# High-throughput biomethane potential (BMP) tests as predictors for commercial-scale anaerobic digester performance

*by*

David John van der Berg

Thesis presented in partial fulfilment

of the requirements for the Degree

*of*

MASTER OF ENGINEERING

(CHEMICAL ENGINEERING)

in the Faculty of Engineering

at Stellenbosch University

*Supervisor*

Prof. Johann F. Görgens

*Co-Supervisors*

Dr. Eugéne van Rensburg and Dr. Funmilayo D. Faloye

April 2022

**DECLARATION**

By submitting this thesis electronically, I declare that the entirety of the work contained therein is my own, original work, that I am the sole author thereof (save to the extent explicitly otherwise stated), that reproduction and publication thereof by Stellenbosch University will not infringe any third party rights and that I have not previously in its entirety or in part submitted it for obtaining any qualification.

Date: April 2022

**PLAGIARISM DECLARATION**

1. Plagiarism is the use of ideas, material and other intellectual property of another's work and to present is as my own.

2. I agree that plagiarism is a punishable offence because it constitutes theft.

3. I also understand that direct translations are plagiarism.

4. Accordingly all quotations and contributions from any source whatsoever (including the internet) have been cited fully. I understand that the reproduction of text without quotation marks (even when the source is cited) is plagiarism.

5. I declare that the work contained in this assignment, except where otherwise stated, is my original work and that I have not previously (in its entirety or in part) submitted it for grading in this module/assignment or another module/assignment.

April 2022

## ABSTRACT

Under steady-state conditions, full-scale anaerobic digestion (AD) plants generate methane gas by utilising industrial organic wastes such as food and beverage processing wastes. The selection and monitoring of operating parameters of AD provides insight into the process dynamics of the system, which presents opportunities to enhance the digester's performance. However, predicting full-scale performance comes with several challenges, including the limitations of using bench-/lab-scale AD tests to accurately estimate industrial-scale AD performance, the impacts of environmental effects on biogas plant operations and the differences in process conditions between AD test scales.

Bench-scale tests such as biomethane potential (BMP) assay tests are used to estimate the methane potential and degradability of a particular feedstock. BMP tests serve as indicators of AD performance and the basis of designing full-scale plants according to an expected biogas output. However, these methods are not always reliable due to the differences in bench- and full-scale AD process conditions, for example different reactor feeding modes. Furthermore, there is a lack of standardisation in BMP test protocols which impacts the reproducibility of BMP results. Very few studies have attempted to predict performance parameters of full-scale AD plants based on bench-scale AD experimental data. Performance parameters such as biogas and methane yields have been estimated for full-scale processes, but not over long durations of time where variations in feedstock compositions are accounted for. This study aimed to utilize bench-scale BMP tests that was efficient in estimating the performance of full-scale AD plants over an operational period spanning three years. The term "high-throughput BMP tests" pertains to the performing of numerous BMP tests simultaneously.

Three full-scale AD plants were included in this study, namely a co-digestion plant of 3200 $m^3$ working volume treating mixed food and agricultural wastes (Plant 1), a full-scale plant of 60 $m^3$ working volume treating tomato wastes (Plant 2) and a liquid-based plant of 2200 $m^3$ working volume treating distillery wastes (Plant 3). BMP tests (500 mL) were performed using a defined standardised BMP protocol on feedstock samples collected over a period of 6 to 8 months. Pilot-scale studies (50 L) were performed under operating conditions replicating those at full-scale AD to assess whether pilot-scale data could predict full-scale performance parameters more accurately than BMP tests. Full-scale performance was predicted using two methods identified from literature: (1) an extrapolation method and a (2) continuous-stirred tank dynamic model. Estimated full-scale performance parameters were then compared to real-time full-scale data to assess the deviation between ideal, bench-scale conditions and full-scale conditions. These deviations were defined as "scale factors" throughout this dissertation, defined as the ratio between real-time and estimated full-scale performance parameters.

The three full-scale AD plants encountered various process disturbances, for example, variations in feedstock composition, which were observed from their full-scale operational datasets. It was found that BMP tests could be used to estimate the performance of full-scale AD processes using the two aforementioned methods identified from literature. Pilot-scale data could not be used to estimate full-scale AD process performance due to errors encountered during experimental procedures. For biogas production and yield estimations, the extrapolation method reflected scale factors of 0.42 for Plant 1 (mixed food wastes), a factor of 1.05 for Plant 2 (TW) and a factor of 0.69 for Plant 3. The dynamic model

provided more accurate estimations of full-scale performance, where scale factors of 0.86, 3.10 and 0.92 were calculated for Plant 1, Plant 2 and Plant 3, respectively. These scale factors have the potential to estimate the energy production potentials of downstream power units for full-scale AD plant by accounting for changes in feedstock composition.

Recommendations for this study included obtaining more reliable datasets of full-scale operational data by ensuring sufficient process monitoring instrumentation (e.g. gas flow meters) is installed at the plant, obtaining operational period spanning a longer time frame (Plants 1 and 2) and by ensuring the design of pilot-scale AD reactors better suit the conditions of full-scale AD plants, e.g. establish the same feeding mode.

**ACKNOWLEDGEMENTS**

The completion of this thesis would not have been possible without the support of many important individuals in my life.

I would like to acknowledge my head supervisor Prof. Görgens for your valuable guidance, expertise and motivation throughout this project. To my co-supervisors Dr. Eugéne van Rensburg and Dr. Funmi Faloye; thank you for your technical insight, wise council and bestowing of knowledge unto me, as well as supporting me through the tough times of industrial-based research.

I would like to thank various staff from Process Engineering; Heinrich Bock, Alvin Petersen, Oliver Jooste and Oom Anton and Jos for supporting and assisting me with my experimental activities. Jaco van Rooyen and Hanlie Botha from the Analytical department for performing my biogas sample analyses. Dr. Danie Diedericks for your contagious laughter and sound advice. Prof. Robbie Pott for keeping my sanity during moments of stress.

Additionally, I would like to extend thanks to the three biogas industries for allowing me to carry out my sample collection and data acquisition plans. It was a privilege to meet such a variety of professional engineers, operators and consultants during my experimental phase and to be exposed to the complexities of AD technologies. This exposure ignited my passion for, one day, working in the renewable energy sector, and hopefully save the world. An extended thank you to the Central Analytical Department (CAF) for carrying out my elemental analyses.

To my dearest friends: Dr. Diane Mostert, my mentor and housemate. You are one the most amazing and intelligent individuals on this planet whose constant support, love and appreciation truly inspired me to finish this thesis. I could never have done this without you. To my fellow Masters colleague, Louis Wentzel. I would have not made it this far without our friendship. I am truly grateful we both took an interest in the biogas field. A few more special friends are worth mentioning: Patrick F., Kyle L., Chandelle N., Anke L., Cody M., Megan W., Joe G., Sasha K., Thomas O., Nicholas E., Adam V., Matt C., Matt T. and Ryan R. All of you played an essential role in this process. Thank you all!

Lastly, to my incredible family: My parents, Margaret and Alan – thank you for your undying support, love and aid through this trying period. You managed to maintain my sanity during these unchartered times and I am forever grateful for your support throughout my Chemical Engineering degree. To my older brother Richard – my idol. Both of us adjusted to incredibly difficult circumstances, yet you continued to push me to “just get on with it”. Our online gaming, face times and phone calls made all the difference to keep me going. Thank you for being my mentor. To my grandparents, June and Peter. You have supported me since day one of preparatory school up until now. I am deeply humbled that my grandfather could witness me receiving this degree. To the memory of Rodney Davison – I wish you could have been here today.

## TABLE OF CONTENTS

**LIST OF TABLES**

## LIST OF FIGURES

## NOMENCLATURE & ABBREVIATIONS

| Symbols/Definitions | | |
|---|---|---|
| $BMP_{max}$ | maximal methane production rate | NL/kg VS/d |
| $BMP_o$ | Ultimate BMP of a feedstock | NL/kg VS |
| $BMP(t)$ | BMP measured at an instance in time | NL/kg VS |
| $BMP_i$ | BMP value used by Holliger *et al*. (2017) | $Nm^3$/t.VS |
| $C$ | Generalized organic content | kg COD or VS/$m^3$ |
| COD | Chemical oxygen demand | mg/L |
| CODR | Chemical oxygen demand removal | % |
| FM | Fresh matter | % |
| $f_{T,P}$ | Temperature-pressure correction factor | - |
| $f_w$ | Water vapor correction factor | - |
| $HRT$ | Hydraulic retention time | d |
| $OLR$ | Organic loading rate | kgVS/$m^3$/d |
| $k_{dis}$ | Kinetic growth constant | $d^{-1}$ |
| $t$ | Time | d |
| $CMP$ | Cumulative methane production | L/d |
| $CMV$ | Cumulative methane volume | L |
| $V_x$ | Digester volume | $m^3$ |
| $WV_x$ | Working volume in digester | $m^3$ |
| SMY | Specific methane yield | NL/kg (VS or COD) |
| $P_{full}$ | Estimated methane production from substrate $i$ | $Nm^3_{CH4}$/week |
| $Q_i$ | Mass flow of material into full-scale digester | ton/week |
| $Se(t)$ | Apparent VS concentration in digester | kg/$m^3$ |
| $So(t)$ | Feedstock VS concentration | kg/$m^3$ |
| $V_o$ | Normalized methane volume | NL |
| $V_{cell}$ | Registered volume for cell opening (AMPTS) | L |
| $T_o$ | Standard temperature | 0°C or 273.15K |
| $P_o$ | Standard pressure | 1.0 atm |
| $T_{gas}$ | Temperature of biogas generated in digester at ambient conditions | °C or K |
| $P_{gas}$ | Pressure of biogas generated in digester at ambient conditions | atm |
| $P_{vap}$ | Vapour pressure of methane gas | mbar |
| $TS$ | Total solids | % wet-weight (w/w) |

| | | |
|---|---|---|
| $VS$ | Volatile solids | % wet-weight (w/w) |
| $\mathrm{VS_{feed}}$ | VS mass fraction in feed | g/kgFM |
| $\mathrm{VS_{dig}}$ | VS mass fraction in digestate | g/kgFM |
| VSR | Volatile solids percentage reduction | % |
| $m_1$ | Mass of empty crucible | g |
| $m_2$ | Mass of crucible with sample | g |
| $m_3$ | Mass of crucible (and sample) after 105°C drying | g |
| $m_4$ | Mass of crucible (and sample) after calcination | g |
| $m(\mathrm{VS})_{add}$ | Mass of VS in the feedstock added do the digester | tonnes |
| $R^2$ | Correlation coefficient for regression model | - |
| **Abbreviations** | | |
| AD | AD | |
| AMPTS | Automatic methane potential test setup | |
| ANOVA | ANOVA | |
| ASBR | Anaerobic sequencing batch reactor | |
| BMP | Biomethane potential | |
| BP | Biogas production | |
| CBP | Cumulative biogas production | |
| CAPEX | Capital expenses | |
| CMP | Cumulative methane production | |
| CMV | Cumulative methane volume | |
| DW | Distillery wastes | |
| FM | Fresh matter | |
| FO | First-order | |
| FVW | Fruit-vegetable waste | |
| FOS/TAC | Ratio of organic acid concentration to buffer capacity of system | |
| ISR | Inoculum-to-substrate ratio | |
| kVA | Kilo-volt ampere | |
| kW | Kilowatt | |
| kWh | Kilowatt hour | |
| MP | Methane production | |
| OPEX | Operating expenses | |
| RSD | Relative standard deviation | |
| SMP | Specific methane production | |
| SMY | Specific methane yield | |

| | |
|---|---|
| STP | Standard temperature and pressure |
| SHW | Slaughterhouse waste |
| STP | Standard temperature & pressure |
| TW | Tomato waste |
| UASB | Up-flow anaerobic sludge blanket |
| VFA | Volatile fatty acids |
| **Sub/Superscripts** | |
| $i$ | Feedstock type |

## GLOSSARY

**Automatic Methane Potential Test System (AMPTS):** Automated bench-scale experimental setup used for BMP tests.

**Biomethane potential (BMP):** The maximum amount of methane gas that can be produced during the AD of a feedstock at bench-scale, as it exists in its individual state.

**Methane potential:** The theoretical maximum amount of methane obtainable from a substrate, based on chemical composition and stoichiometric proportions.

**High-throughput:** The performing of multiple BMP tests simultaneously on AD substrates.

**Scale factor:** The ratio of real-time full-scale performance data to estimated full-scale performance data, expressed as a percentage.

**Specific gas yield (SGY):** The volume of biogas produced per mass of degradable solids, measured from pilot- and full-scale AD systems.

**Specific methane yield (SMY):** The volume of methane gas produced per mass of degradable solids, measured from pilot- and full-scale AD systems.

**Transient effects:** Unpredictable changes in full-scale performance parameters caused by process disturbances.

# CHAPTER 1: INTRODUCTION

In South Africa, the majority of electricity supplementation comes from the use of oil, gas and coal (Ndlovu & Inglesi-Lotz, 2019). Given that the use of fossil fuels to meet energy demands is not sustainable due to the negative effects it has on the environment, alternative energy supplementation systems must be explored to meet the energy demands of rapidly growing populations. Anaerobic digestion (AD) is heralded as one of the most environmentally-friendly and energy efficient conversion technologies for alternative energy production (Amon *et al*., 2006; Walid *et al.,* 2021). AD is a biochemical process involving the breakdown of organic matter in an oxygen-absent environment facilitated by a diverse consortia of microorganisms (FNR, 2012; Meegoda *et al*., 2018; Sarker *et al*., 2019). Organic matter is converted to two useful products, namely biogas and digestate. Biogas predominantly contains methane gas and carbon dioxide ($CO_2$), while digestate can be used for fertilizer production given its richness in nutrients such as nitrogen and phosphorus (Al-Saedi *et al*., 2008).

The selection and monitoring of operating parameters of AD plants provides insight into the process dynamics of the system, which presents opportunities to enhance the digester's performance (Walid *et al.,* 2021). However, predicting full-scale performance comes with several challenges, including the limitations of bench-scale AD tests to accurately estimate full-scale performance, the impacts of environmental effects on biogas plant performance efficiency and the differences in design configurations of full-scale AD plants (Holliger *et al.,* 2017; Koch *et al.,* 2020). Conventionally, bench-scale biomethane potential (BMP) tests are used to assess the methane potentials and degradation capabilities of feedstocks during AD (Angelidaki *et al*., 2009; Esposito *et al*., 2012). BMP tests provide reasonable predictions of full-scale AD performance, however, these methods are not always reliable due to the differences in bench- and full-scale AD process conditions (Sell, 2011; Koch *et al*., 2020). Furthermore, there is a lack of standardisation in BMP test protocols which impacts the validity and comparability of BMP test results (Raposo *et al.,* 2011; Holliger *et al.,* 2016).

In addition to BMP tests, pilot-scale AD tests are performed to optimise or investigate certain process conditions encountered at full-scale like feeding frequencies and the extent of mixing (Lüdtke *et al*., 2017). These tests are, however, more tedious and more costly to operate (Holliger *et al*., 2017; Guendouz *et al*., 2008). Moreover, there is no defined standardised protocol that governs the setup and running of pilot-scale AD tests (Caillet & Adelard, 2020).

Very few studies have attempted to predict the performance of full-scale AD plants using bench-scale tests in order to optimise methane production. Holliger *et al.* (2017) could accurately predict the methane production when they compared two co-digestion full-scale AD plants by extrapolating results from BMP tests. The extrapolation method essentially assumes that methane yields produced from full-scale AD processes will reflect those methane yields produced from BMP tests. Although accurate estimations of methane productions were made, the study did not perform estimations relating to full-scale degradation rates or kinetics. Fiore *et al*. (2016) applied a continuous-stirred tank reactor (CSTR) dynamic model to predict the biogas production rate of a pilot-scale AD system using bench-scale tests. The model assumes that hydrolysis is the rate limiting step for solid-phase feedstocks and that biomass accumulation within

the digester itself was negligible. Fiore *et al.* (2016) did, however, not use BMP tests to estimate full-scale behaviour, nor did they apply the model to a full-scale AD process; only to a 300 L pilot-scale system.

This project aimed to use a high-throughput bench-scale BMP test to estimate the performance of full-scale AD plants, where the term "high-throughput" refers to the performing of many BMP tests simultaneously. Three full-scale AD plants were included in this study, namely a co-digestion plant treating mixed food and agricultural wastes (Plant 1), a full-scale plant treating tomato wastes (Plant 2) and a liquid-based plant treating distillery wastes (Plant 3). BMP tests (500 mL) were performed under the standardised BMP protocol (Holliger *et al*., 2016) on each plants' feedstocks, which were collected over 6 to 8 months to account for feedstock compositional variations. Pilot-scale (50 L) studies were performed under process conditions similar to two of the AD plants: Plant 2 under a semi-continuous feeding mode and Plant 3 under semi-continuous- and batch-fed modes. Batch-mode pilot-scale AD tests were performed under conditions similar to standardised BMP test protocol to assess the effects of changes in process volumes on biogas yields. Scale factors were then calculated as the ratios between the real-time and estimated full-scale performance to quantify the differences between full- and ideal bench-scale test conditions. Estimations of full-scale behaviour were obtained using the extrapolation of BMP test results (Holliger *et al.,* 2017) and a CSTR-based dynamic model (Fiore *et al.,* 2016).

# CHAPTER 2: REVIEW OF LITERATURE

Chapter 2 provides insight into the theoretical framework of this project. The body of the literature review is structured into the following sections: (1) an introduction to AD fundamentals, (2) the implementation of AD in commercial practice and (3) an overview of methods used for estimating the performance of full-scale AD performance, based on experimental data derived from BMP tests.

## 2.1. Fundamentals of AD

AD is a biochemical process that describes the conversion of organic compounds to high-energy by-products in the absence of oxygen (FNR, 2012; Meegoda *et al*., 2018; Sarker *et al*., 2019). This conversion is facilitated by chemoheterotrophic bacteria and methanogenic archaea, where both groups exist in a cultivated medium (Mah, 1981). The by-products given off by these anaerobes are in the form of a gaseous mixture called biogas (Speece, 1996), predominantly containing $CO_2$ and methane.

### *2.1.1. AD reaction pathways*

There are four reaction mechanisms that make up the AD pathway, namely (1) hydrolysis, (2) acidogenesis, (3) acetogenesis and (4) methanogenesis (FNR, 2012). Figure 1 shows the complete AD pathway, where each stage is addressed below.

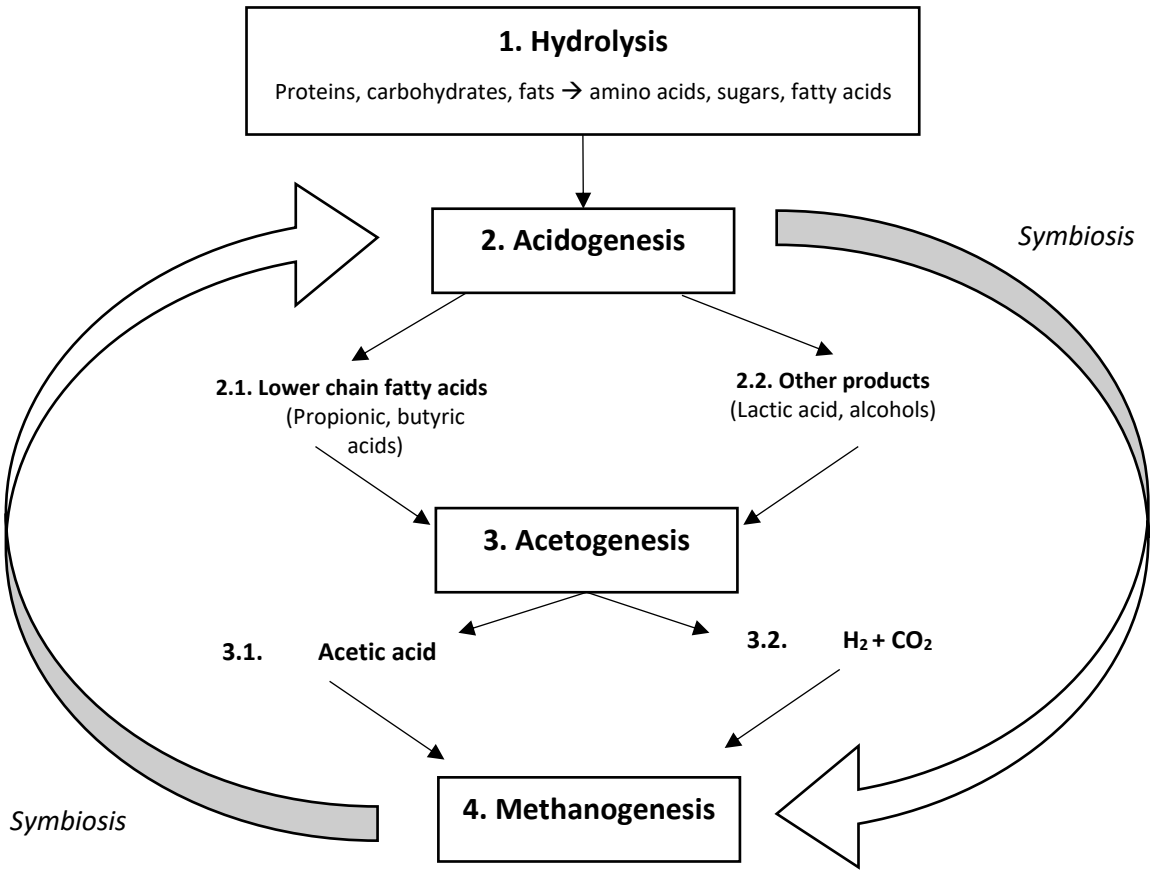


Figure 1: Overview of the anaerobic digestion pathways, adapted from Jewitt *et al*. (2009).

Referring to Figure 1, hydrolysis involves the initial breakdown of large, complex organic molecules into their soluble components (Angelidaki & Sanders, 2004). Large macromolecules like proteins and carbohydrates are broken down to amino acids and monosaccharides (Sarker *et al.,* 2019). If feedstocks composed mostly of solids with little moisture content (highly particulate) are fed to an AD system, hydrolysis may become the rate-limiting step which may slow overall degradation rates (Sayara & Sanchez, 2019). The second stage of AD is called acidogenesis, which involves the breakdown of hydrolysis products into volatile fatty acids (VFA), $CO_2$ and hydrogen gas ($H_2$) by fermentative bacteria (Kalyuzhnyi *et al*., 2000; FNR, 2012). VFAs are subsequently converted to acetates and hydrogen during acetogenesis, which serve as the main precursors for biogas formation (Meegoda *et al.,* 2018). The final stage of methanogenesis involves the conversion of acidogenesis and acetogenesis products ($CO_2$, $H_2$ and acetate) to biogas, facilitated by methanogenic archae (Al-Saedi *et al*., 2008; Jingura & Kamusoko, 2017). Biogas is predominantly composed of methane gas (50 to 75 %vol $CH_4$) with the remaining fraction made up of carbon dioxide (25 to 45 %vol $CO_2$) and trace gases (< 2.0 %vol) (Al-Saedi *et al*., 2008; FNR, 2012; Jingura & Kamusoko, 2017). The volume and concentration of methane in biogas is important for the selection and sizing of downstream co-generation systems that produce electricity (Holliger *et al*., 2017).

### *2.1.2. Conditions for AD*

Microbial communities participating in AD require well-suited environmental conditions to ensure they grow in population. Three important environmental conditions include process temperature, pH level and feedstock nutrient availability, which are discussed below. Organic loading rate (OLR) and hydraulic retention time (HRT) are equally important operating parameters that will be explained in Section 2.2.1.3.

#### *2.1.2.1. Process temperature*

Temperature influences the rate at which AD takes places, specifically its reaction kinetics and metabolic rate of microorganisms involved (Angelidaki & Sanders, 2004; FNR, 2012). There are several temperature ranges at which AD can be operated, namely psychrophilic (< 25$^{o}$C), mesophilic (37 to 42$^{o}$C) and thermophilic (50 to 60$^{o}$C) ranges (Safley & Westerman, 1990; Angelidaki & Sanders, 2004; FNR, 2012).

Mesophilic temperature ranges are commonly employed for full-scale AD processes because they are easy to maintain, have lower heater energy costs and do not pose risks of inhibitions towards anaerobic populations (Meegoda *et al.,* 2018; Sarker *et al.,* 2019). Psychrophilic ranges are rarely adopted at industrial scale because of lower microbial metabolic rates and low biogas production (Connaughton *et al*., 2006). Thermophilic temperature ranges are typically employed to improve the degradability of feedstocks as it enhances the kinetics and growth rates of anaerobic populations (Al-Saedi *et al*., 2008). However, implementing thermophilic temperatures at full-scale is difficult to maintain because thermophilic inoculum is more susceptible to fluctuations in ambient temperatures (Wu *et al.,* 2006). Thermophilic AD plants also have more intense energy demands and thus greater operating expenses compared to mesophilic plants (Ruffino *et al.*, 2015).

#### *2.1.2.2. pH level*

The pH level refers to the balance between acidity and alkalinity of a certain medium. Similar to process temperate the pH of an AD system plays an important role in influencing metabolic activities and the

methane yield (Sarker *et al*., 2019), especially for pH-sensitive methanogens. The optimal pH range for AD has been reported as pH 7.0 to 8.5 (Raposo *et al*., 2012; Holliger *et al*., 2016), but rapid drops (<pH 6.3) or spikes (> pH7.8) have been observed to induce major process instability (Liu *et al*., 2008).

Increases in pH level are associated with free-ammonia accumulation during hydrolysis during the breakdown of protein molecules to amino acids (Angelidaki & Sanders, 2004; Sarker *et al*., 2019). Spikes in free-ammonia concentrations typically arise from protein-rich organic wastes, such as piggery manure or slaughterhouse wastes (Kovács *et al*., 2015). If free-ammonia concentrations exceed a certain threshold in an AD system, then anaerobic bacteria's microbial activities become impeded as free-ammonia negatively affects intracellular pH levels and enzymatic activities (Hashimoto, 1986; Muzenda, 2014; Liu *et al.,* 2019). Decreases in pH level arise from excessive organic acid production, where VFA constituents formed from hydrolysis accumulate due to over feeding (Franke-Whittle *et al*., 2014). If the VFA accumulation becomes too excessive the system pH will drastically decrease, inhibiting the entire AD process (Sarker *et al*., 2019). Declines in system pH are usually associated with feedstocks containing organic wastes too high in carbohydrates or sugars. This is common in plants feeding food and fruit & vegetable wastes (Esposito *et al*., 2012).

#### *2.1.2.3. Feedstock characterizations*

a) Physico-chemical makeup

The suitability of a feedstock for AD depends on its degradation capabilities and methane potential, and thus the concentration of organic and inorganic components in such materials (Kaltschmitt & Hartmann, 2001; Drosg *et al*., 2013). Figure 2 gives an overview of the physical and chemical constituents of feedstock materials. Organic constituents include sugars, proteins and fats/lipids, while inorganic constituents include salts and heavy metals (Al-Saedi *et al*., 2008).

The feedstock (fresh matter) is comprised of solid dry matter (total solids) and water (Liebetrau *et al*., 2016), as depicted in Figure 2. Total solids (TS) represent the portion of fresh matter that constitutes solid dry matter, expressed as a concentration (g/L) or wet-weight percentage (%w/w) (Liebetrau *et al*., 2016; Meegoda *et al*., 2018). The TS content is further categorized into an organic fraction and an inert fraction (ash). The degradable organic fraction is composed of contents such as carbohydrates or proteins. The non-degradable fraction includes components that are not readily digestible such as lignocellulosic components (Goswami & Kreith, 2008; FNR, 2012; Meegoda *et al*., 2018; Sayara & Sanchez, 2019).

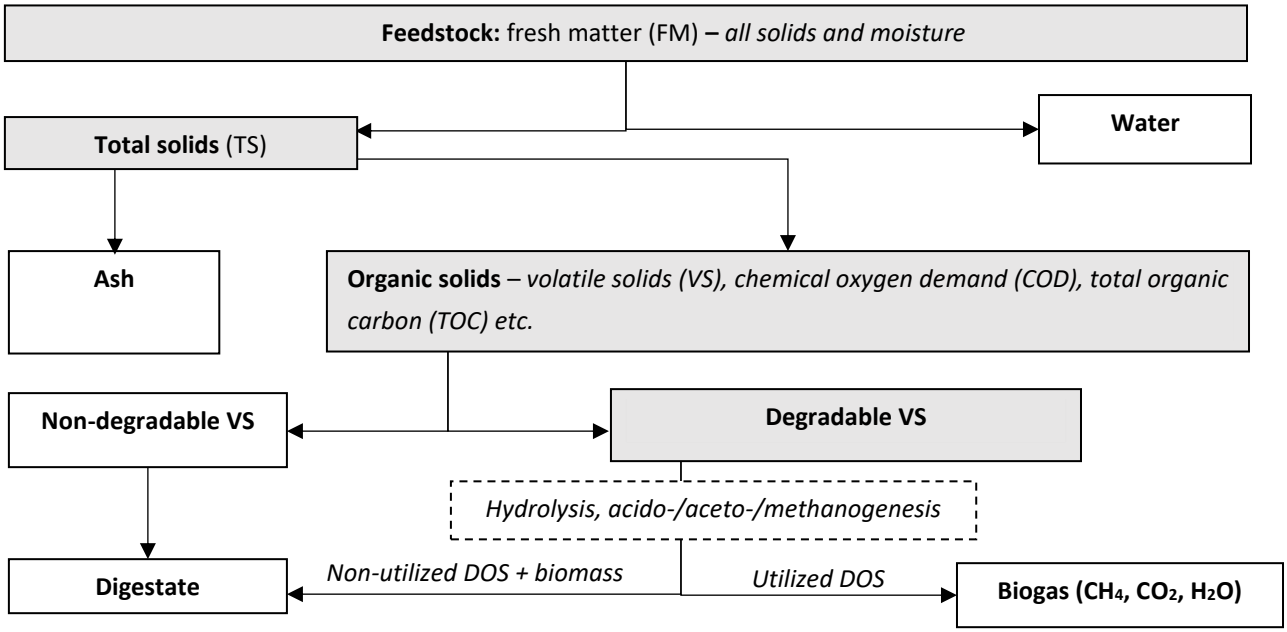


Figure 2: Block-flow diagram showing the degradation pathways of a feedstock via anaerobic digestion, adapted from Liebetrau *et al*. (2016).

Organic content is primarily categorized as volatile solids (VS) or chemical oxygen demand (COD) (Figure 2). The VS content is expressed as the amount of material lost on ignition (American Public Health Association, 1999; FNR, 2012; Liebetrau *et al*., 2016), typically as a percentage of the fresh matter (% wet-weight) or as a fraction of the total solids content (%TS). The VS content is a useful determination of a solid feedstock's organic content, however measuring such a parameter only provides a quantitative analysis of organic content while providing no insight on the nature of organic molecules in an AD system (Schievano *et al.,* 2011; Li *et al.,* 2017).

For feedstocks that are completely liquid, the degradable organic content can be quantified by its chemical oxygen demand (COD). The COD indicates the amount of oxygen consumed by reactions in a sample solution to ensure the complete oxidation of organic constituents (Rajasekharan, 2015; Liebetrau *et al*., 2016). The COD is measured by adding a designated volume of sample to a solution containing potassium dichromate ($K_2CrO_7$) and 50% sulfuric acid ($H_2SO_4$) (Hach, 2020). During this process a strong oxidation reaction takes place, where the amount of $K_2CrO_7$ consumed correlates to the substrate's chemical oxygen demand expressed in milligrams per litre (Hach, 2020). COD content can be determined for any feedstock considered for AD to reflect its organic content; however these measurements consider all material that can be oxidized and quantitative measurements for COD may be less specific (Schievano *et al.*, 2010; Gao *et al*., 2011). In terms of its utilisation for methane production, a theoretical volume of 395 mL of methane gas is produced from 1.0 g of COD at 35 $^{o}$C and at 100% digester efficiency (Speece, 1996).

In addition to the organic content of feedstocks, nutrient availability can be characterized by the carbon-to-nitrogen (C:N) ratio, which compensates for the presence of carbohydrates, lipids/fats and proteins in feedstocks (Meegoda *et al*., 2018). Microorganisms utilize carbon and nitrogen within the optimal ratio

of 25 to 35:1, which is a desirable range for optimising methane yields during the co-digestion of mixed organic wastes (Ward *et al.,* 2008; Weinrich *et al*., 2018).

b) Feedstock sources

AD technology has been applied to a range of industries, with two main sectors being farming and the agricultural processing industries (FNR, 2012). Feedstocks from these sectors include livestock wastes from dairy, poultry and pig farms (Chen at al., 1987; Møller *et al*., 2003; Amon *et al*., 2007; Budiyono *et al*., 2010; Triolo *et al*., 2011; Pham *et al*., 2013; Masse *et al*., 2016; Abdallah *et al*., 2018), crop and plant residues (Amon *et al*., 2007; Triolo *et al*., 2011; Giuliano *et al*., 2013), food wastes (Alveraz, *et al.,* 2008; Arhoun *et al.*, 2019), beverage and distillery wastes (Fountoulakis *et al*., 2008; Da Ros *et al*., 2017), meat processing wastes (Moukazis *et al.,* 2017; Musa *et al.,* 2018) and the organic fraction of municipal solid wastes (OFMSW) sourced from landfill sites (Lemmer & Oechsner, 2002; Esposito *et al.,* 2012). Given the variety of feedstocks considered for AD, each of them will produce different methane yields due to variations in organic content (Drosg *et al*., 2013).

## 2.2. Industrial application of AD

### *2.2.1. Overview*

The implementation of industrial-scale AD is as an effective way for alleviating organic waste accumulation, while promoting the production of renewable energy (De Baere, 2000; Khanal, 2008). In addition to waste valorisation benefits, large-scale AD systems provide environmental and socioeconomic advantages, as listed below (Al-Saedi *et al*., 2008):

1. **Production of biogas as a renewable energy source:** The combustion of methane gas allows for the generation of heat and electricity, serving as an alternative to fossil fuel utilization (Amon *et al*., 2006). It has been reported that full-scale biogas plants typically utilize 15kWh per tonne of feed for self-sustainability purposes, while an excess of 165 to 245 kWh could be repurposed to other industries or sold (De Baere, 2000). AD also enables the diversion of organic wastes from conventional landfill methods, as emissions produced from AD are not emitted directly into the atmosphere (Barragan-Escandon *et al*., 2020).

2. **Contribution to economic and social development:** The establishment and operation of full-scale AD plants can provide employment opportunities to society, especially in undeveloped countries where energy accessibility is limited to many people living in remote and rural areas (Al-Saedi *et al*., 2008).

*2.2.1.1. Process description and flow*

Figure 3 shows a block-flow diagram of a typical commercial-scale anaerobic digester.

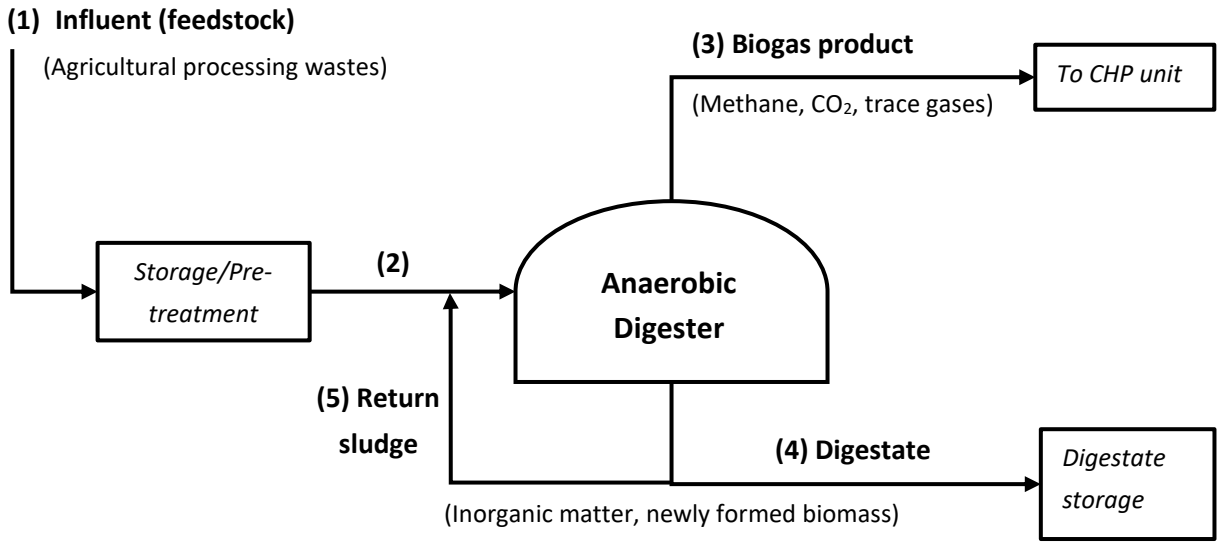


Figure 3: Block flow diagram for a commercial anaerobic digester, adapted from Liebetrau *et al*. (2016).

Waste stream (Stream 1) is fed to a reaction vessel (digester) from a feedstock storage unit. Pre-treatment strategies, such as heating or chemical treatment, may be required for feedstocks that are not readily degradable such as lignocellulosic materials (FNR, 2012; Jingura & Kamusoko, 2017), which may render the hydrolysis stage as rate-limiting (Khanal, 2008). Inside the AD reactor the four stages of AD take place, as the reactor is configured to single-stage digestion, and biogas is subsequently produced. The produced biogas may be directed to downstream processing units such as gas scrubbers or drying units to harness the methane from the mixture (Liebetrau *et al*., 2016). Methane is then used for power generation in downstream combined heat and power (CHP) units (Holliger *et al*., 2017). Alternatively, methane produced from full-scale AD plants can be used as fuel for cars, buses and other vehicles; this is an option explored by developing countries to outlaw the use of fossil fuels for energy production (Fagerström *et al*., 2018).

The other by-product of the AD system is the digestate; a high solids residue rich in nutrients such as nitrogen and phosphates (Al-Saedi *et al*., 2008). Some AD systems post-treat the formed digestate in an attempt to recover water and/or the aforementioned nutrients (Campos *et al*., 2019). Recovered water can be recirculated back to the AD system, while the remaining nutritional mass can be used as fertilizer (Romero-Guiza *et al*., 2015). Dissolved air flotation (DAF) is an example of a post-treatment method used for this water and/or solids recovery, the latter fraction containing nutrients valuable for soil fertilizer applications (Porterfield *et al.*, 2020).

*2.2.1.2. Types of biogas plants*

Numerous anaerobic digester designs and configurations are implemented at industrial scale (Sarker *et al*., 2019). Three types of configurations exist according to total solids (TS) loading requirements for

single-substrate plants, namely (1) conventional wet (TS ≤ 10% w/w), (2) semi-dry (10% to 20% w/w) and (3) modern dry (≥20% w/w) (Yi *et al*., 2014).

Conventional ("wet") AD systems require 10% (w/w) or less solids content, which have served useful for treating and stabilising activated sludge (AS) sourced from wastewater treatment plants (WWTP) (Garcia-Bernet *et al*., 2011). Compared to conventional wet AD, dry AD systems have lower operating expenses (OPEX) and capital costs (CAPEX) due to a lower consumption of dilution water and thus smaller vessels are constructed (Garcia-Bernet *et al*., 2011).

Within the context of conventional wet AD systems, one of the most common digester designs includes a continuous-stirred tank reactor (CSTR) (Achinas *et al*., 2020). A CSTR is a simple yet advantageous reactor design for AD systems as it provides greater consistencies in process conditions such as operating temperature, degree of mixing and reactor concentrations (Usack *et al*., 2012). Moreover, a CSTR design assumes that all material entering the system exits at the same rate and all discharged material has the same concentration as the contents inside the system (Felder & Rousseau, 2005).

In addition to single-feedstock digestion, AD plants implement co-digestion strategies. Co-digestion entails the simultaneous AD of multiple feedstocks in the same system (Esposito *et al*., 2012; Maile *et al*., 2016). Co-digestion strategies have been shown to enhance process stability by providing a better nutrient balance in the feed stream (Tufaner & Avsar, 2016). This is done by adjusting the C:N ratio of a feedstock to the optimal range of 20:1 to 35:1 (FNR, 2012; Weinrich *et al*., 2018). Typically, livestock manure, abundant in elemental nitrogen, is blended with the suitable feedstock adjust the C:N ratio accordingly. (Esposito *et al*., 2012; Maile *et al*., 2016; Tufaner & Avsar, 2016).

*2.2.1.3. Operating parameters*

Full-scale operating parameters such as hydraulic retention time (HRT), organic loading rate (OLR) process temperature and pH level require careful monitoring and control to ensure consistent process stability, performance and production of biogas.

*(a) Hydraulic Retention Time (HRT)*

HRT refers to the amount of time material spent inside an anaerobic digester (Al-Saedi *et al*., 2008; Meegoda *et al*., 2018). HRT is expressed mathematically as Equation (1) (Cooper, 2014):

$$HRT\ [days] = \frac{V_o}{Q_i} \tag{1}$$

Where $V_o$ and $Q_i$ represent the digester volume ($m^3$) and volumetric feed flowrate ($m^3/d$), respectively. The HRT is an important design parameter for sizing AD systems, which can vary for different feedstocks due to differences in composition (Al-Saedi *et al*., 2008). The HRT of a feedstock can be determined in bench-scale batch tests to indicate the time needed for complete degradation to be achieved (Holliger *et al*., 2016). This is also useful for assessing the process kinetics of an AD system (Liebetrau *et al*., 2016).

Longer HRTs may provide sufficient time for methanogenic populations to increase in number, which would, in turn, improve biogas yields of the system (Sarker *et al*., 2019).

HRTs determined from bench-scale tests are usually shorter than for larger AD systems and establishing an HRT that is too short for larger systems may induce volatile fatty acid (VFA) accumulation and AD process inhibition (Kim *et al*., 2013). Ferreira *et al*. (2014), for example, performed 2.0L bench-scale BMP tests on wheat straw feedstock. The methane yield ranged between 293 to 245 mL $CH_4$/kgVS for a corresponding HRT of 43 to 50 days. Shi *et al*. (2017) performed similar tests with wheat straw but at a larger scale (4.0L) under continuously-fed conditions; for a set HRT of 40 days the methane yield was measured as 34.8 mL/kgVS. This yield was lower than that obtained by Feirrera *et al*. (2014), indicating that a 40-day, bench-scale HRT may not be as sufficient for the larger process.

*(b) Organic Loading Rate (OLR)*

For semi-continuously- and continuously-fed anaerobic digester systems the OLR refers to the mass of organic material fed to the digester per digester volume per unit time (Meegoda *et al*., 2018). On a daily basis, OLR is mathematically expressed by Equation (2) (Sarker *et al*., 2019):

$$OLR\left[\frac{kg\ VS\ or\ COD}{m^3 \cdot d}\right] = \frac{C}{HRT} \tag{2}$$

Where $C$ and $HRT$ refers to the organic content (volatile solids or chemical oxygen demand) and the HRT, respectively. Controlling OLR is crucial to the stability of the AD process; if the OLR is too great for the AD system then VFA accumulation would increase, which causes synergistic imbalance between methanogens and acidogenic and acetogenic anaerobes (Ahring, 1995). For AD plants treating animal manure, the OLR typically ranges 2.5 to 3.0 kgVS/$m^3$/d, which, if exceeded, would induce process instability (Coppinger e*t al.,* 1979). Controlling the OLR would therefore ensure the hydrolysis stage remains rate-limiting (Fiore *et al*., 2016). In full-scale AD systems the first signs of VFA accumulation arise from dramatic drops in digester pH level, which creates toxic conditions for microbial consortia (Franke-Whittle *et al*., 2014; Sarker *et al*., 2019).

The HRT and OLR of an AD system are inversely proportional to one another; increasing HRT will lower the organic loading rate. Both the HRT and OLR of an AD system must be well-established and balanced during the start-up phase of any full-scale system so that anaerobic microbes satisfactorily acclimatize to different feeding loads (Akram & Stuckey, 2008). However, from an economic standpoint, higher HRTs increase the digester volume and thus the plant's capital expenses (Meegoda *et al*., 2018).

*(c) Operating temperature and digester pH level*

The operating temperature and pH level of an anaerobic digester must be carefully controlled to maximise methane productivity and minimize process instability. Meeting these control standards can be difficult at full-scale volumes due to fluctuations in feeding rates, environmental factors (e.g. ambient temperature changes during different seasons) and due to the working conditions of process equipment, for example, blockages of pipelines if feed pumps are not suitable for transporting the feedstock

(Coppinger *et al.* 1979. Full-scale digester temperature is controlled using heat exchanger systems using process water and steam, while pH control is regulated via acid or alkaline dosing stations.

*2.2.1.4. Challenges of full-scale operation*

The steady operation of industrial-scale AD plants is challenged by a variety of factors, specifically those that cause transients in process performance. Major process fluctuations can arise from changes in feedstock characteristics (composition) and environmental factors, for example, fluctuations in temperatures in different climates or non-optimal set-up ranges (Cavinato *et al*., 2010).

The composition of feedstocks fed to AD processes can be highly variable, particularly for systems processing complex feedstocks. For example, Illmer & Gstraunthaler (2009) monitored the effects of seasonal changes on biogas production from a 750 $m^3$ plug-flow anaerobic digester. Summer seasons exhibited a period of the highest biogas production (2000 to 3500 $m^3$/d) during peak tourism season, while winter exhibited the lowest production (1500 to 2000 $m^3$/d). Additionally, fluctuations in feedstock composition can give rise to spikes in OLR, which have known to accelerate VFA formation (Sarker *et al*., 2016; Meegoda *et al*., 2018). VFA accumulation decreases digester pH, which inhibits the functionality of methanogenic bacteria (Moeller & Zehnsdorf, 2016). It is difficult to account for variations in organic loading, and, by the time a full-scale system exhibits declining performance, it may be too late for the digester to recover (Schusseler, 2008; Kleybocker *et al*., 2012). Furthermore, reactor overloading is also associated with the formation of foam and floating layers within the digester itself (Moeller & Zehnsdorf, 2016).

Several case studies on full-scale AD plants have reported other challenges with operating such systems. These include inadequate mixing, reactor foam formation, lack of process control and hydrogen sulphide ($H_2S$) build up (Spyridonidis *et al*., 2020). Adequate mixing is essential to ensure sufficient distribution of nutrients inside the digester, as well as to avoid pH, temperature and concentration gradients, scum formation, floating layers and the formation of dead volumes (Singh *et al.,* 2021).

The physical nature of fed organic material to a digester may also impact its mixing efficiencies and thus overall performance. For example, Coppinger *et al.* (1979) monitored the performance of a 172 $m^3$ anaerobic digester treating dairy manure. It was reported that the highly heterogenous manure frequently clogged pipelines and resulted in mixing issues inside the digester, which ultimately impacted daily biogas productivities and yields. Furthermore, AD reactors subject to a high solids loading of 10% to 20% (w/w) can drastically reduce the mass and heat transfer amongst anaerobic bacteria and substrates within the digester (Battista *et al.*, 2016). This is because there is a greater reduction in substrate surface area available to the anaerobic bacteria's enzymes during hydrolysis (Aldin *et al.,* 2011).

### *2.2.2. Design considerations for full-scale AD processes*

The design of a full-scale anaerobic digester plant is based on the degradation capacities and methane potentials of organic materials considered for such systems (Al-Saedi *et al*., 2008). These parameters are typically assessed by performing of AD experiments at smaller process volumes, i.e. bench- and/or pilot-scale AD tests. This section addresses these experimental methods at different scales and their implications on the design of full-scale AD plants.

*2.2.2.1. Bench-scale AD studies*

Methane potential is often referred to as the maximum amount of methane gas that can be produced during the AD of a feedstock at bench-scale, as it exists in its individual state (FNR, 2012; Raposo *et al*., 2012; Holliger *et al*., 2016; Liebetrau *et al*., 2016; Weinrich *et al*., 2018). Bench-scale AD tests are performed to assess the methane potential and degradation capability of different feedstocks at working volumes of 0.1 to 2.0 L (Schievano *et al*., 2008; Angelidaki *et al*., 2009; Raposo *et al*., 2012; Holliger *et al*., 2016). The most common bench-scale AD test method refers to BMP assay tests, originally proposed by Owen *et al*. (1979). According to Holliger *et al*. (2016), methane potential obtained from bench-scale tests is defined as its BMP value, expressed as the volume of dry methane gas per mass of added organic material under standard conditions, that is, the standard temperature and pressure of 273.15 K and 1.0 atm, respectively. As per this definition, the BMP value is expressed by Equation (3):

$$BMP = \frac{CMV}{m_{(VS\ or\ COD)}} \tag{3}$$

Where $CMV$ and $m_{(VS\ or\ COD)}$ represents the cumulative methane volume (mL or L) and mass of volatile solids or COD added (g or kg) to the reactor, respectively. During a bench-scale AD test the cumulative biogas or methane production (CBP or CMP) typically follows a trend that resembles a first-order (FO) model response (Figure 4).

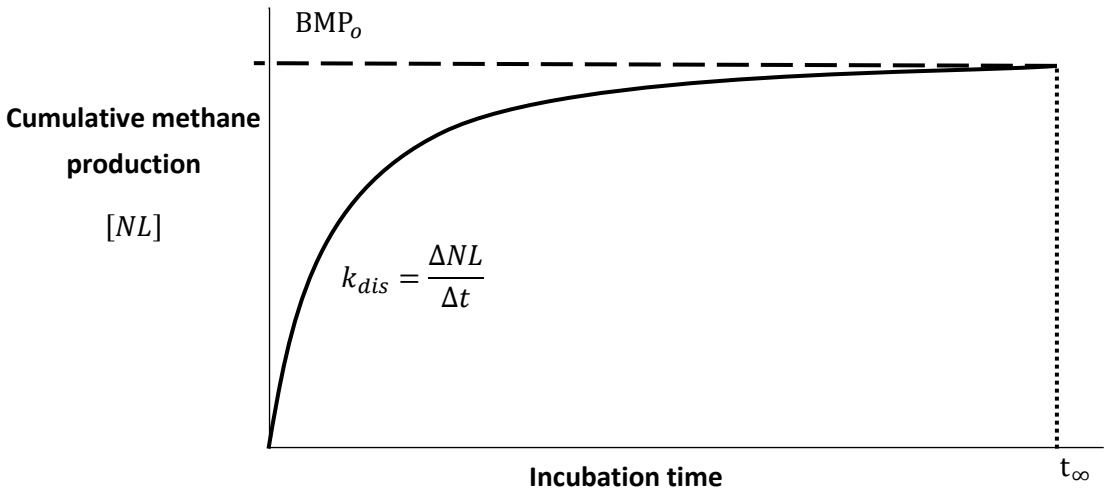


Figure 4: Cumulative specific methane yield versus incubation period during AD tests.

FO modelling of BMP tests are commonly implemented to as first approximations of degradation rates. The response curve shown in Figure 4 can be mathematically expressed as Equation (4):

$$\mathrm{BMP}(t) = \mathrm{BMP}_o(1 - e^{-k_{dis} \times t}) \tag{4}$$

The model above allows for the determination of the biogas production rate $(\mathrm{BMP}(t))$, providing the ultimate methane potential $(\mathrm{BMP}_o)$ and kinetic (degradation) constant $(k_{dis})$ are known. Although useful for first approximations, the application of FO models to full-scale plants is not done due to the extensive differences in process conditions and dynamics between both scales.

Because methane potential strongly depends on a feedstock's organic content, such materials must be physically and chemically categorized in detail (Holliger *et al*., 2016). The degradation pathway showing the major physical and chemical components of feedstocks was previously illustrated in Figure 2. BMP tests are performed under batch conditions, where an aliquot of feedstock (substrate) is digested by active biomass (inoculum) in an anaerobic environment (Raposo *et al*., 2012). Typically, small working volumes are used (0.1 to 2.0 L) for BMP tests (DIN 38414-, 1985; DIN EN ISO 11734, 1998; VDI 4630, 2016), as per the example of the serum bottle below (Figure 5).

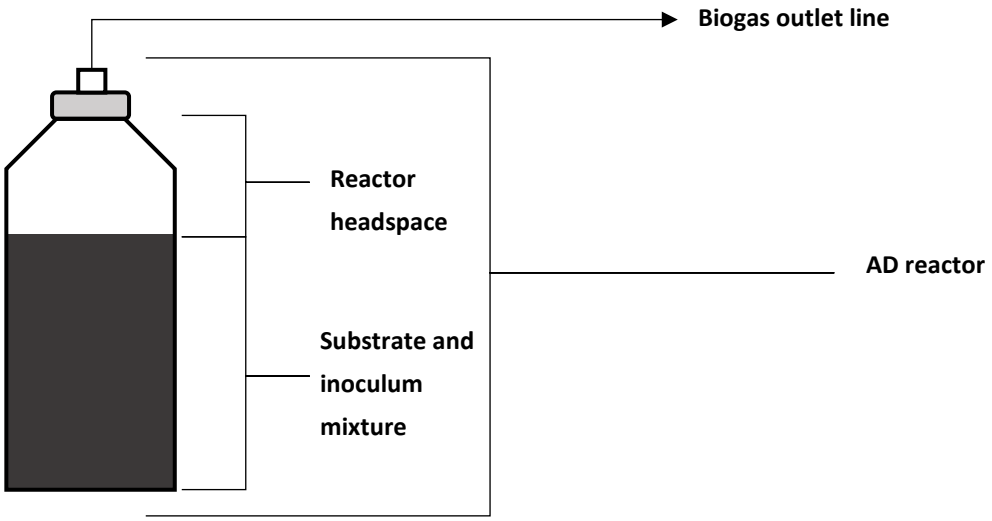


Figure 5: Cross-sectional diagram of a BMP test reactor.

The quantities of loaded substrate and inoculum depend on a parameter called the inoculum-to-substrate ratio (ISR). The ratio is based on the concentration of organic material contained in the substrate and inoculum (Weinrich *et al*., 2018), which can be calculated from a simple VS or COD mass balance. As per the standardised protocol for BMP tests, Holliger *et al*. (2016) recommended an ISR range of 2.0 to 4.0. Higher ISR ranges ensure that the amount of organic material contained in a substrate is always greater than the amount present in inoculum to minimize the risks of VFA accumulation. ISRs lower than this range have been investigated by other researchers. For example, Caillet *et al*. (2020) investigated different ISR ranges for the AD of sugarcane distillery vinasse in BMP tests. On a COD basis, an optimal ratio of 0.5 was recommended for the feedstock as the greatest methane yields were reported from the investigated ratio.

In addition to changes in feedstock compositional makeup, a feedstock's BMP value can be influenced by the process conditions under which AD occurs (Weinrich *et al*., 2018). For example, certain pre-treatment strategies such as pre-heating could influence the methane potential of feedstocks (Weinrich *et al*., 2018), which is why many researchers have reported different methane potentials for the same type of

digested feedstock (Holliger *et al*., 2016). Therefore, there has been much speculation on how bench-scale tests should be standardised to best represent the BMP value of a substrate, as many researchers have explored different test conditions (Holliger *et al*., 2016). The implications of different BMP test conditions will be discussed under Section 2.2.2.3, as well as the standardized protocol recommended for such tests.

*2.2.2.2. Pilot-scale AD studies*

In addition to the small working volumes employed for BMP tests, pilot-scale studies have been investigated to evaluate AD at larger working volumes. Pilot-scale studies allow for the optimisation of operating conditions for full-scale AD processes. For example, Gallert *et al*. (2003) optimised the OLR of a 1200 $m^3$ AD plant using semi-continuously-fed pilot-scale AD tests (8.5 L). The OLR of the pilot-scale system was varied, during which the system exhibited stable process efficiency and biogas productivity. The OLR for the full-scale system was subsequently increased, which encountered no issues associated with major OLR increases.

Pilot-scale studies also allow for the assessment of a number of process conditions, which include evaluating transient conditions (e.g. variations in OLR or temperature), influence of mixing and feeding frequencies, adaption of novel feedstocks for AD or the impact of HRT on system behaviour (Lüdtke *et al*., 2017). For the example of Cavinato *et al*. (2010), a pilot-scale system (380 L) was operated under the same conditions of a 1400 $m^3$ full-scale plant to cross-check certain performance parameters. Under the same process temperature of 47 $^oC$, the pilot-scale produced a biogas yield of 0.54 $m^3$/kgTS while the full-scale process produced a biogas yield of 0.45 $m^3$/kgTS. Given that similar biogas yields were obtained at both scales, the study indicated that the pilot-scale system could be used to monitor other process parameters such as free-ammonia concentrations. Therefore, both of the aforementioned studies indicated that full-scale AD process optimisation was possible using pilot-scale AD tests. This is advantageous over the performing of BMP tests, which do not provide information on the OLR or HRT of full-scale processes because BMP tests are restricted to batch-fed mode (Koch *et al.,* 2020; Sell, 2011).

*2.2.2.3. Scale-up of AD processes*

Bench- and pilot-scale tests are beneficial for assessing the degradation capabilities, methane yields and process parameters at smaller volumes, however the extrapolation of such data to larger AD processes can be complicated due to differences in process conditions (Marques *et al*., 2017). For the example of BMP tests, degradation rates and methane potentials of feedstocks are assessed at a cost-effective scale under controlled operating conditions. These bench-scale datasets then serve as preliminary indicators of feedstock performance, used for sizing full-scale AD plant equipment such as transportation and utilisation system components and digester and biogas collection vessels (Bishop *et al*., 2009). However, many of the indicators determined at bench-scale cannot be extrapolated to full-scale processes because they do not address certain parameters associated with full-scale AD processes, for example, the variations of HRT, OLR or substrate-inoculum interactions (Sell, 2011; Koch *et al.,* 2020). It is, therefore, important to understand how and what scale factors arise from AD processes to understand how and why the conditions between different process volumes change.

a) Fundamentals of scaling up

Scaling involves changing a system's process parameters by a proportional amount, ratio or scale factor in the event of resizing the pre-existing system (Felder & Rousseau, 2005). The general scale-up procedure for bioprocesses involves the primary conduction of bench-scale tests and the progressive development of the process at larger volumes (Clarke, 2013).

In a simplistic view, one scale-up process refers to the principle of geometric similarity, which assumes identical aspect ratios of the vessel and internals on both scales (Clarke, 2013). This method also requires that a process parameter vital to the performance of the system must be identified and kept constant during the scale-up process, for example, constant mixing. The process of geometric similarity is illustrated below for a bench- and pilot-scale bioreactor (Figure 6).

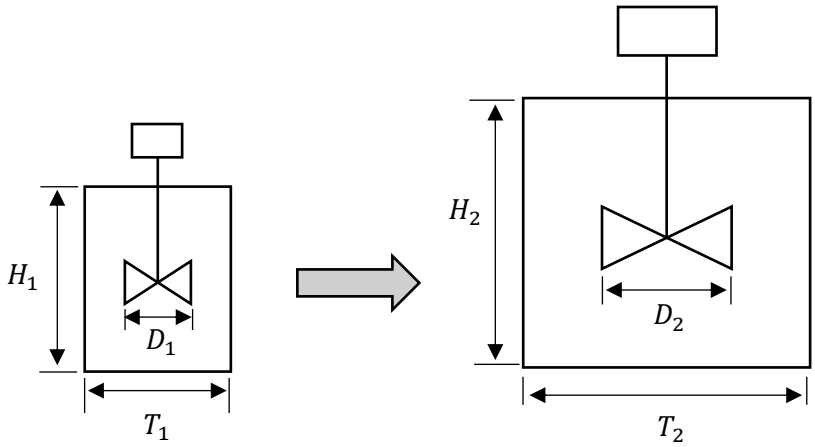


Figure 6: Depiction of geometric similarity between two scales: (a) bench- and (b) pilot-scale bioreactors.

The two bioreactor scales given in Figure 6 are geometrically similar if:

$$\frac{H_1}{T_1} = \frac{H_2}{T_2} \qquad \text{and} \qquad \frac{H_1}{D_1} = \frac{H_2}{D_2}$$

While geometric similarity is useful for the mechanical design of such systems, it does not compensate for changes in microbial physiology, transfer phenomena and chemical dynamics (Marques *et al*., 2010; Clarke, 2013). Moreover, geometric similarity implies that one scale-up criterion remains fixed while others can change (Clarke, 2013). Therefore, it is crucial to address the scale-up factors associated with AD processes at larger volumes.

When an AD system is scaled-up, the increase in process volume induces several complexities associated with transport phenomena and chemical dynamics within the reactor, including mass/heat transfer rates, mixing efficiencies, substrate and product concentrations and temperature and pH distributions (Marques *et al*., 2010). Transfer phenomena like heat distribution are important for maintaining growth kinetics and thus biogas production during AD (Chen *et al*., 2008). Heat transfer is analogous to mass transfer, except that the driving force is temperature difference rather than concentration differences

(Cengel & Ghajar, 2015). At smaller scales, changes in heat distribution (and analogously solids concentration) are considered negligible (Weinrich *et al*., 2018) but they are more significant at larger process volumes. Furthermore, mass transfer rates can be affected by overloading an AD reactor with organic material because introducing more material changes the environmental conditions of anaerobic bacteria, forcing them to re-acclimatise (Lara *et al.,* 2006; Akram & Stuckey, 2008).

To avoid the formation of heat and concentration gradients, adequate mixing of the digester's contents is required (Yu *et al*., 2011). Adequate mixing is ensured when the mixing equipment delivers enough energy to mobilize the digester's contents without inducing major shear forces inhibitory towards microbial growth (Singh *et al.,* 2020). Full-scale digesters experience mixing difficulties when reactors are oversized due to low HRT, and thus insufficient energy is supplied to ensure adequate mixing (Kariyama *et al.,* 2018). Therefore, when scaling up AD processes, scale factors could arise from (1) fluctuations in feedstock composition, (2) differences in process volumes and (3) disruptions in steady-state operations of full-scale processes (e.g. temperature fluctuations).

b) Scaling-up of AD

While BMP tests serve as cost-effective methods for the preliminary assessment of feedstocks' suitability for AD, they do have limitations regarding the assessment of operational parameters and degradation kinetics for larger AD systems (Koch *et al*., 2020). Another limitation includes the lack of standardised experimental designs for BMP tests. Therefore, Holliger *et al*. (2016) compiled a set of standardised protocols for such tests to improve the confidence in produced experimental data for different substrates. Table 1 under lists the standardised conditions for performing BMP tests (Holliger *et al.,* 2016).

Table 1: standardized conditions for BMP assay tests, as defined by Holliger *et al*. (2016).

| **Criterion** | | **Description/Quantification** | **Additional references** |
|---|---|---|---|
| **1. Experimental criteria** | | | |
| 1.1. | Digester volume | • Homogenous feedstocks: < 0.1L<br>• Heterogenous feedstocks: 0.5 to 2.0L | DIN 38414-, 1985; DIN EN ISO 11734, 1998; VDI 4630, 2016 |
| 1.2. | System preparation | • Flush with 50%: 50% v/v nitrogen ($N_2$) and $CO_2$ gas mixture to render anaerobic conditions. | Angelidaki *et al*. (2009) |
| 1.3. | Inoculum-substrate ratio (ISR) | • Fraction of inoculum is typically higher than fraction of substrate in digester. An ISR of 2.0 to 4.0 is the selected norm. | - |
| 1.4. | System incubation | • Temperature: either mesophilic (37°C) or thermophilic (55°C). | - |
| 1.5. | Mixing | • Intermittently (manual) or continuous. | - |
| 1.6. | Gas measurement | • Volumetric, manometric (< 300KPa).<br>• Methane analysis: gas chromatography (GC). | - |

| | | | |
|---|---|---|---|
| | | • Record ambient temperature and pressure at sample port for normalization. | |
| 1.7. | Total organic loading | • On a VS basis: 20 to 60 gVS/L | - |
| **2. Feedstock criteria** | | | |
| 2.1. | Detailed characterization | • Compulsory analyses: TS and VS (and/or COD)<br>• Additional analyses: pH, VFA, elemental analyses, FOS/TAC ratio | VDI 4630 (2016) |
| 2.2. | Substrate preparation/storage | • Sieving and homogenisation (< 10mm) for highly particulate feedstocks.<br>• Short term storage: at 4°C (2 to 5 days)<br>• Long term storage: at -20°C | - |
| **3. Inoculum criteria** | | | |
| 3.1. | Quality control | • Sourced from operational digesters (e.g. WWTP)<br>• Analyses: pH level (7.0 to 8.5), VFA (<1.0 g/L, based on acetic acid), $NH_4^+$ (< 2.5 g/L), alkalinity (> 3g/L, based on calcium carbonate).<br>• Significantly low endogenous methane production relative to total methane produced. | Angelidaki & Sanders (2004) |
| 3.2. | Inoculum preparation/storage | • Minimal preparation (use as sampled)<br>• Stored at ambient temperature (20 to 25°C) for 5 days maximum. | - |
| 3.3. | Blank tests | • Required for evaluating the activity of inoculum, where AD reactors are only loaded with inoculum.<br>• Accounts for methane produced endogenously. | - |
| 3.4. | Positive control tests | • Validate the activity of inoculum with a standard substrate (e.g. micro-crystalline cellulose).<br>• Average methane yield: 350 ± 29 NL $CH_4$/kgVS. | Raposo *et al*., 2011; Bioprocess Control, 2020 |
| **4. Data validation criteria** | | | |
| 4.1. | Number of AD tests | • At least triplicate | - |
| 4.2. | Incubation period (time) | • Experimental time persists until the daily methane production over three consecutive days is <1.0% of the cumulative methane production. | - |
| 4.3. | Results processing | • Normalize BMP data (methane volume) to STP (273.15k and 1 atm) for results comparability.<br>• BMP calculation must account for standard deviation. | - |
| 4.4. | Rejection of results using relative std. deviation (RSD) | BMP results are rejected if:<br>• RSD (blank or positive control) > 5.0%<br>• RSD (homogenous feedstock) > 5.0%<br>• RSD (heterogenous substrate) > 10%<br>• Experimental BMP of positive control tests is <85% and/or >100% of the theoretical BMP. | - |

The standardised BMP test protocol in Table 1 were compiled by a group of 40 researchers that share expertise on the performing of BMP tests. Inter-laboratory discussions were held to identify new routes to render BMP tests more reliable. Such criteria pertaining to experimental conditions and procedures, feedstock and inoculum quality criteria and data validation criteria (Table 1) were formulated to ensure that BMP tests produce results exhibiting high intra- and inter-laboratory reproducibility (Holliger *et al.,*2016). While the standardisation of BMP test protocols is useful for eliminating bias amongst experimental results, there is still speculation on whether BMP tests and if they could be used as sufficient predictors of full-scale AD performance. Typically, BMP tests performed lead to an overestimation of full-scale AD performance due to the inoculum source differing between various scales (Bishop *et al.,* 2009), differences in operating conditions, seasonal variations and mixing inefficiencies (Holliger *et al.,* 2017; Lüdtke *et al*., 2017).

## 2.3. Collection of methods for estimating full-scale AD behaviour

### *2.3.1. Overview*

In addition to experimental methods used to estimate the methane potentials (BMP tests), several theoretical methods have been proposed in literature aimed at predicting full-scale performance parameters. Theoretical specific methane yields (SMY) have been approximated on a nutrient compositional basis (Weinrich *et al.,* 2018). For example, the Buswell formula estimates methane potential based on a feedstock's elemental analyses such as carbon, hydrogen, oxygen, nitrogen and sulphur (Buswell & Muller, 1933; Jingura & Kamusoko, 2017; Filer *et al*., 2019). Other methods include kinetic models used to estimate the degradation/reaction kinetics during the AD of a particular feedstock, which are governed by temperature and pH influences (Gamble *et al*., 2017; Filer *et al*., 2019).

However, the determination of substrates' methane potentials based on chemical and stoichiometric proportions is limited because these methods consider neither the different process conditions nor the interactions amongst microbial communities prevalent during AD (Koch *et al.,* 2020). As such, compositional-based methods are not employed for estimating the behaviour of full-scale AD processes. Experimental methods (bench- and pilot-scale AD tests) provide more depth on the dynamics of actual AD processes than theoretical methods, and it is thus important to consider methods that use experimental data to infer on performance parameters of actual AD processes.

### *2.3.2. Methods for predicting full-scale AD performance*

Several methods investigated by researchers will be addressed in the following section, specifically those that refer to BMP assay tests.

#### *2.3.2.1. Biomethane potential degradation rate*

Conventionally, the reduction in organic content (VS or COD basis) provides an indication of how much material is converted to biogas and thus AD performance (Mei *et al*., 2016; Meegoda *et al*., 2018). Considering a VS organic basis, the Van Kleeck equation is used to compute the VS percentage reduction (VSR), which assumes that the mass of fixed solids in the digester remains constant (Switzenbaum at al., 2003). The Van Kleeck expression is given as Equation (5):

$$\mathrm{VSR}(\%) = \frac{\left(\mathrm{VS_{feed}} - \mathrm{VS_{dig}}\right)}{\left(\mathrm{VS_{feed}} - \left(\mathrm{VS_{feed}} \times \mathrm{VS_{dig}}\right)\right)} \times 100 \quad (5)$$

For liquid feedstocks, Equation (5) can be rewritten on a COD basis, denoted as the COD reduction (CODR). The CODR is expressed as a mass balance from material fed and exiting the digester, as given below:

$$\mathrm{CODR}(\%) = \frac{\left(\mathrm{COD_{feed}} - \mathrm{COD_{dig}}\right)}{\left(\mathrm{COD_{feed}}\right)} \times 100 \quad (6)$$

Volatile solids and COD reductions vary for different feedstocks degraded during AD. Table 2 shows reported values of organic content reductions for different feedstocks.

Table 2: Comparison of volatile solids and COD reduction ranges for anaerobically digested feedstocks.

| **Solid feedstocks** | | | |
|---|---|---|---|
| **Feedstocks** | **AD scale** | **VS reduction (%)** | **Reference** |
| OFMSW [a], pig manure, energy crops, agricultural residues | Three full-scale systems (1600 to 6000 $m^3$) | 70 to 79% | Schievano *et al.,* 2011 |
| Poultry manure, kitchen wastes, OFMSW | Four full-scale (6000 to 39 600 $m^3$) | 50 to 80% | Li *et al.,*2017 |
| Pig manure, food waste, seed sludge | Bench-scale (2.0 L) | 71 to 79% | Wang *et al.,* 2020 |
| Tomato plant wastes | Bench-scale (80 mL) | 8 to 22% | Camara-Martinez *et al.,* 2020 |
| **Liquid feedstocks** | | | |
| **Feedstocks** | **AD scale** [b] | **COD reduction (%)** | **Reference** |
| Pot distillery & beverage effluent | Full-scale UASB [c] (unspecified) | +95% | Melamane *et al.,* 2007 |
| Distillery wastewater (stillage) | Full-scale UASB (420 $m^3$) | +90% | Wolmarans & De Villiers, 2004 |
| Slaughterhouse effluent | Pilot-scale UASB (500 L) | 85 to 90% | Torkian *et al.,* 2002 |

[a] : organic fraction of municipal solid waste; [b] : digester volume given in parentheses; [c] : up-flow anaerobic sludge blanket

VSR ranges are lower than CODR ranges due to the physical nature of feedstocks (Table 2). Solid-based feedstocks may contain non-digestible materials recalcitrant to organic degradation (Schievano *et al.,* 2011; Tambone *et al*., 2010). As such, not all volatile solids are degraded nor converted to biogas. In

contrast to VS reductions, CODRs span much higher ranges (85 to 95%, Table 2) due to the presence of fewer solids in the feedstocks. Liquids are better homogenized than solid feedstocks, and thus more nutrients are accessible to anaerobic populations during anaerobic degradation (Aldin *et al.,* 2011).

The reductions in VS or COD content can be applied to full-scale AD processes to measure performance, however both VS and COD determinations only provide quantitative measurements and say nothing about the nature of organic molecules (Li *et al*., 2017). Schievano *et al*. (2011) proposed an alternative way to measure the efficiency of full-scale AD processes. Instead of measuring the VS or COD reduction percentage, they used the BMP value as the basis for determining AD efficiency. Equation (7) below defines the BMP degradation rate (BDR), also defined as $BMY_1$, which gives an indication of how much the full-scale bio-methane productions approach those obtained in bench-scale BMP tests:

$$\mathrm{BMY}_1(\%) = \frac{(BMP_{in} \times TS_{in} - BMP_{out} \times TS_{out})}{(BMP_{in} \times TS_{in})} \times 100 \tag{7}$$

Where $BMP_{in}$ represents the BMP value of the feedstock in the system, $TS_{in}$ being the TS content of the fed material, $BMP_{out}$ being the BMP value of the output digestate (residual BMP) and $TS_{out}$ being the TS content of digestate. Schievano *et al*. (2011) defined an additional performance parameter quantifying the efficiency of full-scale AD processes. This deviation is termed as a scale factor, and is calculated using Equation (8) below:

$$\text{Scale factor } (\%) = \frac{SMY_{full}}{BMP} \times 100 \tag{8}$$

Where $SMY_{full}$ is the specific methane yield (SMY) obtained from full-scale operational data and $BMP$ is the specific methane yield (methane potential) measured from BMP tests. Schievano *et al*. (2011) used Equation (7) to evaluate the effectiveness of three conventional-wet full-scale AD plants; Plant A treated the OFMSW via four 1000 $m^3$ digesters, Plant B treated liquid swine manure via two 1500 $m^3$ digesters and one 3000$m^3$ post-digester connected in series and Plant C treated swine and cow manure and plant residues in a single 1600 $m^3$ AD reactor. For all three plants, the $BMY_1$ ranged 87% to 93% while the VS removal percentage ranged 70% to 79%, the latter indicating that roughly 21% to 30% of VS were not degraded nor converted to biogas, even under ideal conditions in BMP tests. Schievano *et al*. (2011) also compared the bench- and full-scale methane yields using Equation (8); it was found that the performance (yields) of both AD plants under full-scale conditions were 84 to 93% of the yields obtained from bench-scale tests performed under controlled conditions.

Li *et al*. (2017) performed a study on evaluating full-scale AD performance using a similar equation for determining BMP degradation rate (BDR), as given below:

$$\text{BDR}\ (\%) = \frac{(BMP_{in} - BMP_{out})}{(BMP_{in})} \times 100 \quad (9)$$

The degradation efficiencies were evaluated for four full-scale AD plants by performing BMP tests. Following BMP tests on substrates sourced from all plants, the BDR gave a range of 72 to 90%, while VS degradation gave a range of 50 to 80%. The BDR range essentially indicated that a large portion of organic material remains in digestate discharged from digester vessels. Although a useful indication of digester efficiency, the study did not correspond other performance aspects (biogas production) to BDR.

Considering both studies above, the determined BDRs provided a better indication of AD efficiency than that of VS/COD removal because the parameter compensates for both qualitative and quantitative aspects of the degraded substrate (Schievano *et al*., 2011; Li *et al*., 2017). Although the BDR indicates how much full-scale yields deviate from those obtained under BMP test conditions, the studies did not attempt to correlate BDR to performance parameters such as daily biogas production or yields.

*2.3.2.2. Full-scale performance estimations using bench-scale experimental data*

Several studies have aimed at predicting full-scale AD performance using experimental data obtained from bench-scale AD experiments, which are discussed below.

(a) BMP extrapolation method

Holliger *et al*. (2017) investigated the use of BMP values to calculate the methane production rate for two full-scale AD plants. Equation (10) depicts how full-scale biogas production ($P_{full}$) is calculated from BMP input data:

$$P_{full}\left[\frac{Nm^3_{CH4}}{wk}\right] = \sum\left[Q_i\left[\frac{tonne}{wk}\right] \times TS_i[\%\ w/w] \times VS_i[\%TS]\right] \times \text{BMP}_i\left[\frac{Nm^3}{tonne\ \text{VS}}\right] \quad (10)$$

Where $Q_i$, $TS_i$, $VS_i$ and $\text{BMP}_i$ represent the full-scale mass feed rate, the feedstock's total and volatile solids contents and the experimental BMP value, respectively. The additive property of Equation (10) accounts for blended feedstock streams, i.e. the sum of individual feedstocks' methane productions using individual BMP values amounts to the total methane production from the digester (Holliger *et al*., 2017). For individual feedstocks fed to an AD plant, the additive property of Equation (10) falls away to yield Equation (11):

$$P_{full}\left[\frac{Nm^3\text{CH}_4}{wk}\right] = Q_i\left[\frac{tonne}{wk}\right] \times \text{TS}\%_i \times \text{VS}\%_i \times \text{BMP}_i\left[\frac{Nm^3\text{CH}_4}{tonne\ \text{VS}}\right] \quad (11)$$

A summary of the findings reported by Holliger *et al.* (2017) are given in Table 3 below, where the weekly methane production rates were estimated using Equation (10).

Table 3: Calculation of weekly methane production as performed by Holliger *et al.* (2017).

| Mass feed rate (tonnes/week) | VS[a] feed rate (tonnes/week) | BMP [b] (NL $CH_4$/kgVS) | Calculated MP [c] ($m^3$/week) | Actual MP ($m^3$/week) | Scale factor [d] |
|---|---|---|---|---|---|
| $Q_i \times VS_{fed} \times BMP_i = P_{full}$ | | | | | |
| **Wet-full-scale AD plant** *(feedstocks: waste sludge, food waste, slaughterhouse waste fat, waste alcohol, oil-fat remover sludge and coffee wastewater)* | | | | | |
| 5253 ± 279 | 200.3 ± 10.8 | 463.5 ± 5.3 | 92 860 | 87 247 | 0.94 |
| **Dry-full-scale AD plant** *(feedstocks: household green wastes and food waste from supermarkets)* | | | | | |
| n.r. [e] | ± 123.3 | 259.7 ± 22.3 | 31 645 | 27 450 | 0.87 |

[a] : volatile solids; [b] : biomethane potential determined from bench-scale tests; [c] : methane production; [d] : ratio of real-time data to calculated data; [e] : not reported.

Holliger *et al*. (2017) determined that the full-scale methane production rates were roughly 0.87 to 0.94 times that of the calculated methane productions using Equation (10). These values indicate a marginal overestimation of full-scale performance, which closely resembled the yields measured from BMP tests. Although the aforementioned method was successful in estimating full-scale methane production, it was not used to estimate full-scale degradation rates.

(b) CSTR/Dynamic model

Fiore *et al*. (2016) aimed to model the performance of a 300 L pilot-scale AD reactor using results obtained from batch tests (semi-pilot-scale, 3.0 L working volume). A first-order model was initially proposed for estimating pilot-scale methane productivity, however the disintegration constant $(k_{dis})$ depends upon the digestion period which is subject to change as AD proceeds (Astals *et al*., 2013). Therefore, an alternative model was proposed to estimate daily biogas production based on the robustness of experimental parameters (disintegration constants and feedstock BMPs), based on a continuous-stirred tank reactor (CSTR) design. Daily biogas production is estimated using Equation (12) below:

$$B(t)\left[\frac{Nm^3}{d}\right] = k_{dis}\left[\frac{1}{day}\right] \times Se(t)\left[\frac{kgVS}{m^3}\right] \times \mathrm{BMP}_o\left[\frac{Nm^3}{kgVS}\right] \times V_w[m^3] \quad (12)$$

Equation (12) assumes that solubilisation is the rate-limiting step for complex substrates of a highly particulate nature (Tomei *et al*., 2009; Fiore *et al*., 2016). The daily biogas production on day *t* is given as $B(t)$, which is the product of the degradation constant, the substrate's BMP value ($\mathrm{BMP_o}$), reactor working volume ($\mathrm{V}_w$) and the apparent volatile solids (VS) concentration in the digester, denoted as $\mathrm{Se}(t)$. Both $k_{dis}$ and $\mathrm{BMP_o}$ are determined from bench-scale tests for a particular feedstock.

Because the VS concentration is a time-dependent parameter, it can be solved numerically to approximate daily biogas production. The apparent VS concentration dynamic model is based off a mass balanced around a CSTR, the summarised derivation given below (Felder & Rosseau, 2005):

$$[accumulation] = [input] - [output] + [generation] - [consumption]$$

(13)

Moreover, assuming negligible generation of biomass inside the digester (Fiore *et al*., 2016), the constituent mass balance is based on organic content (apparent VS content) inside the digester, which is given as Equation (14):

$$V_u\left[\frac{dSe(t)}{dt}\right] = q(t)S_o(t) - q(t)S_e(t) + 0 - k_{dis} \times Se(t) \times V_u$$

(14)

Where $q(t)$ represents the input/output flowrate of the anaerobic digester ($m^3$/d) of working volume $V_u$ and $S_o(t)$ being the feed VS concentration of the feedstock. The null value given in Equation (14) indicates that biomass accumulation in the system does not change with time, as per one of the model's assumptions referenced from Fiore *et al.* (2016). Rearranging Equation (14) gives the dynamic model below, which can be solved numerically via MATLAB® software:

$$\frac{dSe(t)}{dt} = \left(\frac{q(t)}{V_u}\right)\left(\mathrm{S_o}(t) - \mathrm{S_e(t)}\right) - k_{dis} \times Se(t)$$

(15)

Fiore *et al*. (2016) applied the CSTR-based model to a pilot-scale AD system of 300L working volume. The dynamically-modelled biogas productions compared well with the pilot-scale biogas productions. Regarding methane yields, for one such feedstock (rice mixture), the 300L system obtained 0.312 $Nm^3$ $CH_4$/kgVS, while the 3.0L batch tests produced 0.386 $Nm^3$ $CH_4$/kgVS. The pilot-scale's methane yield was thus 81% of the methane yield obtained under ideal bench-scale conditions. Both test scales were operated under the same process temperature and utilised the same inoculum. Therefore, deviations in performance were attributed to differences in process volumes, feeding modes and mixing modes.

Although Fiore *et al*. (2016) performed accurate estimations of a pilot-scale system using bench-scale-derived results, the dynamic model was not assessed for full-scale applications. Given that the dynamic model is based off a CSTR design, there is, however, opportunity for applying the model for full-scale performance estimations.

(c) AD Model No. 1 (ADM1)

The ADM1 serves as an extensive model accounting for the complexity of reactions taking place during AD (Daly, 2020). For example, microbial interactions and sulphate reduction processes (Fedorovich *et al*., 2003). The model can be formulated from BMP tests, however, it has rarely been applied to full-scale AD processes due to the large number of input variables and differential equations associated with different

degradation rates for different feedstock composition components (Poggio *et al*., 2016; Nordlander *et al*., 2017).

Otuzalti & Perendeci (2018) used ADM1 to model the AD of a full-scale plant treating waste activated sludge (WAS). The digester system operates under continuous feeding and mesophilic conditions and consists of four 9000m$^3$ digester tanks. Otuzalti & Perendeci (2018) reported that using ADM1 for modelling full-scale performance parameters such as daily biogas and methane productions, VFA, total alkalinity and VS concentrations, digester pH and methane content resulted in a correlation coefficient (R-squared value) range of 0.19 to 0.58. The study indicated that applying ADM1 for full-scale modelling was acceptable. However, most input variables such kinetic constants for different components were derived from literature and there was no evidence of sourcing input data from bench-scale/BMP tests for model development.

## 2.4. Conclusions from literature study

The implementation of AD on industrial-scale is advantageous for the alleviation of organic waste accumulation and for the provision of renewable energy. Estimating process dynamics and efficiency is typically done using BMP tests. These tests are, however, are limited in terms of predicting full-scale performance conditions or accounting for environmental factors like feedstock composition variation. Several methods use BMP tests to estimate full-scale performance, however very few studies have aimed at explaining how and why deviations arise during the scale-up of AD processes. The extrapolation method proposed by Holliger *et al.* (2017) used BMP tests to estimate full-scale performance for solid-based co-digestion plants. Although accurate predictions of full-scale performance were made, the study did not elaborate on what contributed to the scale factors between bench- and full-scale AD systems. The use of the extrapolation method has not been applied to full-scale AD plants processing uniform feedstocks, nor to AD plants processing liquid feedstocks on a COD basis. The dynamic method proposed by Fiore *et al.* (2016) accounts for the BMPs and reaction kinetics measured in bench-scale tests, where accurate approximations of pilot-scale performance were made. Fiore *et al.* (2016) did not apply the model to a full-scale system, nor to AD plants processing uniform and/or liquid-based full-scale processes. Lastly, pilot-scale studies are useful for optimising full-scale behaviour and predicting full-scale process conditions. The use of pilot-scale data has not, however, been used to estimate full-scale performance using the methods proposed by Holliger *et al.* (2017) and Fiore *et al.* (2016). Overall, there is a need to address the common causes of deviations between AD processes of different test volumes.

# CHAPTER 3: PROJECT SCOPE

## 3.1. Aims and objectives

The goal of this research project was utilize BMP test methods to accurately predict the performance of full-scale AD plants. To this end, scale factors were determined by bench- and pilot-scale AD tests to quantify the deviations from full-scale process conditions.

The following objectives were formulated to meet the project's goals:

1. Identify transient effects impacting the performances of full-scale AD plants included in this study.
2. Apply the extrapolation method (Holliger *et al.,* 2017) and CSTR-based dynamic model (Fiore *et al.,* 2016) to estimate performance parameters of three different biogas plants, where estimations are based on bench- and pilot-scale AD tests.
3. Determine the effects of feedstock compositional variation on full-scale methane production potential.
4. Calculate scale factors to quantify the deviations between:
    4.1. Ideal bench-scale/BMP test conditions and full-scale conditions.
    4.2. Pilot-scale test conditions and full-scale conditions.

## 3.2. Research questions

Several key questions were identified for this project:

1. Do the process conditions of full-scale AD systems more representative of a bench- or pilot-scale AD system?
2. How do scale factors determined for solid-based full-scale AD plants compare in magnitude to scale factors determined for a liquid-based AD plant?
3. How does the BMP extrapolation method compare with the dynamic model in terms of accurately predicting full-scale performance for each biogas plant?
4. Do semi-continuously-fed pilot-scale tests approximate full-scale performance more accurately than the use of batch-mode pilot-scale tests?
5. How would the determination of scale factors from bench- and pilot-scale AD tests be beneficial for industrial application?

# CHAPTER 4: MATERIALS AND METHODOLOGICAL APPROACHES

Chapter 4 outlines the materials and equipment used for experimental work, as well as the data acquisition and feedstock and inoculum sampling plans for each full-scale AD plant. Error and statistical analytical methods are also discussed to provide insight on the verification of experimental data.

## 4.1. Experimental methodology & design

### *4.1.1. Overall experimental strategy*

Essentially, three local biogas plants were identified and included in this project, which served as the sources for all feedstock materials and inoculum. Operational data was also obtained from each plant to serve as the full-scale datasets. Bench- and pilot-scale AD tests were conducted with the collected feedstock and inoculum samples. A flow diagram depicting the experimental study is presented in Figure 7.

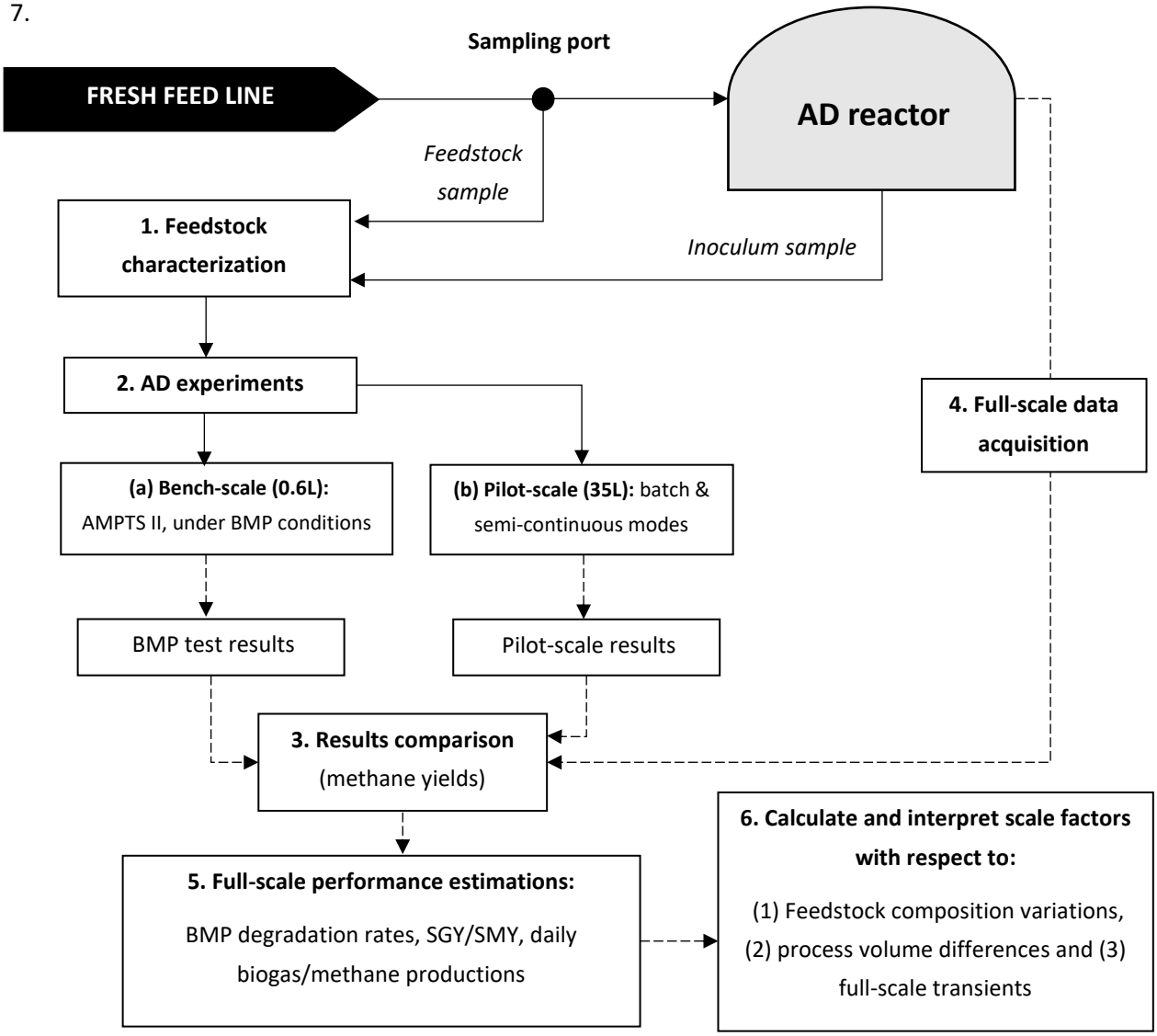


Figure 7: Flow diagram depicting the project's experimental plan, which describes: how feedstocks and inoculum were sampled and analyzed, what AD experiments were conducted and how experimental data were used to predict full-scale AD performance.

Referring to Figure 7, all feedstock and inoculum samples were collected from their respective biogas plants over 6 to 8 months to account for variations in feedstock composition, specifically: Jan-2021 and Feb-2021 for Plant 1, April-2021, May-2021 and June-2021 for Plant 2 and Feb-2020, Oct-2020, Feb-2021, March-2021, May-2021 and June-2021 for Plant 3. Fresh feed was sampled from the relevant line or holding tank located just before the anaerobic digester to best represent the fed material at that point in time. Feedstocks/Inoculum were characterized by their compulsory compositional analyses (total solids, volatile solids, COD and pH level), as specified by the BMP test standardized protocol (Holliger *et al.,* 2016).

All experimental data generated from BMP assay tests and from pilot-scale (semi-continuous & batch modes) were utilized by literature-derived methods to estimate full-scale performance parameters. Estimated parameters for full-scale performance included BMP degradation rate (BDR), daily biogas/methane productions and specific gas and methane yields (Schievano *et al*., 2011; Fiore *et al*., 2016; Holliger *et al*., 2017; Li *et al*., 2017). Scale factors will be subsequently calculated, defined as the ratio of actual performance data to calculated/theoretical performance data. These factors will be statistically compared (95% confidence interval) in terms of the most dominant scale-up effects, i.e. (1) feedstock compositional variations, (2) differences in process volumes and (3) full-scale transients. ANOVA statistical methods will be used to compare predicted performance parameters will actual/full-scale performance parameters.

### *4.1.2. Full-scale data acquisition and feedstock sampling*

#### *4.1.2.1. Description of full-scale biogas systems*

(a) Plant 1: Co-digestion of mixed organic wastes

The first biogas plant (hereon referred to as Plant 1) processes food & beverage and agricultural wastes to produce biogas, specifically rotten fruit and vegetable (apples, watermelon peels, pineapple heads), discarded kitchen wastes (grains, e.g. rice and couscous), beer, expired fruit juice, cattle manure and blood, expired spices and chocolate waste. The system was established on the site of a major fruit juice manufacturing plant, where the biogas is harnessed for the production of electricity and heat via combined heat and power (CHP) technology. A portion of this energy is utilized by facilities in the juice factory, as well as for providing heat to the anaerobic digester.

The biogas installation itself consists of a 3200 $m^3$ concrete vessel, to which the food and beverage wastes are fed. A schematic of the biogas plant is given below as Figure 8. Feedstocks are delivered to a holding area (Stream 1), where they await transport to the primary grinding unit (to reduce particle size). Most feedstocks are stored on site in bins or pallets, with 500 to 1000 kg capacities, respectively, prior to feeding the digester. Process water (Stream 2) and recycled AD sludge (Stream 7) are blended in with the feedstocks, where a total solids loading range of 3.0 to 5.0% is maintained. Following grinding, feedstocks were pre-heated to 37 $^oC$ via a heat exchanger system (steam & water) and subsequently fed to the 3200$m^3$ vessel.

AD is facilitated in the vessel at mesophilic conditions (±37 $^oC$) for a retention time of 40 days; the harnessed biogas (Stream 3) is upgraded via a de-sulphurisation unit and condensate trap processing

between 12 to 28 $m^3$ of biogas per hour. A portion of the upgraded biogas (Stream 4: >95% methane) is then used by the factory's CHP unit to generate electricity and heat, while the other portion is combusted in a boiler system to produce steam.

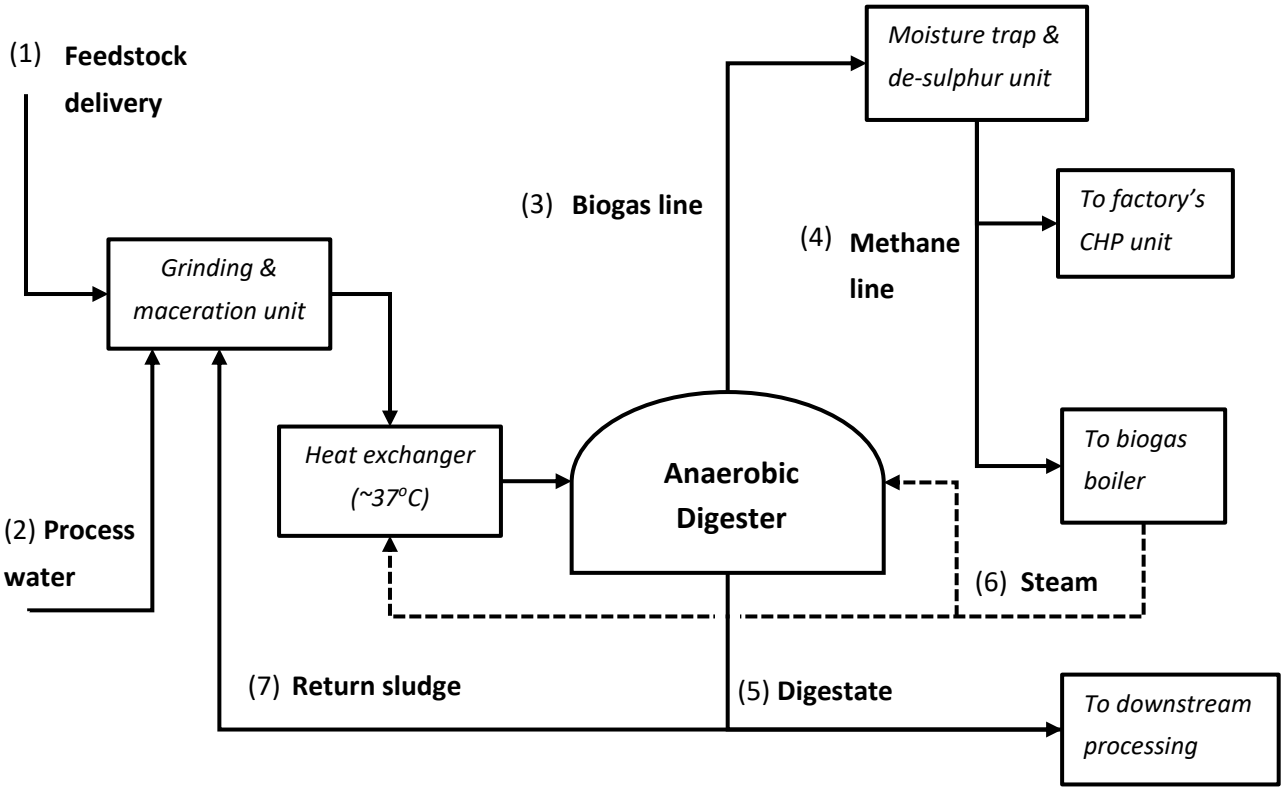


Figure 8: Process overview of biogas Plant 1 (mixed organic wastes).

The steam (Stream 6) is recycled to the biogas plant to maintain digester heating at 37 °C, as well as for feedstock pre-heating purposes. The remaining/digested material (Stream 5) is processed downstream for solids recovery.

The feeding frequency of the digester is dependent on the availability of organic wastes provided by different production processes. The daily OLR thus fluctuates, which, in turn, would induce fluctuations in biogas productivity and yields. The variation in feedstock types would also alter the methane concentration in produced biogas, which can induce transients in energy production for the heating of the digester and for the downstream CHP unit. Moreover, the CBP and flow rate is logged on the condensate product line via an ultrasonic gas flow device.

(b) Plant 2: Tomato waste (TW)

The second biogas installation (hereon referred to as Plant 2) is a pilot-scale AD plant, consisting of a 60$m^3$ primary digester and downstream 120 $m^3$ degasser vessel. The pilot-plant was established by a private company for the AD of tomato waste (TW). The plant is located on site of a tomato farm, where rotten tomatoes are delivered to the biogas plant on a daily basis. Figure 9 represents a block-flow schematic of Plant 2.

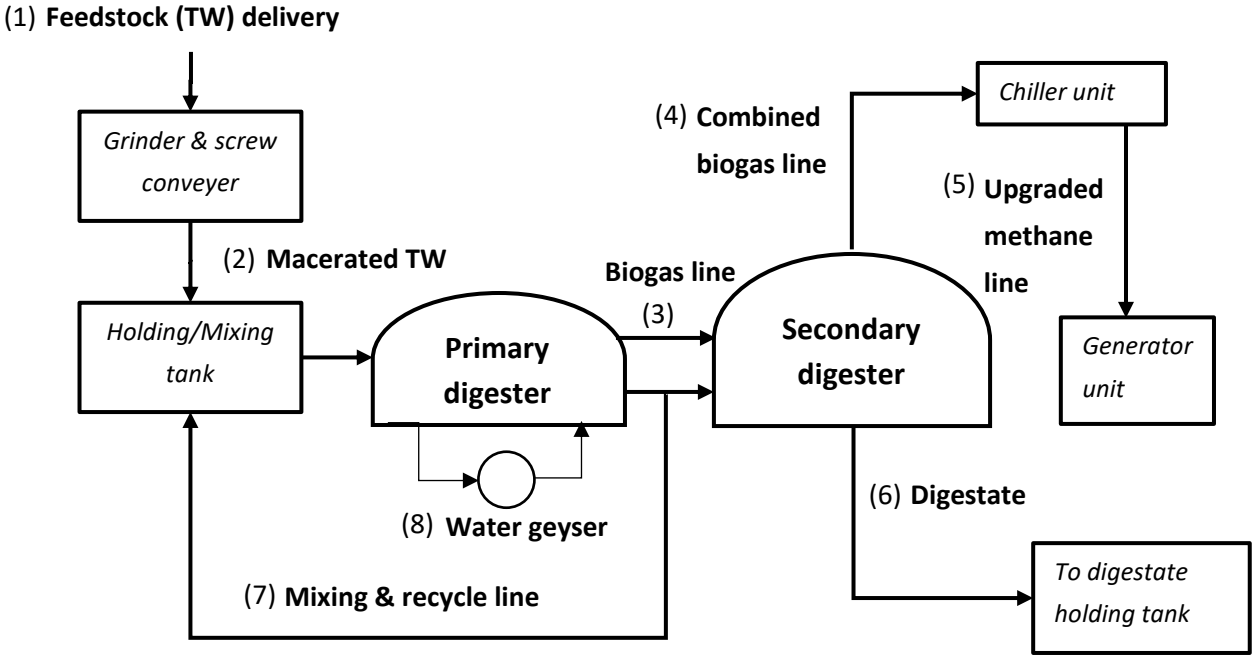


Figure 9: Process overview of biogas Plant 2 (tomato waste).

Tomato waste (Stream 1) is delivered to the pilot-plant in 100 kg crates by farm workers, before being loaded into a grinding machine to reduce particle size. The macerated tomatoes (Stream 2) are subsequently deposited into the holding tank, with a capacity of roughly 15 $m^3$. A sludge recycle line connected to both digesters' sludge lines is also directed to the holding to promote the mixing of anaerobic sludge with the tomato waste. TW is then fed to the primary anaerobic digester (60 $m^3$) via a positive-displacement pump. Moreover, on an irregular basis, roughly 100 L of alcohol/beer effluent was fed to the holding tank per day. This addition of the alcohol waste dosed more nutrients into the holding tank's contents with the goal of boosting biogas production and yield.

The pump has a flow rating of 1500 litres per hour, which automatically feeds the primary digester for 30 to 35 minutes each day (roughly 750 to 875 L of TW loaded). The primary digester's operating temperature is regulated to mesophilic conditions (±37 $^oC$) via a small water geyser (Stream 8). The onset of gas production is often achieved at 24 hours, accompanied with the inflation of the primary digester's balloon/bladder (23 $m^3$ gas storage capacity). Both the primary and secondary digester gas balloons are connected via the same biogas outlet line (Stream 3), and the flow of gas is assisted by an air blower that pressurizes both digesters' bladders.

The final biogas production line (Stream 4) exits the secondary digester (120 $m^3$ liquid volume, 41.2 $m^3$ gas balloon), while the harnessed biogas moves through a chilling unit to condense water, hydrogen sulphide and carbon dioxide from the gas. While the condensate is collected in a water trap, the upgraded biogas (Stream 5) is directed to an 18 kW-rated generator unit. The generator converts produced biogas into useful mechanical power, directed to the farm's borehole pump station. Because the operation of the pump station is seasonal (e.g. dependent on rainfall), the generator does not provide electricity at a constant rate. Therefore, the generator acts as a flare unit for the produced gas.

Similar to the biogas lines, both digesters' digestate pipe lines are connected (Stream 7). All digested material eventually accumulates in the secondary digester, which is not temperature controlled and functions as a degasser unit. The overflow from the secondary digester (Stream 6) is collected in another holding tank, where the liquid is used for irrigation purposes on an irregular basis.

(c) Plant 3: Distillery waste (DW)

The third full-scale AD plant (Plant 3) is a liquid AD plant that utilizes distillery waste (DW) as feedstock, schematically shown as Figure 10. DW is produced as a by-product of distillation and alcohol manufacturing processes, predominantly consisting of winery, beer effluent, spirits effluent and spent process water from on-site utilities. The goal of the plant is to biologically treat the effluent water via AD and recycle treated water to the beverage manufacturing facilities, while the produced biogas is utilized for on-site steam production and process temperature control.

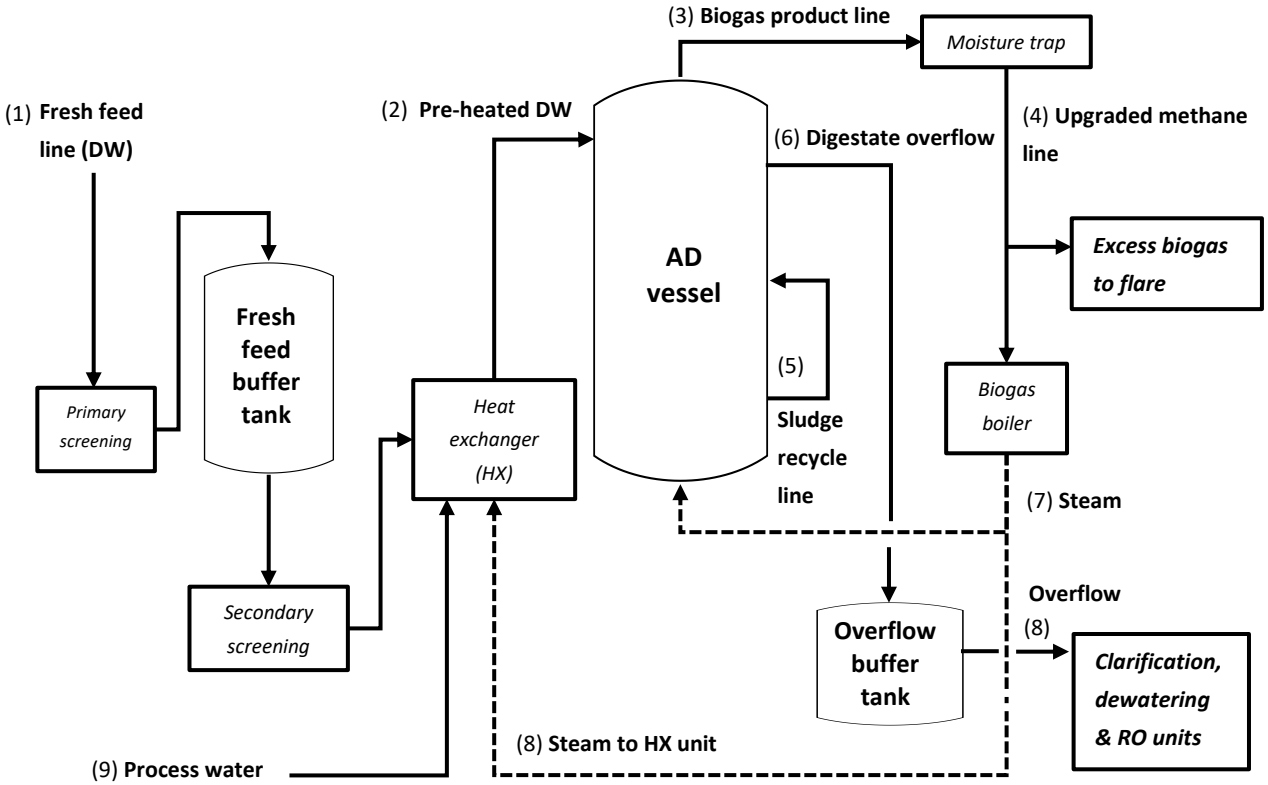


Figure 10: Process overview of biogas Plant 3 (distillery waste).

As shown in Figure 10, raw DW (Stream 1) is primarily screened to remove any entrained solids and is subsequently pumped into a buffer tank (250 $m^3$ capacity). Being comprised of many beverage by-products, the chemical oxygen demand (COD) content varies considerably and ranges around 9319 ± 1346 mg/L. The buffer tank effluent is pumped through a secondary screening unit and is subsequently pre-heated to ±37°C via a plate-and-frame heat exchanger (HX). The pre-heated buffer tank effluent is then pumped to the digester tank (Stream 2), having a diameter of 15.4 m and height of 12.6 m (2200 $m^3$ working volume).

The 2200 $m^3$ reactor facilitates AD, which is controlled at an operating temperature of ± 37 °C. The digester resembles that of a continuously-stirred tank reactor (CSTR), whose contents are mixed via an agitator unit embedded in the side of the vessel. Mixing is also promoted by a recycle line (Stream 5) that continuously recirculates digestate through the tank, typically at a rate of ± 1250 $m^3$/d. The digester operates at a feed rate of approximately ± 550 $m^3$ per day and a HRT of 4 days. Moreover, a sodium hydroxide (NaOH) dosing system is implemented on the heat exchanger's product line to regulate the pH of the fed DW at ± 7.0. The pH of the buffer tank DW has been historically analyzed as 6.50 ± 0.98.

Produced biogas (Stream 3) is directed through a water trap to remove excess moisture. The CBP is measured via an ultrasonic gas flow device in units of normalised cubic-metres ($Nm^3$), where the methane content ranges 65% to 68% vol. The upgraded biogas (Stream 4) is subsequently directed to a biogas boiler, where generated steam is recycled to the plant's heat exchanger unit and digester vessel to regulate process temperature. Excess biogas produced is sent to flare.

All digested material exits the 2200 $m^3$ via an overflow line (Stream 6) and enters another buffer tank vessel. Anaerobic sludge is not directly discharged using pumps so that a higher sludge content is retained in the digester. Digested liquid is pumped from the overflow tank to a clarifier unit (Stream 8). Digestate is subject to clarification to separate the sludge and effluent liquid; settled out sludge is further treated via a centrifuge unit to separate all remaining solids from the effluent, which are collected in a solids disposal bin. The centrifuge overflow is sent to a reverse osmosis (RO) station for a final treatment step, after which the treated water is recycled back to the factory's utilities.

#### *4.1.2.2. Data acquisition plan*

Operational datasets were acquired from each biogas plant to characterize their performances and evaluate their AD efficiencies. This would also assist with identifying the major transients affecting full-scale performance, i.e. fluctuations in feedstock compositions, digester temperatures or pH level. As per the full-scale performance estimation methods discussed under Section 2.3.2.2, several computations require full-scale data as input variables, specifically for BMP extrapolation calculations (Holliger *et al*., 2017), dynamic modelling (Fiore *et al*., 2016) and CSTR residence time distribution function (Ludtke *et al*., 2017). A list of minimum data requirements for the three full-scale plants is given below in Table 4.

Plant 3's installation was the most specialized and controlled out of the three biogas plants selected for this study. The site's operators performed daily COD analyses and pH checks and online instrumentation was employed to track feed/digestate flow rates (ultrasonic flow meters), feed and digestate pH (pH probes) and CBP (ultrasonic gas flow meter). All online measurements and set points were viewed on the control room's supervisory control and data acquisition (SCADA) system.

Plant 1 (co-digestion) had similar instruments installed to monitor some of the parameters listed for Plant 3. The logged mass feed rates of feedstocks were however not accurate representations of feed rates because of the assumptions made with estimating filled bin (500kg) and pallet (1000kg) masses, and due to irregular logging by the site's operators. Plant 2 was not as closely controlled as the previous two plants; only the digester operating temperature is logged and controlled, and the feed pump is set

to a timer to feed between 750 to 875 L of tomato waste per day. There are no pH probes nor gas/flow meters installed at the plant, and thus most performance parameters were measured manually.

Table 4: Full-scale performance parameters that should be measured to track anaerobic digestion performance.

| Operational/Performance parameter | Unit | Purpose to project |
|---|---|---|
| **Feedstock and inoculum characterization** | | |
| Total solids (% w/w) | - | Obtain moisture content; preliminary requirement for measuring VS content. |
| Volatile solids (% w/w) and/or COD (mg/L) | - | Measurement of organic content; requirement for BMP test setup and for calculating gas yields. |
| Chemical Oxygen Demand (COD) | mg/L | Measurement of liquid organic content; for calculation of SGY and SMY data. |
| pH level | - | Process conditions BMP tests and pilot-scale conditions |
| Process temperature | $^{o}C$ | |
| **Digester performance parameters** | | |
| Volumetric or mass feed rate | ($m^3$ or kg)/d | Determination of hydraulic retention time (HRT) for pilot-scale tests; also used for computation of several performance estimating methods. |
| Cumulative biogas production | $Nm^3$ | Comparisons to biogas production obtained at bench- and pilot-scales; computation of SGY. |
| Biogas production | $Nm^3/d$ | |
| Methane content | %vol | Calculation of methane production rate and SMY |

### *4.1.3. Experimental approach*

#### *4.1.3.1. Materials*

A detailed list of all materials, chemicals and laboratory consumables required for experimental work is given under Appendix C in Table 50. The descriptions and assays of each are also given.

#### *4.1.3.2. Feedstock characterization*

All feedstock and inoculum samples were sampled over a duration of 6 to 8 months, or as often as they were available. This was done to make reasonable comparisons between experimental data and full-scale data. Feedstock samples are shown in Figure 11, Figure 12 and Figure 13.


Figure 11: Photographs of feedstock mixtures obtained from Plant 1: (a) Mixture 1 (apples, food waste), (b) Mixture 2 (food waste, spices & beer), (c) Mixture 3 (food waste, spices, beer, cattle blood & manure), (d) Mixture 4 (chocolate processing waste, beer, sugar and cattle blood), (e) Mixture 5 (food waste, beer, fruit juice and cattle blood).


Figure 12: Tomato waste (TW) feedstock; (a) Plant 2's holding & mixing tank, (b) TW sample.


Figure 13: Distillery waste (DW) samples collected from Plant 3.

Feedstock samples from Plant 1 were collected individually, after which 5 mixtures (Figure 11) were aliquoted to represent 5 days of full-scale digester feeding. For selected days the masses of feedstock mixtures/materials fed to the digester were estimated on storage container size and downscaled for bench-scale AD tests. Each feedstock was ground in a food processor to reduce their particle sizes (< 2 mm), after which mixtures were made up (1.0 L) according to the proportions they were fed to Plant 1 on certain days. Table 5 shows the masses of feedstock mixtures fed to the full-scale digester and the downscaled masses used for bench-scale tests.

Table 5: Estimated masses for feedstocks fed to Plant 1's anaerobic digester.

| Date & mixture | | Composition | Crate type | Number | Approx. mass (kg) | Downscaled mass (g) |
|---|---|---|---|---|---|---|
| 30-Jan-21 | Mixture 1 | Apples | Bin | 12 | 6000 | 600 |
| | | Food | Bin | 7 | 3500 | 350 |
| 31-Jan-21 | Mixture 2 | Food | Bin | 10 | 5000 | 500 |
| | | Spices | Bin | 12 | 6000 | 600 |
| | | Beer | Pallet | 10 | 10000 | 1000 |
| 01-Feb-21 | Mixture 3 | Food | Bin | 6 | 3000 | 300 |
| | | Spices | Bin | 6 | 3000 | 300 |
| | | Beer | Pallet | 10 | 10000 | 1000 |
| | | Blood | Pallet | 1 | 1000 | 100 |
| | | Manure | Bin | 1 | 500 | 50 |
| 02-Feb-21 | Mixture 4 | Chocolate | Bin | 5 | 2500 | 250 |
| | | Beer | Pallet | 10 | 10000 | 1000 |
| | | Sugar | Bin | 6 | 3000 | 300 |
| | | Blood | Pallet | 1 | 1000 | 100 |
| 25-Jan-21 | Mixture 5 | Food | Bin | 10 | 5000 | 500 |
| | | Beer | Pallet | 10 | 10000 | 1000 |
| | | Fruit juice | Pallet | 10 | 10000 | 1000 |
| | | Blood | Pallet | 2 | 2000 | 200 |

All solid-based feedstocks (Plant 1 and Plant 2) were characterized by their total solids (TS) content, volatile solids (VS) content, pH level and elemental compositions (carbon, hydrogen, nitrogen and sulphur, CHNS). The pH levels of feedstocks sourced from Plant 1 could not be analysed if they existed completely in the solid phase, e.g. for apples and food waste (Mixture 1 in Table 5). Liquid feedstocks (Plant 3) were characterized by only chemical oxygen demand (COD) and pH level, as the feedstocks exhibited no solids nor could not be analysed for CHNS. In addition to the above analyses, non-compulsory analyses can be determined for feedstocks or during the monitoring of AD performance (Holliger *et al*., 2016), which are given in Table 6 below.

Table 6: List of additional parameters analyzed for feedstock characterization.

| Parameter | Purpose(s) for analysis | Reference |
|---|---|---|
| **Trace element concentrations:** salts, trace metals (e.g. iron, nickel, cobalt) | Important for microorganisms facilitating AD reactions and the associated electron transfer. Also indicative of deficiencies in AD processes | FNR, 2012; Al-Saedi *et al*., 2008 |

| | | |
|---|---|---|
| **Particle size distribution** | Classification of substrates' granulometric state, useful for determining initial degradation rates | FNR, 2012; Raposo *et al*., 2012 |
| **Volatile fatty acid (VFA) concentrations** | Refers to the collective concentration of organic forms during the AD process, e.g. acetic, butyric, propionic and valeric acids. VFA determination assists with monitoring AD process performance; at steady state VFA levels should be constant, and large fluctuations due to accumulation cause inhibition of biogas production | FNR, 2012; Buchauer, 1998; |
| **VFA/TAC ratio** | Defined as the proportion of VFA concentration as determined via titrimetric methods TAC refers to "*the 'consumption A' of 0.1 N sulphuric acid during the titration of a sample to pH 5*" (FNR, 2012). | Liebetrau *et al*., 2016; |

*4.1.3.3. Bench-scale: BMP assay test setup*

BMP assay tests were performed on feedstock samples collected from all three full-scale plants, using the Automatic Methane Potential Test System (AMPTS II) (Bioprocess Control, Sweden). The schematic diagram of the bench-scale setup is presented in Figure 14. The system consists of three major units, namely the thermostatic water bath containing 15 reactor vessels (labelled 1 and 2), the Gas Endeavour and the $CO_2$-adsorption unit (labelled 4 and 6) and the AMPTS II methane detection unit (labelled 9). Table 7 provides a summary of all essential components of the AMPTS II.

Table 7: Major components of the AMPTS II unit, used for BMP assay tests.

| System component | | Description | Quantity |
|---|---|---|---|
| 1 | Thermostatic water bath | Incubation chamber for temperature regulation. | X1 |
| 2 | AD reactor (500mL) | 600 mL glass bottle fitted with a plastic screw thread/motor holder (multifunction brushless DC motor), and two-port stopper with a rotating shaft for mixing.<br>Dimensions of each reactor are indicated in Figure 62 (Appendix C) | X15 |
| 3 | Motor controller | Provides power to each DC motor via the motor cables. Interprets speed signal from the GE and AMPTS units & controls motor speed | X1 |
| 4 | Reactor primary outlet | Biogas production line (clear PVC tubing). | X15 |
| 5 | Gas Endeavour (GE) | Biogas volume measurement device (working principle: liquid displacement & buoyancy), with 15 flotation cells. | X1 |
| 6 | GE outlet line | Biogas production line (clear PVC tubing). | X15 |
| 7 | $CO_2$-adsorption units | 100mL glass bottles fitted with two-port stopper, each bottle containing 3.0 M NaOH and 0.4% Thymolphthalein solutions. | X15 |
| 8 | GE signal output | Biogas production is detected via floatation cell, where volumes are translated to a signal, sent to the computer. | - |
| 9 | $CO_2$-adsorption unit outlets | Methane production line (clear PVC tubing), where all $CO_2$ is removed from produced biogas in each 25 0mL bottle (>98% effective). | X15 |
| 10 | AMPTS II unit | Methane volume measurement device (working principle: liquid displacement & buoyancy), with 15 flotation pegs. | X1 |
| 11 | AMPTS signal output | Methane production is detected via floatation pegs, where volumes are translated to a signal, sent to the computer. | - |
| 12 | Computer control system | Computer system with integrated embedded data acquisition. All input data is entered here, while all results are recorded, displayed and analysed. | X1 |

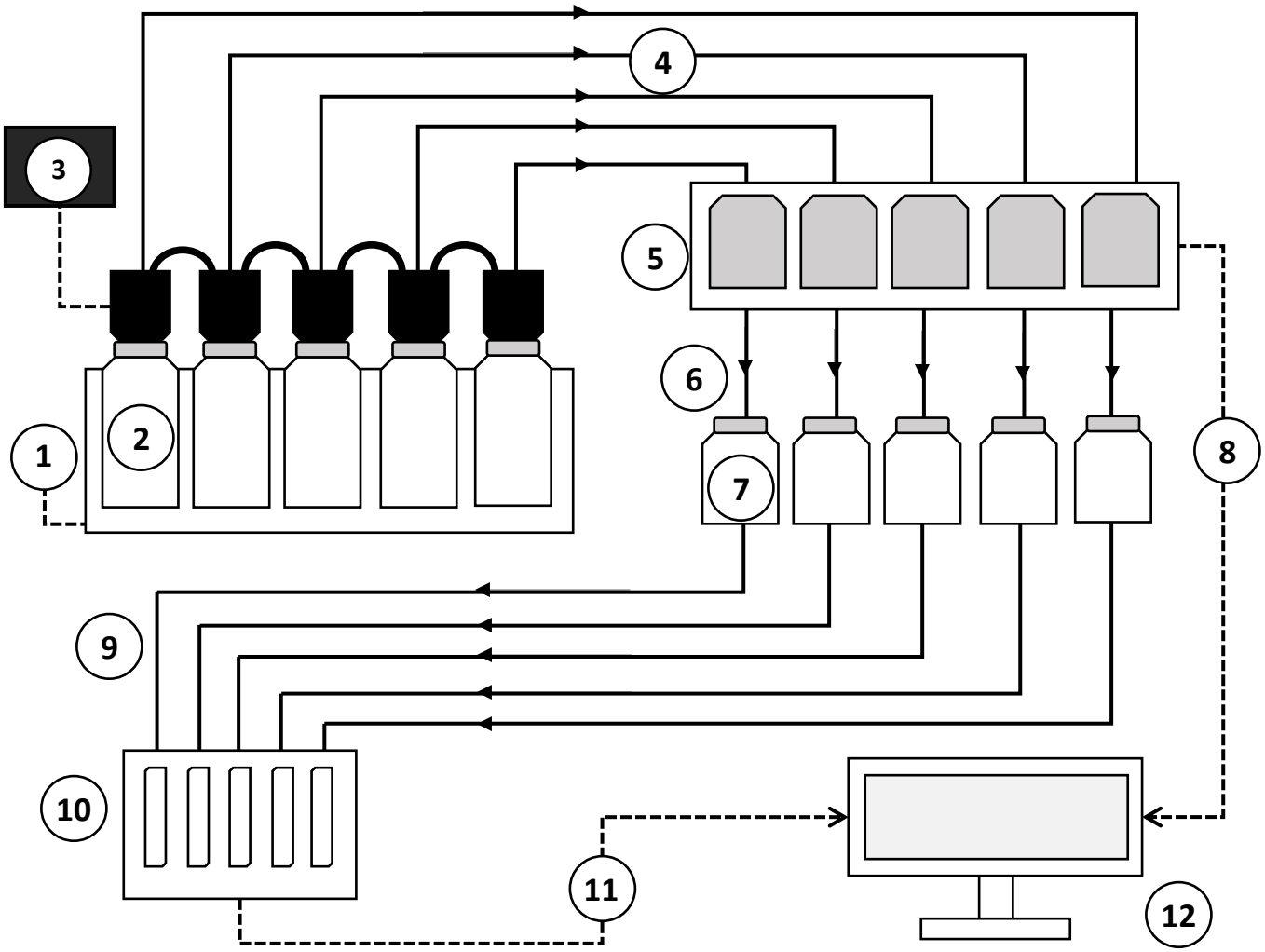


Figure 14: Schematic of the bench-scale biomethane potential (BMP) assay tests, using the Automatic Methane Potential Test System (AMPTS II) (Bioprocess Control, 2020).

Batch-fed AD experiments using the AMPTS II setup have been reported by several authors (Raposo *et al*., 2012; Holliger *et al*., 2016; Holliger *et al*., 2017) based on the standardised BMP protocol (Holliger *et al*., 2016). The automated nature of the system is highly advantageous for reducing test time (i.e. measuring biogas production manually and analysing methane content). The system has also been credited for its generation of reliable data, as many tests can be performed at once (Bioprocess Control, 2020).

Figure 15: Photograph of the bench-scale AMPTS II setup, used for BMP assay tests.

*4.1.3.4. Pilot-scale test setup*

Pilot-scale AD tests were conducted using 50L stainless steel tanks located at the Department of Process Engineering, Stellenbosch University. There are 9 digesters in total, which can be operated in batch, semi-continuous and continuous feeding modes.

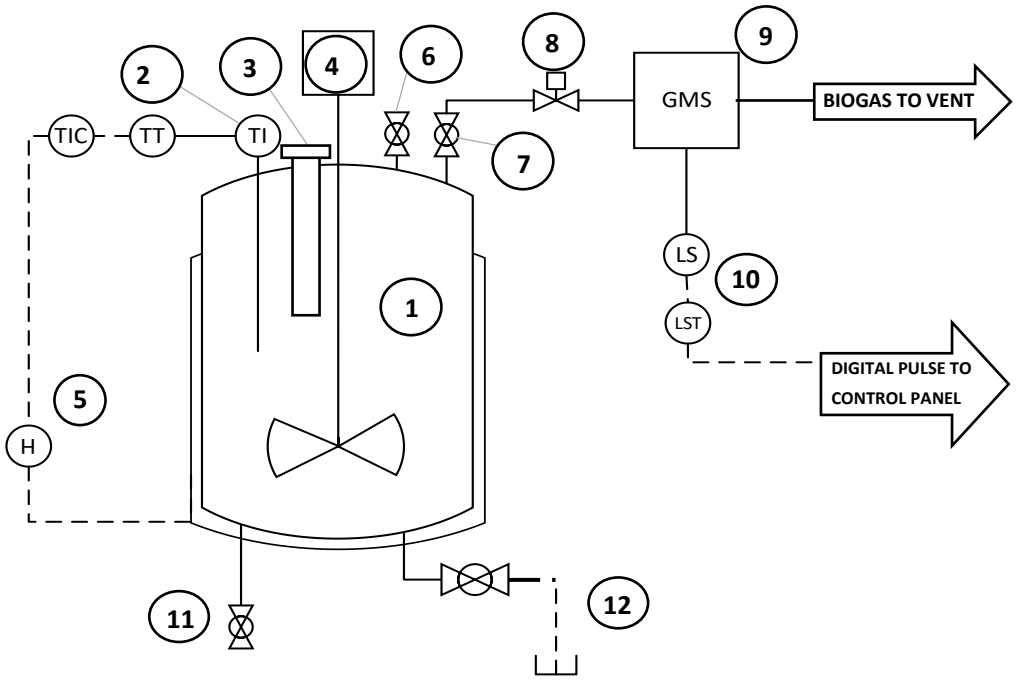


Figure 16: Schematic of 50-litre pilot-scale anaerobic digestion system; (1) continuously-stirred tank reactor (CSTR) digester, (2) temperature regulator, (3) feeding tube, (4) agitator, (5) water-filled heating jacket, (6) gas sampling valve, (7) gas outlet, (8) power/solenoid valve, (9) gas measurement system (GMS), (10) level sensor and transmitter, (11) digestate sample valve, (12) digester drain valve.

Figure 17: Photograph of the pilot-scale (50L) anaerobic digesters.

All pilot-scale systems can be operated individually via the control panel and human machine interface (HMI), where setpoints for the operating temperature (°C) and agitator stirring time (on-off basis) can be established. Each digester is also equipped with a manometric/water displacement gas measurement system (GMS) to automatically measure the daily biogas production. A schematic of the GMS is given below as Figure 18.

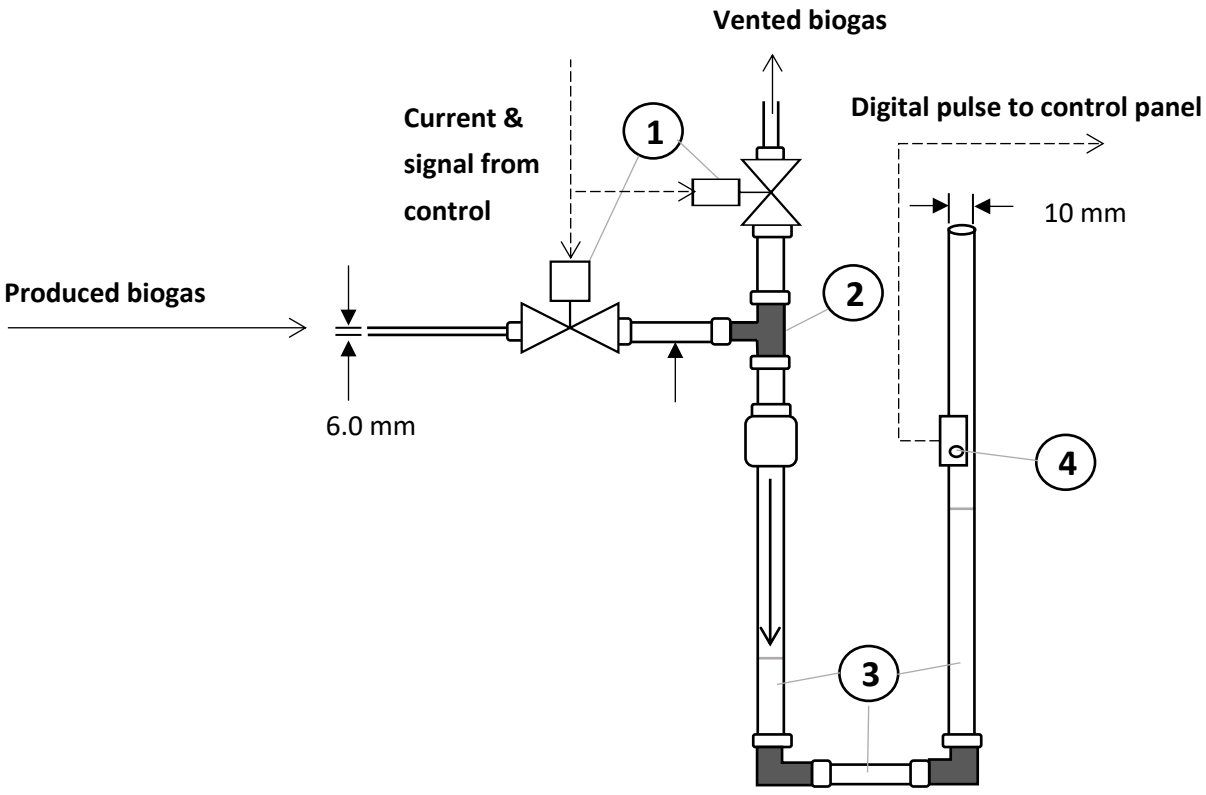


Figure 18: Schematic of micro-digester gas measurement system.

The pilot-scales' gas measurement systems are connected to each biogas outlet line (labelled 7 in Figure 16) to capture daily production. Each GMS consists of two solenoid/power valves, whose functionality is controlled by a level sensor on the outlet line of the manometer (labelled 4 in Figure 18). All piping is made of PVC (6-mm or 10-mm in diameter), which are connected by push-connectors.

The working principle for the GMS is through the water displacement method, in which the produced biogas flows through the first power valve (open position) and subsequently flows into manometer filled with de-ionized water (labelled 3 in Figure 18). As this happens, the second solenoid valve along the venting line is in a closed position. As more gas is produced, the digester headspace pressure increases and pushes the water column down. When the water level in the manometer's outlet tube reaches the level sensor (labelled 4), the sensor transmits a digital pulse to the control panel, which instructs the feedline power valve to close and the venting power valve to open simultaneously. The transmitted digital pulse is registered by the control panel as the volume of biogas produced at that time, which is recorded automatically by the system. After approximately 5 to 10 seconds both valves' positions are reversed and the working principle continues. Biogas production is recorded as liters per day, and the HMI graphically presents this data every hour.

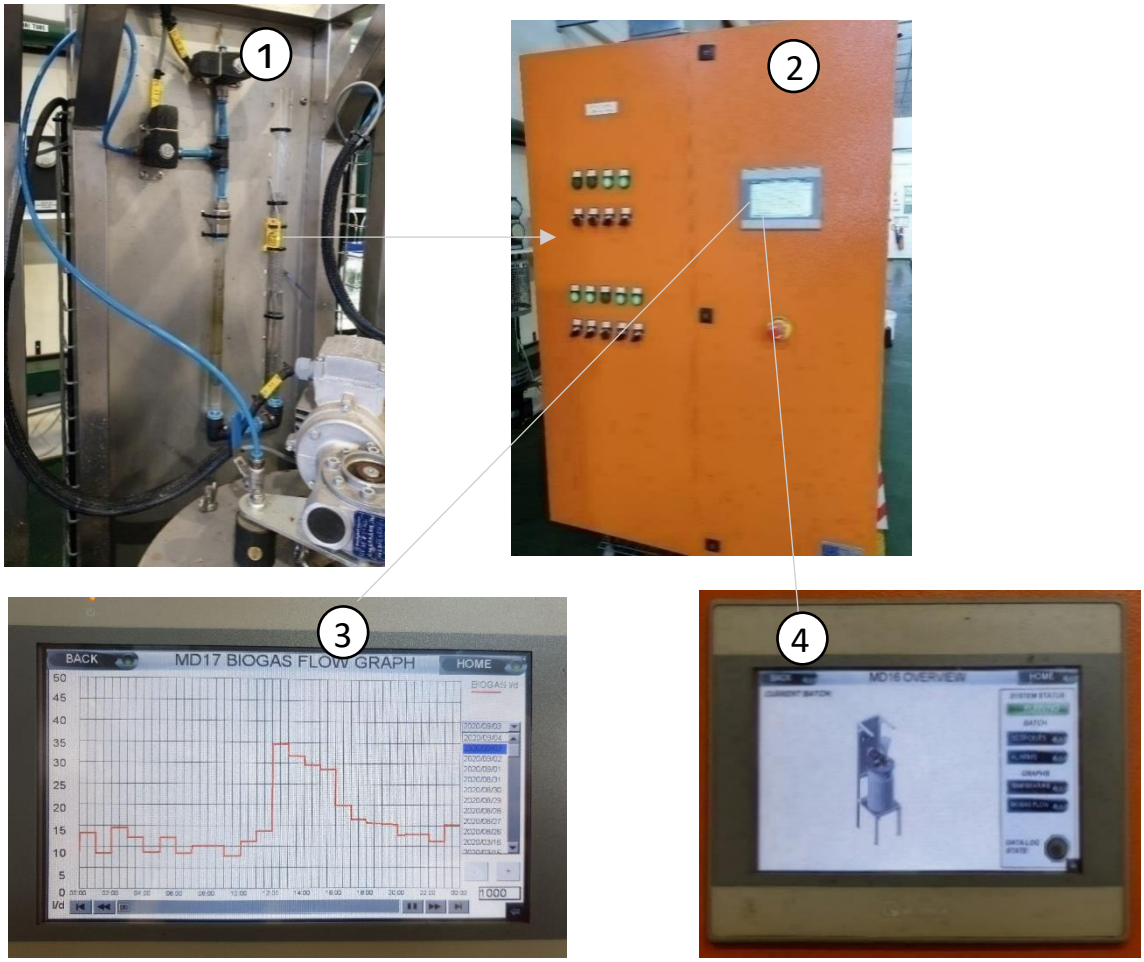


Figure 19: Micro-digester gas monitoring system; (1) GMS transmits level sensor signal to control panel, (2) control panel settings and HMI, (3) biogas production flow graph, (4) digester set point screen.

### *4.1.4. Experimental procedures*

All solutions prepared for bench-scale AD tests were done so in grade-A glassware, which were cleaned thoroughly before and after use with hot water and dishwashing liquid. Because of the large volumes of feedstock and inoculum used for loading pilot-scale AD reactors, plastic containers and buckets (5.0 to 25L) were used for collecting and storing samples.

#### *4.1.4.1. Experimental preparation*

(a) Bench-scale/BMP assay tests

Bench-scale reactors were prepared to a working volume of 400 mL, and tests were performed in triplicate. The proportions of loaded feedstock and inoculum into each vessel were in accordance of an ISR of 2.0, based on both samples' organic contents (VS or COD), and required volumes were measured with glass measuring cylinders and beakers. Furthermore, the initial pH of loaded feedstock was measured and adjusted to the range of 6.8 to 7.2. The pH of feedstock and inoculum mixtures was adjusted with sodium hydroxide (NaOH) and hydrochloric acid (HCl) as required.

The $CO_2$-adsorption units' alkaline solutions consist of alkaline Thymolphthalein solution, which was prepared by dissolving 120 g of NaOH in 250 mL DI water. A magnetic stirrer (Benchmark®) was used to dissolve the added contents, during which 750 mL of DI water was added incrementally to cool the exothermic reaction. Thymolphthalein solution was prepared to 0.4%; 40 mg in 9.0 mL of 99.5%vol ethanol, followed by an addition of 1.0 mL de-ionized (DI) water. The complete alkaline solution was then prepared by adding 5.0 mL of 0.4% Thymolphthalein to 1.0 L of 3.0 M NaOH.

The AMPTS II bench-scale reactors (500 mL) and their rubber stirring caps were thoroughly cleaned with hot water and dishwashing liquid to prevent contamination, after which were left to dry in the water bath. Each reactor bottle was labelled according to the type of test being performed (e.g. blank, positive control tests and the different feedstocks). All PVC tubing/gas lines were also inspected for entrained moisture and fragments of feedstock/inoculum from previous experiments. Entrained moisture was flushed out of the relevant tubing by using an air-filled 50 mL syringe, and fragments of other material were cleaned by soaking tubing in a weak sodium hypochlorite solution.

Because BMP tests were performed automatically, the AMPTS II software was used to input the test conditions for each set of triplicate tests. On the system's *Experiment* web page input data such as ISR and the volatile solids (% w/w) or COD (g/L) content were inputted on the system, which displayed the calculated proportions of substrate and inoculum to add per bottle per test type. These calculations were obtained via a mass balance – details of these calculations are given in Appendix B1 on Page 151. A screen capture of the *Experiment* web page is given below as Figure 20.

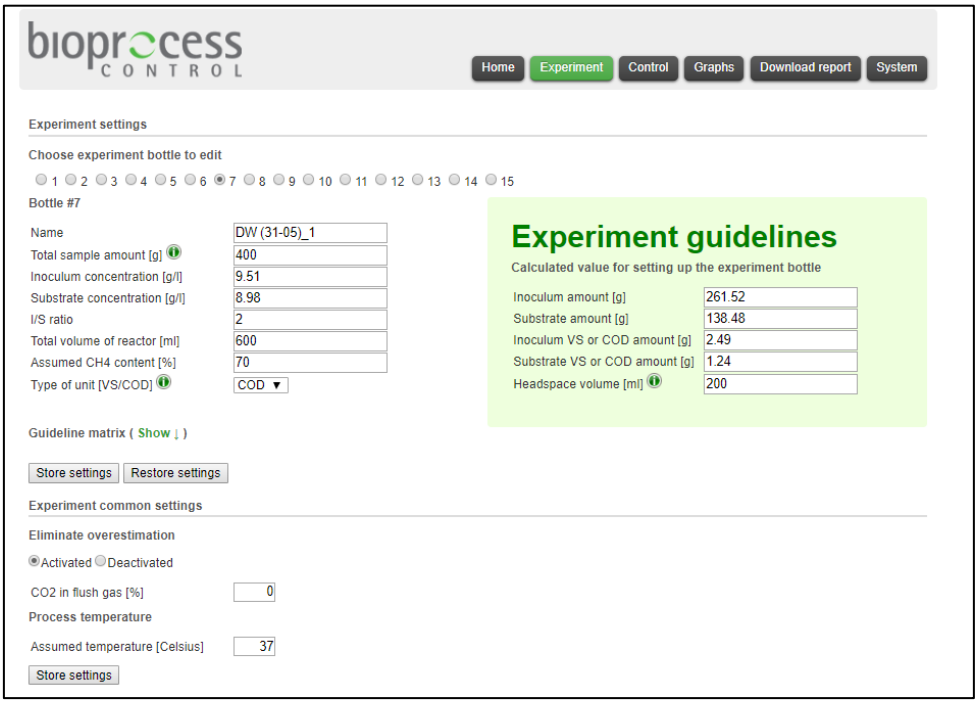


Figure 20: Screenshot of the AMPTS II unit's input variables (*Experiment*) web page.

After the 15 reactors were loaded as required per test type, each bottle was sealed with its screw cap and accompanying DC motor controller. The reactors were purged with 40: 60% nitrogen-$CO_2$ mixture (or pure nitrogen, depending on availability) for at least 60 seconds to ensure anaerobic conditions. The purge ports were fitted with shortened pieces of clear PVC tubing that can be opened and closed during the purging of each bottles' headspace.

The bottles were then placed inside the water bath and each biogas outlet port was connected to the Gas Endeavour (GE) unit via clear PVC tubing. All gas line connections to the GE and AMPTS II units were checked to ensure no gas leaks would occur during experimentation. The water bath and the AMPTS II flotation unit were filled up to the required water level and AD was run at ± 37 °C.

Once all reactors' gas lines were made secure each DC motor head was connected with power cables. The main power cable protruding from the motor controller unit was then connected to one of the reactor's motor heads to interpret speed signals from the GE and AMPTS II, as well as for controlling stirring speed. The stirring motors were also switched on using the same web page and set to 40% of the total rotation speed (80 RPM), for a mixing frequency of 5-minutes-on, 5-minutes-off basis. This mixing frequency was a standardised set point for all BMP tests performed in the bioprocess laboratory (Department of Process Engineering, Stellenbosch University).

The automatic logging of data was initialized on the AMPTS II computer which captures the biogas production (NmL/hour) and CBP (NmL). A screenshot of the *Control* web page is given below as Figure 21. Experiments were terminated when the mean daily biogas production over three consecutive days was less than 1% of the CBP. After shutting down the AMPTS II setup, the reactor bottles' contents were analysed for final pH, total solids and volatile solids or COD content.

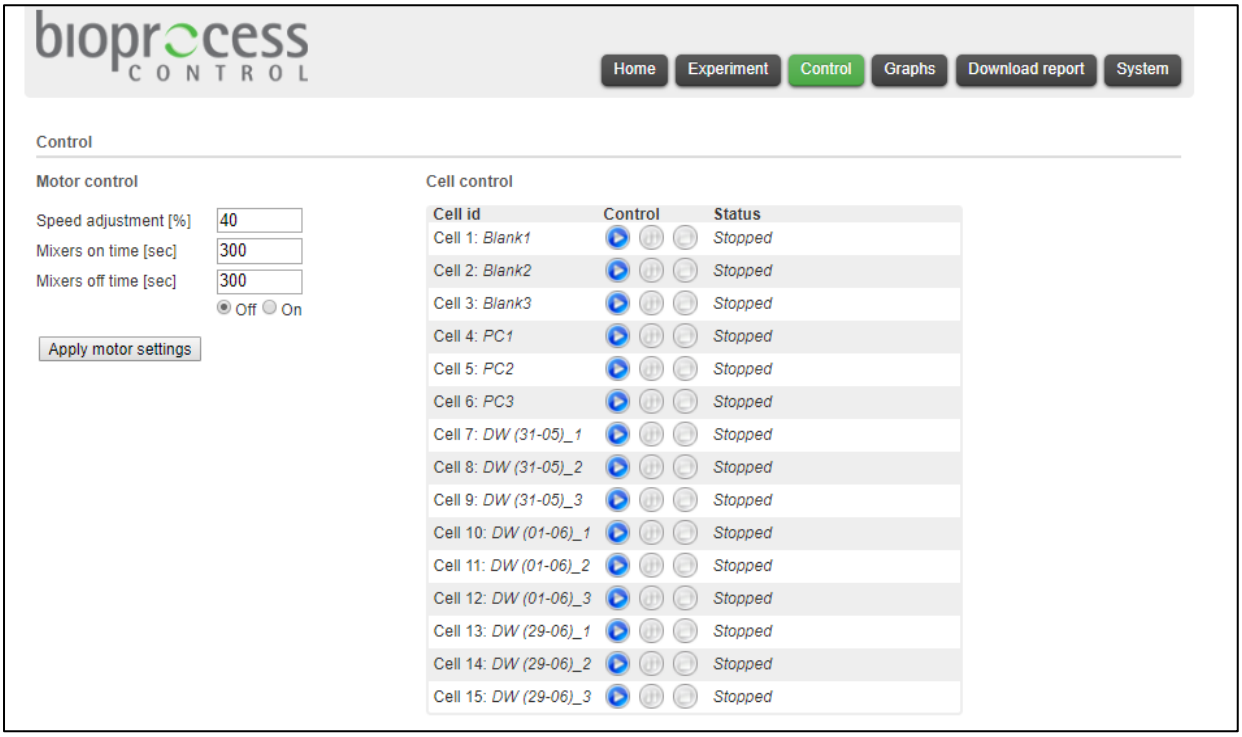


Figure 21: Screenshot of the AMPTS II unit's *Control* web page for a number of BMP tests using distillery waste (DW) samples.

(b) Pilot-scale AD tests

For pilot-scale AD tests, feedstocks had their pH levels adjusted to the desirable range of 6.8 to 7.2, where NaOH or HCl were added to raise or lower the pH as required, respectively. All pre-loaded feedstocks and inoculum were contained in plastic containers. Pilot-scale tests were performed in sealed 50 L stainless steel vessels with a working volume of 35 L. Before setting up any experiments, each vessel, its agitator blades and digestate sample valves were cleaned with hot water and soap and rinsed with DI water. The GMS connections (PVC tubing) were checked for blockages with air-filled 50 mL syringes to ensure the manometer's functionality was not obstructed. The manometer water levels were inspected and topped up with DI water to reset the meter to its baseline water column level. Each level sensor's sensitivity was inspected by physically touching it to trigger the light sensor.

The setting up of a single 50 L reactor entailed the following, regardless of the feeding mode; 35 L of inoculum collected from the relevant biogas plant was loaded into the reactor. The vessel was then closed with a stainless steel lid and securely fastened with eight wing nuts. The headspace of each reactor was flushed for $\geq$ 60 seconds with pure nitrogen gas to ensure anaerobic conditions.

Once the gas product and sampling lines were secured the reactors were switched on and the temperature and stirring time was set to 37°C and 5-minutes on 5-minutes off, respectively. The temperature was set according to the process temperature of the full-scale AD reactors (i.e. 37 °C), while the stirring frequency was set according to the stirring frequency of BMP test reactors. The inoculum-

filled reactor was then left to degas for approximately 1 to 3 days, until the biogas flow graph displayed insignificant biogas production.

*4.1.4.2. Experimental run*

Pilot-scale AD tests were performed for feedstocks obtained from Plant 2 and Plant 3. Pilot studies were not conducted for Plant 1 (mixed organic wastes) due to the complexity of tracking the amounts of feedstocks fed to the full-scale digester per day. Moreover, as indicated by Holliger *et al*. (2017), estimating performance of co-digestion plants requires investigating pilot-studies using different feeding modes (e.g. semi-continuous and continuous), which can be very expensive.

Two feeding configurations were investigated and compared for pilot-scale experiments, namely batch-fed and semi-continuously fed modes. The feeding was performed as follows:

(i) Batch-fed mode

Pilot-scale batch tests were conducted under the same conditions of BMP assay tests; at an ISR of 2.0, feedstock pH of 6.8 to 7.2, an operating temperature of ± 37°C and at a 5-minute on, 5-minute off stirring time. This was done to assess how scaling up digester working volumes would impact performance data such as methane yields. The VS% or COD content of the feedstock were predetermined to calculate the required volume of feedstock to be loaded. The ISR was factored into this calculation via a mass balance of the system. Moreover, it was assumed that the density of loaded feedstocks was the same as water (1.0 kg/m$^3$) for simplification of the mass balance.

Once the reactor under investigation had completely degassed, the relevant reactor vessel was ready for loading. Prior to loading the required volume of feedstock, the same volume of inoculum was removed from the vessel via the drain valve. The biogas product line valve was closed during this process to prevent the backflow of manometer water into the reactor. The ISR-determined volume of feedstock was then loaded into the vessel via the draught tube. The draught tube was then sealed shut and the biogas product line reopened.

(ii) Semi-continuous feeding mode

Semi-continuous modes were carried out under conditions that replicated the operation of the full-scale AD plants. The process temperature for all full-scale AD plants was set to 37°C, had their pH adjusted to the range of 6.8 to 7.2. However, the HRT for the three plants were different, and thus the amount of fed material for semi-continuous experiments was dependent on the full-scale HRT.

The calculation of HRT was previously defined by Equation (1) in Section 2.2.1.3 (Meegoda *et al*., 2018). For the example of AD Plant 3, the plant is operated at an HRT of 4 days. For a working volume of 35L, Equation (1) was rearranged and the daily feed rate ($Q_i$) was calculated as follows:

$$Q_i = \frac{V_o}{HRT} \tag{16}$$

$$\therefore Q_i = \frac{35\ L}{4\ days}$$

$$\therefore Q_i = 8.75\ L/d$$

Similar to the loading of batch mode pilot-scale tests the required daily volume of feedstock was fed to the relevant reactor after removing the corresponding volume of degassed inoculum. After loading, the draught tube was resealed and the biogas product lines reopened.

Pilot-scale experiments were monitored for daily biogas production, cumulative biogas volume and system temperature, and was automatically logged by the control panel system (TF Design [Pty] Ltd). Recorded data was then retrieved from the control panel system with a USB disc.

*4.1.4.3. Analytical methods*

Feedstock/inoculum samples were characterized by the following parameters; alkalinity, TS/VS content, pH measurement, Chemical Oxygen Demand (COD) and elemental analyses. The performance of AD tests (bench- and pilot-scale) was monitored by measuring determining digestate TS/VS% and pH level, as well as the biogas composition (vol%). Volatile fatty acid (VFA) content of digestate was only analysed if drastic changes in pH levels were measured.

Total and volatile solids (TS/VS) analyses were carried out in ± 5.0 mL ceramic crucibles, in triplicate. Before conducting TS/VS analyses crucibles were kept in a drying oven (BENCHOTEC: Term-O-Mat) at ± 50 $^{o}$C for one hour, after which they were placed in a desiccator container to cool. The standard method for TS/VS determination was used, the masses of empty crucibles was first measured, followed by the whole sample-crucible mass after filling it with the relevant feedstock or inoculum sample (Liebetrau *et al*., 2016). The filled crucibles were then placed in the oven for a 24-hour period at 80 $^{o}$C to ensure complete evaporation of moisture. The dried crucible sample masses were measured, and then placed in the muffle furnace (Nabertherm®). The muffle furnace temperature was set to a temperature of 550 $^{o}$C at an initial pre-heating rate of ± 28 $^{o}$C for 15 minutes. Samples were heated at 550 $^{o}$C for two hours, after which the ash-containing crucibles were weighed. All samples were weighed with RADWAG® analytical scale (± 0.0001g accuracy)

All chemical oxygen demand (COD) analyses were performed using a multi-analytical spectrophotometer (Spectroquant® Prove 300). Each time the instrument was used, it performed a self-test to check all functionalities. After the self-test, a reference cell (DI water) was inserted into the cell holder to zero the machine. COD analyses were performed by adding the required volume of substrate to a reaction cell containing potassium dichromate ($K_2CrO_4$) and 50% sulphuric acid ($H_2SO_4$) solution (Hach, 2020). Analyses were then performed by simply inserting the COD reaction cell into the same cell holder, which read the cell's barcode to output the correct analytical result and units. All COD output readings were presented in milligrams per litre (mg/L).

All pH measurements were done using a Hanna pH probe with a ± 0.001 accuracy, whose working principle was based on the concentration of hydrogen ions in solution. The pH meter was calibrated each

time before use with pH buffer solutions 4.01, 7.01 and 10.01 to ensure accurate readings. All feedstock and inoculum samples' pH levels were determined and adjusted to the desirable range of 6.8 to 7.2 and 7.0 to 8.5, respectively, if required. The pH of digestate samples obtained from bench- and pilot-scale tests was also recorded to monitor AD performance, i.e. any indication of VFA accumulation.

Elemental analyses for carbon (C), hydrogen (H), nitrogen (N) and sulphur (S) were performed using the Vario EL Cube Elemental Analyser (Elementar©, Germany) at the Central Analytical Facility, Stellenbosch. Roughly 5.0 mg of feedstock and inoculum samples were dried in the oven at 80 $^{o}$C for 24 hours and milled into a fine powder. Approximately 5.0 mg of tungsten (III) oxide ($WO_3$) was then added to the sample, after which the mixed sample was superheated at 1050 $^{o}$C in a combustion column while injecting oxygen gas. The formed gases ($CO_2$, water vapour, $N_2$, nitrogen oxide and sulphur dioxides) pass over copper wiring to reduce several gases, after which the gaseous component concentrations are detected using adsorption techniques.

For bench-scale/BMP tests, biogas composition (%vol) were not analysed due to issues with the Compact Gas Chromatography (GC) instrument during the test period. For a particular triplicate BMP test, methane content was estimated using the ratio of methane volume (NmL) produced to the volume of biogas volume (NmL) produced. This method was based on the assumption that product gases exiting the $CO_2$ adsorption units contained "pure" methane, i.e. scrubbed from impurities such as $CO_2$ and $H_2S$. The concentrations of $CO_2$ and $H_2S$ in produced biogas were not measured by the AMPTS II system.

Biogas samples obtained from pilot-scale AD tests were analysed for determining the volumetric concentration of $CH_4$, $CO_2$, $O_2$ and $H_2S$ (ppm) using a specialized gas analyser (Biogas 5000, GeoTech). The instrument analyses a gas sample by drawing it in via an air pump, which flows across several sensors before being pushed out its exhaust vent. Methane gas is detected via dual beam infrared absorption sensors. Certified methane mixtures were used to calibrate the sensors, and the presence of other hydrocarbons (e.g. ethane, propane & butane) will influence the actual methane concentration being measured. $CO_2$ content is also detected via infrared absorption at a wavelength specific to $CO_2$; therefore, $CO_2$ concentration is not influenced by the presence of other gases. The oxygen sensor is a galvanic cell-type, and detected oxygen concentrations are not influenced by any other gases (GeoTech, 2020). When switched on, the analyser performs a pre-determined self-test sequence to assess its general operation, gas flow measurement, and calibration status and battery charge level. Once the self-test was passed the instrument was ready for biogas analysis. The analyser's sample line (clear PVC tubing with an in-line moisture trap) was connected to the micro-digester's biogas sample valve. When the system pressure was fixed, the instrument's air pump was switched on while simultaneously opening the sample valve. Biogas was drawn via the pump for one minute or until the gas readings stabilised. The gas volumetric concentrations were recorded, and the analyser was purged with air to clear out the previous gas sample.

The extracted volumes of biogas samples from AD tests were also accounted for in terms of the errors they induced on biogas production and cumulative biogas volume. For a zeroed instrument pressure, the Biogas 5000 device typically draws 550 mL of biogas per minute and thus ± 550 mL of biogas was sampled each day for pilot-scale tests. However, for semi-continuous fed tests, this extracted volume did not affect daily biogas production as biogas samples were only taken once 24 hours had elapsed after feeding a

particular reactor. For CBP, the extracted volumes of biogas were added to the total production by taking the number of test days multiplied by 550mL of biogas. For pilot-scale batch tests biogas samples were taken in duplicate, and thus 1100mL of biogas volume was added to the CBP results at the end of batch experiments. Biogas samples for bench-scale/BMP tests were not performed with the Biogas 5000, as the instrument withdraws a large volume of biogas (550 mL/min). The withdrawing of large volumes of biogas samples would thus result in erroneous recordings of cumulative biogas and methane volumes by the AMPTS II.

## 4.2. Theoretical methodology

Theoretical methodology describes the methods used to process experimental data, specifically the indicators used for model development and the software used to formulate such models. Discussions on experimental and analytical error is also given.

### *4.2.1. Overall data processing plan*

Figure 22 on Page 49 gives an overview of how experimental data were used to calculate scale factors. The major experimental indicators required for developing both models are specific gas and methane yields (SGY and SMY) obtained from bench- and pilot-scale tests, as well as disintegration constants obtained from FM (FO) model approximation of obtained biogas production data. Gas yields are expressed as the normalized produced volume of biogas/methane per mass of organic material fed to the anaerobic digester, previously described by Equation (3):

$$SGY = \frac{Cumulative\ biogas\ volume}{mass\ of\ organic\ material\ added}\left[\frac{NL}{kg\ VS\ or\ COD}\right] \tag{17}$$

$$SMY = \frac{Cumulative\ methane\ volume}{mass\ of\ organic\ material\ added}\left[\frac{NL\ CH_4}{kg\ VS\ or\ COD}\right] \tag{18}$$

When using the AMPTS II setup the calculation of SGY and SMY differs from the calculations above because the system accounts for the endogenous biogas/methane volumes produced from blank tests. This calculation is given below, for a particular time during experimentation:

$$SGY_{AMPTS\ II} = \frac{(VB_{substrate} - VB_{blank} \times \frac{m_{O,RI}}{m_{O,blank}})}{m_{o,RS}} \tag{19}$$

$$SMY_{AMPTS\ II} = \frac{(VM_{substrate} - VM_{blank} \times \frac{m_{O,RI}}{m_{O,blank}})}{m_{o,RS}} \quad (20)$$

Calculating SGY from the AMPTS II considers the volume of biogas ($VB$) produced by the substrate and blank tests. The volume of biogas produced by blank tests is multiplied by the ratio of the mass of organic material in a reactor' bottle's inoculum ($m_{O,RI}$) and the organic mass contained in the blank tests ($m_{O,blank}$). This difference is then divided by the mass of organic material contained in a reactor bottle's substrate ($m_{O,RS}$). The same approach was followed for obtaining SMY data, except cumulative methane volumes ($VM$) were used.

For bench-scale AD tests (AMPTS II) the SMY is also referred to as the BMP value obtained from a particular test. A feedstock's BMP value has been widely used by authors to express the SMY obtained from bench-scale tests, with reference to the standardized protocol (Angelidaki *et al*., 2009; Holliger *et al*., 2016; Holliger *et al*., 2017; Raposo *et al*., 2012).

For pilot-scale tests the SMY is not defined as the BMP value due to differences in experimental conditions. Typically, from the pilot-scale system described in Section 4.1.3.4, the SGY is calculated using CBP data and the known masses of organic content contained in the feedstock. The SMY was calculated after measuring the methane content (%vol) of the produced biogas and multiplying the SGY with this percentage composition. The same approach was followed for calculating the SMY of the full-scale AD plants, where methane content was measured on site via the Biogas 5000.

The development of both models also required input data from the full-scale installations, whose indicators include feed flowrates, full-scale digester volume and feedstock compositional analyses (i.e. total solids, volatile solids and/or total COD). For Plant 1 (mixed organic wastes) and Plant 2 (tomato waste), these compositional analyses were not determined on site, nor were they reflected in their respective operational datasets. Therefore, compositional analyses determined in the laboratory were used by the methods for predicting full-scale AD performance. Plant 3 operators performed frequent feedstock and digestate compositional analyses on site, where specific datasets (e.g. total COD content) were used for in the methods for predicting full-scale AD performance.

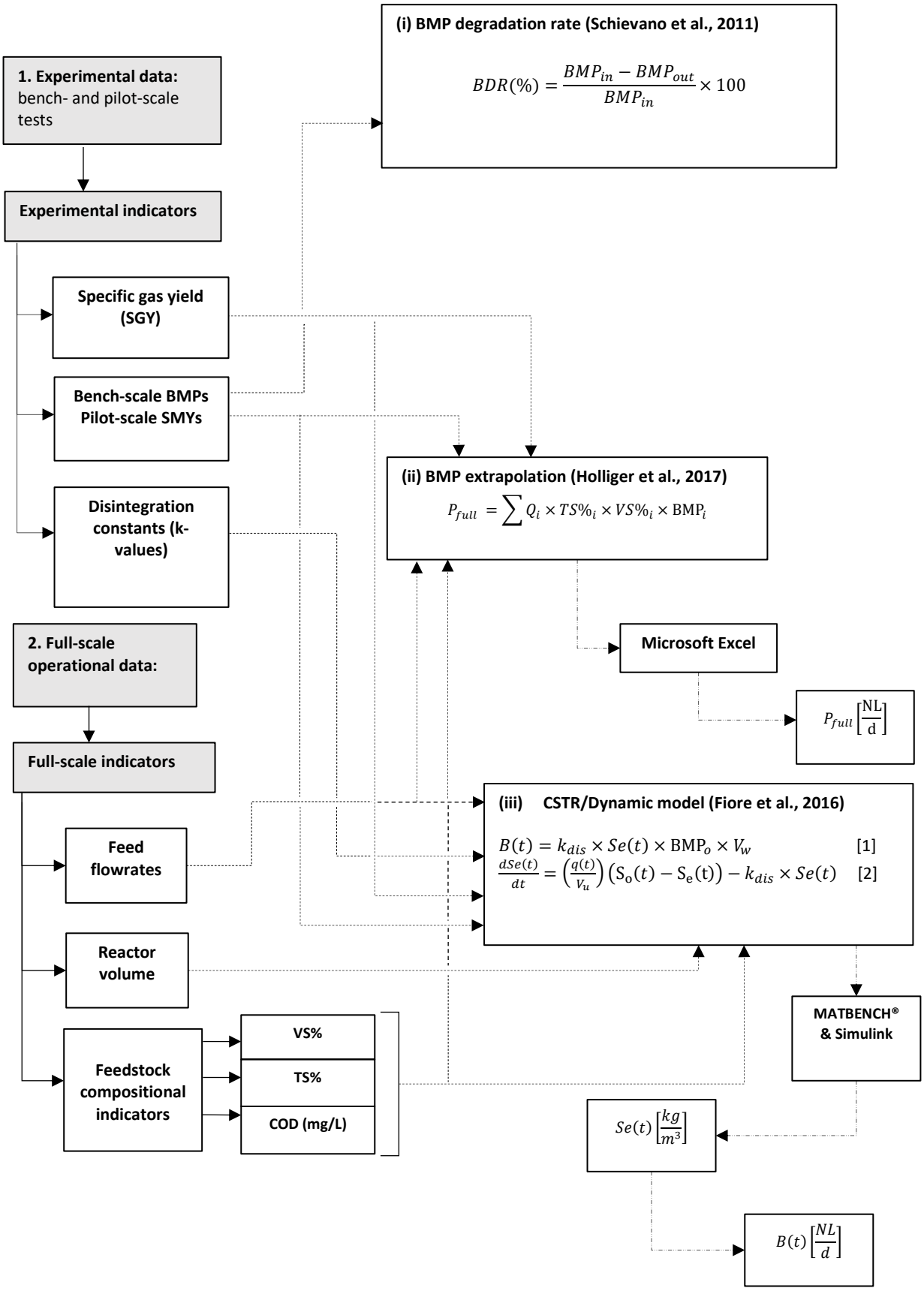


Figure 22: Data processing flow diagram for the methods used to predict full-scale AD performance.

### *4.2.2. Model modifications*

The extrapolation (Holliger *et al*., 2017) and CSTR-based dynamic (Fiore *et al*., 2016) models were originally formulated on organic solids compositional bases (total and volatile solids). For the case of Plant 3 (distillery effluent/liquid plant) both models required modifications to suit a COD basis to model the plant. A simple substitution was performed for each, as shown below:

The original extrapolation model is given below (Holliger *et al*., 2017):

$$P_{full}\left[\frac{NL}{d}\right] = Q_i\left[\frac{kg}{d}\right] \times TS\%_i \times VS\%_i \times BMP_i\left[\frac{NL}{kgVS}\right] \tag{21}$$

Given a certain full-scale volumetric feed flowrate ($Q_i$), the COD content substitutes for the total and volatile solids weight percentages, with the BMP value expressed per mass of added COD:

$$\therefore P_{full}\left[\frac{NL}{d}\right] = Q_i\left[\frac{m^3}{d}\right] \times COD\left[\frac{kg}{m^3}\right] \times BMP_i\left[\frac{NL}{kgCOD}\right] \tag{22}$$

A similar modification was performed on the two original CSTR/dynamic model equations, shown below (Fiore *et al*., 2017):

$$B(t)\left[\frac{Nm^3}{d}\right] = k_{dis}\left[\frac{1}{d}\right] \times Se(t)\left[\frac{kg}{m^3}\right] \times \mathrm{BMP}_o\left[\frac{Nm^3}{kgVS}\right] \times V_w[m^3] \tag{23}$$

$$\frac{dSe(t)}{dt} = \left(\frac{q(t)}{V_u}\right)\left[\frac{m^3}{m^3 \cdot d}\right] \times \left(\mathrm{S_o}(t) - \mathrm{S_e(t)}\right)\left[\frac{kg}{m^3}\right] - k_{dis}\left[\frac{1}{d}\right] \times Se(t)\left[\frac{kg}{m^3}\right] \tag{24}$$

Substituting apparent VS content ($Se(t)$) for apparent COD content ($COD_e(t)$) in the digester, and expressing the BMP value as a COD basis, then:

$$\therefore B(t)\left[\frac{Nm^3}{d}\right] = k_{dis}\left[\frac{1}{d}\right] \times COD_e(t)\left[\frac{kg}{m^3}\right] \times \mathrm{BMP}_o\left[\frac{Nm^3}{kgCOD}\right] \times V_w\ [m^3] \tag{25}$$

$$\therefore \frac{dCOD_e(t)}{dt} = \left(\frac{q(t)}{V_u}\right)\left[\frac{m^3}{m^3 \cdot d}\right] \times [COD_o(t) - COD_e(t)]\left[\frac{kg}{m^3}\right] \times COD_e(t)\left[\frac{kg}{m^3}\right] \tag{26}$$

### *4.2.3. Data processing software*

All experimental results and full-scale operational data were processed using Microsoft Excel 2016. Matrix Laboratories (MATLAB®) and Simulink were used for the computation of the CSTR-based dynamic model. Screen shots of the MATLAB® working spaces and Simulink diagrams for Plants 1 and 2 (Figure 63) and Plant 3 (Figure 64) are given in Appendix C. Additional software includes Easy Converter© (Weintek

Lab., Inc), used for extracting pilot-scale data. Such data was extracted and structured into the following data columns: Record Number, Product T (°C), Jacket T (°C), Biogas Total (L) and Biogas Flow Rate (L/d).

## 4.3. Data verification and error analysis

### *4.3.1. BMP test data validation*

Because of the potential variations in BMP values that could arise in triplicate BMP tests, Holliger *et al.* (2016) compiled a list of data validation criteria for such experimental data. A number of criteria for validating BMP test results, which were previously given in Table 1 (Section 2.2.2.3). If experimental results do not adhere to the listed criteria, they must be rejected and BMP tests should be repeated.

### *4.3.2. Experimental error*

As AD is influenced by the activity of microbial consortia, the conditions in each AD test bottle/vessel may vary. Experimental error arises from varying conditions will therefore influence substrate degradation rates, biogas/methane production and the respective gas yields. As previously mentioned in Section 4.1.4, all bench-scale (BMP tests) were performed in triplicate to minimize the standard error between generated results. Additional experimental error could arise from the sampling of working masses and volumes from reactor vessels.

The adjustment of pH level for feedstocks used for bench-scale AD tests involved the addition of buffer solution (NaOH or HCl) to the stock solution of feedstock. Roughly 500mL stock solution per feedstock per triplicate test was prepared and had its pH adjusted accordingly; approximately 0.1 to 1. 0mL of buffer solution was added to the relevant stock solution, which increased the stock solution volume by roughly 0.0199 to 0.1996%. This increase in volume was deemed insignificant on its effect on each experimental run. The same error was accounted for and deemed negligible during feedstock preparation for pilot-scale experiments.

The sampling of digestate from AD tests also induced error on the reactor's total volume. This was more relevant to semi-continuous pilot-scale AD tests (50L and 35L total and working volumes, respectively); before feeding a certain volume of feedstock the same volume of digestate needed to be extracted from the vessel. A 5.0 L PVC bucket was used for the extraction, having a measuring accuracy of ± 10 mL. The mean quantity of extracted digestate was ± 3.8 L, inducing an error of ± 0.262%, which was also considered negligible.

### *4.3.3. Analytical error*

For biogas compositional analyses via the Biogas 5000, the typical accuracy for measuring methane ($CH_4$), carbon dioxide ($CO_2$), oxygen ($O_2$) and hydrogen sulphide ($H_2S$) concentrations is summarised in Table 8 below. These concentration ranges were specified in the operating manual for the Biogas 5000 instrument (GeoTech, 2020).

Table 8: Biogas 5000 accuracy ranges for detecting various components in biogas.

| Biogas component | Units | Typical accuracy after calibration | |
|---|---|---|---|
| Methane ($CH_4$) | % vol | 0 to 70 (±0.5) | 70 to 100 (±1.5) |
| Carbon dioxide ($CO_2$) | % vol | 0 to 60 (±0.5) | 60 to 100 (±1.5) |
| Oxygen ($O_2$) | % vol | 0 to 25 (±1.0) | |
| Hydrogen sulphide ($H_2S$) | Parts per million (ppm) | 0 to 500 (±2.0% FS [a]); 0 to 5 000 (±2.0% FS); 0 to 10 000 (±5.0% FS) | |

[a] : factory setting

To reiterate from Section 4.1.4.3, the accurate measurement of methane volumetric concentration is influenced by the presence of additional hydrocarbons given off from the anaerobic degradation of a feedstock. For some biogas samples, methane concentration was measured between 72 and 85 % vol, which was out of the calibration range for the Biogas 5000. Therefore, for these highly concentrated methane measurements, a gas chromatography instrument (CompactGC 4.0, Global Analyser Solutions™, The Netherlands) was used to calibrate these readings.

The GC unit was initially calibrated to 0.5% to 10% methane using standard gas mixture calibration standards. However, biogas samples exhibiting >75%vol methane were greater than the initial calibration range, and thus the same concentrated samples were tested on a new GC unit calibrated to 100% methane by the Process Engineering Analytical Laboratory (Stellenbosch University). The calibration method was not very robust nor repeatable due to hardware and software issues, and thus induced some error regarding reproducibility. For a particular biogas sample, when comparing both GC units, the measured methane concentrations differed by roughly ± 1.95%. Therefore, it was decided to analyse all biogas samples on the GC unit calibrated to 0.5% to 10% methane. Extrapolated curve was obtained to interpret the 72% to 85% vol measurements by the Biogas 5000, given in Figure 23.

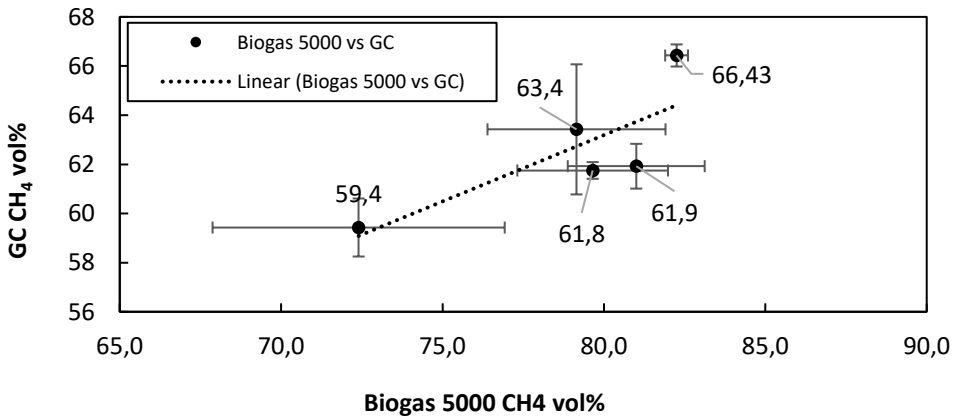


Figure 23: Calibration curve for converting high-range methane concentrations measured by the Biogas 5000 to measurements detected by the Compact GC unit.

The linear trend line equation is given below:

$$\text{Actual } CH_4 \text{ (\%vol)} = 0.54 \times (\text{Biogas 5000 } CH_4 \text{ \%vol}) + 19.995 \quad (27)$$

The linear regression model in Figure 23 shows a correlation ($R^2$-value) of 0.6417 and was used to convert highly-concentrated methane compositions to a more realistic range. A summary of these results is presented in Table 9 for several biogas samples collected from site and from pilot-scale tests fed with distillery effluent from Plant 3.

Table 9: Calibration curve results for several biogas samples.

| Source of biogas sample | Methane concentration (%vol) | | | |
|---|---|---|---|---|
| | Biogas 5000 | Stdev | Compact GC | Stdev |
| Plant 3 gas line | 82.3 | 0.35 | 66.43 | 1.95 |
| Pilot-scale 11 [a] | 79.2 | 2.76 | 63.4 | 2.65 |
| Pilot-scale 12 | 72.4 | 4.53 | 59.4 | 1.18 |
| Pilot-scale 14 | 81.0 | 2.12 | 61.9 | 0.91 |
| Pilot-scale 16 | 79.7 | 2.33 | 61.8 | 0.34 |

[a] : number is indicative of the name of the pilot-scale AD test.

### *4.3.4. Statistical analyses*

Several statistical methods were implemented to evaluate AD experimental data, which includes linear regression modelling, Student t-tests and ANOVA techniques. Linear regression models were used to assess the relationship between dependent and response variables. Student t-tests with unequal variances were used to assess any significant differences between population means for a significance level of 5.0%. ANOVA tests represent a collection of methods for comparing multiple means across different populations. ANOVA was predominantly used to assess any significant differences between experimental and predicted data obtained from methods proposed in Section 2.3.2, for a significance level of 5.0%. All statistical computations were performed in Microsoft Excel 2016.

Additionally, the relative standard deviation (RSD) was calculated for BMP test datasets, also known as the coefficient of variation. RSD calculations were performed as recommended by the standardised BMP test protocol; Holliger *et al.* (2016) provided guidelines from an inter-laboratory conference where it was decided that RSD should serve as the statistical means for validating BMP test results. . The calculation of relative standard deviation was done using the Equation (28), defined as the ratio of standard deviation to the mean for a particular dataset.

$$RSD = \frac{STDEV\ (A_1, A_2, \dots A_n)}{AVG\ (A_1, A_2, \dots A_n)} \times 100\% \quad (28)$$

According to Holliger *et al.* (2016), the following RSD criteria for BMP test data obtained from BMP tests performed on different feedstocks were listed as follows:

- For homogenous feedstocks, RSD < 5.0%
- For heterogenous feedstocks, RSD < 10%

For cases when RSD criteria are not met, BMP test data should be rejected and BMP tests must be redone.

# CHAPTER 5: RESULTS AND DISCUSSION

Chapter 5 presents the findings from performed experimental work and the interpretations thereof. Results pertaining to full-scale feedstock characterization, bench- and pilot-scale tests and full-scale performance estimations for each biogas plant are discussed in individual sections.

## 5.1. Feedstock characterization

All materials sampled from the three full-scale AD plants were characterized by their total solids (TS) content, organic content and elemental compositions as pre-requisites for setting up experiments and for determining their suitability for AD.

### *5.1.1. Plant 1: Co-digestion of mixed organic wastes*

Five representative feedstock mixtures (denoted by the letter M) and inoculum were collected from Plant 1, where all materials were characterized by their chemical compositions. Table 10 gives the total solids (TS) and volatile solids (VS) contents, pH level and elemental analyses for each material.

Table 10: Feedstock characterization for feedstock mixtures fed to Plant 1.

| Analysis | Units | Inoculum | M1 [a] | M2 [b] | M3 [c] | M4 [d] | M5 [e] |
|---|---|---|---|---|---|---|---|
| TS | % w/w | 1.67 ± 0.02 | 15.5 ± 0.98 | 25.9 ± 0.37 | 18.4 ± 0.18 | 39.0 ± 0.33 | 30.0 ± 2.71 |
| VS | % w/w | 1.01 ± 0.03 | 14.7 ± 0.95 | 12.1 ± 0.38 | 9.48 ± 0.20 | 38.7 ± 0.33 | 22.9 ± 2.28 |
| | %TS [f] | 60.6 ± 2.52 | 95.2 ± 0.19 | 46.8 ± 0.81 | 51.4 ± 0.58 | 99.3 ± 0 | 76.4 ± 1.18 |
| pH | - | 7.41 | n.d.[h] | 4.58 | 4.77 | 5.86 | 5.88 |
| C | % | n.d. | 48.0 | 23.5 | 25.8 | 50.1 | 43.5 |
| N | % | n.d. | 2.39 | 1.05 | 1.64 | 0.80 | 1.25 |
| H | % | n.d. | 7.31 | 3.75 | 3.79 | 7.49 | 6.95 |
| S | % | n.d. | 0.13 | 0.17 | 0.22 | BDL [g] | 0.09 |
| C:N | - | n.d. | 20.1 | 22.4 | 15.8 | 63.7 | 34.8 |

[a] : Apples, food waste; [b] : beer, food waste, spices; [c] : beer, cow blood & manure, food waste, spices; [d] : beer, cow blood, chocolate waste, sugar; [e] : beer, cow blood, food waste, fruit juice; [f] : portion of total solids constituting volatile solids; [g] : below detection limit; [h] : not determined.

As given in Table 10, Mixture 2 and Mixture 5 exhibited C:N ratios of 22.4 and 34.8, respectively. These ratios were in accordance with the desirable C:N ratio of 20 to 35:1, which suggests both mixtures are suitable for AD (Ward *et al.,* 2008; Weinrich *et al*., 2018). Mixture 3 exhibited the lowest C:N ratio of 15.8 compared to the other feedstock mixtures. This was attributed to the presence of cow blood and manure, the former feedstock containing large quantities of protein and nitrogen (Kovács *et al*., 2015; Moukazis *et al*., 2018; Nazifa *et al*., 2021). The greatest C:N ratio was determined for Mixture 4 as 63.7, which far exceeded the recommended range of 20 to 35:1 (Ward *et al.,* 2008; Weinrich *et al*., 2018).. The abundance of carbon in Mixture 4 was attributed to the presence of starches and sugars in feedstocks such as beer, chocolate waste and sugar. This large C:N ratio of 63.7 may have a negative impact on AD

performance; according to the study by Hills (1979), increased C:N ratios in cow manure decreased methane yields during AD. Moreover, large quantities of sugar could pose risks of VFA accumulation during acidogensis (FNR, 2012; Buchauer *et al*., 1998).

The TS and VS contents of Plant 1's inoculum were determined as 1.67% and 1.01% (w/w), respectively, which are lower than what has been reported by other studies. For example, Schievano *et al.* (2011) reported a TS content range of 3.7% to 5.8% (w/w) for digestate samples collected from three full-scale co-digestion plants. The dilute nature of Plant 1's inoculum may be due to the dilute nature of certain feedstock mixtures, which had moisture contents of 61% to 85% (w/w) as shown in Table 10. Moreover, Plant 1's pH level was measured as 7.41, which is consistent with the range of pH 7.0 to 8.5 as reported for healthily-functioning AD plants (Angelidaki *et al*., 2009; Holliger *et al*., 2016; Raposo *et al*., 2012).

### *5.1.2. Plant 2: Tomato waste (TW)*

Six TW samples were collected over 3 months from Plant 2, which were analysed for essential parameters TS, VS, total COD and pH level, as shown in in Table 11 below.

Table 11: Compositional variation of tomato waste (TW) samples collected during times of the year.

| TW sample date | Parameter | | | | |
|---|---|---|---|---|---|
| | Total COD (mg/L) | TS (% w/w) | VS (% w/w) | VS (%TS) [a] | pH level |
| **Inoculum** | 7145 ± 7.071 | 0.71 ± 0.07 | 0.51 ± 0.09 | 71.43 ± 4.55 | 7.75 |
| **15-Apr-21** | 49745 ± 106.5 | 2.67 ± 0.50 | 2.57 ± 0.33 | 87.4 ± 3.14 | 4.08 |
| **22-April-21** | 54365 ± 1506 | 2.70 ± 0.02 | 2.26 ± 0.04 | 83.7 ± 1.01 | 4.01 |
| **29-April-21** | 53643 ± 125.0 | 3.29 ± 0.18 | 2.75 ± 0.20 | 85.4 ± 1.36 | 3.98 |
| **18-May-21** | 34615 ± 120.2 | 3.39 ± 0.28 | 3.15 ± 0.20 | 92.9± 1.77 | 4.08 |
| **10-Jun-21** | 26085 ± 2920 | 2.18 ± 0.20 | 2.00 ± 0.03 | 92.4 ± 7.16 | 4.29 |
| **14-Jun-21** | 45590 ± 950 | 2.45 ± 0.35 | 2.26 ± 0.10 | 92.83 ± 11.2 | 4.38 |
| **TW mean values** | **44007 ± 11358** | **2.78 ± 0.47** | **2.50 ± 0.41** | **89.1 ± 4.12** | **4.14 ± 0.16** |

[a] : portion of total solids that constitutes volatile solids.

Amongst the compositional parameters given in Table 11, the mean moisture content (i.e. difference between 100 and the mean TS content) of 97% (w/w) suggests that the TW samples were suitable for AD. As described by Fujishima *et al.* (2000), during the AD of sewage sludge in a continuously-fed pilot-scale AD reactor of unspecified working volume, a decrease in feedstock moisture content from 97% to 89% (w/w) resulted in a decrease in methane yields. Therefore, the mean moisture content of 97% (w/w) of TW will favour biogas production via AD because a feedstock's nutrients must first be dissolved in the liquid phase before being assimilated by anaerobic microbes (Liotta *et al.,* 2014). Moreover, these compositional analyses indicate minimal variations in feed composition over the 3-month period, which suggests that biogas and methane production rates would be consistent during Plant 2's operational period.

For one particular TW sample, the C:N ratio was measured as 12.2, which was not shown in Table 11. Elemental analyses were not performed for other TW samples due to time constraints during the time of analysis. This ratio suggests an imbalance between carbon and nitrogen, as it fell short of the desirable C:N range of 20 to 35:1 (Ward *et al.,* 2008; Weinrich *et al*., 2018). This analysis was also lower than what has been reported in literature, for example, Szilagyi *et al*. (2020) measured a C:N ratio of 21.1 ± 0.77 for rotten tomatoes. Low C:N ratios may cause free-ammonia concentrations to exceed threshold levels such that anaerobic populations' abilities to produce methane gas become inhibited (Hashimoto, 1986; Muzenda, 2014). However, methanogenic bacteria could acclimatise to free-ammonia concentrations within an AD system providing drastic increases are not encountered from overfeeding the system (Fujishima *et al.,* 2000). The low pH level of 4.14 ± 0.16 for TW samples was also of concern to the stability of the AD pathways due to the risk of volatile fatty acid (VFA) accumulation (Raposo *et al*., 2012). The pH level of the digestate, however, reflects a satisfactory value by falling within the recommended range of pH 7.0 to 8.5 (Angelidaki *et al*., 2009; Raposo *et al*., 2012; Holliger *et al*., 2016).

Overall, the compositional analyses for TW samples given in Table 11 indicate suitable feedstock conditions for AD, as reflected by their moisture contents (97% w/w) and volatile solids content (89.1 ± 4.12 %TS), however the undesirable C:N ratio and pH level given as 12.2 and pH 4.14 ± 0.16, respectively, could induce potential inhibitions towards AD.

### *5.1.3. Plant 3: Distillery waste (DW)*

Plant 3 performed their own compositional analyses on distillery wastes (DW) and inoculum to monitor the digester's performance. Table 12 contains data that characterizes the DW and digestate on a daily basis.

Table 12: Mean historical compositional analyses of distillery waste (DW), as determined by Plant 3's operators.

| Analysis | Unit | Mean values | |
|---|---|---|---|
| | | Distillery waste (DW) | Inoculum |
| Alkalinity | mg/L | 543 ± 294 | n.d [d] |
| Total COD | mg/L | 11876 ± 5540 | n.d |
| Soluble COD | mg/L | 5989 ± 4533 | 893 ± 855 |
| pH level | - | 6.50 ± 0.98 | 6.97 ± 0.10 |
| TS [a] | % (w/w) | 0.52 ± 0.29 | 1.29 ± 0.38 |
| VS [b] | % (w/w) | n.d | n.d |
| TKN [c] | mg/L | 4.69 ± 4.94 | n.d |

[a] : Total solids; [b] : volatile solids; [c] total Kjeldahl nitrogen, reported as a concentration by Plant 3 operators; [d] : not determined

In addition to the analyses presented in Table 12, DW samples collected over a 9-month period were characterized by their pH levels and chemical oxygen demand (COD) contents. Table 13 shows the variations in feedstock COD contents and pH levels for DW samples, as well as the total COD contents for inoculum samples. For certain months, inoculum COD concentrations were the same because, at the

beginning of certain months, collected DW was frozen until later use. The effects of feedstock freezing on feedstock composition were not accounted for in this project. At the end of the month inoculum was collected for BMP tests.

Table 13: Organic content and pH level variation for distillery waste (DW) samples and inoculum collected during different months.

| DW sample date | Total COD (mg/L) | pH level | Inoculum COD (mg/L) |
|---|---|---|---|
| 19-Feb-20 | 15400 ± 226.3 | 5.33 | 13280 ± 876.8 |
| 23-Sep-20 | 9855 ± 70.71 | 6.10 | 7360 ± 115.2 |
| 19-Oct-20 | 11775 ± 487.9 | 5.22 | 11050 ± 268.7 |
| 26-Oct-20 | 15290 ± 106.1 | 7.37 | 11050 ± 268.7 |
| 05-Feb-21 | 10295 ± 1407 | 4.24 | 11050 ± 268.7 |
| 11-Feb-21 | 9980 ± 66.57 | 4.48 | 11050 ± 268.7 |
| 22-Feb-21 | 12160 ± 155.6 | 4.45 | 11050 ± 268.7 |
| 04-Mar-21 | 16680 ± 113.1 | 4.38 | 5000 ± 169.7 |
| 06-May-21 | 11610 ± 859.2 | 7.09 | 7393 ± 308.6 |
| 07-May-21 | 9820 ± 777.8 | 6.47 | 7393 ± 308.6 |
| 19-May-21 | 10510 ± 28.28 | 5.77 | 7393 ± 308.6 |
| 25-May-21 | 8890 ± 120.2 | 6.32 | 7393 ± 308.6 |
| 31-May-21 | 8980 ± 54.86 | 6.20 | 9510 ± 155.6 |
| 01-June-21 | 7810 ± 38.50 | 6.45 | 9510 ± 155.6 |
| 29-June-21 | 9350 ± 565.7 | 6.26 | 9510 ± 155.6 |
| **Mean values** | **11227 ± 2639** | **5.74 ± 1.01** | **9268 ± 2233** |

The mean COD content for all analysed DW samples was measured as 11227 ± 2639 mg/L, where variations in COD arose from waste streams originating from different alcohol production processes on-site of Plant 3 (Vlissidis & Zouboulis, 1993; Melamane *et al*., 2007; Vital-Jacome *et al*., 2020). These fluctuations would, in turn, cause fluctuations in methane yields produced by the full-scale system (Drosg *et al*., 2013). Fluctuations in feed pH could also be problematic for digester stability (Liu *et al*., 2008), as methanogenic bacteria are sensitive to pH changes. In fact, historical pH analyses of digestate shown in Table 12 reflected a value of pH 6.97 ± 0.10, which was marginally lower than the optimal pH range for a healthy anaerobic digester (Holliger *et al*., 2016; Raposo *et al*., 2012).

The historical compositional analyses given in Table 12 are compared with other analyses performed on different distillery effluents, as compared in Table 14. The DW sourced from Plant 3 corresponds more closely to wine distillery wastewater (WDW) in terms of total COD (DW = 11 876 ± 5540 mg/L and WDW = 15 150 ± 17 041 mg/L, in Table 14). The pH of DW reflected a neutral value of pH 6.50 ± 0.98 while WDW had a more acidic pH of 4.50 ± 0.80). Plant 3's pH was attributed to the dilution of DW by other factory process waters. A neutral pH suggests more stable conditions for AD, as the recommended pH range for feedstocks range of pH 6.8 to 7.2 (Holliger *et al*., 2016). Therefore, given the compositional analyses for DW samples in Table 12 and the close comparisons to other distillery waste samples in Table 14, Plant 3's distillery effluent was considered suitable for AD.

Table 14: Feedstock characterizations of distillery waste (DW) by different studies, adapted from Melamane *et al*. (2007).

| Parameter | Unit | DW analysed by Plant 3 (± standard deviation) | DW samples reviewed by Melamane et al. (2007) | | | |
|---|---|---|---|---|---|---|
| | | | Distillery wastewater [a] (± standard deviation) | Wine distillery wastewater [b] (± standard deviation) | Vinasse [c] (± absolute values) | Raw spent wash [d] (± absolute values) |
| Total COD | mg/L | 11 876 ± 5540 | 110 000 ± 14 142 | 15 150 ± 17 041 | - | ± 37 500 |
| Soluble COD | mg/L | 5989 ± 4533 | - | - | ± 97 500 | - |
| pH level | - | 6.50 ± 0.98 | 3.55 ± 0.78 | 4.50 ± 0.70 | ± 4.4 | ± 4.2 |
| TS | % (w/w) | 0.53 ± 0.29 | 7.58 ± 3.43 | 0.033 ± 0.023 | ± 0.362 | ± 0.28 |
| VS | % (w/w) | - | 5.0 | 0.028 ± 0.21 | - | - |
| TN [e] | mg/L | 4.70 ± 4.94 | - | 42.7 ± 30.2 | - | ± 2020 |

[a] : Mean values from two included studies (Harada *et al*., 1995; Nataraj *et al*., 2006), [b] : Eusébio *et al*., 2004; [c] : Martin *et al*., 2002, [d] : Ramana *et al*., 2002c; [e] : total nitrogen.

## 5.2. Full-scale AD performance data

Operational datasets were acquired from each of the three biogas plants to identify the prevailing transient effects influencing the steady operation of such systems. Full-scale data included biogas and methane production rates, organic loading and feeding rates, organic matter removals, digester pH levels and process temperatures.

### *5.2.1. Plant 1: Co-digestion of mixed organic wastes*

Performance data was obtained from industrial operations of Plant 1, represented as weekly mean values. These datasets span a 28-week operational period which include: daily biogas production and total mass feed rates in Figure 24 (a), power and daily methane production rates and composition in Figure 24 (b), individual feedstock mass feed rates per week in Figure 24 (c) and digester operating temperature and pH level in Figure 24 (d).

Transient effects in mean daily biogas productions were attributed to variations in the feed rates of mixed organic wastes to the digester, shown in Figure 24 (a). Because Plant 3 does not control its feeding rates nor frequencies, the feeding of mixed organic wastes was highly erratic, as emphasised by the given mass feed rates of individual feedstocks in Figure 24 (c). These feeding rates were also subject to seasonal availability of such materials, which is a common issue for co-digestion plants. For example, Holliger *et al.* (2017) reported a large extent of feed rate variation for green wastes fed to a dry-AD plant during certain months. OLR fluctuations could also influence downstream energy supply to on-site facilities, however, according to Figure 24 (b), daily power generation (kWh) was consistent around 588 ± 179 kWh/d over the 28-week period, as was mean daily methane production (391 ± 118 $Nm^3$/d). These consistencies were possibly due to the inaccuracies of measurements detected by the ultrasonic gas flow

meter, which could have arisen from pressure drops in the biogas product line (Water Technology, 2015). However, there were no reports of fluctuating pressure drops within Plant 1's biogas product line.

Over the 28-week period the mean total daily feed rate was recorded as 15.0 ± 7.51 tonnes per day, which, for a digester volume of 3200 $m^3$, corresponds to an HRT of roughly 213 days. This HRT far exceeds those established for other co-digestion plants. For example, Holliger *et al*. (2017) reported an HRT of 18 to 20 days for a co-digestion plant processing 5253 ± 279 tonnes of mixed liquid wastes per week. Kübler *et al.* (2000) assessed the operation of a full-scale co-digestion plant for 18 months, where the full-scale HRT was reported as 7 to 15 days during the treatment of the organic fraction of municipal solid waste (OFMSW). The HRT of 213 days for Plant 1 was greater because, under standard operation, the digester was meant to be fed 60 tonnes of mixed wastes per day, resulting in an HRT of roughly 49 days. However, during the study period the digester could only be fed 15.0 ± 7.51 ton/day due to issues with draining the digester as reported by on-site operators.

The system's process temperature and pH level were also logged over the 28-week period, given in Figure 24 (d). For weeks 1 to 10 the digester's process temperature was consistent around 36.8 ± 0.45$^oC$, as was the digester's pH level at 7.18 ± 0.04. After week 10, process temperature fluctuated between 18 and 47$^oC$ due to issues with biogas-fired boiler system. These temperature fluctuations would have disrupted the metabolic and growth rates of anaerobic bacteria in the digester (Angelidaki & Sanders, 2004; FNR, 2012), which resulted in a drastic decrease in daily biogas production from 1438 $Nm^3/d$ (week 13) to an all-time low of 29.5 $Nm^3/d$ (week 17). These fluctuations would have also made it difficult to re-distribute heat within the reactor, which, in turn, would slow the biogas production recovery rate (Chen *et al*., 2008; Marques *et al*., 2010). Furthermore, the digester pH dropped to 6.83 by week 16 while the biogas-fired boiler's malfunction persisted. By week 18 the digester system made a recovery and biogas production increased to 1055 $Nm^3/d$. Although the changes in process temperature was a once-off event, it emphasised the importance of regulating temperature, as large changes can impact overall digester performance. But, for weeks 0 to 10 and 20 to 28, digester temperature was stable and thus it was not clear that temperature changes were more impactful on full-scale performance than the variations in feedstock loading rates.

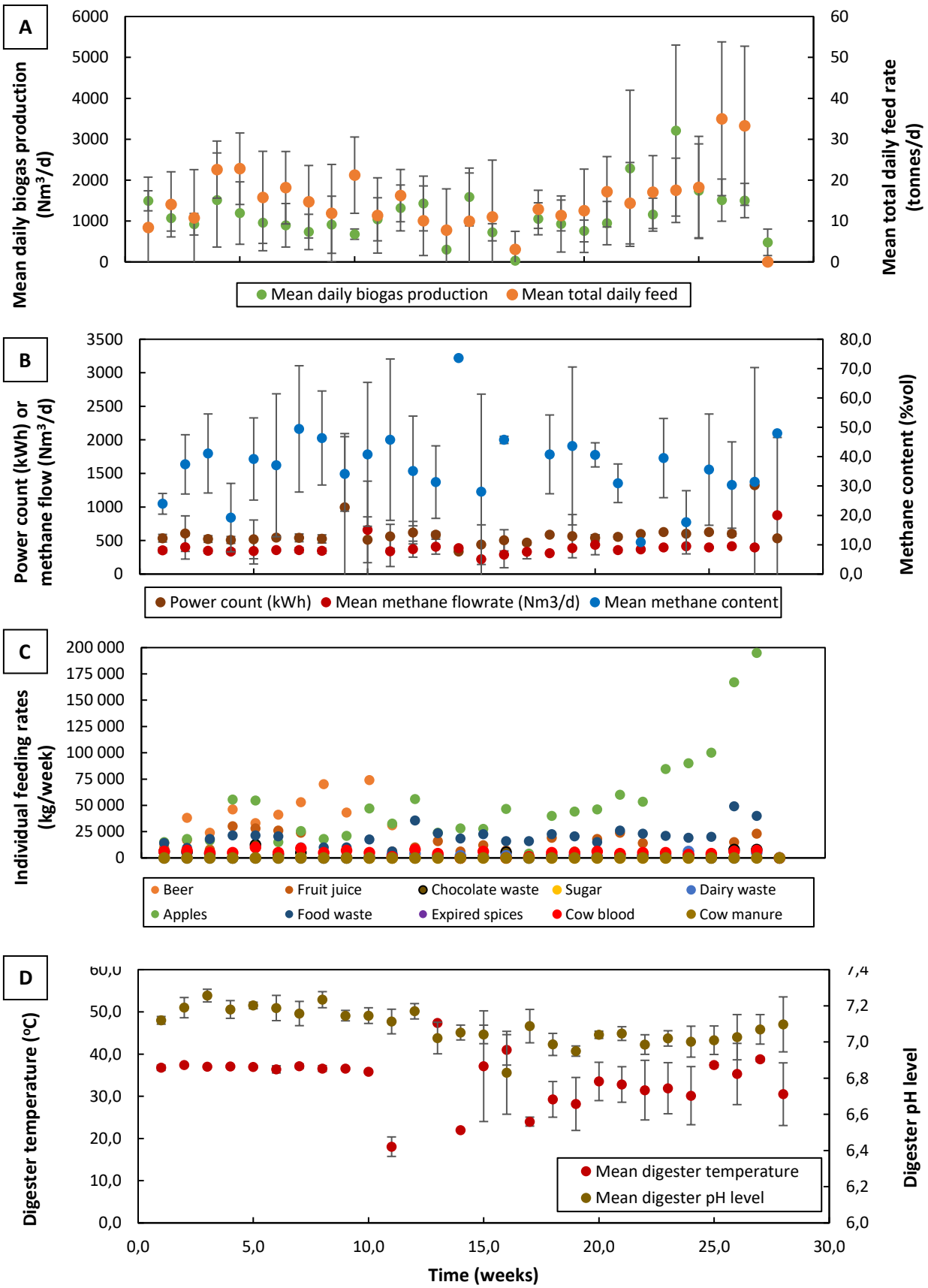


Figure 24: Full-scale operational data for Plant 1 treating mixed organic wastes; (a) total mass feed rates vs. daily biogas production, (b) power production and methane production rates and concentrations, (c) individual feedstock mass feed rates, (d) digester temperature and pH level. Error bars indicate the standard deviations for a sample size of $n$ = 7.

### *5.2.2. Plant 2: Tomato waste (TW)*

The major obstacles for obtaining full-scale data from Plant 2 operations included the lack of instrumentation such as gas flow measurement devices, pH probes and flow meters, as well as the lack of monitoring the digester's process conditions. An alternative plan was carried out to log power readings from the on-site 18 kW generator unit. However, such data could only be acquired when the borehole pump station on site was activated. These pumps were operated seasonally, and, when rainfall was not significant, typically ran for 8 to 12 hours.

Plant 2 also encountered highly erratic feeding and off-take over the past 6 months due to power failures and equipment malfunctions. Therefore, only one day's worth of generator output data was obtained in April-2021. A power range of 7.0 to 7.2 kVA, or 7.0 to 7.2 kW power output, was obtained, which was used to determine the plant's daily biogas production rate (Table 15).

Table 15: Generator power readings and biogas production data for Plant 2.

| Parameter | Unit | Value |
|---|---|---|
| Pump run time | Hours | 8.0 |
| Generator power reading | kW | 7.10 ± 0.10 |
| Thermo-electric efficiency | - | 32% |
| Generator efficiency | - | 20% |
| Actual power reading | kW | 2.27 ± 0.03 |
| | kWh | 18.2 ± 0.26 |
| Tomato waste feed basis | kg/d | 750 to 1000 |
| Estimated methane production | $m^3$ $CH_4$/d | 9.65 ± 0.14 |
| Estimated biogas production | $m^3$/d | 15.1 ± 0.21 |
| Full-scale methane content | % vol | 63.7 ± 0.66 |

An estimated daily biogas and methane production of 14.0 ± 0.20 and 8.92 ± 0.13 $Nm^3$/d were determined for Plant 2, respectively. Historically, it was observed that the primary digester's balloon took almost two days to inflate to maximum capacity; therefore, for a digester balloon volume of 23 $m^3$ at the current estimated biogas production rate, the balloon took roughly 1.5 days to completely fill.

As only one day's worth of generator readings was recorded, there was no compensation for variability in feedstock composition, digestate quality nor daily biogas production and methane concentrations. Attempts were made to measure the daily biogas production manually using water displacement methods, however, due to numerous power disruptions these manual measurements could not be performed. Above all, estimated biogas and methane production rates were deemed unreliable for Plant 2 because the generator's efficiency and run time during this duration were also only estimated. More reliable datasets could have been obtained if instrumentation was installed at the facility (e.g. a gas flow meter) to sufficiently monitor full-scale performance over longer periods of time.

### *5.2.3. Plant 3: Distillery waste (DW)*

Full-scale data operational data was acquired from the SCADA system of Plant 3, which spanned a period of almost three years. All data was plotted as daily mean values for each month of plant operation, where Figure 25 (a) shows the daily volumetric feed rates versus total COD, Figure 25 (b) shows daily biogas production versus OLR, Figure 25 (c) shows digester pH and feed pH levels and Figure 25 (d) shows ambient and digester temperature fluctuations.

In Figure 25 (a) the mean daily feed flows are inversely proportional to the mean total feed COD content, i.e. when low COD concentrations are measured (< 10 000 mg/L) in the fresh feed the digester feed rate set point is manually increased to roughly 586 $m^3$/d. This was done to ensure sufficient nutrients are supplied to the full-scale system when DW streams are more dilute. Changes in feed flowrates cause subsequent fluctuations in OLR, which, in turn, caused fluctuations in mean daily biogas production as shown in Figure 25 (b). Biogas production was most consistent over months 18 to 24 (1082 ± 157 $Nm^3$/d) and months 27 to 34 (1046 ± 165 $Nm^3$/d) when the OLR ranged from 2.1 to 2.6 kgCOD/$m^3$/d. Therefore, variations in OLR was identified as the major factor influencing daily biogas production. The regulation of OLR was difficult as feed COD concentrations were influenced by what was produced by the alcohol manufacturing processes (Melamane *et al*., 2007). However, the installation of an additional feed equalisation tank at the biogas installation could assist with minimizing compositional variations over time, i.e. improve the degree of homogenisation of the feedstock.

Referring to Figure 25 (c), the handheld-measured pH of the fed DW ranged pH 4.79 to 7.01, whose standard deviations ranged ± 0.28 to ± 1.94 over the 34-month period. The digester's pH was not majorly influenced by variations in feed pH and was maintained within a range of pH 6.85 to 7.30 over the 34-month operational period. Effects of feed pH on full-scale biogas production were deemed negligible due to implementation of an alkaline-dosing station on the feed line that regulated feed pH level. In contrast to pH control, the digester's operating temperature fluctuated seasonally. This was evident in Figure 25 (d); from January (month 0) to May 2018 (month 5) the digester temperature declined from 29.5 to 21.5 $^oC$ as a result of summer transitioning to winter. The recovery of process temperature to mesophilic conditions was gradual because heat needed to be uniformly redistributed within the large process volume of 2200 $m^3$ (Chen *et al*., 2008; Marques *et al*., 2010). Furthermore, a possible solution for improving digester temperature control entails the following: an additional boiler unit could be installed at the biogas plant to utilize excessively produced biogas instead of frequently flaring off the excess. This boiler unit could thus produce more steam to assist with combatting declines in process temperature during winter months. However, it was not clear how much excess biogas was sent to flare during different seasons.

Although changes in ambient temperature influenced the process temperature of Plant 3's 2200 $m^3$ digester, it was not clear that these changes impacted full-scale performance. More extreme effects of ambient temperature changes were observed by Coppinger *et al*. (1979), who monitored the performance of a full-scale dairy manure AD plant. Freezing temperatures were encountered in winter which disrupted overall biogas productivity due to the freezing of water vapour in biogas product lines.

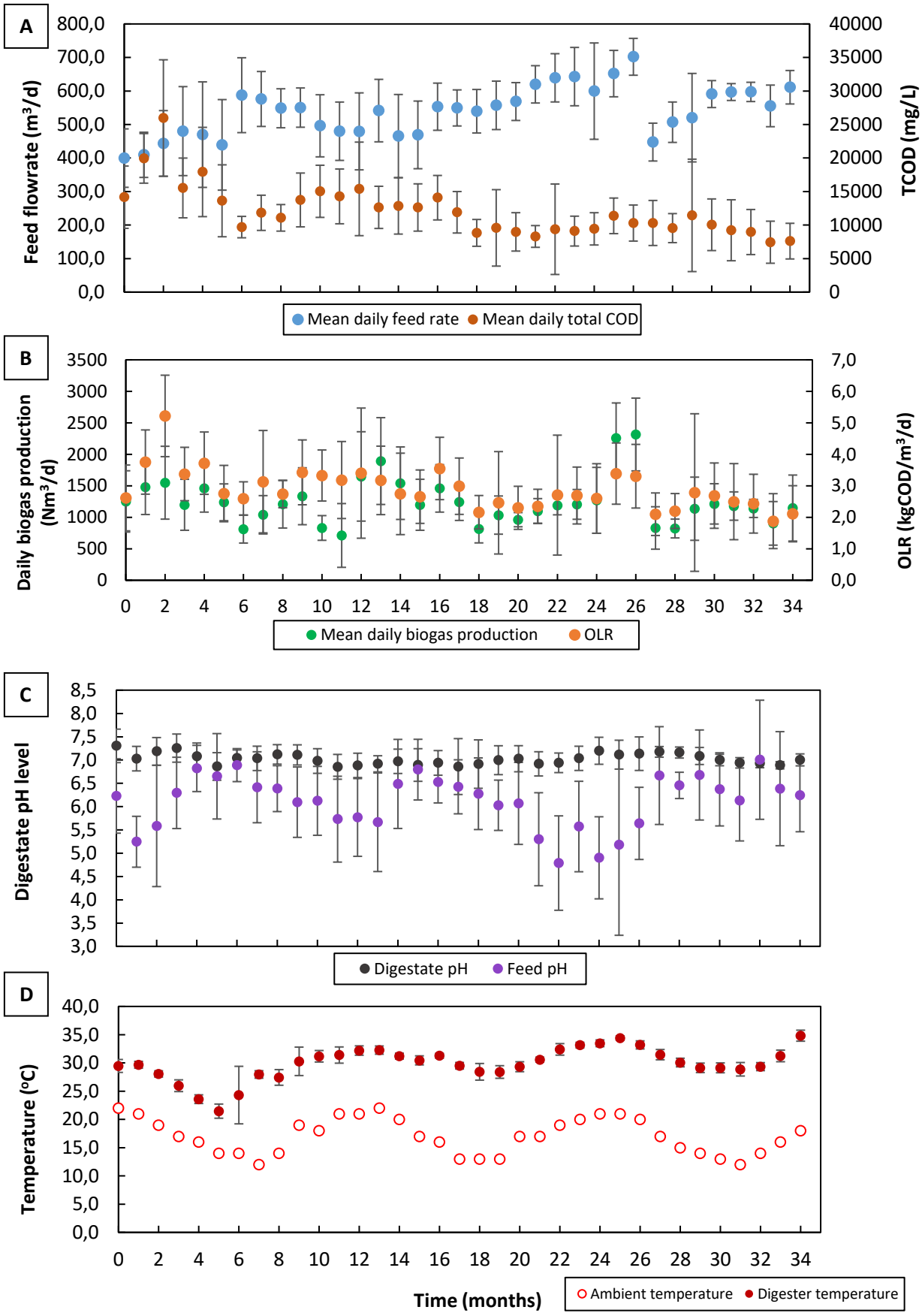


Figure 25: full-scale operational data for Plant 3; (a) feed flow vs. feed TCOD, (b) biogas production vs. OLR, (c) digestate and feed pH levels, (d) ambient and digester temperatures. Error bars indicate the standard deviations for a sample size of $n$ = 22.

## 5.3. Bench-scale results

The following section provides and discusses the experimental results obtained from bench-scale tests (500 mL) performed under standardised BMP test conditions. Bench-scale data included cumulative biogas and methane productions, yields and AD performance indicators determined for different feedstock samples collected from Plant 1 (mixed organic wastes), Plant 2 (tomato waste) and Plant 3 (distillery wastes). Bench-scale results were then evaluated on their ability to predict the performances of the full-scale systems.

### *5.3.1. AD Plant 1: Co-digestion of mixed organic wastes*

#### *5.3.1.1. BMP test results*

Cumulative biogas and methane curves are presented in Figure 26 (ab), determined from BMP tests performed on the following mixtures (M): M1 (apples & food waste), M2 (food waste, spices & beer), M3 (food waste, spices, beer, cow blood & manure), M4 (chocolate waste, beer, sugar & cow blood) and M5 (food waste, beer, fruit juice and cow blood).

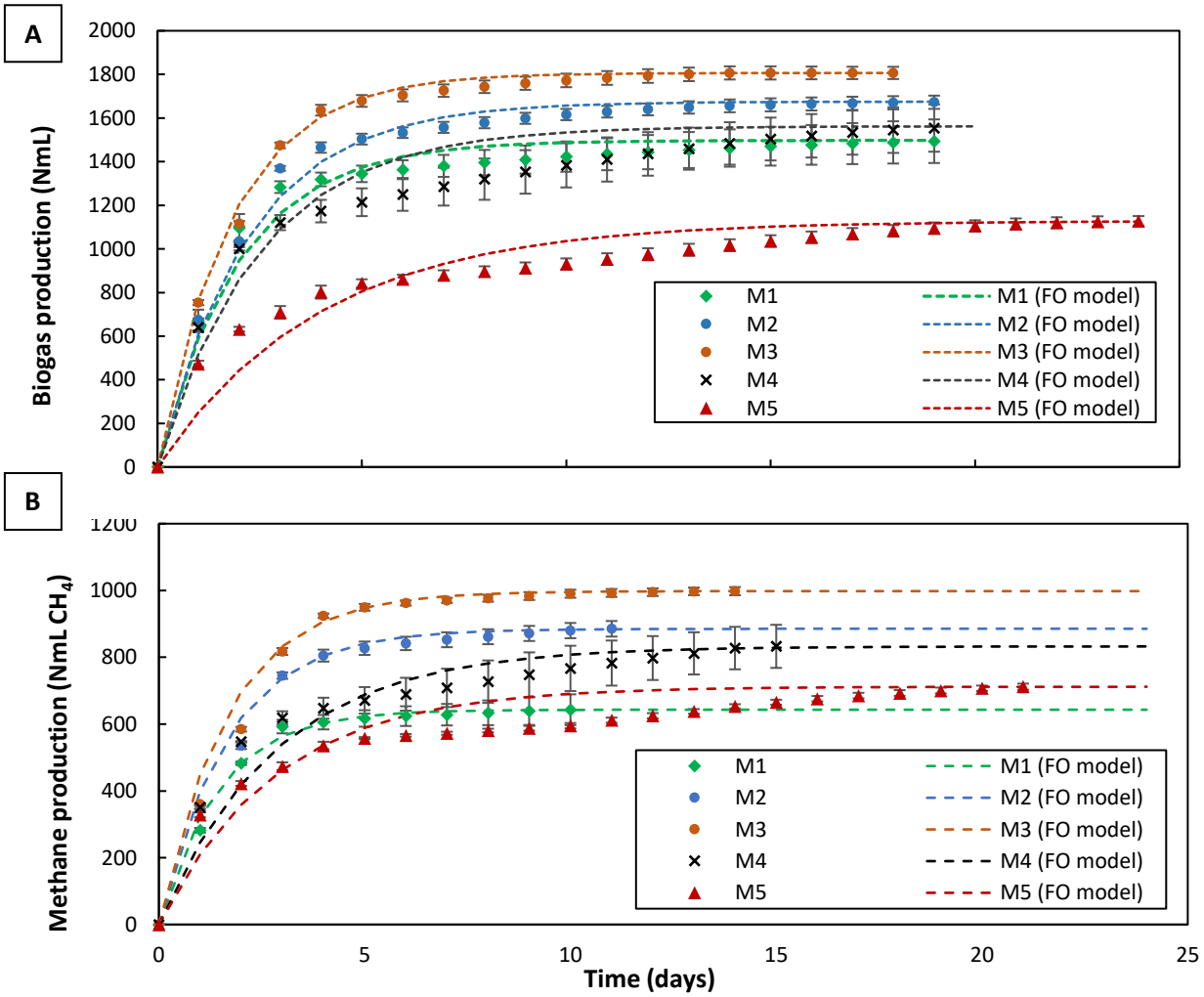


Figure 26: BMP gas production curves for Plant 1 feedstock mixtures; (a) cumulative biogas production, (b) cumulative methane production. Error bars indicate the standard deviations for a sample size of *n* = 3.

The bench-scale experimental data for the respective feedstock mixtures allowed for the determination of HRT, disintegration constants ($k_{dis}$), specific gas yields (SGY) and BMP. This data is summarised in Table 16 below.

Table 16: Summary of BMP assay test data for Plant 1's feedstock mixtures.

| Mixture | Reaction kinetics | | Biogas production | | Methane production | | $CH_4$ content (% vol) |
|---|---|---|---|---|---|---|---|
| | HRT [a] (days) | $k_{dis}$ [b] (1/day) | Cumulative volume (NmL) | SGY [c] (NL/kgVS) | Cumulative volume (NmL $CH_4$) | BMP [d] (NL $CH_4$/kgVS) | |
| 1 | 20 | 0.70 | 1498 ± 103.8 | 699 ± 53.2 | 643 ± 46.1 | 292 ± 23.6 | 41.9+ ± 2.32 |
| 2 | 20 | 0.60 | 1672 ± 30.41 | 793 ± 15.7 | 885 ± 23.3 | 418± 12.0 | 52.7 ± 1.30 |
| 3 | 18 | 0.60 | 1807 ± 30.26 | 878 ± 15.8 | 998 ± 12.2 | 480 ± 6.33 | 55.1 ± 0.27 |
| 4 | 20 | 0.35 | 1562 ± 112.7 | 716 ± 56.6 | 833 ± 64.5 | 379 ± 32.4 | 52.9 ± 0.61 |
| 5 | 24 | 0.35 | 1128 ± 22.49 | 645 ± 14.3 | 712 ± 9.10 | 372 ± 5.80 | 57.7 ± 1.16 |

[a] : hydraulic retention time; [b] : disintegration constant; [c] : specific gas yield; [d] : biomethane potential

The results presented in Table 16 indicate that Mixture 1 resulted in the lowest BMP of 292.4 ± 23.6 NL $CH_4$/kgVS. The mixture ratio of apples to food waste was roughly 2: 3 on a total solids basis, based on TS contents of 13% (w/w) for apples and 31% (w/w) for food waste as analysed by Kell (2019). Compared to other studies, Mu *et al*. (2019) obtained an SMY of 336 NL/kgVS from bench-scale AD tests performed on apples and food wastes using the same mixing ratio (2: 3 TS basis). Kell (2019) reported a much lower BMP and methane content of 2.51 NL $CH_4$/kgVS and 5.80 %vol for a 50:50 apples and food waste mixture, respectively, because of the large concentrations of VFA produced during the BMP test runs. Moreover, lower BMPs may have arisen from the inability of anaerobes to break down lignocellulosic components present in apples and food wastes (Goswami & Kreith, 2008; FNR, 2012; Yang *et al*., 2015; Abraham *et al*., 2020).

Mixture 3 (food waste, spices, beer and cow blood & manure) resulted in the largest BMP of 480 ± 6.33 NL $CH_4$/kgVS compared to Mixtures 2 to 5. It was not clear whether the presence of expired spices negatively impacted biogas production rates for certain mixtures, but one study reported that salt (sodium chloride) concentrations exceeding 12 g/L could induce inhibitory effects towards anaerobic digestion (Li *et al.* 2018). Again, the concentrations of spices/salts contained in certain mixtures were not determined in this study. A Student's t-test for unequal population variances verified that specific gas yields obtained for Mixture 3 were significantly different than specific gas yields obtained for Mixtures 2 to 5 ($p<0.05$). Mixture 3 was the only mixture to contain cow manure, which has shown to enhance methane yields during co-digestion (Li *et al*., 2021). The C:N ratio of Mixture 3 was also obtained as 15.8, which falls within the desirable C:N ratio range of 15 to 30 for co-digestion mixtures containing cow manure (Font-Palma, 2019). These BMP test results suggest that, if feedstock mixtures fed to Plant 1's digester were blended with cow manure, full-scale methane yields and productivities would improve but this strategy would require improving the control of feeding rates to the full-scale system.

Additionally, Mixtures 2 to 5 contained large quantities of beer, which contains small concentrations of unfermented sugars, extractives, water and alcohols. Anaerobic bacteria would rapidly break down these sugars and alcohols to produce acetates, which are utilized by methanogens to produce methane (Speece, 1996; Zhu *et al.*, 2011). Therefore, AD of beer could have improved methane yields due to the boost in acetates production.

To validate the experimental results determined from BMP tests, relative standard deviations (RSD) were calculated, as recommended by Holliger *et al.* (2016). The RSD provides an indication of how certain data points are scattered around their mean values. Validating BMP values was important because, as discussed by Holliger *et al.* (2016), large variations in triplicate tests could arise. Mean BMP data, standard deviations and RSD computations are given in Table 17.

Table 17: Data validation criteria for Plant 1 BMP assay tests.

| Mixture | BMP [a] (NL $CH_4$/kgVS) | RSD [b] | RSD > 10%? | Accept/Reject result |
|---|---|---|---|---|
| 1 | 292 ± 23.6 | 8.08% | No | Accept |
| 2 | 418 ± 12.0 | 2.87% | No | Accept |
| 3 | 480 ± 6.33 | 1.32% | No | Accept |
| 4 | 379 ± 32.4 | 8.56% | No | Accept |
| 5 | 372 ± 5.80 | 1.56% | No | Accept |

[a] : biomethane potential; [b] : relative standard deviation

For heterogenous substrates BMP test results should be rejected if the RSD exceeds 10% (Holliger *et al.*, 2016). The BMP results shown in Table 17 are satisfactory with these validation criteria and are thus not rejected. Moreover, positive control tests yielded an SGY and BMP of 697.8 ± 11.80 NL/kgVS and 331.2 ± 6.195 NL $CH_4$/kgVS, respectively, with the BMP being satisfactory with the literature-derived BMP of 350 ± 29 NL/kgVS for micro-crystalline cellulose (Holliger *et al.*, 2016).

The AD efficiencies for each BMP test were evaluated by analyzing the composition of final digestate samples collected from each test. These analyses included the final digestate pH level, final total solids (TS) content, final volatile solids (VS) content and the VS reduction (VSR), given in Table 18 below.

Table 18: Performance parameters for BMP tests performed on Plant 1 feedstocks.

| BMP test | Mixture pH | | Final/Digestate pH | Total solids (% w/w) | | Volatile solids (% w/w) | | |
|---|---|---|---|---|---|---|---|---|
| | Initial | Adj. | | Initial [a] | Final | Initial | Final | VSR [b] (%) |
| Blank | 7.48 | - | 7.43 ± 0.07 | 1.67 ± 0.02 | 1.34 ± 0.14 | 1.01 ± 0.03 | 0.815 ± 0.06 | 19.5 |
| M1 | - | - | 7.81 ± 0.03 | 15.5 ± 0.98 | 1.00 ± 0.24 | 14.7 ± 0.95 | 0.698 ± 0.07 | 95.9 |
| M2 | 4.56 | 6.99 | 7.95 ± 0.06 | 25.9 ± 0.37 | 1.62 ± 0.33 | 12.1 ± 0.38 | 0.816 ± 0.11 | 94.0 |
| M3 | 4.77 | 7.05 | 7.90 ± 0.10 | 18.4 ± 0.18 | 1.56 ± 0.03 | 9.48 ± 0.20 | 0.761 ± 0.01 | 92.7 |
| M4 | 5.86 | 7.16 | 7.84 ± 0.12 | 39.0 ± 0.33 | 1.19 ± 0.20 | 38.7 ± 0.33 | 0.803 ± 0.04 | 98.7 |
| M5 | 6.36 | 7.01 | 7.45 ± 0.06 | 30.0 ± 2.71 | 1.32 ± 0.22 | 22.9 ± 2.28 | 0.795 ± 0.004 | 97.3 |

[b] : volatile solids reduction

The final pH values of digestate samples extracted from each mixture BMP test ranged pH 7.43 to 7.95, as shown in Table 25. This range falls within the stable pH range of 7.0 to 8.5, as recommended by digestate quality standards (Raposo *et al*., 2012; Holliger *et al*., 2016). It was only mixtures M2 and M3 where the pH levels rose by 0.42 and 0.47, respectively, possible due to free-ammonia formation due to each mixtures' low C:N ratios (Table 10) (Raposo *et al*., 2012).

The VS reductions (VSR) for each BMP test bottle were calculated using Equation (5) to determine the quantity of organic material converted to biogas during AD. As shown in Table 18 the VSR ranged 92.7% (M3) to 98.7% (M4). The VSRs given in Table 18 are greater than what has been reported by other studies; Wang *et al*. (2020) reported a VSR range of 71% to 79% from the co-digestion of pig manure, food waste and seed sludge in 2.0L batch tests. Lee *et al*. (2015) reported a VSR range of 41% to 64% from food waste leachate and animal manure feedstocks co-digested in full-scale AD plants. The VSRs for each BMP mixture tests indicate a high conversion of organic solids to biogas, which may have been due to well acclimatized nature of Plant 1's inoculum. Reportedly, the feeding of multiple feedstocks to an AD reactor promotes greater diversification in microbial populations, subsequently increasing their metabolic activities and degradation capabilities (Rabii *et al.,* 2019; Kim *et al.*, 2018).

#### *5.3.1.2. Bench-scale results as predictors of full-scale performance*

(a) BMP degradation rates (BDR)

Experimental data obtained from BMP tests Plant 1 feedstock mixtures (Table 16 and Table 18) were used to predict relevant full-scale performance parameters of Plant 1. BMP test data was used to compute BMP degradation rates (BDR) and full-scale biogas and methane production rates using methods propsoed by Schievano *et al.* (2011), Holliger *et al.* (2017) and Fiore *et al.* (2016).

The calculation of BDR was defined in Section 2.3.2.2, which gives an indication of how much organic material is converted to biomethane potential during AD in BMP tests. BDRs calculated for Plant 1 feedstock mixtures are compared with VS reductions, as shown in Figure 27.

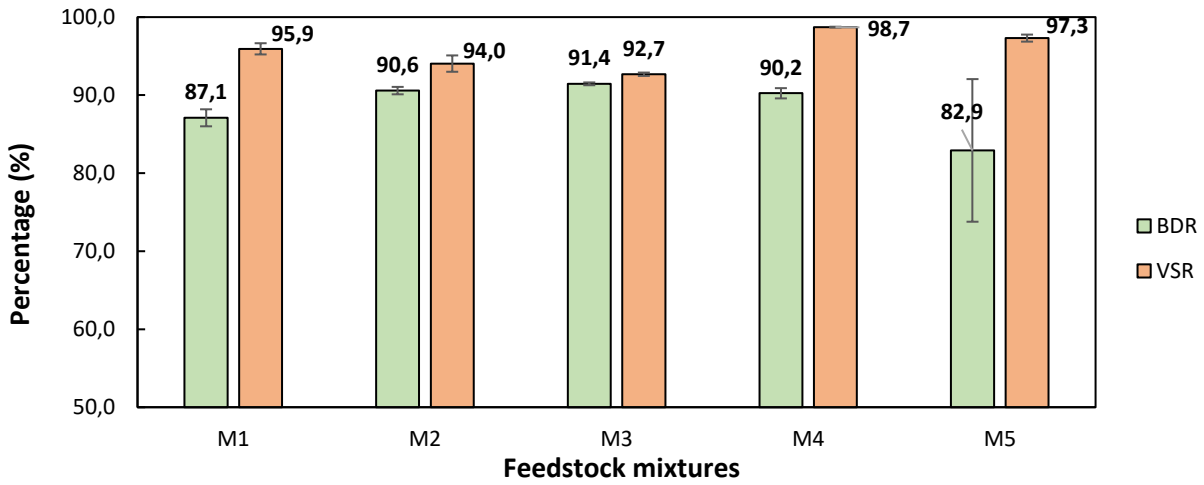


Figure 27: comparison of BMP degradation rates (BDR) and VS reductions (VSR) for Plant 1 feedstock mixtures.

The calculated BDRs shown in Figure 27 ranged from 87% to 91% for the given feedstock mixtures. These percentages essentially provide quantitative and qualitative estimations of how much total organic material was converted to methane gas during AD. That is, 87% to 91% of the organic material contained in each feedstock was converted to methane gas. The obtained VSR range of 91% to 99% was greater than the BDR range, indicating that most organic material was converted to biogas and not biomethane potential. Compared to other studies, Schievano *et al*. (2011) calculated a greater BDR range (87 to 93%) than VSRs (70 to 79%) for three full-scale co-digestion plants. Li *et al*. (2017) compared VS and BMP degradation rates measured from BMP tests for four different full-scale plants treating poultry manure, kitchen waste and the organic fraction of municipal solid waste (OFMSW). All four plants reflected a VSR of 50% to 80%, while BDRs ranged from roughly 72% to 90% (Li *et al*., 2017).

Therefore, for Plant 1, the VSR range was greater than the calculated BDR range because of more recalcitrant components contained in each feedstock mixture duirng BMP tests. Feedstocks containing lignocellulosic materials are inhibitory towards methane production (Jingura & Kamusoko, 2017), and thus produced biogas from BMP tests would have a lower methane concentration. This is supported by full-scale operational data for Plant 1 given in Figure 24 (a-d), which shows the variations in mean daily biogas and methane productions with time. From the 28-week period, mean methane content was calculated as 36 ± 17.5 %vol, which does not fall within the typical methane composition of biogas of 50 to 75 %vol (Al-Saedi *et al*., 2008; FNR, 2012; Jingura & Kamusoko, 2017). Ultimately, the BDR range provided a more quantitative and qualitative measurement of AD efficiency but under ideal BMP test conditions. As such, it was not possible to use bench-scale BDRs to approximate full-scale behaviour.

(b) Extrapolation method

Bench-scale datasets previously given in Table 16 for all 5 feedstock mixtures were used to predict the daily biogas production rates and specific gas yields (SGY) of Plant 1 using the extrapolation method proposed by Holliger *et al*. (2017). However, because feedstock mixtures were collected over 5 days, predictions of full-scale performance were done over the same period. Table 19 shows operational data for Plant 1 collected over the respective 5-day period. Note the datasets below do not form part of operational datasets previous given in Figure 24 (a-d).

Table 19: Full-scale operational data obtained from AD Plant 1 over 5 days.

| Date | Feedstock mixture | Digester monitoring | | Biogas monitoring | | Methane flow [a] | |
|---|---|---|---|---|---|---|---|
| | | Full-scale feed rate ($m^3$/d) | Feed VS content (% w/w) [b] | Gas flow count ($Nm^3$/d) | Power count (kWh/d) | Production ($Nm^3$ $CH_4$/d) | Content (%vol) |
| 30-Jan-21 | 1 | 9 500 | 14.8 ± 0.953 | 820 | 481 | 318 | 38.8 |
| 31-Jan-21 | 2 | 21 000 | 12.1 ± 0.384 | 1000 | 491 | 325 | 32.5 |
| 01-Feb-21 | 3 | 17 500 | 9.48 ± 0.202 | 658 | 510 | 337 | 51.3 |
| 02-Feb-21 | 4 | 16 500 | 38.7 ± 0.326 | 873 | 511 | 338 | 38.7 |
| 25-Jan-21 | 5 | 27 000 | 22.9 ± 2.28 | 566 | 489 | 323 | 57.1 |

[a] : calculated from power count value (calculations shown in Appendix B3); [b] : VS compositions determined in the laboratory

Full-scale performance parameters such as daily biogas and methane productions and yields were calculated using Equation (11) using data presented in Table 19, specifically full-scale feed rates, feed VS content and specific gas and methane yields determined from BMP tests. Actual and predicted full-scale performance parameters are compared in Table 20.

Table 20: Estimated gas production rates and yields for Plant 1 feedstock mixtures.

| **Biogas productions and yields** | | | | |
|---|---|---|---|---|
| **Feedstock mixture** | **Full-scale data [a]** | | **Calculated full-scale data [b]** | |
| | **Biogas production ($Nm^3/d$)** | **SGY (NL/kgVS)** | **Biogas production ($Nm^3/d$)** | **SGY (NL/kgVS)** |
| Mixture 1 | 820 | 585 ± 38.3 | 979 | 699 ± 53.2 |
| Mixture 2 | 1000 | 392 ± 12.3 | 2023 | 793 ± 15.7 |
| Mixture 3 | 658 | 396 ± 8.36 | 1457 | 878 ± 15.8 |
| Mixture 4 | 873 | 137 ± 1.14 | 4576 | 716 ± 56.6 |
| Mixture 5 | 566 | 91.4 ± 8.89 | 3996 | 645 ± 14.3 |
| **Methane productions and yields** | | | | |
| **Feedstock mixture** | **Full-scale data** | | **Calculated full-scale data** | |
| | **Methane production ($Nm^3/d$)** | **SMY (NL $CH_4$/kgVS)** | **Methane production ($Nm^3/d$)** | **SMY (NL $CH_4$/kgVS)** |
| Mixture 1 | 318 | 227 ± 14.9 | 410 | 372 ± 23.6 |
| Mixture 2 | 325 | 127 ± 4.00 | 1065 | 418 ± 12.0 |
| Mixture 3 | 337 | 203 ± 4.29 | 797 | 480 ± 6.33 |
| Mixture 4 | 338 | 52.9 ± 0.44 | 2420 | 379 ± 32.4 |
| Mixture 5 | 323 | 52.2 ± 5.08 | 2305 | 372 ± 5.79 |

[a] : Real-time full-scale data obtained from Plant 1; [b] : estimated full-scale performance parameters calculated from Equation (11) (Holliger *et al.,* 2017).

All calculated full-scale performance parameters given Table 20 (biogas & methane production rates and yields) were greater than actual full-scale performance data obtained from industrial operations of Plant 1, which suggest that the performance of Plant 1 was overestimated. Regarding gas yields, single-factor ANOVA tests (5.0% significance level) confirmed that actual and estimated SGYs were not significantly different from each other ($p = 0.11, > 0.05$), while SMYs were significantly different ($p << 0.05$), the latter being attributed to the different methane concentrations of produced biogas from the bench- and full-scale systems. Results from ANOVA tests are given in Table 44 (Appendix A).

These overestimations were quantified as scale factors, i.e. the ratios of real-time full-scale performance data to estimated full-scale performance data, where performance was expressed in terms of specific gas and methane yields (SGY & SMY). Figure 28 compares calculated scale factors for each feedstock mixture, specifically for specific gas and methane yields presented in Table 20. The full-scale OLR is also given for each mixture.

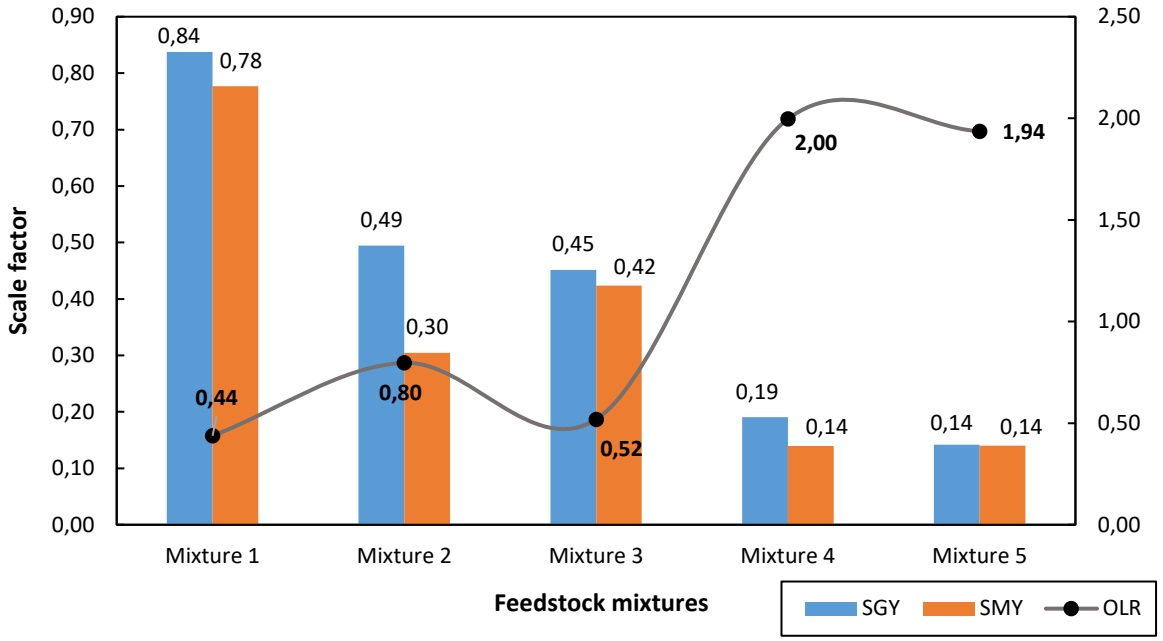


Figure 28: Calculated scale factors for Plant 1 feedstock mixtures, with corresponding organic loading rates.

In Figure 28 the full-scale specific gas and methane yields were roughly 14% to 84% and 14% to 78% of the calculated yields, as determined from Equation (11). These percentages essentially quantify the deviations between ideal BMP test conditions and full-scale conditions established for Plant 1, where the most notable difference was attributed to differences in process volumes. Due to the large volume of Plant 1's digester (3200m$^3$), there is a risk of inadequate mixing of the digester's contents. Inadequate mixing may also be factor of Plant 1's digester being oversized, however this effect was deemed negligible given the large mean HRT) of 213 days previously calculated from feed rate data in Figure 24 (a). Instead, inadequate mixing may have been due to the feeding of complex and non-homogenised material to Plant 1's digester (Kariyama *et al.,* 2018). For example, food waste fed to the Plant 1 contained large pieces of watermelon peels, pineapple tops and fruit skins that clogged the feed line on a regular basis. Highly particulate, non-homogenised feedstocks will restrict the availability of nutrients to anaerobic populations (Aldin *et al.,* 2011). In contrast, feedstock mixtures were homogenised for BMP tests to ensure maximum accessibility of nutrients to microbial populations.

The OLR for each feedstock mixture were also presented in Figure 28, where it appears that the deviations between bench- and full-scale process conditions worsened with increased OLR. When more organic material of different varieties is introduced into the 3200 m$^3$ digester, anaerobic populations are constantly exposed to changing environments. As such, these microbial communities are constantly acclimatising to the newly-fed material which ultimately affects their culture performance and their abilities to convert organic material to biogas (Akram & Stuckey, 2008; Lara *et al*., 2006). In contrast, BMP tests were loaded with finite quantities of feedstock mixture where organic loading was not varied. Overall, considering these scale-up effects, biogas and methane productivities and yields were greater in BMP tests than what was measured for the full-scale system (Koch *et al.*, 2020).

In addition to the scale factor ranges shown in Figure 28, a cumulative scale factor was determined from full-scale data spanning the 5-day period. Actual/Full-scale and calculated cumulative productions and gas yields are compared below in Figure 29.

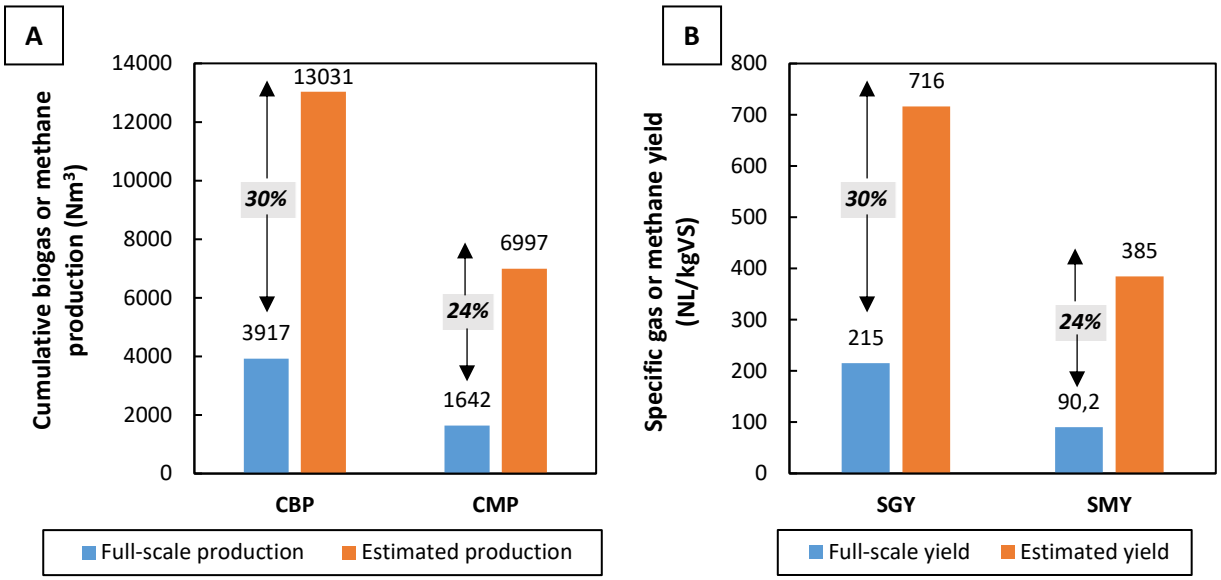


Figure 29: Comparison of full-scale and calculated (a) cumulative biogas and methane productions (CBP & CMP) and (b) specific gas and methane yields (SGY & SMY) for Plant 1.

Referring to Figure 29, the full-scale CBP/SGY and CMP/SMY were 30% and 24% of their calculated values, respectively. These scale factors further emphasize the transient effects encountered in the full-scale AD process over the 5-day period, specifically the scale-up of process volumes and variations in feeding rates and feed compositions.

Holliger *et al*. (2017) performed a similar study on co-digestion AD plants, where a scale factor range of 89% to 94% was obtained, based on the comparison of bench- and full-scale SMYs. However, the study adopted a different approach for bench-scale experiments, where BMP tests were performed on individual feedstock materials sourced from the relevant full-scale plants. The specific methane yields of full-scale feedstock mixtures were then estimated using the sum of individual feedstock BMP values using Equation (10). For Plant 1, BMP values were measured from feedstock mixtures to best represent the feed streams fed to the system but calculated scale factors were much lower (0.24 to 0.30) than what Holliger *et al.* (2017) reported. This was because only 5-days' worth of full-scale data from Plant 1 was obtained, as opposed to Holliger *et al.* (2017) who compared bench-scale results to 37-weeks' worth of data.

(c) CSTR/Dynamic model

As a comparison to the method proposed by Holliger *et al.* (2017), a continuous-stirred tank reactor (CSTR) dynamic model (Fiore *et al*., 2016) was utilized to estimate the performance of Plant 1. The CSTR model differs from the method investigated by Holliger *et al*. (2017) because it includes reaction kinetics data measured from BMP tests. Table 21 shows the required input variables for computing the model.

Table 21: Input variables required for dynamic modelling of Plant 1's performance.

| Feedstock mixture | Full-scale data | | Bench-scale/BMP test data | | |
|---|---|---|---|---|---|
| | Feed rate ($m^3/d$) [a] | VS content ($kg/m^3$) [b] | Disintegration rate (1/day) | SGY (NL/kgVS) [c] | BMP (NL $CH_4$/kgVS) [d] |
| 1 | 9 500 | 0.44 ± 0.03 | 0.70 | 699 ± 53.2 | 292 ± 23.6 |
| 2 | 21 000 | 0.80 ± 0.02 | 0.60 | 793 ± 15.7 | 418 ± 12.0 |
| 3 | 17 500 | 0.52 ± 0.01 | 0.60 | 878 ± 15.8 | 480 ± 6.33 |
| 4 | 16 500 | 2.00 ± 0.02 | 0.35 | 716 ± 56.6 | 378 ± 32.4 |
| 5 | 27 000 | 1.94 ± 0.19 | 0.35 | 645 ± 14.3 | 372 ± 5.80 |

[a] : Total mass feed rates for each mixture; [b] : VS mass per digester volume; [c] specific gas yield; [d] biomethane potential.

The data given in Table 21 served as inputs for the dynamic model, which was solved using MATLAB® and Simulink software. The Simulink diagram is given as Figure 63 under Appendix C. Estimated full-scale performance parameters are compared with actual/full-scale performance parameters, as given in Table 22.

Table 22: Actual and dynamically modelled performance parameters for Plant 1.

| **Biogas productions and yields** | | | | |
|---|---|---|---|---|
| Feedstock mixture | Full-scale data [a] | | Dynamically modelled data [b] | |
| | Biogas production ($Nm^3/d$) | SGY (NL/kgVS) | Biogas production ($Nm^3/d$) | SGY (NL/kgVS) |
| Mixture 1 | 820 | 585 | 541 | 386 |
| Mixture 2 | 1000 | 392 | 1111 | 436 |
| Mixture 3 | 658 | 396 | 786 | 474 |
| Mixture 4 | 873 | 137 | 1493 | 234 |
| Mixture 5 | 566 | 91.4 | 1304 | 211 |
| **Methane productions and yields** | | | | |
| Feedstock mixture | Full-scale data | | Dynamically modelled data | |
| | Methane production ($Nm^3/d$) | SMY (NL $CH_4$/kgVS) | Methane production ($Nm^3/d$) | SMY (NL $CH_4$/kgVS) |
| Mixture 1 | 318 | 227 | 226 | 205 |
| Mixture 2 | 325 | 181 | 586 | 230 |
| Mixture 3 | 337 | 339 | 430 | 259 |
| Mixture 4 | 338 | 57.8 | 790 | 124 |
| Mixture 5 | 323 | 79.2 | 752 | 121 |

[a] : Real-time full-scale data obtained from Plant 1; [b] : dynamically-modelled full-scale performance parameters calculated from Equation (12) (Fiore *et al.,* 2016).

As shown in Table 22, the dynamic model overestimated the performance of Plant 1 for feedstock Mixtures 2, 3, 4 and 5. For these mixtures, the scale factor ranges for daily biogas production and daily methane productions were calculated as 0.43 to 0.90 and 0.43 to 0.79, respectively. The scale factors indicate that full-scale daily biogas productions and methane productions were roughly 43% to 90% and 43% to 79% of the dynamically modelled productions, respectively. It was only for Mixture 1 that the dynamic model underestimated full-scale biogas and methane productions by 152% and 141%, respectively. These underestimations may have been due to the specific gas yields (699 ± 53.2 NL/kgVS), disintegration constants (0.70 1/day) and BMP values (292 ± 23.6 NL $CH_4$/kgVS) obtained from Mixture 1 during BMP tests. Given that the disintegration constant was the largest for Mixture 1 compared to the

other feedstock mixtures (0.35 to 0.60 1/day) along with its SGY and BMP values, the dynamical model outputted a daily biogas and methane productions lower than actual production rates according to Equation (12).

Because the scale factor ranged reflected an over- and underestimation of full-scale performance, a cumulative scale factor was calculated from the results given in Table 22. Actual/Full-scale and calculated cumulative productions and gas yields are compared below in Figure 30.

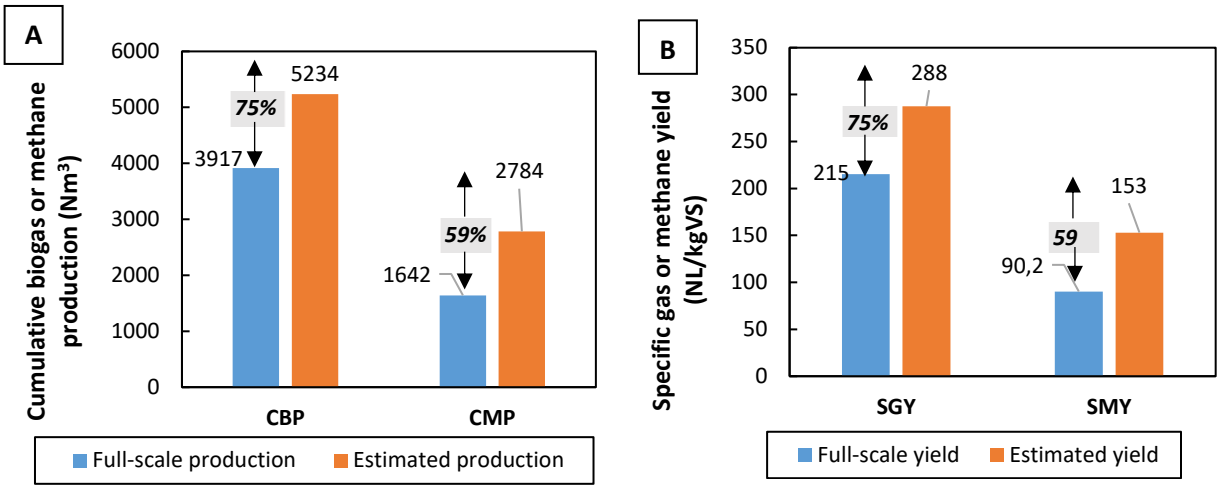


Figure 30: Comparison of full-scale and dynamically-modelled (a) cumulative biogas and methane productions (CBP & CMP) and (b) specific gas and methane yields (SGY & SMY) for Plant 1.

The results graphically shown in Figure 30 indicate that full-scale performance was better estimated over the cumulative 5-day operating period. The dynamic model approximated full-scale daily biogas production/SGY and daily methane production/SMY as 75% and 59% of the performance parameters measured under ideal BMP test conditions, respectively. Single-factor ANOVA tests (5.0% significance level) confirmed that there were significant differences between actual and estimated SGYs ($p = 0.003$, $< 0.05$) and for SMYs ($p = 0.002$, $<0.05$). These results are given in Table 45 (Appendix A).

The scale factor ranges obtained by the methods proposed by Holliger *et al*. (2017) and Fiore *et al*. (2016) are compared in Figure 31 for each feedstock mixture. On average, scale factors using the dynamic model were roughly 51% greater than the factors calculated from the extrapolation method. Therefore, the dynamic model approximated full-scale performance and conditions more similar towards ideal BMP test conditions than the use of the extrapolation method. This was because the BMP tests' disintegration constants exhibited reaction kinetics of feedstocks with a highly particulate nature, as per one of the dynamic model's assumptions specified under Section 2.3.2.2 (b) (Fiore *et al*., 2016). The extrapolation method does not consider the reaction kinetics prevalent in bench-scale tests, which is important for making approximations on the rates of biogas and methane productions. Therefore, it is recommended to employ the dynamic model for industrial use than the extrapolation method, however, more BMP tests should be carried out to assess the reaction kinetics and methane potentials of more feedstock mixture combinations.

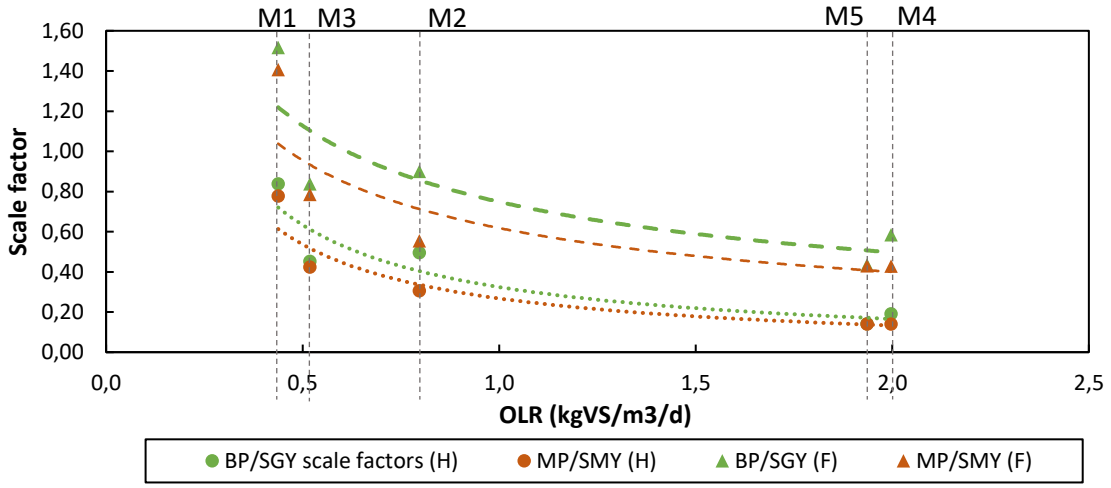


Figure 31: Comparison of scale factors determined for Plant 1; using the extrapolation (denoted as *H*) and dynamic modelling methods (denoted as *F*), for a range of organic loading rates.

### *5.3.2. AD Plant 2: Tomato waste (TW)*

#### *5.3.2.1. BMP test results*

BMP assay tests were performed on TW samples that were collected over a duration of 3 months. Cumulative biogas and methane production curves are plotted in Figure 32 (ab).

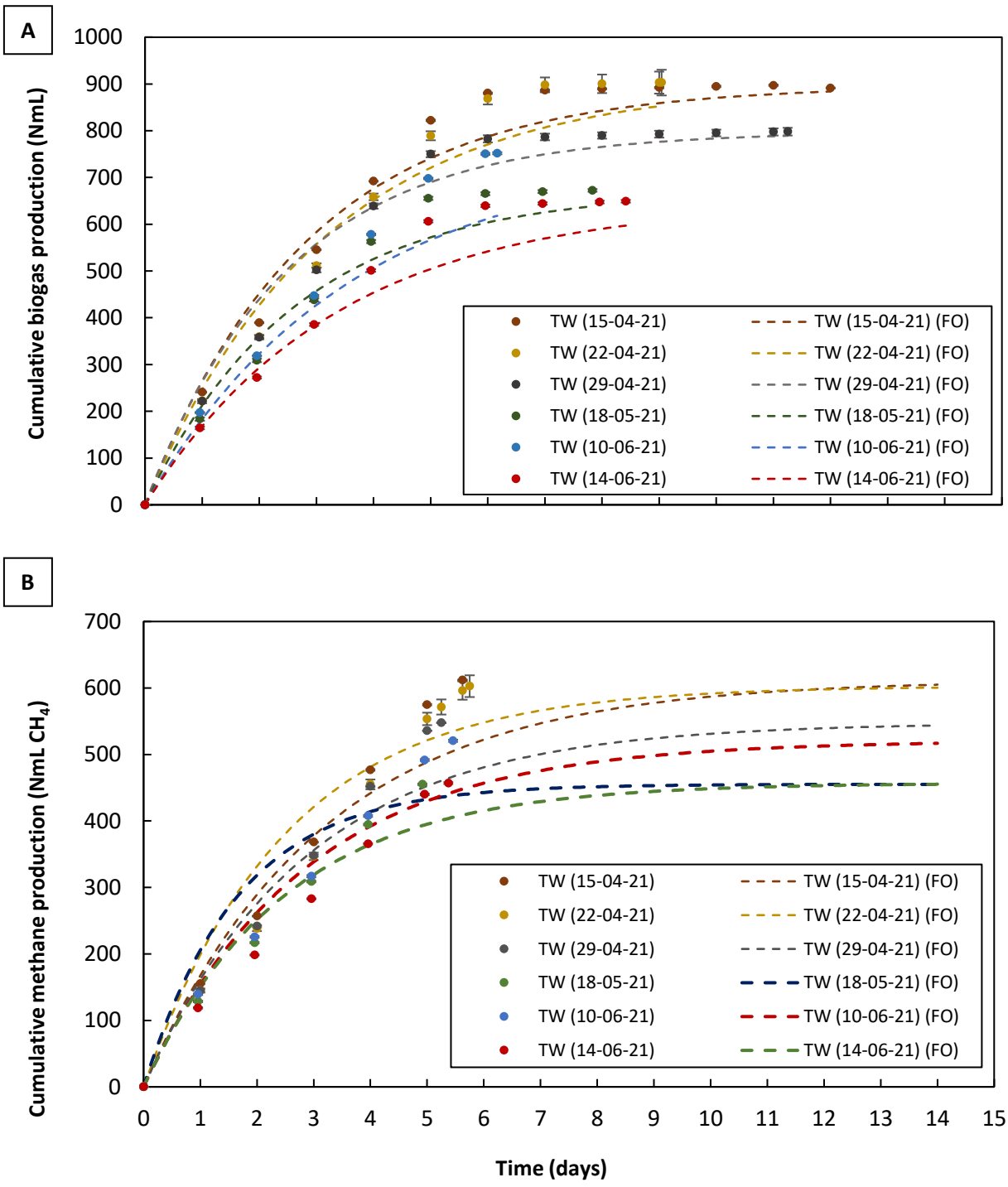


Figure 32: BMP gas production curves for tomato waste samples collected from Plant 2; (a) cumulative biogas production, (b) cumulative methane production. Error bars indicate the standard deviations for a sample size of $n$ = 3.

FO kinetic models were fitted to the cumulative biogas and methane production curves to obtain disintegration kinetic constants. It was observed that daily methane productions in Figure 32 (b) stopped after roughly 5.8 days of incubation time, while biogas productions shown in Figure 32 (a) continued to day 12. Larger volumes of biogas are registered by the AMPTS II system than methane volumes because of the presence of more components ($CO_2$) in produced biogas, and thus the gaseous mixture had a greater partial pressure as opposed to the "pure" methane stream exiting the $CO_2$ adsorption units (label 7 in Figure 14). Biogas and methane production data obtained from BMP tests are summarised in in Table 23 below:

Table 23: Summary of BMP assay test data for tomato waste (TW) samples collected from Plant 2.

| TW sample | Reaction kinetics | | Biogas production | | Methane production | | $CH_4$ content (% vol) |
|---|---|---|---|---|---|---|---|
| | HRT [a] (days) | $k_{dis}$ [b] (1/day) | Cumulative volume (NmL) | SGY [c] (NL/kgVS) | Cumulative volume (NmL $CH_4$) | BMP [d] (NL $CH_4$/kgVS) | |
| 15-April-21 | 11.0 | 0.35 | 897 ± 17.3 | 652 ± 15.1 | 612 ± 13.3 | 456 ± 11.6 | 70.0 ± 0.26 |
| 22-April-21 | 9.04 | 0.32 | 903 ± 35.9 | 664 ± 31.4 | 603 ± 76.4 | 453 ± 67.0 | 68.2 ± 7.33 |
| 29-April-21 | 11.3 | 0.40 | 798 ± 12.6 | 554 ± 10.8 | 548 ± 10.6 | 392 ± 9.03 | 70.8 ± 0.64 |
| 18-May-21 | 7.83 | 0.38 | 673 ± 3.13 | 509 ± 2.73 | 455 ± 1.65 | 346 ± 1.44 | 68.0 ± 0.10 |
| 10-June-21 | 6.17 | 0.28 | 752 ± 4.24 | 617 ± 3.89 | 521 ± 2.70 | 427 ± 2.48 | 69.2 ± 0.11 |
| 14-June-21 | 8.42 | 0.30 | 649 ± 12.7 | 507 ± 11.4 | 457 ± 6.44 | 361 ± 5.80 | 71.2 ± 5.80 |

[a] : hydraulic retention time; [b] : disintegration constant; [c] : specific gas yield; [d] biomethane potential.

The biogas and methane production volumes were consistent for all periodically-collected TW samples assessed in BMP tests. The methane concentrations in Table 23 ranged 68% to 71% by volume, which suggests there may have been an excess of hydrogen in the feed as according to the stoichiometric mass balance below occurring during anaerobic digestion:

$$\mathrm{CH_{2.8}O_{0.6}} \rightarrow 0.7\mathrm{CH_4}(g) + 0.3\mathrm{CO_2}(g) \tag{29}$$

As previously mentioned in Section 4.1.2.1, Plant 2 feeds additional alcohol/beer wastewater into the tomato waste holding tank. It is possible that the addition of this waste stream may have introduced more hydrogen into the feedstock, and the concentration of hydrogen may not have been reflected in volatile solids analyses. However, these statements are speculative because compositional analyses were not performed on the alcohol wastewater.

Referring to Table 23, each TW sample had a different initial volatile solids content (% w/w), giving slight variations in methane yields. Figure 33 shows the relationship between VS content and resulting BMPs for different TW samples:

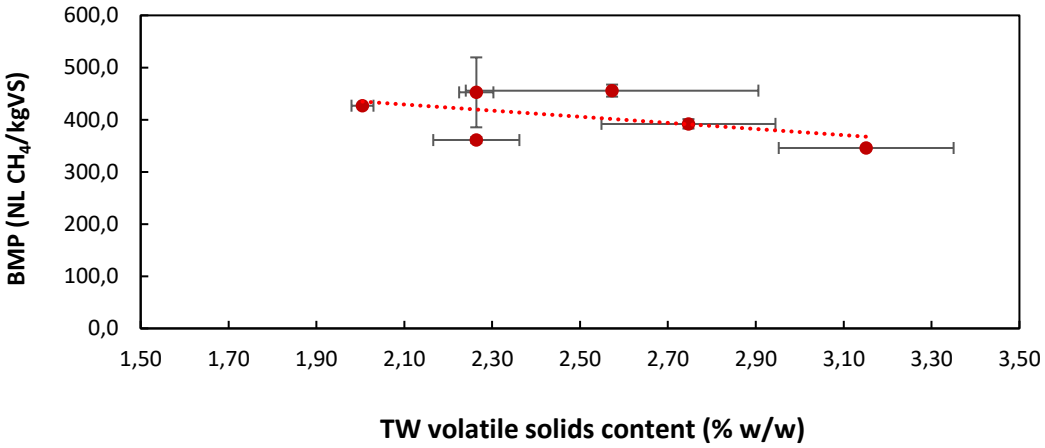


Figure 33: Relationship between feed VS content and biomethane potentials (BMP) for different TW samples.

The linear trend line plotted Figure 33 indicates a poor correlation between VS content and BMP data ($R^2$ = 0.2679), which indicates that BMPs do not change with variations in VS content for TW samples. Instead, variations in BMP values may have been attributed to different inoculum used during BMP tests, i.e. inoculum samples collected in April, May and June of 2022. This statement was in support of the results measured from positive control tests (micro-crystalline cellulose); for TW samples collected on 15-, 22- and 29-April-21, the BMP for triplicate positive control tests was obtained as 316 ± 3.93 NL $CH_4$/kgVS. For samples collected on 18-May, 10- and 14-June, the BMP for triplicate positive control tests was 297 ± 2.55 NL $CH_4$/kgVS. These BMP values were lower than the literature value of 350 ± 29 NL $CH_4$/kgVS for BMP tests performed on micro-crystalline cellulose (Holliger *et al*., 2016). The positive control BMP measured for inoculum samples collected on 18-May, 10- and 14-June of 297 ± 2.55 NL $CH_4$/kgVS suggests that the inoculum's health was not up to acceptable standards, which may have been influenced by the erratic feeding rates and power disruptions to Plant 2 encountered during this sampling period.

Overall, referring to Table 23, the mean SGY and BMP were obtained as 584 ± 69.9 NL/kgVS and 406 ± 46.7 NL $CH_4$/kgVS, respectively. These yields were greater than what was determined by other studies; Gunaseelan (2004) obtained a BMP of ± 211 NL $CH_4$/kgVS for rotten tomatoes (VS content of 95.8 ± 0.141 %TS) using 135 mL BMP test bottles. This yield was lower because the 135mL bottles contained roughly 2.0 g of volatile solids, as determined from compositional analyses (Gunaseelan, 2004). The mean mass of VS from TW samples loaded into each BMP test bottle was 3.40 ± 0.09 g, and thus greater BMPs were obtained due to more organic material in each bottle. Calabrò *et al*. (2015) measured a BMP of 330 ± 10 NL $CH_4$/kgVS for BMP tests (1.1 L) performed on tomato processing waste's without alkaline pre-treatment, which was also lower than what was measured from Plant 2's TW. Saghouri *et al*. (2018) also performed AD tests on tomato-processing wastes (VS content of 96.2 %TS) using an 8.0 L digester, where a methane yield of ± 140 L $CH_4$/kgVS was obtained after 40 days HRT. Both these methane yields were lower than what was obtained in this study (405.7 ± 46.72 NL $CH_4$/kgVS) due to differences in process conditions; Calabrò *et al*. (2015) conducted BMP tests in 1.1 L vessels where biogas productions were approximated by measuring digester pressure and converting these values to moles of methane

generated, assuming ideal gas behaviour. Saghouri *et al*. (2018) performed batch tests in 8.0 L vessels where the digester loading was established on an 8.0% total solids basis, and biogas production was recorded using water displacement methods. Furthermore, the mean HRT for all tests was observed as 9.0 days (Table 23), which indicates relatively rapid degradation time compared to the aforementioned studies of 30 to 40 days (Gunaseelan, 2004; Calabrò *et al*., 2015; Saghouri *et al*., 2018).

Data validation via relative standard deviation (RSD) was also computed for the SGY-SMY data presented in Table 23, as stated by Holliger *et al*. (2016). These computations are given in Table 24 below.

Table 24: Data validation criteria for Plant 2 BMP assay test results.

| TW sample | BMP [a] (NL $CH_4$/kgVS) | Stdev | RSD [b] | RSD > 5.0%? | Accept/Reject result |
|---|---|---|---|---|---|
| 15-Apr-21 | 456 ± 11.6 | 11.6 | 2.54% | No | Accept |
| 22-Apr-21 | 453 ± 67.0 | 67.0 | 14.8% | Yes | Reject |
| 29-Apr-21 | 392 ± 9.03 | 9.03 | 2.30% | No | Accept |
| 18-May-21 | 346 ± 1.44 | 1.44 | 0.41% | No | Accept |
| 10-Jun-21 | 423 ± 2.48 | 2.48 | 0.58% | No | Accept |
| 14-Jun-21 | 361 ± 5.80 | 5.80 | 1.61% | No | Accept |

[a] : biomethane potential; [b] : relative standard deviation

For homogenous substrates, under which TW is categorized, calculated RSDs must not exceed 5.0% (Holliger *et al*., 2016). Therefore, from the results presented in Table 23 and Table 24, all BMP tests results are acceptable except for tests performed on TW sampled from 22-April 2021.

Final analytical results for digestate samples are summarized in Table 25 below, which include final pH, total & volatile solids contents and VS reductions (VSR).

Table 25: Performance parameters determined from BMP tests performed on different tomato waste (TW) samples.

| BMP test | TW pH [a] | | Final digestate pH | Total solids (% w/w) | | Volatile solids (% w/w) | | |
|---|---|---|---|---|---|---|---|---|
| | Initial | Adj. | | Initial | Final | Initial | Final | VSR (%) |
| Blank tests | 7.63 | - | 8.20 ± 0.01 | 0.76 ± 0.21 | n.d. | 0.63 ± 0.04 | n.d. | n.d. |
| 15-Apr-21 | 4.08 | 6.96 | 8.10 ± 0.05 | 2.67 ± 0.50 | 0.98 ± 0.04 | 2.57 ± 0.33 | 0.58 ± 0.04 | 77.8 |
| 22-Apr-21 | 4.01 | 6.96 | 8.17 ± 0.02 | 2.70 ± 0.05 | 0.92 ± 0.10 | 2.26 ± 0.04 | 0.53 ± 0.11 | 76.9 |
| 29-Apr-21 | 3.98 | 6.87 | 8.08 ± 0.04 | 3.29 ± 0.18 | 0.99 ± 0.07 | 2.75 ± 0.20 | 0.71 ± 0.11 | 74.6 |
| 18-May-21 | 4.08 | 7.13 | 7.90 ± 0.03 | 3.39 ± 0.28 | 1.09 ± 0.02 | 3.15 ± 0.20 | 0.78 ± 0.05 | 76.0 |
| 10-Jun-21 | 4.29 | 6.81 | 7.92 ± 0.04 | 2.18 ± 0.20 | 1.05 ± 0.06 | 2.01 ± 0.03 | 0.68 ± 0.02 | 66.5 |
| 14-Jun-21 | 4.38 | 6.97 | 7.93 ± 0.03 | 2.45 ± 0.35 | 1.12 ± 0.04 | 2.26 ± 0.10 | 0.68 ± 0.04 | 70.5 |

[a] : pH measured for raw TW samples.

As indicated in Table 25 all BMP tests with different TW samples exhibited stable AD performance as the final pH range of 7.63 to 8.20 fell within the quality criteria range for digestate pH levels of 7.0 to 8.5 (Raposo *et al*., 2012; Holliger *et al*., 2016). The VS reductions ranged from 66.5% to 77.8% for all TW samples assessed in BMP tests, which indicates excellent AD efficiencies. The lowest VS reductions were

obtained for TW samples collected in June 2021 (Table 25), which were 66.5% and 70.5%. A reason why they were the lowest was due to possible issues with the inoculum collected from Plant 2 during this time; the 60m$^3$ digester's temperature dropped due to power cuts on site which would have disrupted the metabolic functionalities of microbial populations (Chen *et al*., 2008). Moreover, the BMP obtained from positive control tests on this inoculum sample was 297 ± 2.55 NL $CH_4$/kgVS, which was less than the literature-derived value of 350 NL $CH_4$/kgVS (Holliger *et al*., 2016).

#### *5.3.2.2. Bench-scale results as predictors of full-scale performance*

(a) BMP degradation rates (BDR)

BMP degradation rates (BDR) were calculated to assess the AD efficiency of Plant 2. Calculated BDRs are compared with VS reductions below in Figure 34.

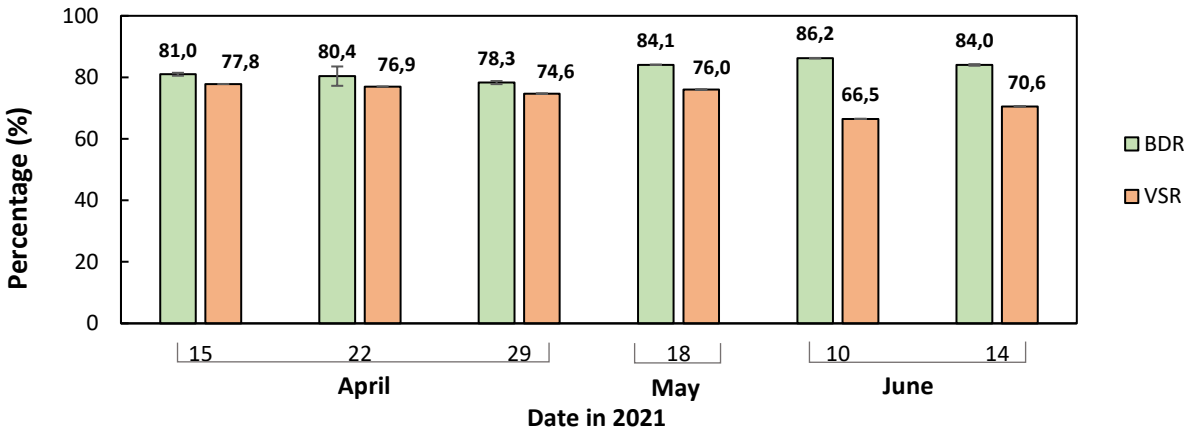


Figure 34: Comparison of BMP degradation and volatile solids reduction efficiencies for different TW samples assessed in BMP tests.

According to Figure 34, BMP degradation rates exceeded the VS reduction efficiencies, whose ranges were determined as 80 to 86% and 65 to 78%, respectively. These results are in accordance with BDRs reported by Schievano *et al*. (2011) and Li *et al*. (2017), where the BDR ranges were greater than VSR ranges. For the TW samples assessed in BMP tests, lower VS degradation rates may have been attributed to the presence of lignin, which is recalcitrant to the formation of biogas (Tambone *et al*., 2010). The relevant non-degradable components of a TW sample were analyzed for their concentrations, as given in Figure 35.

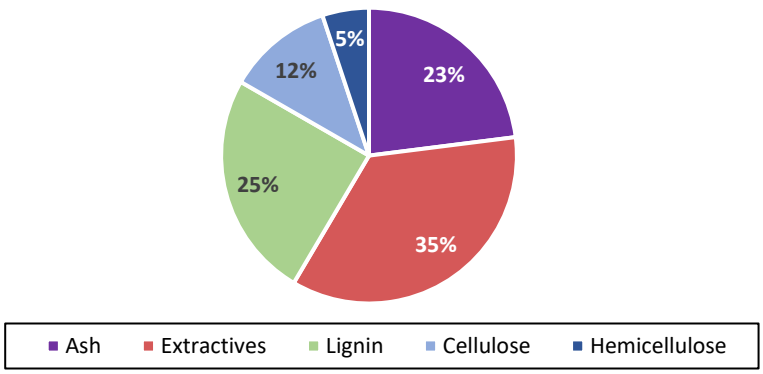


Figure 35: Composition of non-degradable fractions of tomato waste sourced from Plant 2.

According to Figure 35, lignocellulosic components make up roughly 42% of total solids of the analyzed TW sample. According to VSR calculations, roughly 22% to 35% of the total organic matter was not converted to methane gas, even under ideal bench-scale (BMP) test conditions, and given that nearly half of the total solids fraction was attributed to the presence of lignocellulosic materials. Moreover, the BDR range of 80% to 86% (Figure 34) was complemented by the concentration of methane in biogas produced from BMP tests, which ranged 68% to 71 %vol (Table 23). Overall, the BDR ranges indicate sufficient conversion of organic material to methane gas, but under bench-scale/BMP test conditions.

(b) Extrapolation method

Experimental data obtained from BMP tests performed on different TW samples were used to infer on the performance of Plant 2 using the extrapolation method proposed by Holliger *et al*. (2017). Table 26 shows the experimental data. The dataset pertaining to 22$^{nd}$ April 2021 was excluded from Table 26 as obtained BMP data did not adhere to BMP data validation criteria.

Table 26: BMP test datasets used for estimating Plant 2's performance.

| TW sample | VS content (% w/w) | SGY (NL/kgVS) | BMP (NL $CH_4$/kgVS) | $CH_4$ content (% vol) |
|---|---|---|---|---|
| 15-April-21 | 2.57 ± 0.333 | 652 ± 15.1 | 456 ± 11.6 | 70.0 ± 0.26 |
| 29-April-21 | 2.75 ± 0.198 | 554 ± 10.8 | 392 ± 9.03 | 70.8 ± 0.64 |
| 18-May-21 | 3.15 ± 0.199 | 509 ± 2.73 | 346 ± 1.44 | 68.0 ± 0.10 |
| 10-June-21 | 2.01 ± 0.025 | 617 ± 3.89 | 427 ± 2.48 | 69.2 ± 0.11 |
| 14-June-21 | 2.26 ± 0.098 | 507 ± 11.4 | 361 ± 5.80 | 71.2 ± 5.80 |
| **Mean** | **2.55 ± 0.44** | **568 ± 64.9** | **396 ± 45.5** | **69.8 ± 1.28** |

The daily biogas and methane productions and yields were estimated using Equation (11) for a digester feed rate of 1.0 tonnes TW per day. The mean VS content of TW (2.55 ± 0.44 % w/w), SGY (568 ± 64.9 NL/kgVS) and specific methane yield (396 ± 45.5 NL/kgVS) in Table 26 were also used for these estimations. Actual and estimated full-scale behaviour is presented in Figure 36.

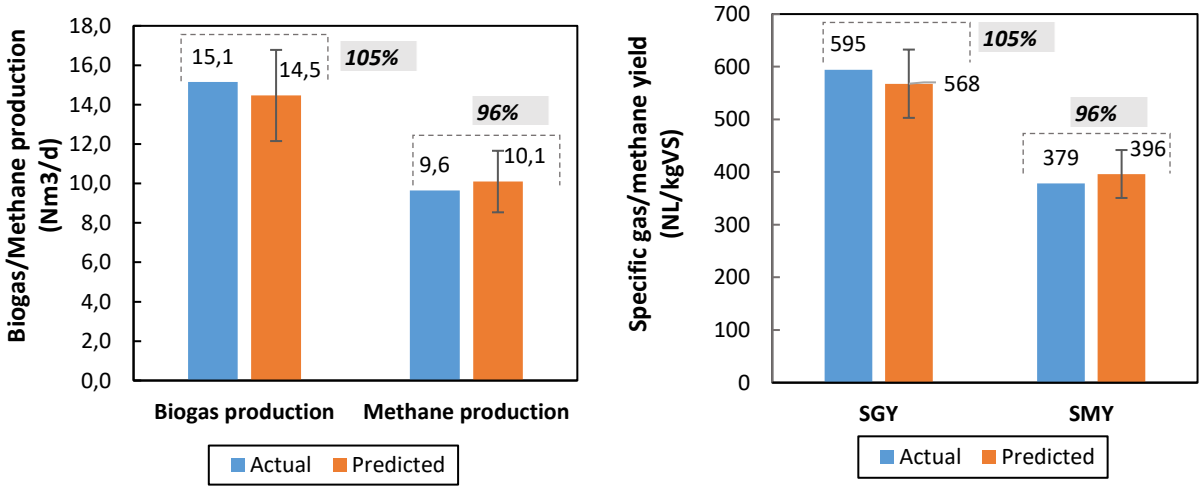


Figure 36: Actual and extrapolated full-scale performance using bench-scale results: (a) daily biogas & methane productions, (b) specific gas & methane yields.

It is clear from Figure 36 that estimated full-scale gas productions and yields closely compared with actual data, despite the crude method of acquiring such data from Plant 2. This was indicated by the given scale factors, where actual biogas production and SGY were 105% of the calculated values while actual methane production and SMY were 96% of the calculated values. The accuracy of these estimations were attributed to lack of compositional variability in the fed tomato waste, as Plant 2 was fed a uniform feedstock. This statement is supported by the marginal variations in VS content (2.55 ± 0.44 % w/w) for all of the collected TW samples, as shown in Table 26.

There were minimal variations in SGYs (568 ± 64.9 NL/kgVS) and BMPs (396 ± 45.5 NL $CH_4$/kgVS) produced from BMP tests which suggests that biogas productions and yields measured at full-scale would have also been consistent. This is, however, speculative as only one day's worth of full-scale data was obtained and thus full-scale transient effects could not be identified over time. For example, it was reported by site operators that Plant 2's 60 $m^3$ digester's temperature dropped from 35°C to less than 30°C during the winter months, but again the effects of these fluctuations on full-scale behavior could not be evaluated.

(c) CSTR/Dynamic model

The CSTR/dynamic model was used to assess the behavior of Plant 2. Degradation kinetics determined from BMP tests (Table 23) were included for solving the model, for a feeding basis of 1.0 tonnes of TW fed to Plant 2's digester per day. Figure 37 compares actual/full-scale data with estimated performance parameters, with each bar graph labelled with corresponding scale factors.

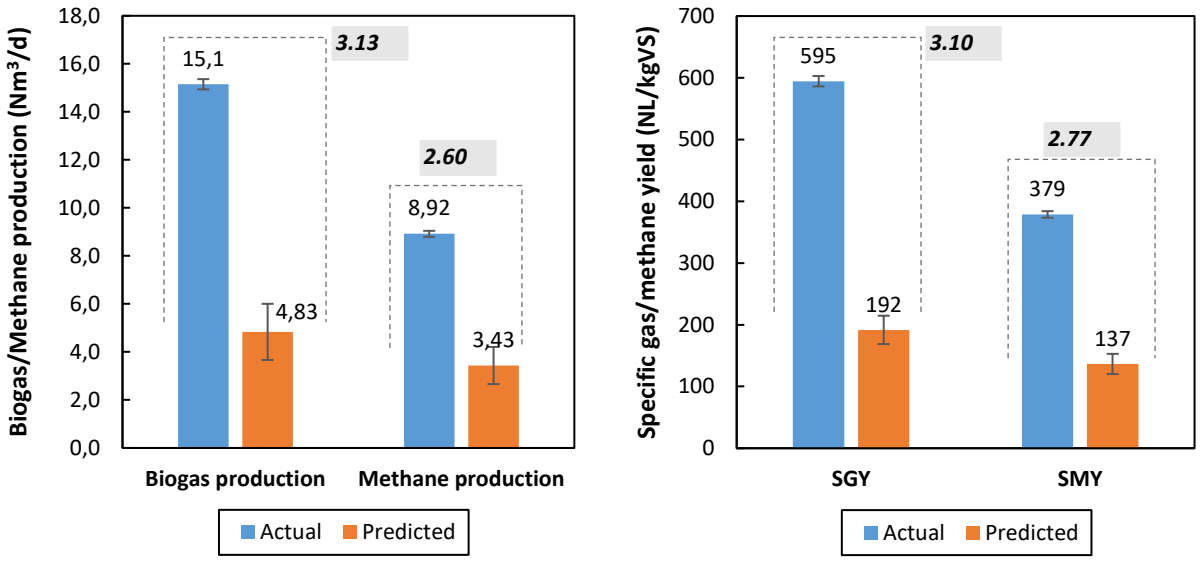


Figure 37: Actual and dynamically-modelled full-scale performance using bench-scale results: (a) daily biogas & methane productions, (b) specific gas & methane yields.

The calculated scale factors shown in Figure 37 were roughly 3.1 for biogas production/SGY estimates and 2.7 for methane production/SMY estimates. These scale factors indicate that actual full-scale performance was 270% to 310% of their dynamically estimated values, which indicated an extreme

underestimation of full-scale behavior. One reason for these overestimations pertains to the dynamic model's assumption that the hydrolysis and disintegration stages are rate-limiting for complex substrates of a highly particulate nature (Fiore *et al*. 2016). This was, however, not the case for TW samples assessed in BMP tests; the BMP curves (Figure 32) exhibited no lag phases with kinetic constants ranging 0.30 to 0.40 per day (Table 23). The TW samples used in this study were also sufficiently homogenised, and their mean moisture content of ± 97**%** (w/w) was indicative of the samples' un-particulate nature. It is possible, however, that degradation constants obtained from BMP tests (Table 23) may not have been reliable approximations of degradation kinetics due to imprecise fittings of first-order models to BMP test data. Compared to other studies, Rodrigues (2017) reported a kinetic constant of 0.61 per day for BMP tests performed on tomatoes with no indications of lag phases during AD. Therefore, if degradation constants were more reliably measured from BMP tests, the dynamic model would have potentially made better estimates of full-scale performance parameters. This remark is however speculative due to the absence of operational data collected over longer sampling durations.

Furthermore, the CSTR dynamic model itself may have not been a suitable model to estimate the performance of Plant 2 because of how the digester is mixed. Essentially, the 60 $m^3$ digester is mixed via a sludge recirculation pump that operates on a timer basis. Therefore, it is possible that the reactor does not mix as sufficiently as a CSTR digester, and rather approaches a plug-flow mixing regime. In a plug-flow digester there is minimal length-wise mixing of feedstocks under digestion as they are circulated in the reactor (Gomez *et al.,* 2019), which, to reiterate, may have been promoted by Plant 2's sludge recirculation line. As such, the CSTR dynamic model may have not been suitable to estimate biogas and methane production rates of Plant 2.

Overall, there is little confidence for the application of the extrapolation and dynamic-model methods for estimating Plant 2's behavior. The extrapolation of BMP data for estimating full-scale biogas/methane productions and yields may be more feasible than the dynamic model according to the accurate scale factors calculated (96% to 105%), but more operational data is required for future studies to expand on these scale factors.

### *5.3.3. AD Plant 3: Distillery waste (DW)*

#### *5.3.3.1. BMP test results*

Cumulative biogas and methane production curves obtained from BMP tests performed on different DW samples are presented in Figure 38 and Figure 39, respectively. Each DW sample is named according to the date they were collected from Plant 3, with corresponding COD concentrations given in Table 27.

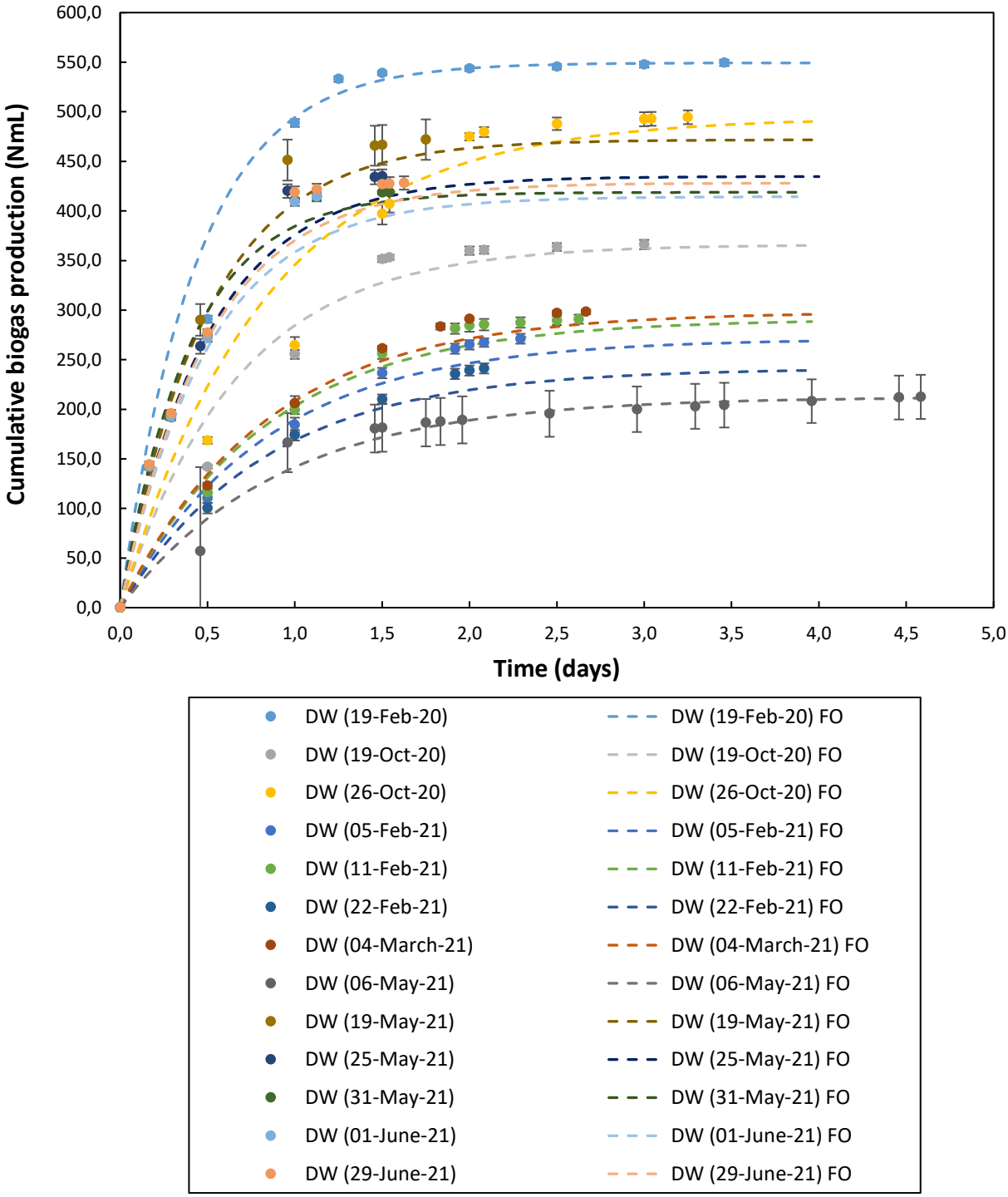


Figure 38: Cumulative biogas production curves for different distillery waste (DW) samples, with fitted first-order (FO) models. Error bars represent the standard deviations for a sample size $n$ = 3.

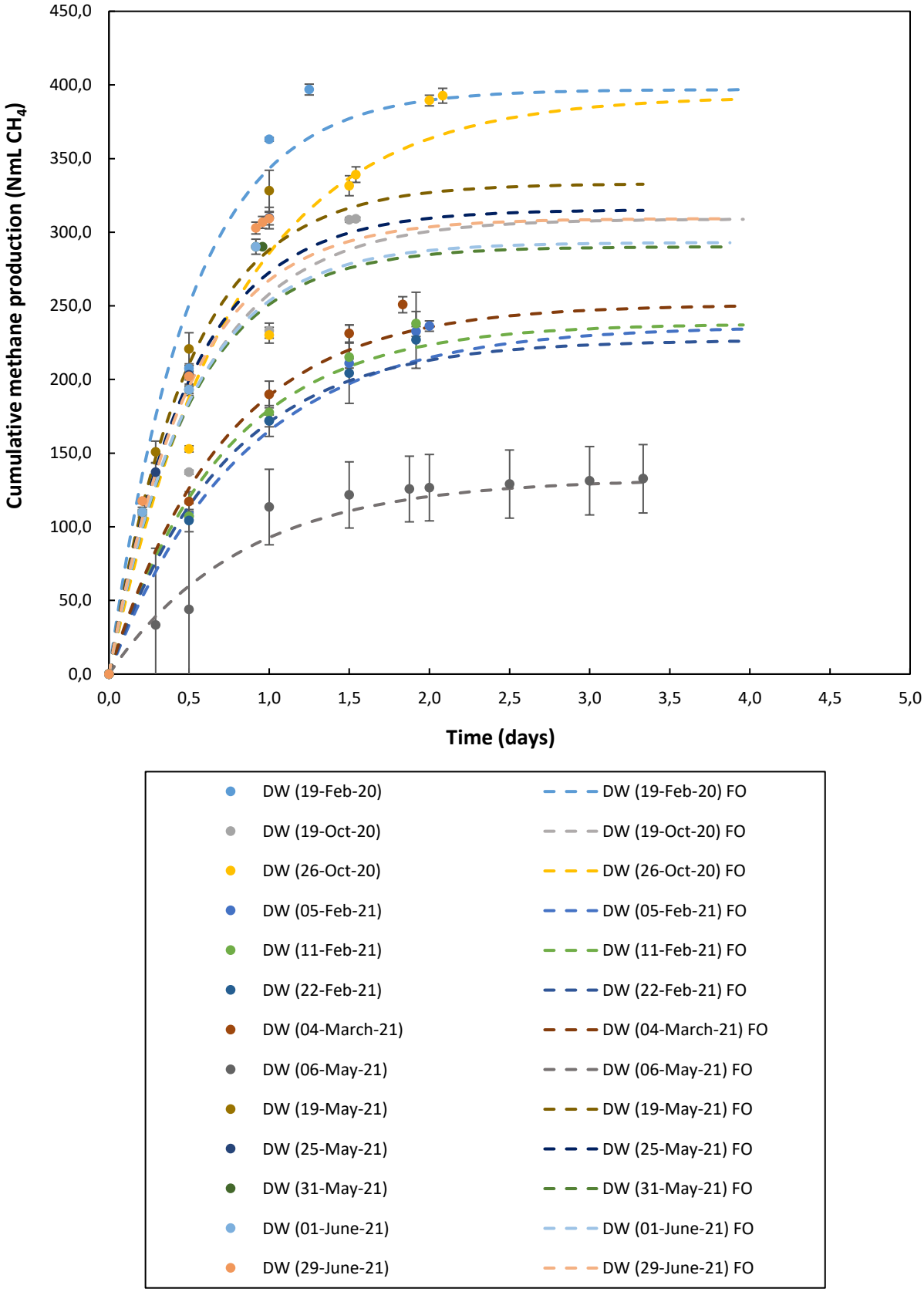


Figure 39: Cumulative methane production curves for different distillery waste (DW) samples with fitted first-order (FO) models. Error bars represent the standard deviations for a sample size *n* = 3.

All experimental data obtained from BMP tests on DW samples is summarised below in Table 27, as well as estimated disintegration constants $(k_{dis})$ and HRT for different total COD concentrations (TCOD).

Table 27: Summary of BMP assay test data for distillery waste (DW) samples collected from Plant 3.

| DW sample | | Reaction kinetics | | Biogas production | | Methane production | | $CH_4$ content (% vol) |
|---|---|---|---|---|---|---|---|---|
| Date | TCOD (mg/L) | HRT (days) | $k_{dis}$ (1/day) | Cumulative volume (NmL) | SGY [a] (NL/kgCOD) | Cumulative volume (NmL $CH_4$ | BMP [b] (NL CH4/kgCOD) | |
| 01-06-21 | 7810 ± 38.50 | 1.1 | 2.0 | 415 ± 4.82 | 323 ± 4.09 | 293 ± 3.64 | 230 ± 3.08 | 71.3 |
| 25-05-21 | 8890 ± 120.2 | 1.5 | 2.0 | 435 ± 7.16 | 303 ± 7.16 | 315 ± 2.17 | 223 ± 1.74 | 73.7 |
| 31-05-21 | 8980 ± 54.86 | 1.5 | 2.5 | 419 ± 1.65 | 306 ± 1.33 | 290 ± 0.81 | 216 ± 0.65 | 70.5 |
| 29-06-21 | 9350 ± 565.7 | 1.6 | 2.0 | 428 ± 6.76 | 308 ± 5.36 | 309 ± 4.22 | 227 ± 3.35 | 73.7 |
| 11-02-21 | 9980 ± 66.57 | 2.6 | 1.2 | 291 ± 4.47 | 307 ± 5.58 | 238 ± 21.3 | 247 ± 26.6 | 80.4 |
| 05-02-21 | 10295 ± 1407 | 2.3 | 1.2 | 271 ± 1.13 | 284 ± 6.16 | 236 ± 3.57 | 244 ± 4.46 | 86.2 |
| 19-05-21 | 10513 ± 28.28 | 1.8 | 2.0 | 472 ± 20.4 | 309 ± 15.4 | 333 ± 13.1 | 224 ± 9.92 | 72.5 |
| 06-05-21 | 11613 ± 859.2 | 4.6 | 1.1 | 213 ± 22.2 | 82.7 ± 16.3 | 133 ± 22.2 | 52.8 ± 17.1 | 63.8 |
| 19-10-20 | 11775 ± 487.9 | 3.0 | 1.5 | 366 ± 4.66 | 233 ± 3.11 | 309 ± 1.13 | 202 ± 0.75 | 86.9 |
| 22-02-21 | 12160 ± 155.6 | 2.1 | 1.2 | 241 ± 5.07 | 236 ± 6.11 | 227 ± 19.3 | 220 ± 23.3 | 93.0 |
| 26-10-20 | 15290 ± 106.1 | 3.3 | 1.2 | 495 ± 6.99 | 293 ± 4.31 | 393 ± 5.01 | 236 ± 3.09 | 80.6 |
| 19-02-20 | 15400 ± 226.3 | 3.5 | 2.3 | 549 ± 3.17 | 269 ± 1.70 | 397 ± 3.70 | 203 ± 1.99 | 75.5 |
| 04-03-21 | 16680 ± 113.1 | 2.7 | 1.2 | 298 ± 2.27 | 287 ± 2.61 | 251 ± 5.49 | 238 ± 6.32 | 83.1 |

[a] : Specific gas yield; [b] : biomethane potential

Specific gas yields and BMPs given in Table 27 ranged 82.7 ± 16.3 to 309 ± 15.4 NL/kgCOD and 52.8 ± 17.1 to 247 ± 26.6 NL $CH_4$/kg COD, respectively. These ranges compare well with other studies; Rodrigues (2017) performed BMP tests in 3.75L-reactors on winery wastes. For an ISR of 2.0, specific gas yields and BMPs reflected mean values of 359 NL/kgVS (or 139 NL/kgCOD) and 237 NL/kgVS (or 91.9 NL/kgCOD), respectively. Compared to the results in Table 27, these yields were much lower, possibly attributed to differences in compositional makeup between DW samples, for example, the presence of solids in the separate feedstocks. Because DW samples already exist in a liquid phase, organic components are dissolved in solution and anaerobic populations can easily assimilate the available nutrients (Liotta *et al.,* 2014). Therefore, degradation rates were more rapid during the AD of DW samples, ranging 1.1 to 2.5 per day in Table 27. Rodrigues (2017) reported slower degradation velocities of 0.58 per day for winery wastes because of the waste's higher TS content of 3.0 ± 0.1% (w/w).

Borja *et al*. (1993) investigated the reaction kinetics of 3.0L bench-scale reactors loaded with different biomass support material, for example, supports made from micronized sepiolite, bentonite and saponite. Different volumes (ranging 60 to 600 mL) of wine distillery wastewater was fed to each system in batch mode to determine reaction kinetics for the different supporting material. From these tests, the specific methane yield was obtained as ± 327 NL/kgCOD. Compared to specific methane yields in Table 27, this yield was much greater due to the improved immobilisation of anaerobic biomass in the AD reactor as a result of the reactor's supporting material.

The obtained BMP range in Table 27 was validated according to BMP test validation criteria. Relative standard deviations (RSD) were calculated from each DW sample's BMP data set, as shown in Table 28.

Table 28: Data validation criteria for Plant 3 BMP assay test results.

| DW sample | BMP [a] (NL $CH_4$/kgVS) | RSD [b] | RSD > 5%? | Accept/Reject result |
|---|---|---|---|---|
| 01-06-21 | 230.2 ± 3.08 | 1.34 | No | Accept |
| 25-05-21 | 223.1 ± 1.74 | 0.78 | No | Accept |
| 31-05-21 | 216.0 ± 0.65 | 0.30 | No | Accept |
| 29-06-21 | 227.1 ± 3.35 | 1.48 | No | Accept |
| 11-02-21 | 247.1 ± 26.6 | 10.8 | Yes | Reject |
| 05-02-21 | 244.4 ± 4.46 | 1.83 | No | Accept |
| 19-05-21 | 224.0 ± 9.92 | 4.43 | No | Accept |
| 06-05-21 | 52.8 ± 17.1 | 32.4 | Yes | Reject |
| 19-10-20 | 201.9 ± 0.75 | 0.37 | No | Accept |
| 22-02-21 | 219.9 ± 23.3 | 10.6 | Yes | Reject |
| 26-10-20 | 235.7 ± 3.09 | 1.31 | No | Accept |
| 19-02-20 | 203.0 ± 1.99 | 0.98 | No | Accept |
| 04-03-21 | 238.1 ± 6.32 | 2.65 | No | Accept |

[a] : biomethane potential; [b] : relative standard deviation

As distillery wastes were considered homogenized substrates, calculated RSDs must not exceed 5.0% (Holliger *et al*., 2016). Therefore, only 3 BMP data sets were rejected (dates 11-Feb-21, 06-May-21 and 22-Feb-21) and not used for the formulation of predictive models. Furthermore, the methane content determined from BMP tests performed on DW collected on 22-Feb-21 reflected a value of 93%vol; a value not consistent with the literature range of 50 to 75%vol (Al-Saedi *et al*., 2008; FNR, 2012; Jingura & Kamusoko, 2017). This methane content of 93%vol may have been attributed to an outlier in measured cumulative methane volumes for the 22-Feb-21 dataset. BMP values of 249.2, 216.0 and 215.5 NL $CH_4$/kgCOD were measured. After removing the value of 249.2 NL/kgCOD the mean BMP was 215.8 ± 0.35 NL $CH_4$/kgCOD, which resulted in a methane content of roughly 88%vol.

Ten of the BMP datasets that adhered to RSD criteria are correlated to different total COD concentrations analyzed for DW samples, given in Figure 40. For the range of analyzed COD contents, there are no clear trends visible in Figure 40, with poor correlations visible between SGY ($R^2$ = 0.228) and SMY ($R^2 = 5 \times 10^{-5}$) and total COD content. Although poor correlations were visible in Figure 40 the equations of both trend lines will be used to assess the performance of Plant 3 by accounting for a range of COD concentrations measured for DW.

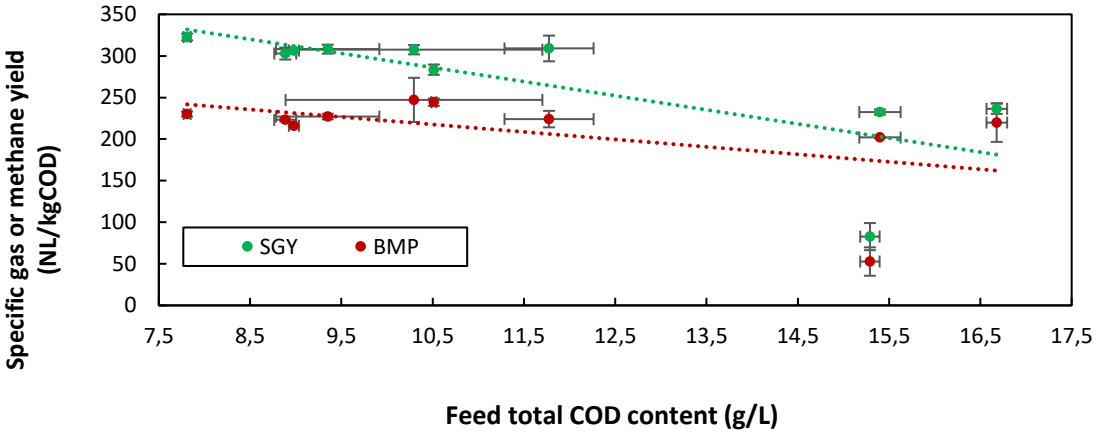


Figure 40: Regression models correlating total COD and specific gas and methane yields obtained from BMP tests. Error bars represent the standard deviations for a sample size *n* = 3.

AD performance parameters from resulting BMP tests were determined, as shown in Table 29.

Table 29: Performance parameters for distillery waste BMP tests.

| BMP test | DW pH level [a] | | Final digestate pH | TCOD (mg/L) | | |
|---|---|---|---|---|---|---|
| | Initial | Adj. | Final | Initial | Final | CODR [b] (%) |
| 01-06-21 | 5.62 | 6.88 | 7.68 | 7810 ± 38.50 | 217 ± 84.9 | 97.2 |
| 25-05-21 | 6.29 | 6.97 | 7.62 | 8890 ± 120.2 | 90 ± 5.66 | 99.0 |
| 31-05-21 | 6.47 | 7.02 | 7.66 | 8980 ± 54.86 | 306 ± 244 | 96.6 |
| 29-06-21 | 7.45 | 7.08 | 7.68 | 9350 ± 565.7 | 235 ± 91.2 | 97.5 |
| 11-02-21 | 3.98 | 7.06 | 7.59 | 9980 ± 66.57 | 219 ± 7.78 | 97.8 |
| 05-02-21 | 3.58 | 7.19 | 7.67 | 10295 ± 1407 | 408 ± 4.95 | 96.0 |
| 19-05-21 | 6.15 | 7.06 | 7.56 | 10513 ± 28.28 | 141 ± 60.8 | 98.7 |
| 06-05-21 | 6.25 | 6.99 | 7.62 | 11613 ± 859.2 | 95.0 ± 1.41 | 99.2 |
| 19-10-20 | 3.54 | 7.09 | 7.47 | 11775 ± 487.9 | 223 ± 1.41 | 98.1 |
| 22-02-21 | 4.13 | 6.82 | 7.57 | 12160 ± 155.6 | 246 ±27.6 | 98.0 |
| 26-10-20 | 6.54 | 6.91 | 7.47 | 15290 ± 106.1 | 124 ± 5.66 | 99.2 |
| 19-02-20 | 5.24 | 7.12 | 7.49 | 15400 ± 226.3 | 162 ± 0.00 | 98.9 |
| 04-03-21 | 4.07 | 6.97 | 7.56 | 16680 ± 113.1 | 209 ± 6.36 | 98.8 |

[a] : pH level of raw DW samples; [b] : Chemical oxygen demand reduction

All BMP tests exhibited stable process conditions, as the final pH values ranged 7.47 to 7.68 and fall within the satisfactory range of 7.0 to 8.5 for anaerobic sludge (Holliger *et al*., 2016). The reductions in organic/COD content indicated superior AD efficiencies, which ranged 96% to 99.2%. These removal efficiencies are consistent with efficiencies obtained for full-scale systems treating distillery and beverage wastes, where COD removals of + 95% are obtained for up-flow anaerobic sludge blanket (UASB) reactors (Melamane *et al*., 2007). Wolmarans & De Villiers (2004) reported COD removals higher than 90% during

the monitoring of a full-scale UASB. These removal efficiencies are lower than those measured from BMP tests as the UASB was operated at a lower HRT of 4 to 11 hours compared to 4 days for Plant 3.

*5.3.3.2. Bench-scale results as predictors of full-scale performance*

(a) BMP degradation rates (BDR)

Figure 41 compares the COD reduction percentages with BMP degradation rates to assess how much organic material contained in DW samples was converted to biomethane potential during bench-scale BMP tests.

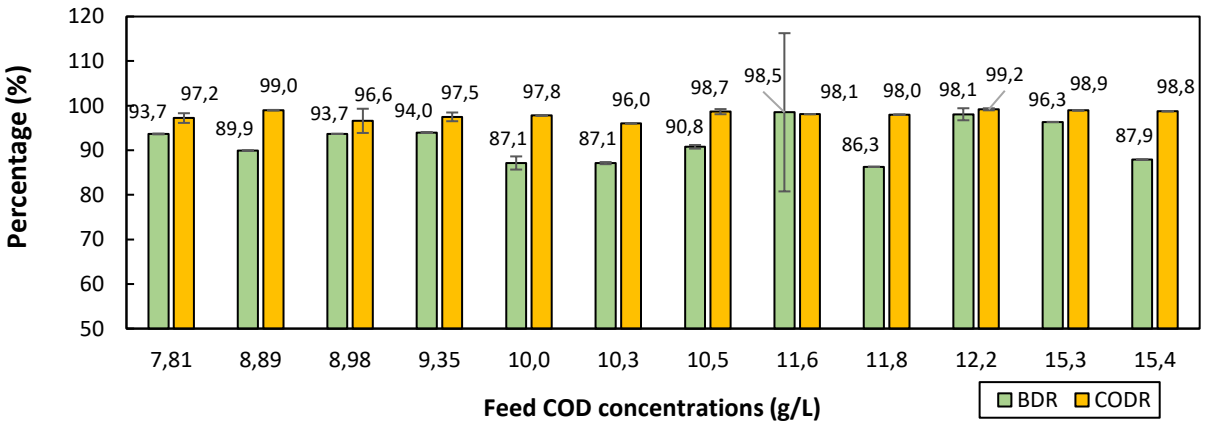


Figure 41: Comparison of COD reductions (CODR) and BMP degradation rates (BDR) for DW samples investigated in BMP tests.

The BDR range of 86.3% to 98.5% in Figure 41 indicates that roughly 1.5% to 13.7% of organic material contained in DW samples was not converted to biomethane. This may have been due to the presence of polyphenolic compounds in the alcohol wastewater, for example, gallic acids formed as by-products from beer and wine fermentation can be inhibitory towards anaerobic digestion (Mousa & Forster, 1999; Goodwin *et al.*, 2001). The obtained BDR range has not been reported for feedstocks based on COD concentrations, which provides some novelty on the application of BDRs for liquid AD plants. Again, the calculated BDRs were applicable to bench-scale tests performed under BMP test conditions and thus BDRs for Plant 3 were determined from full-scale specific gas yields. Therefore, COD reductions obtained from BMP tests and full-scale operational data were compared to assess the deviation of organic removal efficiencies between scales. Figure 42 below compares the bench- and full-scale COD reductions.

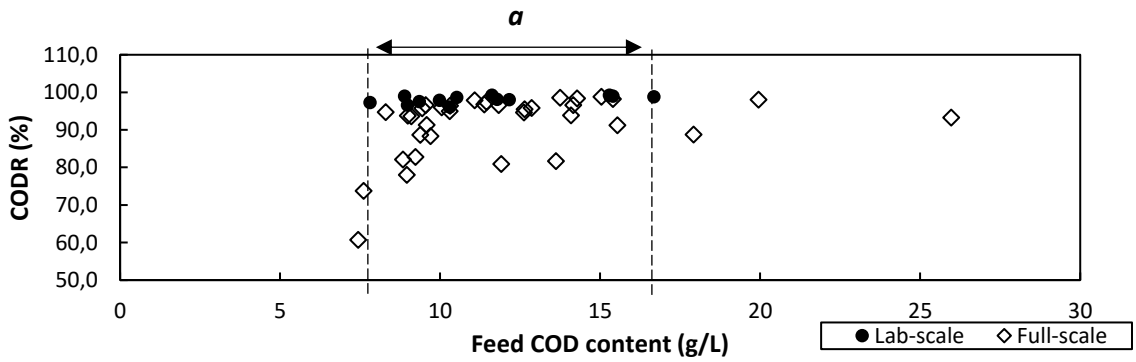


Figure 42: Comparison of COD removal (CODR) efficiencies obtained from BMP tests (bench-scale) and Plant 3's (full-scale) operational data (*a* = comparable COD range).

For the COD range of 7.81 to 16.7 g/L (letter *a* in Figure 42), the mean bench- and full-scale CODRs were obtained as 98 ± 1.0% and 93 ± 6.0%, respectively. Therefore, for the given COD range, the full-scale's COD removal efficiency can be estimated as roughly 95% of the removal efficiency measured from BMP tests. The deviations between bench- and full-scale CODRs are a result of the different feeding modes between both scales; Plant 3 is continuously-fed distillery wastes, exposing the 2200 $m^3$ digester's microbes to a highly dynamic environment and thus affecting culture performance (Lara *et al*., 2006). BMP tests were performed under batch-mode under a set inoculum-to-substrate ratio (ISR) where environmental conditions were considered uniform through the experimental period. Therefore, BMP tests provided reasonably accurate approximations of organic content removal for Plant 3.

(b) Extrapolation method

Results from BMP tests (Table 27) were used to predict the biogas production rate and SGY of Plant 3. A linear regression model was previously constructed (Figure 40) to show the relationship between feed COD concentrations (mg/L) and specific gas and methane yields for each of the DW samples assessed in BMP tests. Equations (30) and (31) below represent the straight line equations for calculating SGY and SMY data, respectively.

$$SGY_{trend} = -3.885 \times [COD] + 336 \quad (30)$$

$$SMY_{trend} = -0.0188 \times [COD] + 225 \quad (31)$$

The expressions were used to calculate specific gas and methane yields for a range of feed COD concentrations. If applied to a full-scale system for different COD ranges, the extrapolation method assumes that full-scale yields will eventually approach those measured from BMP tests. The expression proposed by Holliger *et al*. (2017) was used to estimate average daily biogas production rates and SGYs (Equation (11)) for different full-scale flowrates ($m^3$/d), feed COD concentrations and calculated gas yields. Mean daily methane productions and yields were not predicted as full-scale methane productions were not logged consistently. Actual/full-scale datasets are compared with estimated daily biogas productions (Figure 43) and daily biogas yields (Figure 44).

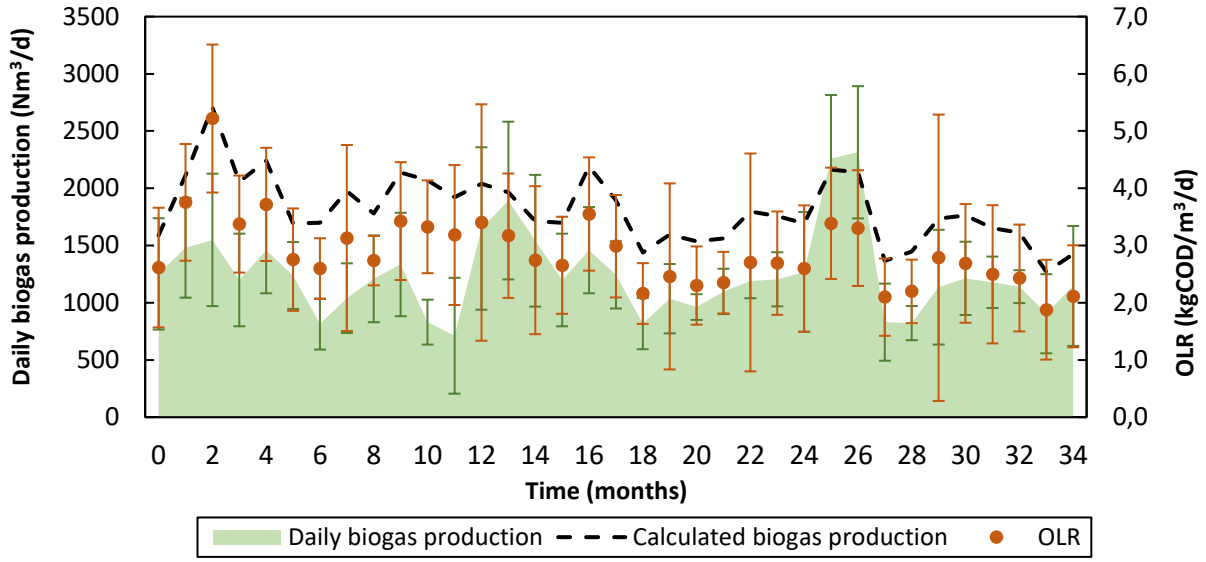


Figure 43: Comparison of actual and calculated mean daily biogas productions for Plant 3 for a range of organic loading rates (OLR). Error bars indicate the standard deviations for a sample size *n* = 22.

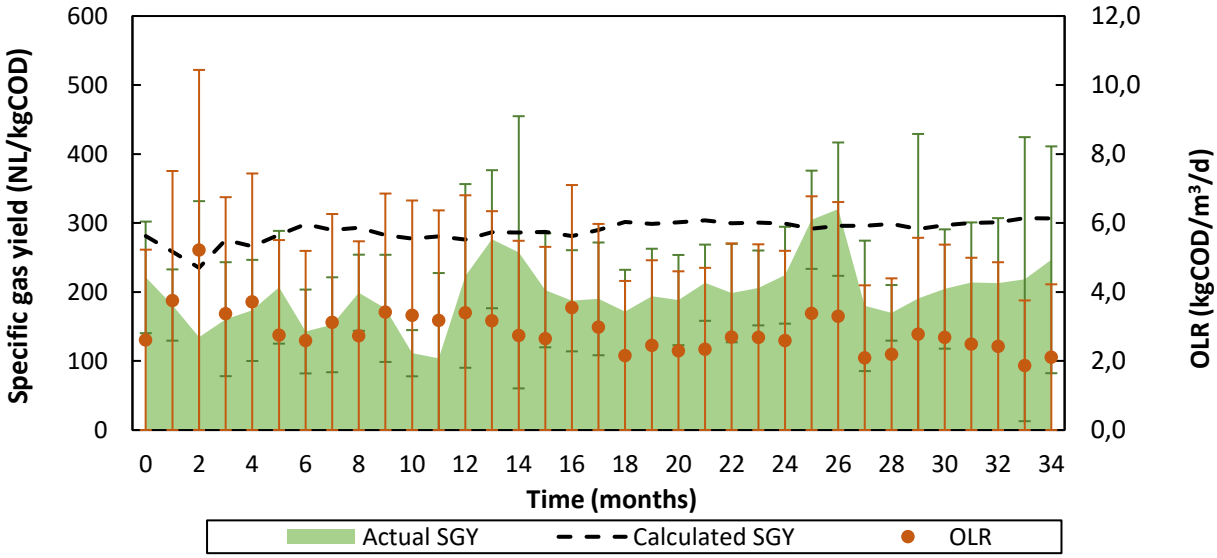


Figure 44: Comparison of actual and calculated mean specific gas yields (SGY) for Plant 3 for a range of organic loading rates (OLR). Error bars indicate the standard deviations for a sample size *n* = 22.

According to Figure 43 and Figure 44, estimated daily biogas productions and yields exceeded the actual/full-scale productions and yields for most of the 34-week operational period. That is, actual biogas productions and yields were 68.7 ± 15.1% (scale factor) of their calculated values. Therefore, for a certain feed COD concentration, full-scale flowrate and SGY determined from BMP tests, the full-scale daily biogas production can be estimated as 0.69 of the productions calculated from Equation (11). Single-factor ANOVA tests (Table 46) confirmed that there were major significant differences between actual and estimated daily biogas productions (p = 1E-09, < 0.05) and for actual and estimated SGY datasets (p = 7.8E-17, < 0.05), confirming that full-scale performance parameters do indeed differ from those measured from bench-scale tests.

The deviations between full-scale and estimated performance (68.7 ± 15.1%) are attributed to differences in bench- and full-scale AD conditions. Because BMP tests are controlled at optimal conditions and are assumed to be ideally mixed at small working volumes (Van't Riet & Van der Lans, 2011), anaerobic microbes will always exhibit maximum degradation rates and gas yields under bench-scale conditions (Koch *et al*., 2020). The variations in heat and concentration distributions at bench-scale were also considered negligible (Weinrich *et al*., 2018) compared to those encountered at full-scale volumes.

At a process volume of 2200 $m^3$ phenomena transfer such as mass and heat transfer rates will be slower at than the rates in smaller process volumes, which is further influenced by the degree of homogeneity and mixing within the full-scale digester (Lara *et al*., 2006; Marques *et al*., 2010; Clarke, 2013). These changes are further influenced by increased OLRs to the full-scale system. As shown on Figure 43 and Figure 44, when OLR increased the deviations between actual and estimated daily biogas productions become worse. This is the case because, as more material enters the 2200 $m^3$ digester, the digester's contents become more heterogeneous. As anaerobic microbes travel through these concentration gradients they are continuously exposed to changing environments, which, in turn, will affect their culture performance (Lara *et al*., 2006). Constantly changing reactor environments will impact the communities' reproduction and acclimatisation rates, impeding microbial communities' abilities to convert organic material to biogas (Akram & Stuckey, 2008; Theuerl *et al.*, 2019). Considering these full-scale process conditions, the activities and physiology of microbial communities are thus much different at full-scale compared to those encountered at bench-scale (Marques *et al*., 2010; Clarke, 2013).

In comparison to a study performed by Holliger *et al*. (2017), actual daily methane productions measured for a liquid-based full-scale plant were roughly 94% of their calculated productions. Holliger *et al*. (2017) obtained a more accurate scale factor than what was obtained for Plant 3, possibly due to the type of performance datasets compared with estimated data. Holliger *et al*. (2017) obtained methane production data from measured methane volumes on site, the biomethane injected into the electrical grid and the surplus flared gas. Multiple datasets reduced uncertainties with variations in methane yields, potentially attributing to the greater scale factor of 94%. Only biogas production rates were recorded by Plant 3 using an ultrasonic gas flow meter, whose recordings could have been inaccurate due to phenomena such as pressure drops in the biogas product line (Water Technology, 2015).

(c) CSTR/Dynamic model

A limitation of the extrapolation method is that it did not account for reaction kinetics of anaerobic populations observed for the full-scale process, which, on a continuously-fed basis, could potentially influence achievable daily biogas productions and yields. The use of bench-scale disintegration constants to predict daily biogas productions and biogas yields of Plant 3 were thus assessed using the CSTR-based dynamic model (Fiore *et al*., 2016). A linear regression model was constructed (Figure 45) to depict the relationship between disintegration constants and feed COD concentrations (Table 27) obtained from BMP tests.

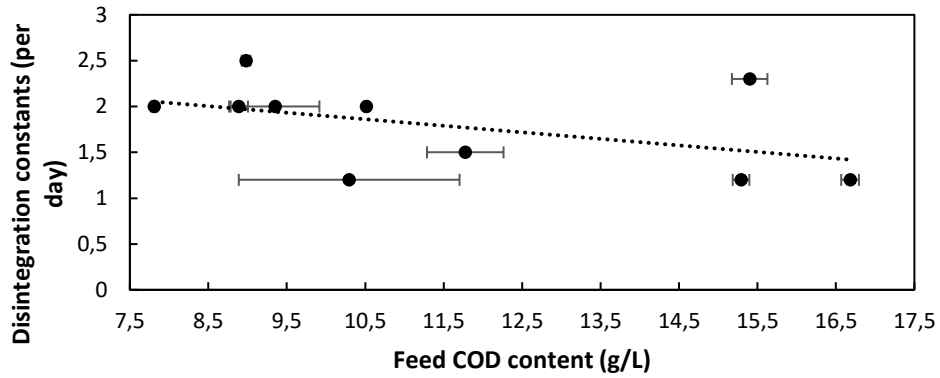


Figure 45: Relationship between disintegration constants and feed COD content of DW samples.

The linear trend line in Figure 45 is mathematically given as Equation (32).

$$k_{dis} = -0.0713 \times [COD] + 2.6102 \quad (32)$$

The 34-month dataset of regression-modelled SGY, SMY and k-values for the full-scale system are presented in Table 39, along with dynamically-modelled biogas data (Appendix A). Approximations of full-scale behaviour are given in Figure 46 and Figure 47.

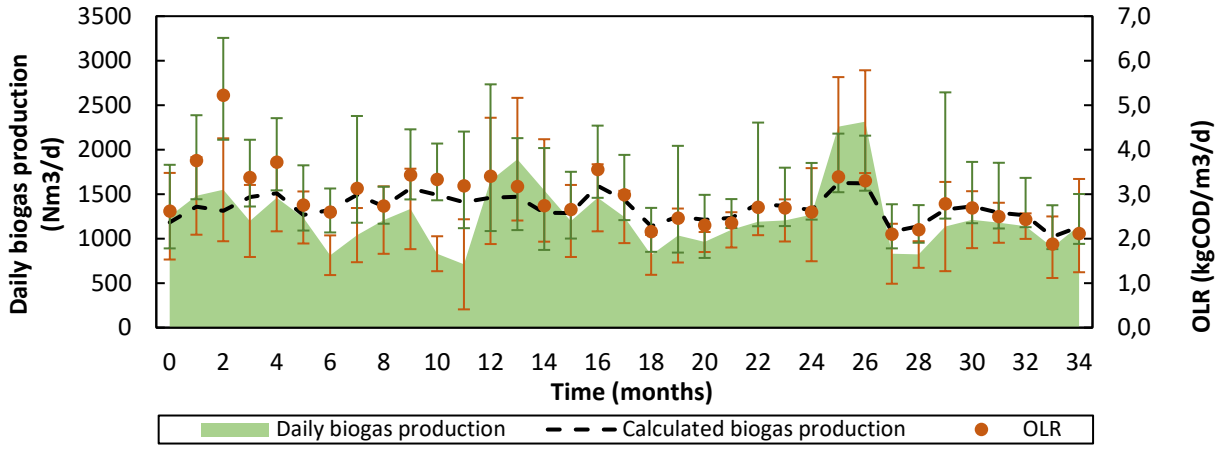


Figure 46: Comparison of actual and dynamically-modelled daily biogas production for Plant 3.

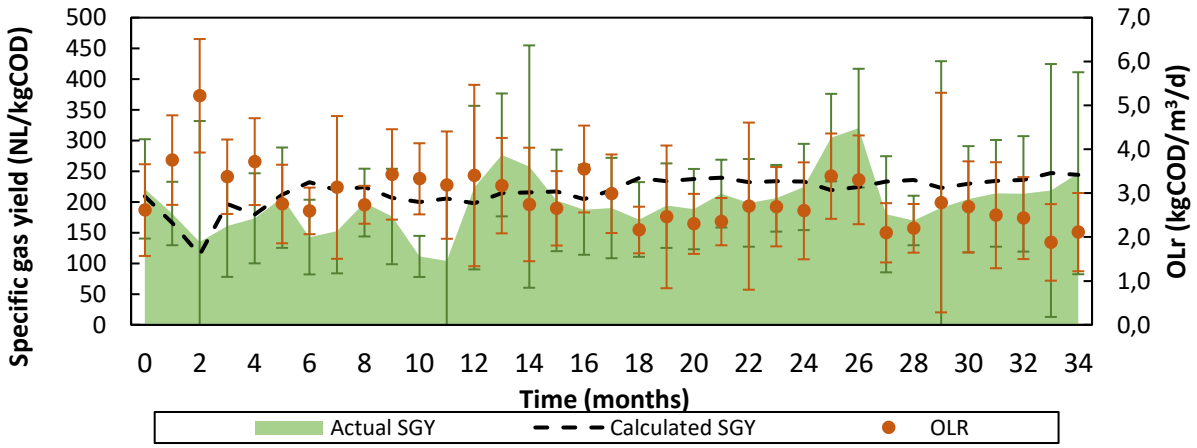


Figure 47: Comparison of actual and dynamically-modelled daily specific gas yields for Plant 3.

Over the 34-week operating period, the full-scale daily biogas productions (Figure 46) and specific gas yields (Figure 47) were roughly 92 ± 20.8% of the values estimated by the dynamic model. These percentages indicate that the full-scale system is moving more towards ideal bench-scale behaviour. This mean scale factor was greater than the value calculated from the extrapolation method (68.7 ± 15.1%), which may have been due to the inclusion of degradation kinetic constants (1.1 to 2.0 per day, Table 27) in the dynamic model, accounting for biogas production rates inside the full-scale reactor. Furthermore, single-factor ANOVA tests (Table 47) confirmed that actual and dynamically-modelled daily biogas production rates were not significantly different from each other ($p = 0.15$, $> 0.05$) for a significance level of 5.0%. This may indicate that similar reaction kinetics and COD degradation rates were obtained for both full- and bench-scale tests. In contrast, actual and modelled specific gas yields were significantly different ($p = 0.041$, $< 0.05$), possibly due to the variation in feed flow and organic loading rates to the system.

Apparent COD concentrations were also determined from the dynamic model using Equation (12). A comparison between the actual and estimated digestate COD contents is given in Figure 48.

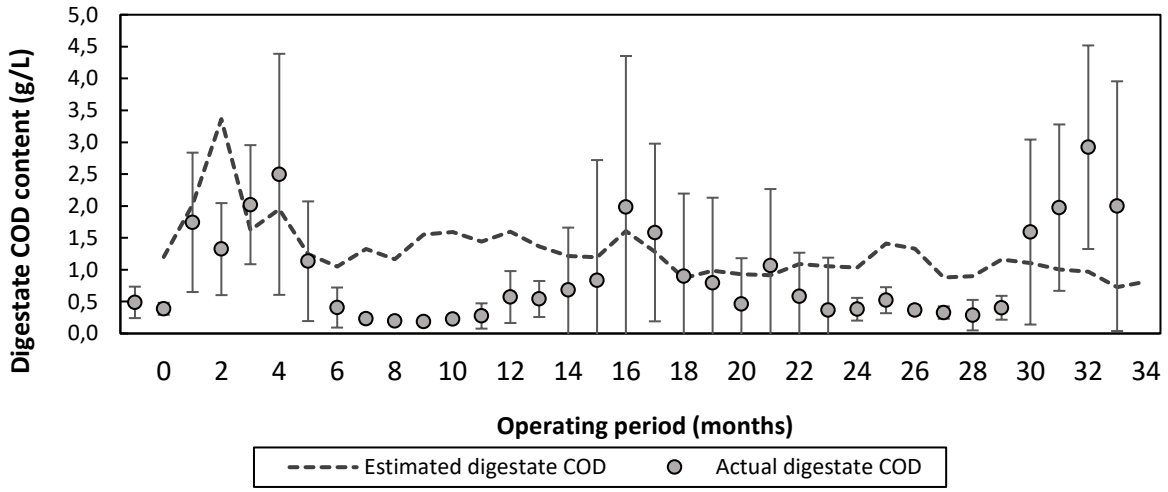


Figure 48: Actual and apparent (estimated) COD concentrations for Plant 3's digestate.

Apparent COD concentrations are time-dependent parameters, which were solved according to the disintegration constants determined from BMP tests, the full-scale feed rates and COD contents (Equation (12)). The model also assumes that there is no accumulation of biomass inside the digester. However, in full-scale processes, the growth rates of microorganisms are considerable, where biomass accumulation can be influenced by process parameters like organic loading, temperature and pH level (Meegoda *et al.,* 2018; Sarker *et al.*, 2019). Therefore, with reference to Figure 48, the estimated digestate COD content mostly exceeds the actual digestate COD content for most of the 34-week period because biomass accumulation in the system was significant. The deviation between actual and estimated digestate COD concentration was roughly 82 ± 81%, which quantifies the deviation between ideal reactor conditions and actual full-scale reactor conditions. Single-factor ANOVA tests (Table 48) confirmed that, for a significance level of 5.0%, actual COD concentrations and apparent COD

concentrations were significantly different from each other ($p = 0.02, < 0.05$) due to the accumulation of biomass within the full-scale digester.

The dynamically modelled daily biogas productions and yields plotted in Figure 46 and Figure 47 (dashed lines) do not give a clear indication of whether changes in OLR are proportionate to changes in modelled performance parameters. This may be due to nature of the DW streams fed to the full-scale system; DW samples do not adhere to the model's assumption that hydrolysis becomes rate-limiting for complex feedstocks of a highly particulate nature (Fiore *et al.*, 2016) because they are categorized as purely liquid feedstocks (total solids of 0.53 ± 0.3 % w/w, Table 12) and no lag phases were observed from biogas and methane production curves shown in Figure 38 and Figure 39.

Fiore *et al*. (2016) applied the dynamic model to a 300 L pilot-scale AD system being fed mixed food wastes under a semi-continuous feeding mode. The model was developed using data (disintegration constants and specific gas and methane yields) derived from semi-pilot-scale AD tests performed in 6.0 L vessels. It was found that, towards the end of the pilot-scale's experimental period, actual daily biogas production was 7.1% to 8.5% less than what was estimated by the dynamic model. That is, actual daily biogas production produced by the 300 L system was ± 93% of the dynamically estimated production. Although Fiore *et al*. (2016) estimated the performance of a 300 L AD system, the deviation between pilot- and bench-scale conditions was similar to the deviation measured between bench- and full-scale (Plant 3) conditions, which was 92 ± 20.8%. Fiore *et al*. (2016) did not apply this model to a full-scale study, nor did they apply it to an AD system operating on a COD concentration basis. Therefore, the results obtained from dynamically-modelling Plant 3 demonstrate some novelty in the work performed.

## 5.4. Pilot-scale results

Pilot-scale AD tests (50 L) were conducted using feedstocks collected from Plant 2 (tomato waste) and Plant 3 (distillery waste) under conditions similar to the full-scale AD plants. Pilot-scale tests were not performed for Plant 1 (co-digestion of mixed organic wastes) due to the complexities of feeding schedules and hazards associated with working with large quantities of cow blood in the laboratory. The goal of pilot-scale tests to assess whether full-scale performance parameters can be better approximated than performing BMP tests.

### *5.4.1. AD Plant 2: Tomato waste (TW)*

Performance data for the TW-fed semi-continuous pilot-scale AD reactor was obtained over a 30-day operational period, which includes daily biogas and methane productions and OLR (Figure 49a), digestate total solids content and pH level (Figure 49b), and feed volatile solids content and removal efficiencies (Figure 49c).

Referring to Figure 49a, the semi-continuous pilot-scale reactor was fed ± 438 mL of TW per day (OLR of 0.31 ± 0.03 kgVS/$m^3$/d) during the first 8 days of operation, which corresponded to an HRT of 80 days. This HRT replicated the HRT of the full-scale system, where, the 60$m^3$ digester's feed rate was set to 750L per day. The daily biogas and methane productions were measured as 0.53 ± 0.06 NL/d (SGY = 49.0 ± 6.46 NL/kgVS) and 0.32 ± 0.04 NL $CH_4$/d (SMY = 30.2 ± 4.35 NL $CH_4$/kgVS), respectively. From Day 9 to 18 (Figure 49a) the pilot-scale's feed rate was increased to ± 510 mL of TW fed per day (HRT of 69 days)

because the feed rate to the Plant 2's digester was increased to 875 L/d, i.e. at an HRT of 69 days. The OLR subsequently increased to 0.36 ± 0.12 kgVS/$m^3$/d, and mean biogas and methane productions were recorded as 0.59 ± 0.18 NL/d (SGY = 46.6 ± 7.22 NL/kgVS) and 0.37 ± 0.1 NL/day (SMY = 29.0 ± 4.41 NL $CH_4$/kgVS), respectively.

On Day 24 the reactor was fed according to an HRT of 30 days, which increased the OLR from 0.36 to 0.75 kgVS/$m^3$/d (Figure 49a). The SGY and SMY were obtained as 27.1 ± 5.17 NL/kgVS and 16.9 ± 3.17 NL $CH_4$/kgVS, respectively. On Day 28 the HRT was further reduced to 12 days (OLR = 1.88 kgVS/$m^3$/d), where SGY and SMY data were obtained as 22.1 ± 7.68 NL/kgVS and 13.1 ± 4.19 NL $CH_4$/kgVS, respectively. Overall, for an HRT range of 12 to 80 days (OLR range of 0.31 to 1.88 kgVS/$m^3$/d), the SGY and SMY ranged from 22 to 49 NL/kgVS and from 13 to 30 NL $CH_4$/kgVS, respectively.

The aforementioned biogas and methane yield results are not in agreement with results presented by other studies. Sarada & Joseph (1994) performed AD tests in 5.5 L digesters, which were semi-continuously fed tomato-processing wastes. For an investigated HRT range of 4 to 32 days, SGY and SMY datasets ranged from roughly 40 to 600 NL/kgVS and 20 to 420 NL $CH_4$/kgVS. Belhadj *et al*. (2014) investigated co-digested sewage sludge and rotten tomatoes in 3.5 L reactors operated under semi-continuous feeding. The HRT was not reported but an OLR range of 0.4 to 2.2 kgVS/$m^3$/d was investigated, where a methane yield of 159 NL/kgVS was obtained after 30 days of experimental run time.

Compared to literature, the biogas and methane yields obtained from the 35 L pilot-scale system were much lower, which may have been due to performance issues with the system's inoculum. Over the 30-day operating period, digester pH was measured as 8.06 ± 0.27 (Figure 49b), which falls within the stable pH range of 7.0 to 8.5 for anaerobic sludge (Raposo *et al*., 2012; Holliger *et al*., 2016). There were, however, increases in digester pH on Day 14 (pH 8.56) and Day 16 (pH 8.73) which may have been due to free-ammonia accumulation in the system. This is because the C:N ratio for TW samples was determined as 12.2, which falls short of the desirable C:N range of 20 to 35:1 (Ward *et al.,* 2008; Weinrich *et al*., 2018). This low C:N ratio indicates that more nitrogen may have been present in the reactor than carbon, however free-ammonia concentrations were not measured in collected digestate samples.

Although the digester's pH reflected alkaline conditions (pH > 8.0), the methane composition of produced biogas ranged 54% to 65 %vol for the 30-day period. This volumetric concentration range was in accordance of the typical composition of methane gas of 50% to 75%vol as produced during AD (Al-Saedi *et al*., 2008; FNR, 2012; Jingura & Kamusoko, 2017). Therefore, if free-ammonia accumulation majorly disrupted process performance, methane concentrations would have decreased (Raposo *et al*., 2012). Lastly, the pilot-scale exhibited sufficient reductions in VS content, which ranged 75% to 88% for the 30-day period, as shown in Figure 49c. Therefore, given that semi-continuously-fed pilot-scale system exhibited an acceptable pH level, adequate methane content in produced biogas and efficient VS reductions, it was possible that low biogas and methane productions and yields were attributed to calibration of the pilot-scale's gas measurement system (GMS).

It was found that specific methane yields (SMY) measured from BMP tests were also much greater than pilot-scale yields, which ranged 346 to 456 NL $CH_4$/kgVS, as given in Table 23. Pilot-scale SMYs were thus 6.5% to 8.5% of SMYs measured in BMP tests, indicating major deviations between bench- and pilot-scale

test conditions. In terms of full-scale performance parameter estimates, for a feed basis of 1.0 tonnes TW/d, a TW VS content of 2.55 ± 0.44 % w/w and using pilot-scale biogas and methane yields (50.6 ± 7.18 NL/kgVS and 31.1 ± 4.94 NL $CH_4$/kgVS) in Equation (11), the full-scale daily biogas and methane production rates were calculated as 1.29 $Nm^3$/d and 0.793 $Nm^3$ $CH_4$/d, respectively. However, the actual full-scale biogas and methane production rates for Plant 2 were obtained as 14.0 ± 0.20 $Nm^3$/d and 8.92 ± 0.13 $Nm^3$ $CH_4$/d, respectively. Therefore, because poor specific gas and methane yields were measured from semi-continuous pilot-scale tests, full-scale performance estimations of Plant 2 were not reliable. As such, the dynamic model was not computed for estimating Plant 2's behaviour.

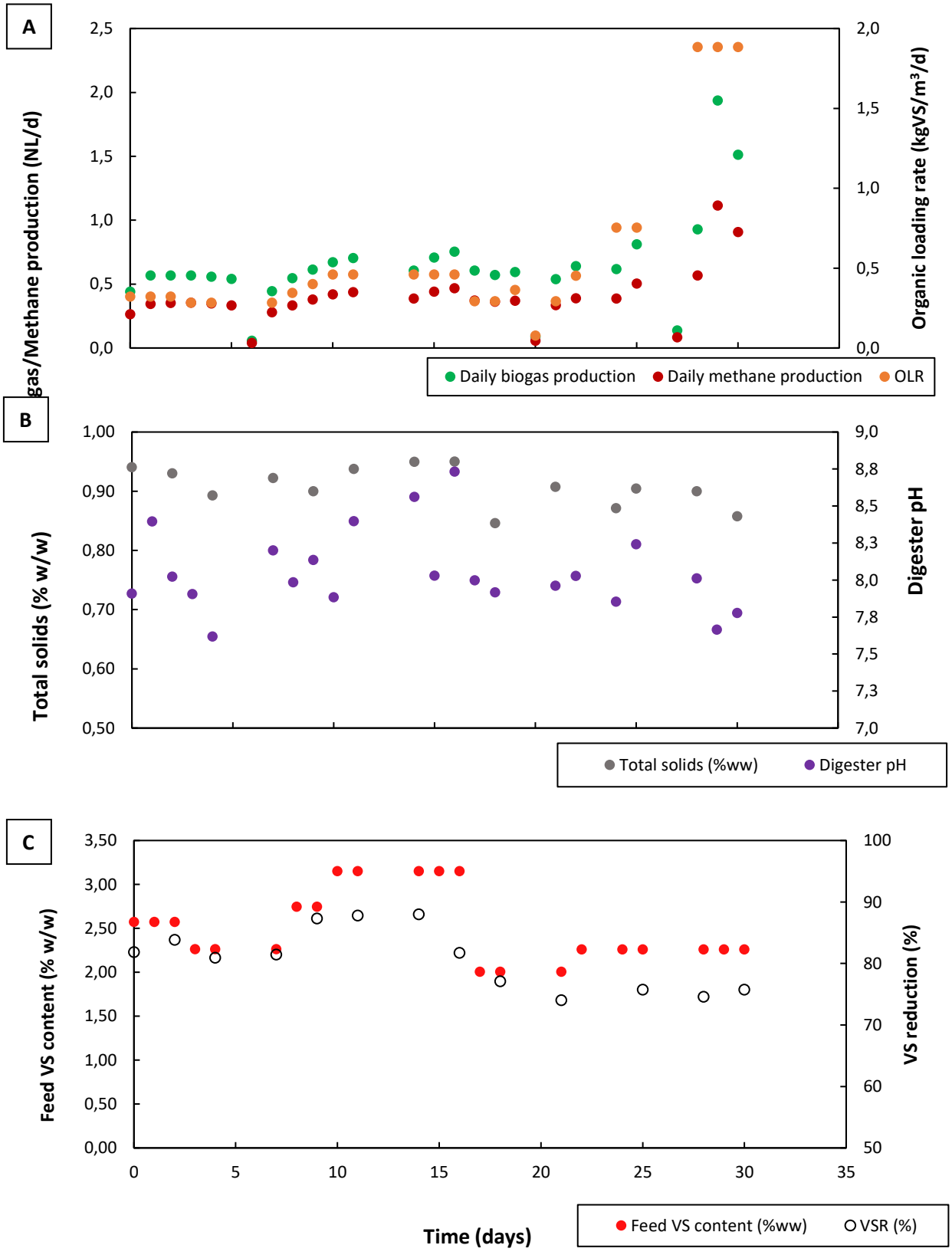


Figure 49: Experimental data for semi-continuous pilot-scale AD reactors fed with tomato wastes; (a) daily biogas/methane production & organic loading rate, (b) digester TS% and pH level, (c) feed VS content and reduction.

### *5.4.2. AD Plant 3: Distillery waste (DW)*

Two types of configurations were investigated for pilot-scale AD tests performed on DW sourced from Plant 3, namely: (1) a semi-continuous-fed reactor operated under conditions similar to Plant 3 and (2) batch-fed reactors under conditions similar to BMP test protocols.

#### *5.4.2.1. Semi-continuous feeding mode*

Experimental data obtained from semi-continuous pilot-scale (35 L) AD tests is presented graphically below, specifically daily biogas & methane production rates and OLR (Figure 50a), digestate TS content and digester pH level (Figure 50b) and feed COD content and COD removal (Figure 50c).

For Days 0 to 11 the system's loading rate ranged 0.67 to 1.75 kgCOD/$m^3$/d (Figure 50a), corresponding to an HRT range of 18 to 8.8 days. A higher HRT was established to give the microbial communities sufficient time to acclimatise to the environment of the 35 L reactor. For Days 16 to 29 the system's feed rate was gradually lowered to an HRT of 4.4 days (OLR increased to 2.28 kgCOD/$m^3$/d) to replicate the feeding rate of the full-scale system. However, between Days 20 to 30, notable changes in reactor performance were observed. The digester pH level decreased from 7.23 to 5.82 and the TS content of sampled digestate dropped from 0.56% to 0.20% (w/w), as shown in Figure 50b. Daily biogas and methane production rates also decreased from 5.86 to 0.54 NL/d and from 4.58 to 0.34 NL $CH_4$/d, respectively (Figure 50a).

Under the established HRT of 4.4 days, the pilot-scale system exhibited a decline in process performance. Poor AD performance may have resulted from a combination of over feeding and poor reactor design. Under semi-continuous feeding digestate samples are removed from the bottom of the vessel via a sampling tap (Label 11, Figure 16), after which the reactor was fed via the draught tube (Label 3, Figure 16). This extraction process may have caused a wash-out of microorganisms from the system because of too low retention times (4.4 days) and greater organic loading rates (2.28 kgCOD/$m^3$/d), resulting in a loss of essential process functionality (Schnürer, 2016). The 35 L system could have been better designed to retain more biomass during feeding. For example, Garcia-Calderon *et al*. (1998) investigated the AD of wine distillery wastewater in a 5.0L anaerobic fluidized-bed reactor for an HRT range of 3.3 to 1.3 days. When the HRT was reduced from 1.6 to 1.3 days, daily biogas production decreased by roughly 22%. In this study, daily biogas production decreased by 91% when the HRT was decreased from 8.8 to 4.4 days. The decreases in biogas production observed by Garcia-Calderon *et al*. (1998) were smaller as the fluidized-bed pilot-scale system retained a higher biomass content due to system's well-suited design, specifically the implementation of a sludge recycle loop, perlite packing material and an overflow line to discharge digestate.

Goodwin *et al*. (2001) also reported process performance issues for a continuously-fed bench-scale UASB reactor (1.1 L) fed malt whiskey distillery pot ale. For an HRT of 4.2 days (OLR = 4.19 kgCOD/$m^3$/d), daily biogas production was ± 1.5 L/d due to VFA accumulations within the system. This daily biogas production was greater than what was achieved by the 35L-pilot-scale reactor operating at a similar HRT of 4.4 days but at a lower OLR (2.28kgCOD/$m^3$/d), which was measured 0.54 NL/d on Day 29 (Figure 50a). Compared to Goodwin *et al*., (2001), this daily production was lower due to the overfeeding of the system.

On Day 34 the pilot-scale reactor was emptied and reloaded with fresh inoculum; for Days 34 to 58 an OLR range of 0.30 to 3.45 kgCOD/$m^3$/d was investigated, as shown in Figure 50a, where the HRT was gradually reduced from 56 to 4.8 days. The greatest SGY and SMY were measured on Day 54 as 405 NL/kgCOD and 298 NL $CH_4$/kgCOD (73.6 %vol methane content), respectively, at an OLR of 0.20 kgCOD/$m^3$/d (HRT = 85 days). During Days 34 to 58 the digester system exhibited healthy conditions, where system pH ranged 6.90 to 7.45 (Figure 50b) and the mean COD reduction obtained as 97.6 ± 0.42% (Figure 50c).

Although the digester was stable for the aforementioned HRT and OLR ranges, the resulting methane yields were lower than yields reported in literature. For example, Farina *et al*. (2004) conducted a pilot-scale study on the AD of different DW using an anaerobic sequencing batch reactor (ASBR) with a working volume of 180 L. For a mean COD loading rate of 4.0 kgCOD/$m^3$/d a methane yield range of 300 to 350 L $CH_4$/kgCOD was obtained. For the 35 L pilot-scale, an SMY of 63.7 NL $CH_4$/kgCOD was obtained for an OLR of 3.45 kgCOD/$m^3$/d (Day 42 in Figure 50a). These differences may have been due to differences in reactor design, as the ASBR investigated by Farina *et al*. (2004) contained an inert support mesh along the overflow digestate line to improve the sludge retention time. However, the study did not indicate that the support mesh improved system productivity or yield but, as suggested by Garcia-Calderon *et al*. (1998), the implementation of support media in AD vessels assists with retaining more biomass in the system.

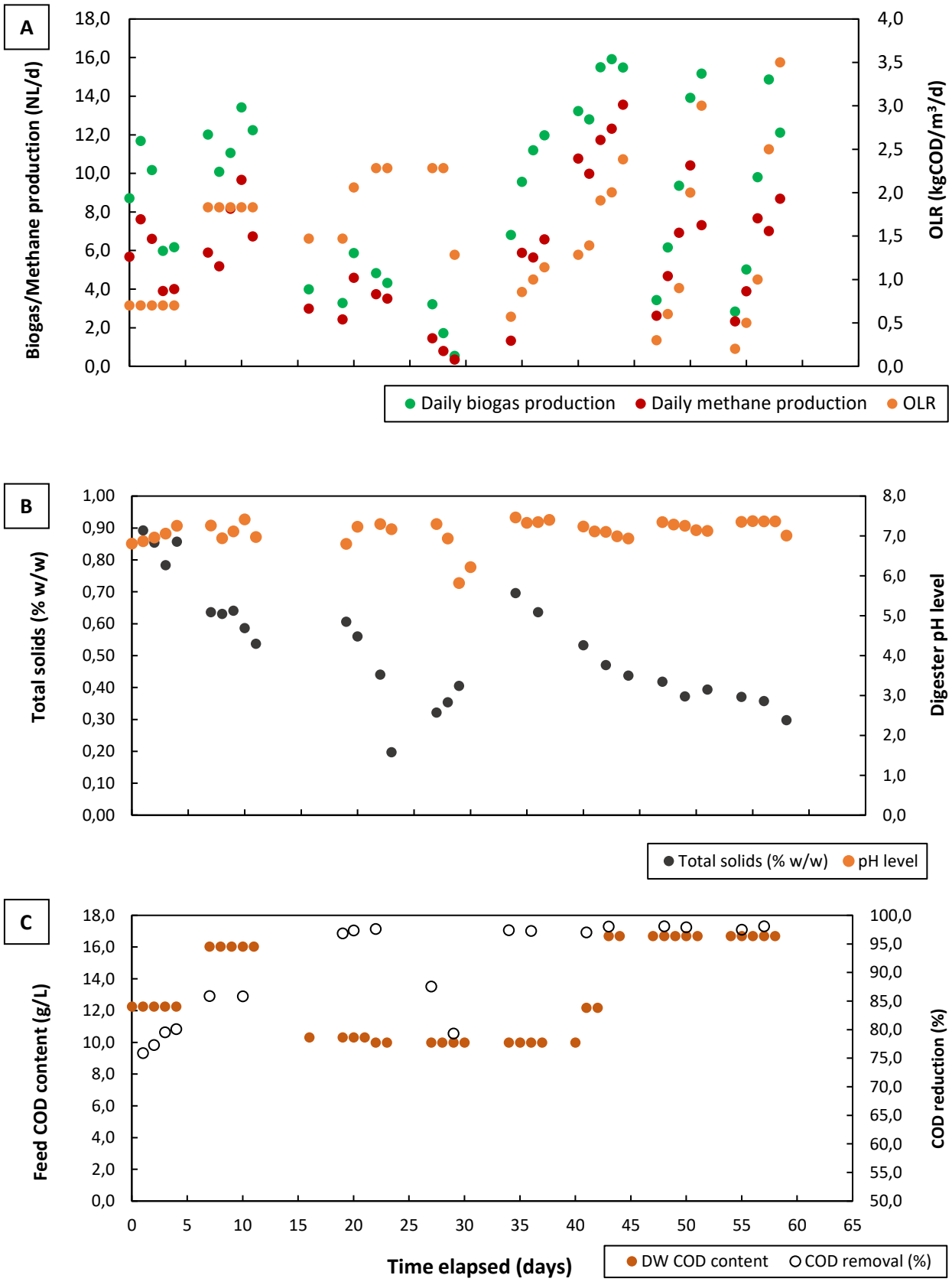


Figure 50: Experimental data for semi-continuously-fed pilot-scale AD reactors; (a) daily biogas/methane production & organic loading rate, (b) digester TS% (w/w) and pH level, (c) feed COD content and reduction.

The semi-continuous pilot-scale system fed with DW were performed under conditions that replicated the conditions of Plant 3, them being mesophilic conditions (± 37 °C), pH adjustment of the feed (pH 6.8 to 7.2) and under a target HRT of 4 days. For a range of organic loading rates, semi-continuous pilot- and full-scale performance data is compared below; daily biogas productions (Figure 51a) and specific gas yields (Figure 51b).

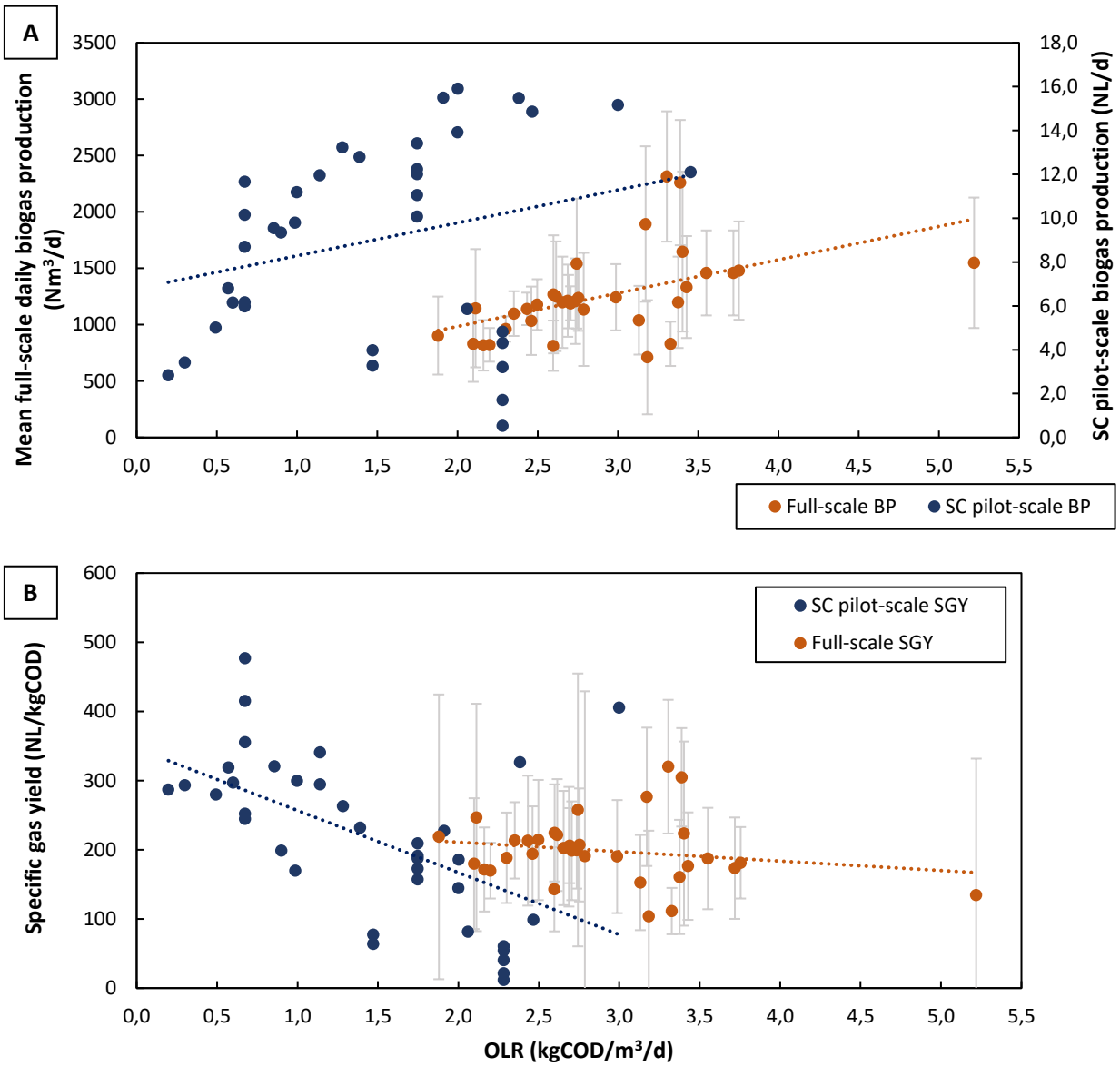


Figure 51: Comparison of performance data between semi-continuously-fed pilot- and full-scale AD systems for Plant 3; (a) daily biogas productions (BP, (b) specific gas yields (SGY).

In Figure 51a, the full-scale AD plant was operated at an OLR range of 2.0 to 3.75 kgCOD/m$^3$/d, where mean daily biogas production was consistent around 1248 ± 371 Nm$^3$/d (SGY of 201 ± 45.9 NL/kgCOD). The pilot-scale system was operated for a range of organic loading rates and could not be maintained at the same OLR as the full-scale system because of biomass wash-out (Schnürer, 2016). This was evident in Figure 51ab, where the pilot-scale's daily biogas production and SGY dropped for a corresponding HRT of 4.4 days. This was due to the fed DW being dilute in COD content (9.98 g/L) at the time. However, even for some OLR ranges maintainable by both the pilot- and full-scale systems (2.06, 2.28, 2.38, 2.47, 3.0

and 3.4 kgCOD/$m^3$/d, given on Figure 51ab), pilot- and full-scale performance data did not correspond. For these corresponding OLRs, the pilot-scale SGY (139 ± 61.0 NL/kgCOD) was roughly 68% of the full-scale SGY (205 ± 20.3 NL/kgCOD). These results did not correspond to results obtained by Gallert *et al*. (2003); for an OLR of 15 kgCOD/$m^3$/d, the full-scale biogas productivity (± 4.5 $m^3$/$m^3$/d) was roughly 75% of the productivity measured by the pilot-scale system (6.0 $m^3$/$m^3$/d). Cavinato *et al*. (2010) reported a similar finding; AD tests were performed using a 380 L pilot-scale CSTR that replicated the conditions of a 1400 $m^3$ full-scale AD plant. For a total solids loading of 5.0 kgTS/$m^3$/d, the full-scale's SGY was roughly 83% of the SGY measured at pilot-scale.

Both of the aforementioned studies found that biogas yields obtained from pilot-scale are greater than what would be achieved at full-scale for the same operating conditions. The difference in results obtained from the pilot- and full-scale systems was attributed to the different feeding modes implemented. Under continuous feeding the full-scale system ensures a consistent production of biogas, provided that no process disturbances are encountered. The pilot-scale system was fed semi-continuously, which resulted in spikes in daily biogas production due to rapid degradation of the fed DW. Figure 52 illustrates these remarks, which shows pulses in daily biogas production for an arbitrary feeding period (19-Oct to 31-Oct 2020):

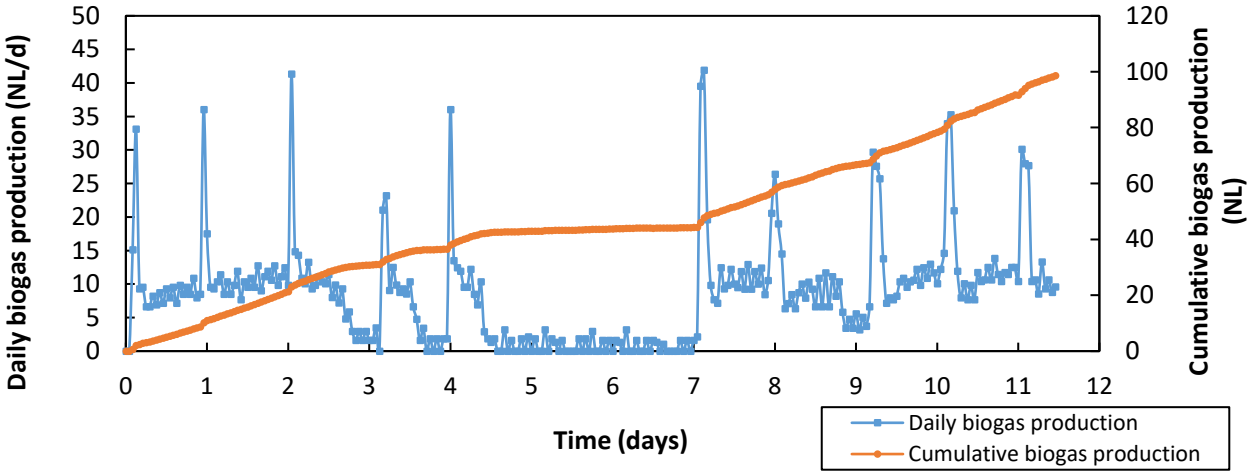


Figure 52: Responses in daily biogas production for the 35L-pilot-scale AD system, operated under semi-continuous feeding (Days 0 to 4: COD = 122.2 g/L; Days 7 to 11: COD = 16.0 g/L).

Figure 52 indicates that, as soon as the pilot-scale system is fed a required volume of DW, biogas production sharply increases. After several hours production then decreased and remained consistent until the next feeding cycle. The reactor was not fed over weekends (Days 4 to 7 in Figure 52), but it is important to note that 12 hours after feeding the system's biogas production decreased rapidly. Therefore, because the full-scale system is continuously-fed, greater volumes of biogas are produced over time, essentially increasing overall biogas yield.

With the aforementioned discussions in mind, results from the semi-continuous pilot-scale system was used to infer on the performance of the full-scale system. Only the extrapolation method (Holliger *et al*., 2017) was considered for full-scale estimations as disintegration constants could not be reliably

determined for semi-continuously-fed AD tests. A linear regression plot was constructed (Figure 53) to obtain the relationship between OLR and SGY for the semi-continuous pilot-scale system.

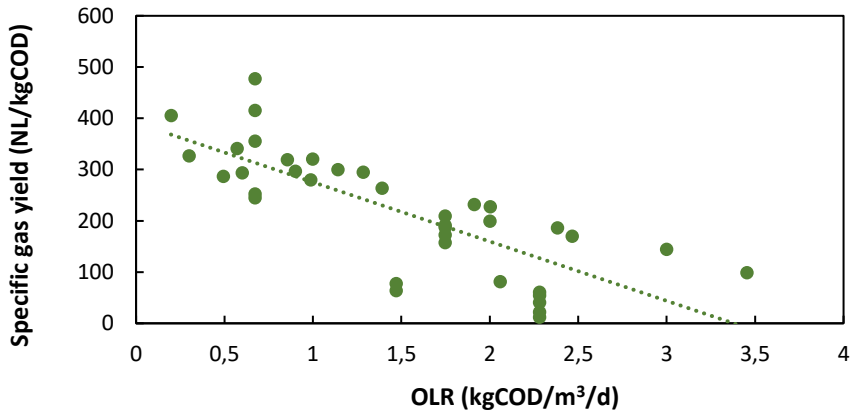


Figure 53: Linear regression plot for semi-continuous pilot-scale organic loading rates and specific gas yields.

The trend line given in Figure 53 is described by Equation (33), where $SGY_{trend}$ and $OLR$ represent specific gas yields and organic loading rates from semi-continuous pilot-scale tests, respectively.

$$SGY_{trend} = -116 \times [OLR] + 391 \quad (33)$$

The full-scale daily biogas production was estimated for a range of OLRs using Equation (33) and the extrapolation calculation. Actual and estimated production parameters are compared in Figure 54.

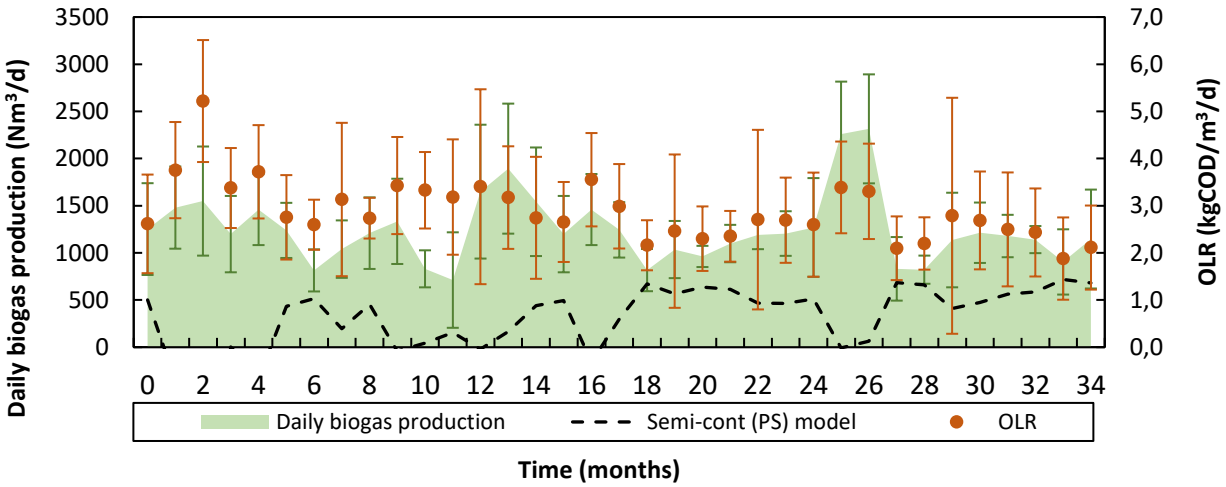


Figure 54: Comparison of actual and extrapolated full-scale daily biogas production rates using semi-continuous pilot-scale AD experimental data.

It is clear that the semi-continuous pilot-scale system underestimated the performance of the full-scale system. For the 34-week period, actual full-scale daily biogas productions were 40-times greater than the estimated biogas productions. These differences are extreme compared to the use of BMP test specific gas yields for estimating full-scale biogas productions (Figure 43), where full-scale biogas productions were roughly 69% of the extrapolated biogas productions. The fluctuations of estimated biogas

production in Figure 54 are a result of the poor correlations between OLR and SGY (Figure 53). Therefore, the application of the semi-continuous pilot-scale to estimate full-scale performance was not feasible.

#### *5.4.2.2. Batch-fed mode with a process protocol similar to BMP tests*

Pilot-scale batch tests were performed on DW samples collected from Plant 3 under conditions that replicated BMP test protocols. The aim of these tests was to assess the changes in performance parameters (gas yields) when AD volumes are scaled-up from bench- (500 mL) to pilot-scale (35 L). Cumulative biogas and methane production (CBP & CMP) data from pilot-scale (PS) batch-fed AD tests are presented in Figure 57 for different DW COD contents. Obtained biogas and methane production data are summarised in Table 30, where batch-mode pilot-scale tests were performed in duplicate.

Table 30: Summary of biogas production data from batch-mode pilot-scale (PS) AD tests.

| Pilot-scale name | DW COD (mg/L) | Inoculum COD (mg/L) | Biogas production data | | Methane production data | | |
|---|---|---|---|---|---|---|---|
| | | | CBP (NL) [a] | SGY (NL/kgCOD) [b] | CMP (NL $CH_4$) [c] | SMY (NL $CH_4$/kgCOD) [d] | $CH_4$ %vol |
| PS1 | 7.81 ± 0.36 | 9.51 ± 0.16 | 12.5 ± 1.13 | 121 ± 10.9 | 7.75 ± 0.70 | 74.9 ± 6.76 | 62.2 ± 1.20 |
| PS2 | 8.89 ± 0.12 | 9.59 ± 0.62 | 17.8 ± 4.19 | 163 ± 38.5 | 10.9 ± 2.57 | 100 ± 23.6 | 61.4 ± 2.56 |
| PS3 | 8.98 ± 0.06 | 9.51 ± 0.16 | 13.0 ± 11.2 | 119 ± 103 | 8.16 ± 7.04 | 75.0 ± 64.7 | 63.0 ± 1.11 |
| PS4 | 9.35 ± 0.57 | 9.51 ± 0.16 | 2.21 ± 0.76 | 20.0 ± 6.90 | 1.36 ± 0.47 | 12.3 ± 4.24 | 61.4 ± 2.82 |
| PS5 | 10.5 ± 0.56 | 9.45 ± 0.54 | 2.52 ± 1.08 | 22.1 ± 9.46 | 1.57 ± 0.67 | 13.8 ± 5.89 | 62.3 ± 0.34 |

[a] :Cumulative biogas production; [b] : specific gas yield; [c] : cumulative methane production; [d] : specific methane yield

According to the pilot-scale results in Table 30, it appears that biogas and methane cumulative volumes and yields decreased with increased feed COD concentrations. The largest SMY was obtained as 100 ± 23.6 NL $CH_4$/kgCOD for PS2 and the lowest SMY was obtained as 12.3 ± 4.24 NL $CH_4$/kgCOD for PS4. These yields are substantially lower than yields measured from BMP tests performed on the same DW samples. A comparison of bench- and pilot-scale yields are compared in Figure 55 below for corresponding COD concentrations.

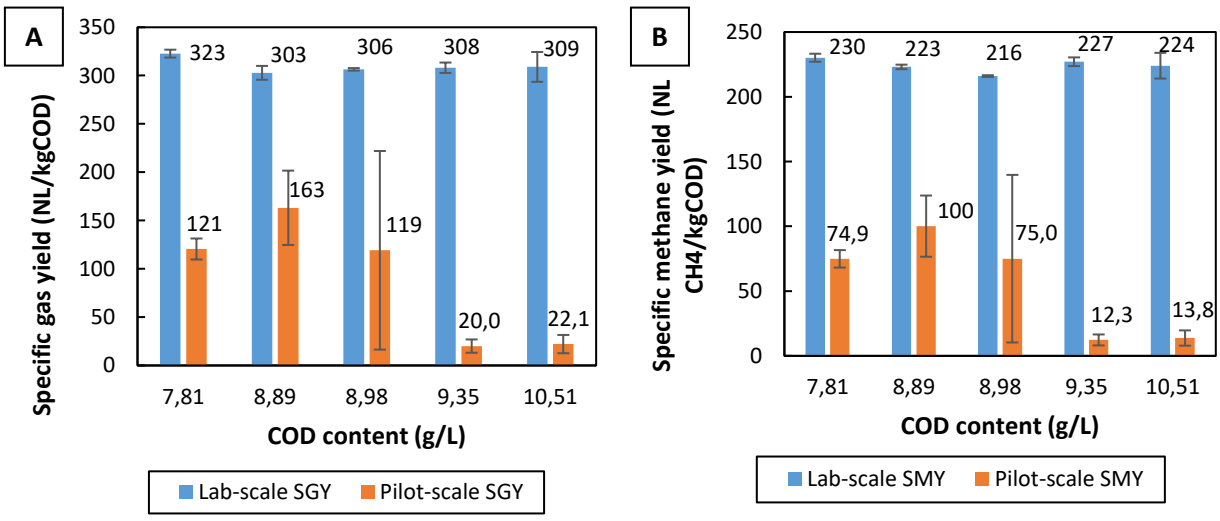


Figure 55: Comparison of bench-scale/BMP test and batch-mode pilot-scale gas yields, measured under BMP test conditions: (a) specific gas yields (SGY) and (b) specific methane yields (SMY).

As shown in Figure 55 none of the specific gas and methane yields correspond between bench- and pilot-scale batch tests. In terms of scale factors, pilot-scale SGYs were roughly 7.16 to 54.0% of SGYs measured from BMP tests, while pilot-scale SMYs were 5.42 to 44.9% of SMYs measured from BMP tests. These scale factors become worse with increased COD concentrations because pilot-scale SGYs and SMYs worsened. The pilot-scale's yields were not attributed to poor process performances, as final digestate analyses reflected stable process conditions. Performance parameters for these tests are shown in Table 31; pH levels for all pilot-scale reactors ranged 7.40 to 7.62, which falls within the stable pH range of 7.0 to 8.5 (Holliger *et al*., 2016; Raposo *et al*., 2012). There rapid changes in pH levels were measured, indicating no accumulations of VFAs. COD reductions (CODR) ranged 96.3 to 97.6%, which exceeds the CODR values typically measured for the AD of DW (>95%, Melamane *et al*., 2007), indicating sufficient degradation of organic material.

Table 31: Summary of performance parameters from batch-mode pilot-scale (PS) AD tests.

| Test | Feed conditions | | | | Performance parameters | | | | |
|---|---|---|---|---|---|---|---|---|---|
| | DW COD (g/L) | DW $pH_{initial}$ | DW $pH_{adj}$ | Inoculum $pH_{initial}$ | Final pH | TS (% w/w) | VS (% w/w) | Final COD (mg/L) | CODR (%) |
| PS1 | 7.81 ± 0.36 | 5.72 | 6.90 | 7.36 ± 0.02 | 7.40 | 0.55 ± 0.03 | 0.37 ± 0.03 | 242 ± 83.4 | 96.9 |
| PS2 | 8.89 ± 0.12 | 6.29 | 7.12 | 7.46 ± 0.04 | 7.43 | 0.63 ± 0.02 | 0.42 ± 0.02 | 331 ± 121 | 96.3 |
| PS3 | 8.98 ± 0.06 | 6.45 | 7.10 | 7.39 ± 0.02 | 7.37 | 0.60 ± 0.04 | 0.41 ± 0.03 | 256 ± 82.0 | 97.2 |
| PS4 | 9.35 ± 0.57 | 6.26 | 7.05 | 7.42 ± 0.01 | 7.40 | 0.56 ± 0.18 | 0.37 ± 0.12 | 224 ± 42.4 | 97.6 |
| PS5 | 10.5 ± 0.56 | 5.79 | 6.95 | 7.20 ± 0.26 | 7.62 | 0.55 ± 0.07 | 0.36 ± 0.05 | 282 ± 85.6 | 97.3 |

Therefore, because bench- and batch-mode pilot-scale tests were performed under identical process conditions, the deviations in biogas and methane yields between both test scales were attributed to the differences in working volumes. Bench- and batch-mode pilot-scale tests were operated under the same mixing frequencies (5-min-on, 5-min-off) but the mixing speed (RPM) of pilot-scale tests was unknown and not reported. Therefore, at larger volumes there may be an increase in shear stress within the system (Clarke, 2013) because the mixing speed may have been faster at pilot-scale. Increased shear stress induces more mechanical stress on the reactor's contents, consequently destroying methanogenic communities and decreasing biogas and methane yields (Singh *et al.,* 2020; Singh *et al.,* 2021). In contrast, under smaller working volumes of bench-scale tests, mixing was assumed to be ideal for non-viscous media with a low TS content (Van't Riet & Van der Lans, 2011.

Another reason contributing to the differences in bench- and batch-mode pilot-scale yields include the differences in microbial physiology (Clarke, 2013). Different inoculum samples were collected over 6 to 8 months exhibited varying compositional characteristics, where inoculum used for BMP tests had total COD contents that ranged from 5000 to 13 280 mg/L, while COD contents for inoculum used in pilot-scale batch tests ranged 9450 to 9590 mg/L (Table 30). These differing COD concentrations suggest that the anaerobic bacteria in different inoculum samples exhibited different microbial growth rates, consequenty impacting obtainable biogas production rates. As such, the disintegration constants between each scale were different. Kinetic data obtained from BMP and pilot-scale tests are compared below in Figure 56ab.

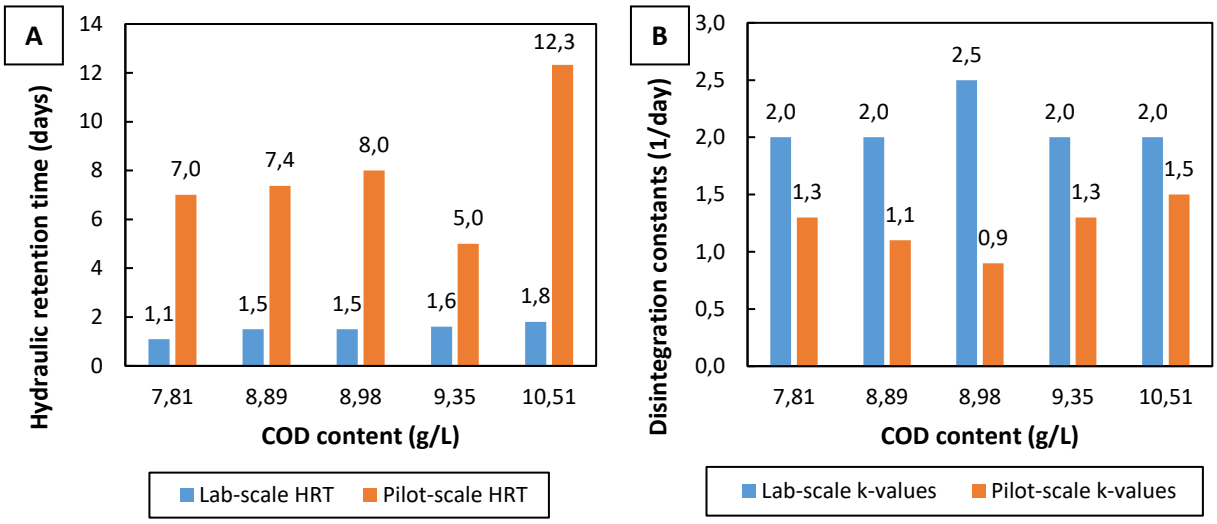


Figure 56: Comparison of hydraulic retention times and disintegration constants (*k*-values) for bench- (a) and (b) pilot-scale tests performed under BMP test conditions.

The bar graphs in Figure 56a show that longer HRTs were obtained for pilot-scale batch tests than the HRTs measured in BMP tests. Reaction kinetic constants also indicated that biogas production rates were faster in BMP tests (2.0 to 2.5 per day) than those obtained from pilot-scale tests (0.9 to 1.5 per day). These results emphasise that, at larger AD test volumes, AD occurs at slower rates and for longer digestion times, indicating a retarding of mass transfer rates. Caillet *et al*. (2020) reported even slower reaction kinetics when BMP tests were performed on sugarcane distillery vinasse, ranging 0.14 to 0.31 per day. This is however due to the more particulate nature of the vinasse, having a TS content of 6.64% (w/w) compared to DW samples having a TS content of ± 0.52% (w/w) (Table 12). Degradation kinetic data has not been reported for large-scale (50 L) AD batch tests performed on distillery effluents. Moreover, as recommended by Weinrich *et al*. (2018), large-scale batch tests (10 to 20 L) should be performed only on non-homogenous (particulate) feedstocks, while BMP tests are typically performed at working volumes of 0.1 to 2.0 L (DIN 38414-, 1985; DIN EN ISO 11734, 1998; Angelidaki *et al*., 2009; VDI 4630, 2016; Holliger *et al*., 2016).

Another reason explaining the low biogas and methane yields measured from pilot-scale batch tests relates to the inoculum-substrate-ratio (ISR) established for loading the reactors. An ISR of 2.0 was selected for both BMP and pilot-scale tests, as according to the BMP protocol guidelines proposed by Holliger *et al*. (2016). This ratio, however, may have been too large for the AD of DW. For example, Caillet *et al*. (2020) investigated different ISRs in BMP tests for sugarcane distillery effluents. The study found that the greatest methane yields were obtained for an ISR of 1.0, on a VS basis. On a COD basis, this ratio corresponds to 0.512. Therefore, if a lower ISR of 0.5 was established for pilot-scale batch tests, biogas and methane yields may have been more similar to BMP test yields, but further batch-mode pilot-scale tests would need to be performed to identify the optimal ISR for such tests.

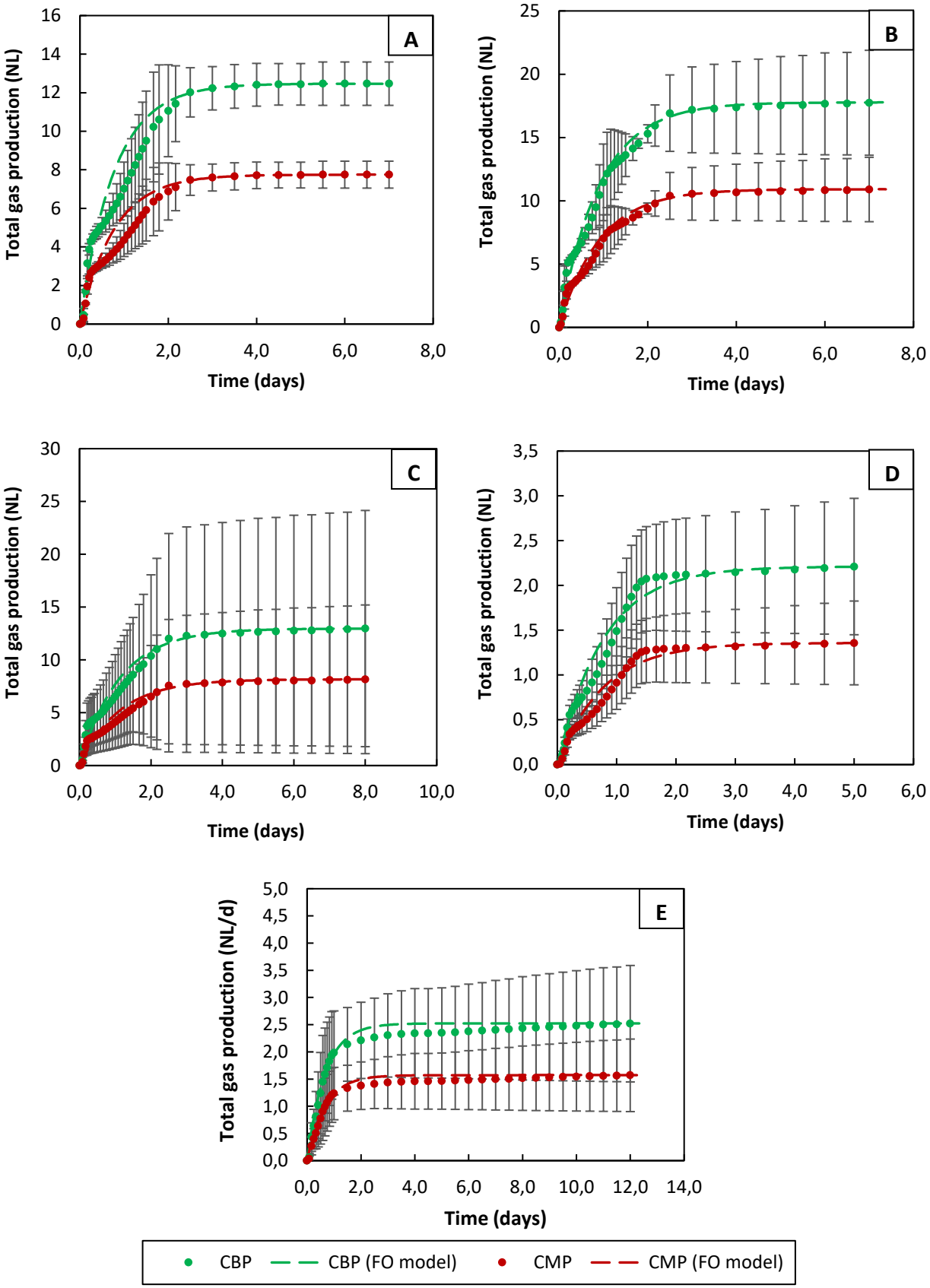


Figure 57: Cumulative biogas and methane production curves from pilot-scale AD batch tests; (a) PS1 (COD = 7.81 mg/L), (b) PS2 (COD = 8.89 mg/L), (c) PS3 (COD= 8.98 mg/L), (d) PS4 (COD = 9.35 mg/L), (e) PS5 (COD = 10.5 mg/L). Error bars represent the standard deviations for a sample size *n* = 2.

Experimental results obtained from batch-mode pilot-scale AD tests were used to infer on the performance of Plant 3. BMP degradation rates (BDR) were not calculated from such datasets as blank pilot-scale tests were not performed. The extrapolation method proposed by Holliger *et al*. (2017) (Equation (11)) was used to estimate full-scale biogas productions and yield. A linear regression model was constructed to correlate batch-mode pilot-scale SGY and SMY data to feed COD concentrations (Figure 58).

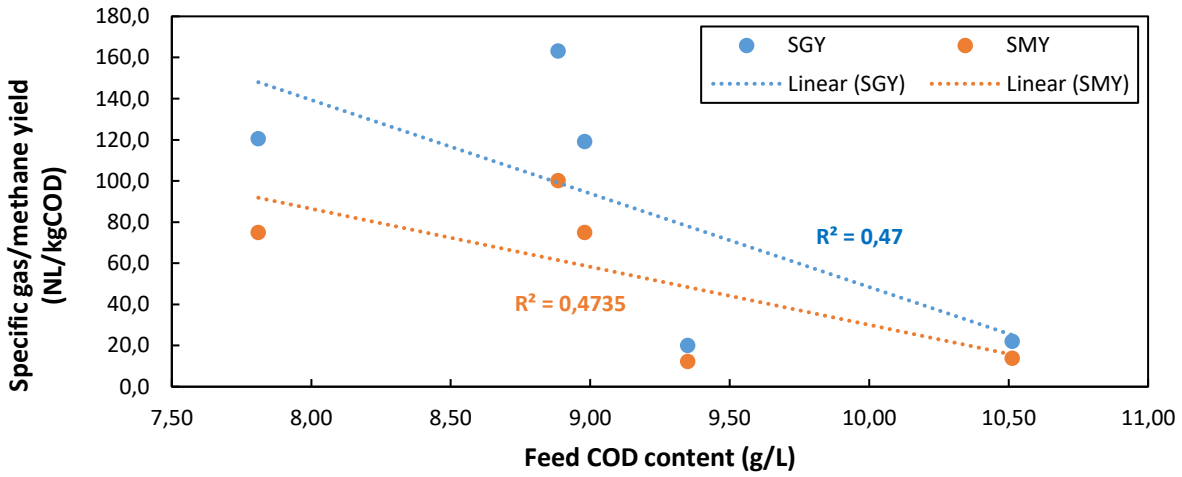


Figure 58: Linear regression plots for specific gas and methane yields obtained from batch pilot-scale AD tests.

The linear regression models' trend lines for SGY ($SGY_{trend}$) and SMY ($SMY_{trend}$) for different COD concentrations are described by Equation (34) and Equation (35) below:

$$SGY_{trend} = -45.5 \times [COD] + 503 \quad (34)$$

$$SMY_{trend} = -28.2 \times [COD] + 312 \quad (35)$$

The linear regression models were restricted to a COD concentration range of 7.8 to 10.5 g/L because estimating full-scale biogas production rates beyond 10. 5 g/L would have resulted in negative values, as visible on Figure 58. The actual full-scale mean daily biogas productions and SGYs for a COD range of 7.8 to 10.5 g/L are given below in Table 32. Estimations of the mean daily biogas production are compared with actual/full-scale daily biogas productions in Figure 59.

Table 32: Full-scale datasets corresponding to batch-mode pilot-scale for different COD contents.

| Month | Feed rate (m3/d) | Actual feed COD (mg/L) | Biogas production data | | Methane production data | |
|---|---|---|---|---|---|---|
| | | | $Nm^3/d$ | SGY (NL/kgCOD) | $Nm^3\ CH_4/d$ | SMY (NL $CH_4$/kgCOD) |
| Jul-18 | 588 ± 112 | 9.70 ± 1.60 | 814 ± 223 | 1423 ± 60.8 | 528.9 ± 145 | 92.8 ± 39.5 |
| Jul-19 | 540 ± 64.9 | 8.83 ± 2.00 | 817 ± 224 | 172 ± 60.8 | 531.3 ± 146 | 112 ± 53.1 |
| Aug-19 | 557 ± 72.3 | 9.58 ± 5.70 | 1035 ± 303 | 194 ± 68.8 | 672.8 ± 197 | 126 ± 44.7 |
| Sep-19 | 569 ± 56.5 | 8.98 ± 2.87 | 962 ± 112 | 188 ± 65.4 | 625.3 ± 73.1 | 122 ± 42.5 |
| Oct-19 | 620 ± 55.7 | 8.30 ± 1.62 | 1099 ± 198 | 214 ± 55.2 | 714.1 ± 129 | 139 ± 35.9 |
| Nov-19 | 639 ± 72.0 | 9.37 ± 6.75 | 1190 ± 151 | 199 ± 71.4 | 773.4 ± 98.0 | 129 ± 46.4 |
| Dec-19 | 643 ± 87.0 | 9.10 ± 2.23 | 1205 ± 237 | 206 ± 54.3 | 783.0 ± 154 | 134 ± 35.3 |
| Jan-20 | 600 ± 144 | 9.43 ± 2.41 | 1269 ± 523 | 224 ± 70.2 | 825.0 ± 340 | 14 ± 45.6 |
| Mar-20 | 702 ± 55.0 | 10.3 ± 2.69 | 2315 ± 578 | 320 ± 96.6 | 1504 ± 376 | 208 ± 62.8 |
| Apr-20 | 448 ± 56.5 | 10.3 ± 3.36 | 830.3 ± 337 | 180 ± 94.5 | 539.7 ± 241 | 117 ± 61.4 |
| May-20 | 507 ± 60.3 | 9.54 ± 2.17 | 821.6 ± 149 | 170 ± 40.3 | 534.0 ± 97.1 | 110 ± 26.2 |
| Jul-20 | 591 ± 40.2 | 10.05 ± 3.85 | 1213 ± 320 | 204 ± 86.5 | 788.5 ± 208 | 133 ± 56.2 |
| Aug-20 | 597 ± 25.2 | 9.22 ± 4.55 | 1178 ± 225 | 214 ± 86.8 | 766.0 ± 146 | 139 ± 56.4 |
| Sep-20 | 597 ± 28.7 | 8.96 ± 3.36 | 1141 ± 144 | 213 ± 93.9 | 741.4 ± 93.3 | 139 ± 61.1 |

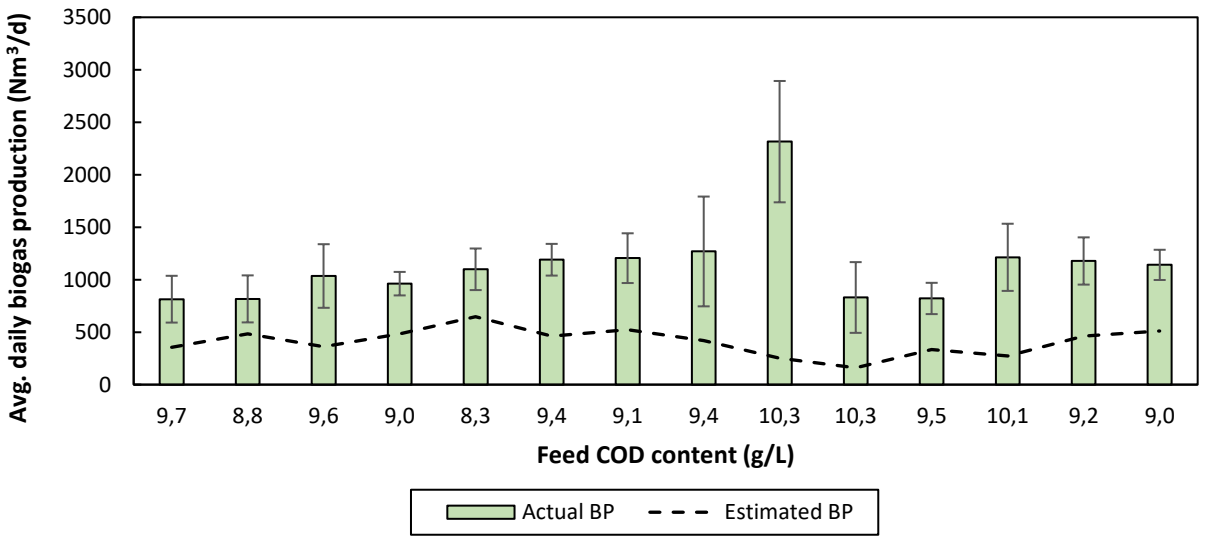


Figure 59: Actual and estimated daily biogas productions (BP) for Plant 3, using batch-mode pilot-scale test data.

From Figure 59, it is clear that the estimated daily biogas productions for Plant 3 were underestimated for the given COD concentration range due to low biogas yields measured during batch-mode pilot-scale AD tests. For the whole COD range given in Figure 59, actual daily biogas production was roughly 3.18-times greater than the calculated productions. These underestimations emphasize the extreme deviations in the conditions between either scales. BMP tests resulted in greater biogas and methane yields, where it was shown that the extrapolation of these results for estimating full-scale behaviour (Figure 43 and Figure 44) resulted in a mean scale factor of 68.7 ± 15.1%. Therefore, the extrapolation of

batch-mode pilot-scale SGY data for full-scale estimations was deemed unreliable due to the low biogas yields measured at these larger volumes (35L).

The dynamic model (Fiore *et al.*, 2016) was used to estimate full-scale behaviour using the same results measured from batch-mode pilot-scale results (Table 30), with the inclusion of disintegration constants measured from such tests. A linear regression model was constructed to show the relationship between disintegration constants measured from pilot-scale tests and feed COD content (Figure 60).

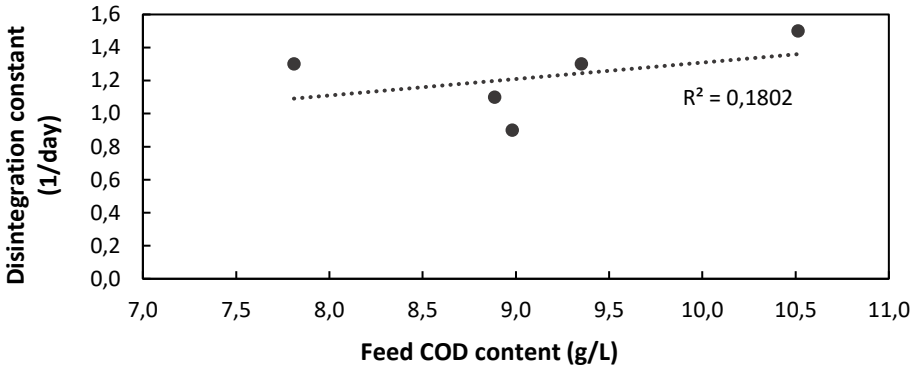


Figure 60: Disintegration constants versus feed COD content, according to batch-mode pilot-scale results.

The equation for the linear trend line in Figure 60 is expressed below as Equation (36), which correlates disintegration constant values with feed COD concentrations. Actual and dynamically-modelled daily biogas productions are compared in Figure 61.

$$k_{dis} = 0.0995 \times [COD] + 0.3134 \quad (36)$$

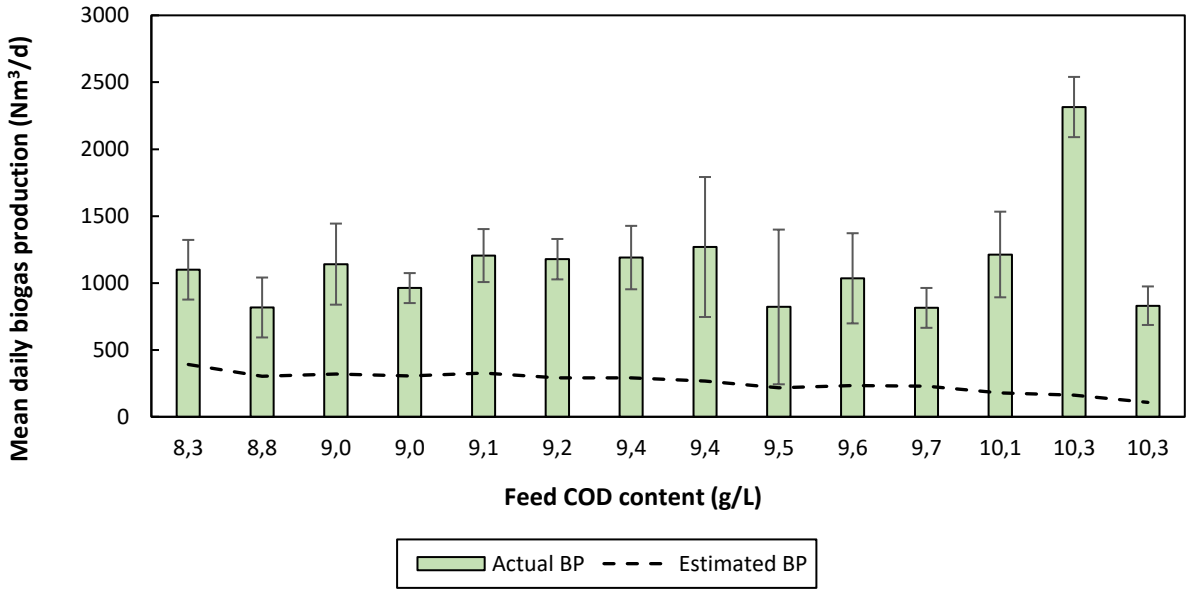


Figure 61: Actual and dynamically-modelled daily biogas productions (BP) for Plant 3, using batch-mode pilot-scale test data.

Similar to what was observed in Figure 59, the dynamic model's estimates were less than the actual full-scale daily biogas productions, as shown in Figure 61. These results indicate greater deviations between pilot- and full-scale process conditions, where, on average, actual biogas productions were 4.95-times greater than their estimated values. This scale factor was greater than that calculated from using the extrapolation method (3.18), which was due to the inclusion of reaction kinetics data in the model. The regression-estimated kinetic constants ranged from 1.0 to 1.60 1/day, as determined from batch-mode pilot-scale AD tests. Therefore, the scale factor of 4.95 indicates that process conditions regarding reaction kinetics in batch-mode pilot-scale tests were different than those of the full-scale system. Once again, BMP tests provided more accurate estimations of full-scale behavior, where the scale factor was calculated as 92 ± 20.8%. Therefore, estimating full-scale behaviour using results generated from pilot-scale tests replicating BMP test conditions did not improve the precision of full-scale behaviour estimates and BMP tests themselves provided better approximations based on bench-scale gas yields and disintegration constants.

## 5.5. Summary of scale factors

Biogas installations Plant 1 (co-digestion of mixed organic wastes), Plant 2 (tomato waste) and Plant 3 (distillery effluent) all had their process performances evaluated by BMP degradation rates (BDR) (Schievano *et al*., 2011; Li *et al*., 2017) and two methods proposed from literature (Fiore *et al*., 2016; Holliger *et al*., 2017). A summary of performance estimations are given in Table 33 for each biogas plant.

Table 33: Overview of scale factors obtained for each biogas plant for different AD test scales.

| **Full-scale biogas plant** | **Extrapolation scale factors** | | **Dynamic model scale factors** | | **Degradation efficiencies** | |
|---|---|---|---|---|---|---|
| **Plant 1: co-digestion of mixed organic wastes** | | | | | | |
| **Full-scale behaviour estimated by:** | **BP [a] & SGY [b]** | **MP [c] & SMY [d]** | **BP & SGY** | **MP & SMY** | **VSR (%) [e]** | **BDR (%) [f]** |
| Bench-scale (BMP tests) | 0.42 ± 0.28 | 0.36 ± 0.26 | 0.86 ± 0.42 | 0.72 ± 0.41 | 95.7 ± 2.43% | 88.5 ± 3.51% |
| Pilot-scale | No pilot-scale tests performed | | | | | |
| **Plant 2: AD of tomato wastes (TW)** | | | | | | |
| **Full-scale behaviour estimated by:** | **BP & SGY** | **MP & SMY** | **BP & SGY** | **MP & SMY** | **VSR (%)** | **BDR (%)** |
| Bench-scale (BMP tests) | 1.05 | 0.96 | 3.10 | 2.69 | 73.7 ± 4.36% | 82.3 ± 2.93% |
| Pilot-scale (semi-cont.) | 10.9 | 11.2 | n.d. [g] | n.d. | n.d. | n.d. |
| **Plant 3: AD of distillery wastes (DW)** | | | | | | |
| **Full-scale behaviour estimated by:** | **BP & SGY** | **MP & SMY** | **BP & SGY** | **MP & SMY** | **VSR (%)** | **BDR (%)** |
| Bench-scale (BMP tests) | 0.69 ± 0.15 | n.d. | 0.92 ± 0.21 | n.d. | 98.1 ± 1.01% | 87.3 ± 17.8% |
| Pilot-scale (semi-cont.) | 40.0 ± 32.2 | n.d. | n.d. | n.d. | n.d. | n.d. |
| Pilot-scale (batch) | 3.18 ± 1.99 | n.d. | 4.95 ± 3.04 | n.d. | n.d. | n.d. |

[a] : Biogas production; [b] : specific gas yield; [c] methane production; [d] : specific methane yield; [e] : VS reduction; [f] : BMP degradation rate; [f] : not determined.

From the results given in Table 33, the scale factors indicate that BMP tests served as better approximations of full-scale AD performance than the use of pilot-scale AD tests. The mean scale factors calculated via the extrapolation method for Plant 1, Plant 2 and Plant 3 were obtained as 0.42, 1.05 and 0.69, respectively, with Plant 2 leaning more towards ideal bench-scale behaviour. Moreover, scale factors calculated from the dynamic model were greater than those calculated from the extrapolation method. These mean scale factors for Plant 1, Plant 2 and Plant 3 were calculated as 0.86, 3.10 and 0.92, respectively. Plant 3 reflected more ideal conditions that Plant 1 and Plant 2 when its performance was estimated with the dynamic model, indicating the reaction kinetics between bench- and full-scale were similar. Therefore, the dynamic model serves as a better tool for estimating full-scale using BMP tests.

In contrast, scale factors calculated from pilot-scale data for Plant 2 and Plant 3 were much greater than those calculated from BMP tests. Scale factors calculated from extrapolated semi-continuous pilot-scale biogas productions and yields for Plant 2 and Plant 3 reflected values of 10.9 and 40.0, respectively, indicating a tremendous difference in process conditions between pilot- and full-scale systems. Pilot-scale batch tests for Plant 3 also reflected high scale factors compared to the use of BMP test data. The extrapolation method gave a scale factor of 3.18 while the dynamic model gave a factor of 4.95, thus indicating that the full-scale system does not exhibit the same conditions established for pilot-scale tests, even if BMP protocol conditions are established at these scales.

For each biogas plant, the calculated scale factors could be used to optimise full-scale performance. Plant 1 produces electricity and heat using a combined-heat-and-power (CHP) unit, whose function depends on the flow rate of methane gas produced from the 3200 $m^3$ digester. The mean scale factor of 0.72 calculated from the dynamic model for methane production indicates that 72% of methane produced in BMP tests will be produced at full-scale. This is potentially useful for predicting the energy output of the CHP unit for a given VS content range for different feedstocks. For Plant 2, full-scale performance was estimated using one day's worth of operational data. This limited the application of the obtained scale factors to optimise full-scale performance over longer durations. Plant 3 employs full-scale AD for the biological treatment of DW, where produced biogas is used for regulating process temperature or is flared. The mean scale factor of 0.92 calculated from dynamical modelling and BMP tests indicates that full-scale biogas yields will be 92% of yields measured at bench-scale. This scale factor may be useful if Plant 3 considers the implementation of a CHP unit on site for electricity production. Estimating biogas production will provide an indication of energy production potential for a range of DW samples of differing COD concentrations. However, given that methane concentrations were not measured on Plant 3, energy production estimates could only be based on biogas production rates.

## CHAPTER 6: CONCLUSIONS

The goal of this research project was to utilize BMP tests for predicting the performance of full-scale AD plants. Two methods were used to estimate the performances of full-scale plants using standardised BMP tests and pilot-scale AD tests namely: (1) an extrapolation method and (2) a CSTR dynamic model. Full-scale performance parameters were estimated with such methods and scale factors were calculated by finding the ratios of real-time full-scale performance data to estimated full-scale performance data. It was found that BMP tests could be used to estimate the performance of full-scale AD processes. For both the extrapolation method and CSTR dynamic model, scale factors calculated for the liquid AD plant (Plant 3, DW) were greater in magnitude (0.69 to 0.92) than scale factors calculated for the solid-based AD plant (Plant 1, treating mixed food and agricultural wastes), whose scale factors were calculated as 0.42 to 0.86). A scale factor of 1.05 for Plant 2 (TW) was calculated but this result was limited by the lack of full-scale operational data (lack of process monitoring instrumentation) acquired from Plant 2. Considering the use of BMP tests as predictors for full-scale AD performance, the CSTR dynamic model gave more accurate estimations than the extrapolation method. This was because the dynamic model accounted for anaerobic degradation kinetics, which influenced the estimations of full-scale biogas production rates. These results were more conclusive for Plant 3 (distillery waste), where scale factors calculated from the dynamic model and extrapolation method reflected values of 92 ± 21% and 69 ± 15%, respectively, for a 34-month operational period. It was not possible to verify whether the extrapolation method or dynamic model gave better estimations of full-scale behaviour for Plant 1 and Plant 2 due to limited full-scale operational datasets. In this study, pilot-scale AD tests could not be used to accurately estimate full-scale AD performance due to errors encountered during experimental procedures. The poor biogas and methane yields measured from pilot-scale tests resulted in underestimations of full-scale performance, where real-time full-scale performance data were roughly 3.2-times greater than estimated full-scale performance data. Overall, for the example of results obtained for Plant 3 (distillery waste), the CSTR dynamic model could be considered for industrial AD applications, providing a sufficient number of BMP tests are performed on substrates collected during different times of the year. Performing BMP tests on seasonally-collected feedstocks accounts for changes in feedstock composition, which subsequently allows for the assessment of changes in biogas and methane yields. Furthermore, the dynamic model could be used to estimate electricity production potential for downstream combined-heat-and-power (CHP) units. Changes in peak and baseload electricity requirements can be predicted for changes in feedstock composition (i.e. seasonal effects), however this may be a complex project as additional full-scale AD performance data (e.g. methane productions and yields) and biogas-fired engine data (e.g. power output, availability, efficiencies etc.) are required.

.

# CHAPTER 7: RECOMMENDATIONS

The following section provides insight on the limitations encountered during this study. Recommendations for future investigation are also discussed as guidelines for future work.

## 1. Full-scale AD plant challenges:

**1.1.** Plant 1 (mixed organic wastes) logged full-scale data inconsistently, which were often not representative of certain process parameters. For example, daily feed masses were logged per container, where mass feed rates were based on the capacities of the container (500 kg for bins, 1000kg for pallets). It was observed that feedstock containers were not filled to capacity, which, in turn, introduced inaccuracies with estimating feed rates and thus achievable methane yields. Plant 1 should thus employ better control of feeding rates to the system by recording actual container masses.

**1.2.** Plant 2 did not log any full-scale performance data and rarely monitored the conditions of the 60$m^3$, and thus the application of the extrapolation and dynamic modelling methods to estimate full-scale performance was limited. Plant 2 should employ instrumentation on site to better monitor actual full-scale performance parameters. Moreover, Plant 2 was subject to numerous disturbances that disrupted full-scale performance. For example, power outages affected the health of the 60$m^3$ digester due to losses in process temperature.

**1.3.** Plant 3 was the most specialized and controlled full-scale AD plant, however the methane concentrations of produced biogas were not monitored. Recording methane concentrations would have allowed for the prediction of methane production rates, which are, for example, more sensitive to variations in feedstock composition than biogas production rates.

## 2. Experimental challenges:

**2.1.** For Plant 1, full-scale performance estimations were based on 5 days'-worth of feed rate data. It is recommended to collect all individual feedstocks from Plant 1, freeze them and aliquot mixtures for future BMP tests to expand on the sample size of BMP test data. Moreover, mixture proportions should be based on weekly proportions as opposed to daily proportions.

**2.2.** Pilot-scale AD tests were not performed for Plant 1 due to the complexity of feeding frequencies and due to the hazards associated with aliquoting large quantities of cow blood.

**2.3.** The gas measurement system (GMS) for the semi-continuous pilot-scale AD system for Plant 2 was not calibrated to ensure accurate recordings of daily biogas productions. This deduction was made based on the stable conditions monitored for the pilot-scale system throughout its operational period. It is recommended for future work to calibrate the pilot-scale GMS using the water displacement method to ensure accurate recordings of gas production.

**2.4.** Semi-continuous pilot-scale tests for Plant 3 were limited in their abilities to replicate the conditions of the full-scale system. This was due to the unsuited design of the reactor system for the semi-continuous feeding of liquid feedstocks (DW). Biomass wash-out occurred at low HRTs when digestate was extracted during feeding cycles. The lack of retaining biomass in the system thus impacted biogas and methane production rates. It is recommended to reconfigure the design of pilot-scale reactors according to semi- and/or continuous feeding modes. For example, the implementation of an overflow line for digested material to exit the system and/or digester packaging material to improve biomass immobilisation. It is recommended to investigate continuously-fed feeding modes for AD reactors treating liquid-based feedstocks, especially if such feedstocks are rapidly degradable. This would improve biogas and methane production rates for better comparability to full-scale productions. Furthermore, batch-mode pilot-scale tests performed under BMP test protocol were operated at an ISR of 2.0, at which low biogas and methane yields were obtained. Therefore, lower ISRs (e.g. 0.5 to 1.0) should be investigated to determine if gas yields would improve. This would potentially allow for better estimations of full-scale performance.

## LIST OF REFERENCES


1. Abraham, A., Mathew, A.K., Park, H., Choi, O., Sindhu, R., Parameswaran, B., Pandey, A., Park, J.H., Sand, B-I. (2020). *Pretreatment strategies for enhanced biogas production from lignocellulosic biomass.* Bioresource Technology, 301, 122725.

2. Abdallah, M., Shanableh, A., Adghim, M., Ghenai, C., Saad, S.A. (2018) *Biogas production from different types of cow manure*. In: Advances in Science and Engineering Technology International Conferences, 6-7 February 2018, Dubai. Dubai: IEEE.

3. Achinas, S., Longinos, S.N., Achinas, V., Euverink, G.J.W. (2020). *Scale-up operations for biogas production: Analysis on critical factors governing large-scale operations.* Biogas Production, Springer, 263-284.

4. Ahring, B.k. (1995). *Methanogenesis in thermophilic biogas reactors.* Antonie van Leeuwenhoek, 67(1), 91-102.

5. Akram, A., and Stuckey, D. (2008). *Biomass acclimatization and adaption during start-up of a submerged anaerobic membrane reactor (SAMBR).* Environmental Technology, 29, 1053-1065.

6. Aldin, S., Nakhla, G., Ray, M.B. (2011). *Modeling the influence of particulate protein size on hydrolysis in AD.* Industrial & Engineering Chemistry Research, 50(18), 10843-10849.

7. Al-Saedi, T., Rutz, D., Prassl, H., Kottner, M., Finsterwalder, T., Volk, S., Janssen, R. (2008). *Biogas Handbook.* University of Denmark Esbjerg, Niels Bohrs.

8. Amaral, A. C. do, Kunz, A., Steinmetz, R. L. R., Cantelli, F., Scussiato, L. A., & Justi, K. C. (2014). *Swine effluent treatment using AD at different loading rates.*

9. American Public Health Association. (1999). *Standard methods for the examination of water and wastewater.* American Water Works Association, Water Environment Federation.

10. Amon, T., Amon, B., Kryvoruchko, V., Zollitsch, W., Mayer, K., Gruber, L. (2007). *Biogas production from maize and dairy cattle manure – influence of biomass composition on the methane yield.* Agriculture, Ecosystems & Environment, 118(1-4), 173-182.

11. Angelidaki, I., and Sanders, W. (2004). *Assessment of the anaerobic biodegradability of macropollutants.* Reviews in Environmental Science and Bio/Technology, 3(2), 117-129.

12. Angelidaki, L., Alves, M., Bolzonella, D., Borzacconi, L., Campos, J.L., Guwy, A.J., Kalyuzhnyi, S., Jenicek, P., Van Lier, J.B. (2009). *Defining the biomethane potential (BMP) of solid organic wastes and energy crops: A proposed protocol for batch assays.* Water, Science & Technology, 59, 927-934.

13. Arhoun, B., Villen-Guzman, M., Gomez-Lahoz, C., Rodriguez-Maroto, J.M., Garcia-Herruzo, F., Vereda-Alonso, C. (2019). *Anaerobic Co-digestion of Mixed Sewage Sludge and Fruits and Vegetable Wholesale Market Waste: Composition and Seasonality Effect.* Journal of Process Engineering, 31, 100848.

14. Arikan, O. A., Mulbry, W., Lansing, S. (2015). *Effect of temperature on methane production from field-scale anaerobic digesters treating dairy manure.* Waste Management, 43, 108-13.

15. Battista, F., Fino, D., Mancini, G., Ruggeri, B. (2016). *Mixing in digesters used to treat high viscosity substrates: The case of olive oil production wastes.* Journal of Environmental Chemical Engineering, 4(1), 915-923.

16. Barragan-Escandon, A., Ruiz, J.M.O., Tigre, J.D.C., Zalamea-Leon, E.F. (2020). *Assessment of power generation using biogas from landfills in an equatorial tropical context.* Sustainability, 12, 2669-2677.

17. Belhadj, S., Joute, Y., El Bari, H., Serrano, A., Gil, A., Lopez, J.A.S., Chica, A.F., Martin, M.A. (2014). *Evaluation of the anaerobic co-digestion of sewage sludge and tomato waste at mesophilic temperature.* Applied Biochemistry and Biotechnology, 172(8).

18. Bioprocess Control, Sweden. (2020). Available from: https://www.bioprocesscontrol.com/products/ampts-ii/ [Accessed 12 February 2020].

19. Bishop, G.C., Burns, R.T., Shepherd, T.A., Moody, L.B., Gooch, L.A., Spajic, R., Pronto, J.L. (2009). *Evaluation of Laboratory Biochemical Methane Potentials as a Predictor of Anaerobic Dairy Manure Digester Biogas and Methane Production*. Reno, Nevada, June 21 - June 24.

20. Borja, R., Martin, A., Luque, M., Duran, M.M. (1993). *Kinetic study of AD of wine distillery wastewater.* Process Biochemistry, 28, 83-90.

21. Buchauer, K. (1998). *A comparison of two simple titration procedures to determine volatile fatty acids in influents to waste-water and sludge treatment processes.* Water SA, 24(1), 49-56.

22. Budiyono, I.N., Widiasa, S., Johari, and Sunarso. (2010). *The Kinetic of Biogas Production Rate from Cattle Manure in Batch Mode.* International Journal of Chemical and Biological Engineering, 3(1), 39-44.

23. Buffière P., Frederic S., Marty B., Delgènes J.P. (2008). *A comprehensive method for organic matter characterization in solid wastes in view of assessing their anaerobic biodegradability*. Water Science and Technology. 58, 1783–8.

24. Buswell, A.M., Symons, G.E. (1933). *The methane fermentation of carbohydrates*. Journal of the American Chemical Society, 55, 2028–2036

25. Calabrò, P.S., Greco, R., Evangelou, A., Komilis, D. (2015). *AD of tomato processing waste: Effect of alkaline pretreatment.* Journal of Environmental Management, 163, 49-52.

26. Caillet, H., and Adelard, L. (2020). *Start-up strategy and process performance of semi-continuous AD of raw sugarcane vinasse.* Waste and Biomass Valorization, 12, 185-198.

27. Caillet, H., Lebon, E., Akinbenchi, E., Madyira, D., Adelard, L. (2019). *Influence of inoculum to substrate ratio on methane production in Biochemical Methane Potential (BMP) tests of sugarcane distillery waste water.* 2nd International Conference on Sustainable Materials Processing and Manufacturing (SMPM 2019), 35, 259 – 264.

28. Camarena-Martinez, S., Martinez-Martinez, J.H., Saldana-Robles, A., Nunez-Palenius, H.G., Costilla-Salazar, R., Valdez-Vazquez, I., Lovanh, N., Ruiz-Aguilar, G.M.L. (2020). *Effects of experimental parameters on methane production and volatile solids removal from tomato and pepper plant wastes.* BioResources, 15(3), 4763-4780.

29. Camarillo, R. and Rincón, J. (2009). *Effect of inhibitory compounds on the AD performance of diluted wastewaters from the alimentary industry*. Journal of Chemical Technology & Biotechnology, 84(11), 1615–1623.

30. Campos, J.L., Crutchik, D., Franchi, O., Pavissich, J.P. Belmonte, M., Pedrouso, A., Mosquera-Corral, A., del Rio, A.V. (2019). *Nitrogen and phosphorus recovery from anaerobically pretreated agro-food wastes: A review.* Sustainable Food Systems, 2(9).

31. Cavinato, C., Fatone, F., Bolzonella, D., Pavan, P. (2010). *Thermophilic anaerobic co-digestion of cattle manure with agro-wastes and energy crops: Comparison of pilot and full scale experiences.* Bioresource Technology, 101(2), 545–550.

32. Cengel, Y.A., and Ghajar, A.J. (2015). *Heat and mass transfer: Fundamentals & applications.* McGraw Hill Education, New York.

33. Chen, C.H., Day, D.L., Steinberg, M.P. (1987). *Methane Production from Fresh Versus Dry Dairy Manure.* Biological Wastes. Agricultural Engineering Department, 24(4), 297-306.

34. Chen, Y., Cheng, J.J., Creamer, K.S. (2008). *Inhibition of anaerobic process: A review.* Bioresource Technology, 99(10), 4044-4064.

35. Chen, G., Zheng, Z., Yang, S., Fang, C., Zou, X., Zhang, J. (2010). *Improving conversion of* Spartina alterniflora *into biogas by co-digestion with cow feces*. Fuel Processing Technology, 91(11), 1416–1421.

36. Chouinard, T.M. (2014). *Evaluation of Multiple Feedstocks for Co-digestion.* The University of North Carolina, U.S.A.

37. Clarke, K.G. (2013). *Bioprocess engineering: An introductory engineering and life science approach.* Woodhead Publishing.

38. Climate-Data.org (2021). Available online: https://en.climate-data.org/ [Accessed: January 2021]

39. Connaughton, S., Collins, G., O'Flaherty, V. (2006). *Psychrophilic and mesophilic AD of brewery effluent. A comparative study.* Water Research, 40(13), 2503-2510.

40. Cooper, C.D. (2014). *Introduction to environmental engineering.* Waveland Press: Long Grove, I.L., USA.

41. Coppinger, E., Brautigam, J., Lenart, J., Baylon, D. (1979). *Report on the Design and Operation of a Full-Scale Anaerobic Digester: final report*. Solar Energy Research Institute, Colorado.

42. Da Ros, C., Cavinato, C., Pavan, P., Bolzonella, D. (2017). *Mesophilic and Thermophilic Anaerobic Co-digestion of Winery Wastewater Sludge and Wine Lees: An Integrated Approach for Sustainable Wine Production.* Journal of Environmental Management, 203, 745-752.

43. Daly, S.E. (2020). *Biochemical methane potential testing and modelling for insight into anaerobic digester performance.* Final Dissertation, Department of Agricultural and Biological Engineering, West Lafayette, Indiana.

44. De Baere, L. (2000). *Anaerobic digestion of solid waste: state-of-the-art*. Water, Science & Technology, 41(3), 283-290.

45. DIN 38 414-8: 1985-06. (1985). *German standard methods for the examination of water, waste water and sludge: sludge and sediments (group S): determination of the amenability to AD*. Berlin: Beuth Verlag.

46. DIN-EN-ISO 11734. (1998). *Water quality: evaluation of the "ultimate" anaerobic biodegradability of organic compounds in digested sludge: method by measurement of the biogas production.* Berlin: Beuth Verlag.

47. Drosg, B., Braun, R., Bochmann, G., Al-Saedi, T. (2013). *Analysis and characterisation of biogas feedstocks.* The Biogas Handbook: Science, Production and Applications. Wellinger, A., Murphy, J., David, B., Eds.; Woodhead Publishing: Sawston, UK.

48. Dubrovskis, V., Plume, I., Straume, I. (2009). *Investigation of Biogas Production from Mink and Cow manure.* Engineering for Rural Development, Latvia University of Agriculture.

49. Esposito, G., Frunzo, L., Panico, A., Pirozzi, F. (2012). *Enhanced bio-methane production from co-digestion of different organic wastes. Environmental Technology,* 33(24), 2733–2740.

50. Eusébio, A., Petruccioli, M., Lageiro, M., Federici, F. (2004). *Microbial characterisation of activated sludge in jet-loop bioreactors treating winery wastewaters.* Industrial Microbiology and Biotechnology, 31(1), 29-34.

51. Fachagentur Nachwachsende Rohstoffe (FNR), 2012. *Guide to Biogas: From production to use*. Fifth Edition. Federal Ministry of Food, Agriculture and Consumer Protection. Dag-Hammarskjöld-Weg 1-5. 65760 Eschborn, Germany.

52. Fagerström, A., Al-Saedi, T., Rasi, S., Briseid, T. (2018). *The role of AD and biogas in the circular economy.* Murphy, J.D. (Ed.), IEA Bioenergy Task 37, 8.

53. Farina, R., Cellamare, C.M., Stante, L., Giordano, A., (2004). *Pilot scale anaerobic sequencing batch reactor for distillery wastewater treatment.* In: Proceedings of the 10th World Congress AD 2004: Anaerobic conversion for sustainability, from 29 August to 2 September, Montreal, Canada.

54. Fedorovich, V., Lens, P., & Kalyuzhnyi, S. (2003). *Extension of AD Model No. 1.* Applied Biochemistry and Biotechnology, 109, 33–45.

55. Feirrera, L.C., Nilsen, P.J., Fdz-Polanco, F., Perez-Elvira, S.I. (2014). *Biomethane potential of wheat straw: Influence of particle size, water impregnation and thermal hydrolysis.* Chemical Engineering Journal, 242, 254-259.

56. Felder, R.M., Rousseau, R.W. (2005). *Elementary Principles of Chemical Processes; Third Edition.* John Wiley & Sons, U.S.A.

57. Filer, J., Ding, H.H., Chang, S. (2019). *Biochemical methane potential (BMP) assay method for anaerobic digestion research.* Water, 11(5), 921-950.

58. Fiore, S., Ruffino, B., Campo, G., Roati, C., Zanetti, M.C. (2016). *Scale-up evaluation of the anaerobic digestion of food-processing industrial wastes.* Renewable Energy, 96(A), 949-959.

59. Font-Palma, C. (2019). *Methods for the treatment of cattle manure: A review.* Journal of Carbon Research, 5(2).

60. Fountoulakis, M. S., Drakopoulou, S., Terzakis, S., Georgaki, E., & Manios, T. (2008). *Potential for methane production from typical Mediterranean agro-industrial by-products.* Biomass and Bioenergy, 32(2), 155–161.

61. Franke-Whittle, I.H., Walter, A., Ebner, C., Insam, H. (2014). *Investigation into the effect of high concentrations of volatile fatty acids in AD on methanogenic communities.* Waste Management, 34(11), 2080-2089.

62. Fujishima, S., Miyahara, T., Noike, T. (2000). *Effect of moisture content on AD of dewatered sludge: ammonia inhibition to carbohydrate removal and methane production*. Water, Science & Technology, 41(3), 119–127.

63. Gallert, C., Henning, A., Winter, J. (2003). *Scale-up of AD of the biowaste fraction from domestic wastes*. Water Research, 37, 1433-1441.

64. Gamble, K.J., Houser, J.B., Hambourger, M.S., Hoepfl, M.C. (2015). *Anaerobic digestion from the laboratory to the field: An experimental study into the Scalability of anaerobic digestion.* Department of Technology and Environmental Design, Appalachian State University, U.S.A.

65. Gao, D.-W., Tao, Y., An, R., Fu, Y., Ren, N.-Q. (2011). *Fate of organic carbon in UAFB treating raw sewage: Impact of moderate to low temperature.* Bioresource Technology, 102(3), 2248-2254.

66. Garcia-Bernet, D., Biffiere, P., Latrille, E., Steyer, J.P., Escudie, R. (2011a). *Water distribution in biowastes and digestates of dry AD technology.* Chemical Engineering Journal, 172, 924-928.

67. Garcia-Calderon, D., Buffiere, P., Moletta, R., Elmaleh, S. (1998). *Anaerobic digestion of wine distillery wastewater in down-flow fluidized bed.* Water Research, 32(12), 3593-3600.

68. Giuliano, A., Bolzonella, D., Pavan, P., Cavinato, C., Cecchi, F. (2013). *Co-digestion of Livestock Effluents, Energy Crops and Agro-waste: Feeding and Process Optimization in Mesophilic and Thermophilic Conditions.* Bioresource Technology, 128C: 612-618.

69. Gomez, D., Ramos-Suarez, J.L., Fernandez, B., Munoz, E., Tey, L., Romero-Guiza, M., Hansen, F. (2019). *Development of a modified plug-flow anaerobic digester for biogas production from animal manures.* Energies, 12(13), 2628-2645.

70. Goswami, Y.D., and Kreith, F. (2008). *Energy Conversion*. London New York: CRC press, Taylor and Francis Group, Boca Raton.

71. Guendouz, J., Buffiere, P., Cacho, J., Carrere, M., Delgenes, J.P. (2008). *High-solids AD: comparison of three pilot scales.* Water, Science & Technology, 58(9), 1757-1763.

72. Gunaseelan, V. N. (2004). *Biochemical methane potential of fruits and vegetable solid waste feedstocks.* Biomass and Bioenergy, 26(4), 389–399.

73. Harada, H., Uemura, S., Chen, A-C., Jayadevan, J. (1995). *Anaerobic treatment of recalcitrant distillery wastewater by a thermophilic UASB reactor.* Bioresource Technology, 55, 215-221.

74. Hashimoto, A.G. (1986). *Ammonia inhibition of methanogenesis from cattle wastes.* Agricultural Wastes, 17, 241-261.

75. Hills, D.J. (1979). *Effects of carbon: nitrogen ratio on AD of dairy manure.* Agricultural Wastes, 1, 267-278.

76. Holliger C., Fruteau de Laclos, H., Hack, G. (2017). *Methane production of full-scale anaerobic digestion plants calculated from substrate's biomethane potentials compares well with the one measured on-site.* Frontiers in Energy Research, 5: 12.

77. Holliger, C., Alves, M., Andrade, D., Angelidaki, I., Astals, S., Baier, U., Bougrier, C., Buffière, P., Carballa, M., Wilde, V., Ebertseder, F., Fernández, B., Ficara, E., Fotidis, I., Frigon, J., Fruteau, H., Ghasimi, D., Hack, G., Hartel, M., Wierinck, I. (2016). *Towards a standardization of biomethane potential tests*. Water Science & Technology. 74..

78. Illmer, P., and Gstraunthaler, G. (2009). *Effect of seasonal changes in quantities of biowaste on full-scale anaerobic digester performance.* Waste Management, 29(1), 162-167.

79. Jewitt, G., Wen, H., Kunz, R., Rooyen, A.V. (2009). *Scoping study on water use of crops/trees for biofuels in South Africa.* WRC Report.

80. Jingura, R.M., and Kamusoko, R. (2017). *Methods for determination of biomethane potential of feedstocks: A review.* Biofuel Research Journal, 14, 573-586.

81. Kaltschmitt, M., Hartmann, H. (2001). *Energie aus Biomasse – Grundlagen, Techniken und Verfahren.* Springer Verlag, Berlin.

82. Kalyuzhnyi, S., Veeken, A., Hamelers, B. (2000). *Two-particle model of anaerobic solid state fermentation*. Water Science and Technology, 41, 43-40.

83. Kariyama, I.D., Zhai, X., Wu, B. (2018). *Influence of mixing on AD efficiency in stirred tank digesters: A review*. Water Research, 143, 503-517.

84. Kell, C.J.K. (2019). *Anaerobic co-digestion of fruit juice industry waste with lignocellulosic biomass.* Thesis (MEng), Stellenbosch University.

85. Kleyböcker, A., Liebrich, M., Verstraete, W., Kraume, M., & Würdemann, H. (2012). *Early warning indicators for process failure due to organic overloading by rapeseed oil in one-stage continuously stirred tank reactor, sewage sludge and waste digesters.* Bioresource Technology, 123, 534–541.

86. Khanal, S.K. (2008). *Anaerobic Biotechnology for Bioenergy Production: Principles and Applications.* Iowa, U.S.A. University of Hawaii, Manoa.

87. Kim, W., Shin, S.G., Lim, J. Hwang, S. (2013). *Effect of temperature and hydraulic retention time on volatile fatty acid production based on bacterial community structure in anaerobic acidogenesis using swine wastewater.* Bioprocess and Biosystems Engineering, 36, 791-798.

88. Koch, K., Hafner, S.D., Weinrich, S., Astals, S., Holliger, C. (2020). *Power and limitations of biochemical methane potential (BMP) tests.* Frontiers in Energy Research, 8, 63.

89. Kovács, E. Wirth, R. Maróti, G. Bagi, Z. Nagy, K. Minárovits, J. Rákhely, G. Kovács, K.L. (2015). *Augmented biogas production from protein-rich substrates and associated metagenomic changes*. Bioresource Technology, 178, 254–261.

90. Kübler, H., Hoppenheidt, K., Hirsch, P., Kottmair, A., Nimmrichter, R., Nordsieck, H., Mücke, W., Swerev, M. (2000). *Full-scale co-digestion of organic waste.* Water, Science & Technology, 41(3), 195-202.

91. Lara, A.R., Galindo, E., Ramirez, O.T., Palomares, L.A. (2006). *Living with heterogeneities in bioreactors.* Molecular Biology, 34, 355-381.

92. Lee, D-J., Lee, S-Y., Bae, J-S., Kang, J-G., Kim, K-H., Rhee, S-S., Park, J-H., Cho, J-S., Chung, J., Seo, D-C. (2015). *Effect of volatile fatty acid concentration on anaerobic degradation rate from field anaerobic digestion facilities treating food waste leachate in South Korea.* Journal of Chemistry.

93. Lehtomaki, A., Huttunen, S., Rintala, J.A. (2007). *Laboratory investigations on co-digestion of energy crops and crop residues with cow manure for methane production: Effect of crop to manure ratio.* Resources, Conservation and Recycling, 51, 591-609.

94. Lemmer, A., and Oechsner, H. (2002). *Use of Grass or Field Crops for Biogas Production*. Budapest, Hungary: Proceeding of the AgEng.

95. Levenspiel, O. (2012). *Fluid mechanics and its applications – tracer technology.* Springer New York, New York, NY.

96. Li, C., Nges, I.A., Lu, W., Wang, H. (2017). *Assessment of the degradation efficiency of full-scale biogas plants: A comparative study of degradation indicators.* Bioresource Technology, 244, 304-312.

97. Li, X., Huang, J., Liu, Y., Huang, T., Maurer, C., Kranert, M. (2019). *Effects of salt on anaerobic digestion of food waste with different component characteristics and fermentation concentrations.* Energies, 12(18), 3571-3585.

98. Liu, Y., Ngo, H.H., Guo, W., Peng, L., Wang, D., Ni, B. (2019). *The roles of free ammonia (FA) in biological wastewater treatment processes: A review.* Environment International, 123, 10-19.

99. Li, Y., Zhao, J., Krooneman, J., Euverink, G.J.W. (2021). *Strategies to boost AD performance of cow manure: Laboratory achievements and their full-scale application potential.* Science of the Total Environment, 755, 142940.

100. Liebetrau, J., Pfeiffer, D., Thran, D. (2016). *Collection of methods for biogas: Methods to determine parameters for analysis purposes and parameters that describe processes in the biogas sector.* German Biomass Research Center (DBFZ), Volume 7.

101. Liotta, F., d'Antonio, G., Esposito, G., Fabbricino, M., Frunzo, L., Van Hullebusch, E.D., Lens, P.N.L., Pirozzi, F. (2014). *Effect of moisture content on disintegration kinetics during AD of complex organic substrates.* Waste Management & Research, 32(1), 40-48.

102. Liu, D., Zeng, R.J., Angelidaki, I. (2008). *Effects of pH and hydraulic retention time on hydrogen production versus methanogenesis during anaerobic fermentation of organic household solid waste under extreme=thermophilic temperature (70$^{o}$C).* Biotechnology and Bioengineering, 100, 1108-1114.

103. Lüdtke, M., Nordberg, A., Baresel, C. (2017). *Experimental power of laboratory-scale results and transferability to full-scale AD.* Water, Science & Technology, 76(4), 983-991.

104. Ma, J., Frear, C., Wang, Z., Yu, L., Zhao, Q., Li, X., & Chen, S. (2013). *A simple methodology for rate-limiting step determination for AD of complex substrates and effect of microbial community ratio. Bioresource Technology, 134, 391–395.* doi:10.1016/j.biortech.2013.02.014

105. Mah, R. A., Smith, M.R. (1981). *The methanogenic bacteria.* p. 948-977. In M. P. Starr, H. Stolp, H. G. Truper, A. Balows, and H. G. Schlegel (ed.), The prokaryotes, vol. I. SpringerVerlag, Berlin.

106. Maile, I., Muzenda, E., Mbohwa, C. (2016). *Optimization of biogas production through AD of fruit and vegetable waste: A review.* Int. Conference on Biology, Environment and Chemistry, Volume 98.

107. Martín, M., Raposo, F., Borja, R., Martín, A. (2002). *Kinetic study of the AD of vinasse pretreated with ozone, ozone plus ultraviolet light, and ozone plus ultraviolet light in the presence of titanium dioxide.* Process Biochemistry, 37(7), 699–706.

108. Marques, M.P.C., Cabral, J.M.S., Fernandes, P. (2010). *Bioprocess scale-up: Quest for the parameters to be used as criterion to move from microreactors to bench-scale.* Journal of Chemical Technology and Biotechnology, 85(9), 1184-1198.

109. Massé, D. I., Jarret, G., Benchaar, C., Hassanat, F., Saady, N. (2016). *Effect of increasing levels of corn silage in an alfalfa-based dairy cow diet and of manure management practices on manure fugitive methane emissions*. Agricultural Ecosystems & Environment, 221, 109–114.

110. Meegoda, J.N., Li, B., Patel, K., Wang, L.B. (2018). *A review of the processes, parameters and optimization of AD.* Environmental Research and Public Health, 15, 2224 -2240.

111. Melamane, X., Strong, J., Burgess, J. (2007). *Treatment of wine distillery wastewater: A review with emphasis on anaerobic membrane reactors.* South African Journal for Enology and Viticulture, 28, 25-36.

112. Møller, H.B., Sommer, S.G., Ahring, B.K. (2003). *Methane Productivity of Manure, Straw and Solid Fractions of Manure.* Biomass and Bioenergy, 26, 485-495.

113. Moeller, L., and Zehnsdorf, A. (2016). *Process upsets in a full-scale AD bioreactor: Over-acidification and foam formation during biogas production.* Energy, Sustainability and Society, 6(1).

114. Moody, L., Burns, R., Wu-Haan, W. (2009). *Use of biochemical methane potential (BMP) assays for predicting and enhancing anaerobic digester performance.* Agricultural Engineering, 44th Croatian & 4th International Symposium of Agriculture.

115. Moukazis, I., Pellera, F.-M., Gidarakos, E. (2018). *Slaughterhouse by-products treatment using anaerobic digestion.* Waste Management, 71, 652–662.

116. Mousa, L., and Forster, C.F. (1999). *The use of trace organics in anaerobic digestion.* Process Safety and Environmental Protection, 77(1), 37-42.

117. Musa, M.A., Idrus, S., Hasfalina, C.M., Daud, N.N.N. (2018). *Effect of organic loading rate on anaerobic digestion performance of mesophilic (UASB) reactor using cattle slaughterhouse wastewater as substrate.* International Journal of Environmental Research and Public Health, 15, 2220.

118. Muzenda, E. (2014). *Bio-methane generation from organic waste: A review.* In Proceedings of the World Congress on Engineering and Computer Science, San Francisco, CA., USA.

119. Mu, H., Zhao, C., Zhao, Y., Hua, D., Li, Y., Zhang, X., Cao, Y. (2019). *Optimizing methane production from anaerobic bacth co-digestion of apple pomace and vegetable waste.* Journal of Biobased Materials and Bioenergy, 13(4), 508-516.

120. Nataraj, S.K., Hosamani, K.M., Aminabhavi, T.M. (2006). *Distillery wastewater treatment by the membrane-based nanofiltration and reverse osmosis processes.* Water Research, 40(12), 2349-2356.

121. Naumann, K., and Bassler, R. (1976). *Chemische Untersuchung von Futtermitteln*. VDLUFA Methodenhandbuch, 3. Auflage, Neumann-Neudamm.

122. Nazifa, T.H., Saady, N.M.C., Bazan, C., Zendehboudi, S., Aftab, A., Albayati, T.M (2021). *AD of blood from slaughtered livestock: A review*. Energies 2021, 14, 5666-5691.

123. Ndlovu, V., and Inglesi-Lotz, R. (2019). *Positioning South Africa's energy supply mix internationally: Comparative and policy review analysis.* Journal of Energy in Southern Africa, 30(2), 2413-3051.

124. Nordlander, E., Thorin, E., and Yan, J. (2017). *Investigating the possibility of applying an ADM1 based model to a full-scale co-digestion plant.* Biochemical Engineering Journal, 120, 73– 83.

125. NIST Chemistry WebBook, Methane. Available from: https://webbook.nist.gov/cgi/cbook.cgi?Name=methane&Units=SI, [Accessed 12-Aug-2021].

126. Otuzalti, M.M., and Perendeci, N.A. (2018). *Modeling of real scale waste activated sludge AD process by AD Model 1 (ADM1).* International Journal of Green Energy, 15:7, 454-464.

127. Owen, W. F., Stuckey, D. C., Healy, J. B. Jr., Young, L. Y., McCarty, P. L. (1979). *Bioassay for monitoring biochemical methane potential and anaerobic toxicity*. Water Research, 13, 485–492.

128. Pham, C.H., Triolo, J.M., Cu, T.T.T., Pedersen, L., Sommer, S.G. (2013). *Validation and Recommendation of Methods to Measure Biogas Production Potential of Animal Manure.* Asian-Australas. Journal of Animal Science, 26, 864–873

129. Pilarski, K., Pilarska, A.A., Piotr, B., Niedbala, G. (2020). *The efficiency of industrial and - laboratory anaerobic digesters of organic substrates: The use of the biochemical methane potential correction coefficient.* Energies, 1280-1293.

130. Poggio, D., Walker, M., Nimmo, W., Ma., L., Pourkashanian, M. (2016). *Modelling the anaerobic digestion of solid organic waste – Substrate characterization method for ADM1 using a combined biochemical and kinetic parameter estimation approach.* Waste Management, 53, 40 – 54.

131. Porterfield, K.K., Faulkner, J., Roy, E.d. (2020). *Nutrient recovery from anaerobically digested dairy manure using dissolved air flotation (DAF).* ACS Sustainable Chemical Engineering, 8(4), 1964-1970.

132. Rabii, A., Aldin, S., Dahman, Y., Elbeshbishy, E. (2019). *A review on anaerobic co-digestion with a focus on the microbial populations and the effect of multi-stage digester configuration.* Energies, 12, 1106-1131.

133. Ramana, S., Biswas, A., Singh, A., Yadava, R. B. (2002). *Relative efficacy of different distillery effluents on growth, nitrogen fixation and yield of groundnut*. Bioresource Technology, 81(2), 117–121.

134. Rajasekharan, V.V. (2015). *Apparatus, composition and method for determination of chemical oxidation demand*. US Patent 20150108009.

135. Raposo, F., Fernandez-Cegri, V., De la Rubia, M. A., Beline, F., Cavinato, C., Demirer, G., Fernandez, B., Fernandez-Polanco, M., Frigon, J-C., Ganesh, R., Kaparaju, P., Koubova, J., Mendez, R., Menin, G., Peene, A., Scherer, P., Torrijos, M., Uellendahl, H., Wierinck, I., de Wilde, V. (2011). *Biochemical methane potential (BMP) of solid organic substrates: evaluation of anaerobic biodegradability using data from an international interlaboratory study.* Journal of Chemical Technology & Biotechnology, 86(8), 1088-1098.

136. Raposo, F., De la Rubia, M.A., Fernandez-Cegri, V., Borja, R. (2012). *Anaerobic digestion of solid organic substrates in batch mode: An overview relating to methane yields and experimental procedures.* Renewable and Sustainable Energy Reviews, 16, 861-877.

137. Rico, C., Rico, J. L., Tejero, I., Muñoz, N., Gómez, B. (2011). *AD of the liquid fraction of dairy manure in pilot plant for biogas production: Residual methane yield of digestate.* Waste Management, 31(9-10), 2167–2173.

138. Rodrigues, R.P. (2017). *Anaerobic digestion process for agro-industrial wastes valorization: experimental and theoretical biochemical methane potential prediction.* Master's Dissertation, Faculty of Science and Technology, University of Coimbra.

139. Romero-Guiza, M.S., Mata-Alvarez, J., Rivera, J.M.C., Garcia, S.A. (2015). *Nutrient recovery technologies for anaerobic digestion systems: An overview.* Revista ION, 29(1), 7-26.

140. Ruffino, B., Fiore, S., Roati, C., Campo, G., Novarino, D., Zanetti, M. (2015). *Scale effect of anaerobic digestion tests in fed-batch and semi-continuous mode for the technical and economic feasibility of a full scale digester.* Bioresource Technology, 182, 302-313.

141. Safley, L.M., and Westerman, P.W. (1990). *Psychrophilic AD of animal manure: Proposed design methodology.* Biological Wastes, 34, 133-148.

142. Saghouri, M., Mansoori, Y., Rohani, A., Khodaparast, M.H.H., Sheikhdavoodi, M. J. (2018). *Modelling and evaluation of AD process of tomato processing wastes for biogas generation.* Journal of Material Cycles and Waste Management, 20, 561-567.

143. Sarada, R., and Joseph, R. (1994). *Studies on factors influencing methane production from tomato-processing wastes.* Bioresource Technology, 47(1), 55-57.

144. Sarker, S., Lamb, J.J., Hjelme, D.R., Lien, K.M. (2019). *A review of the role of critical parameters in the design and operation of biogas production in plants.* Applied Sciences, 9, 1915-1953.

145. Sayara, T., and Sanchez, A. (2019). *A review on AD of lignocellulosic wastes: Pretreatments and operational conditions.* Applied Sciences, 9, 4655-4678.

146. Schnürer, A. (2016). *Biogas production: Microbiology and Technology.* In *Anaerobes in Biotechnology;* Advances in Biochemical Engineering/Biotechnology. Springer: Cham, Switzerland, 156, 195–234.

147. Schievano, A., Pognani, M., DÍmporzano, G., Adani, F. (2008). *Predicting anaerobic biogasification potential of ingestates and digestates of a full-scale biogas plant using chemical and biological parameters.* Bioresource Technology, 99, 8112-8117.

148. Schievano, A., DÍmporzano, G., Malagutti, L., Fragali, E., Ruboni, G., Adani, F. (2010). *Evaluating inhibition conditions in high-solids AD of organic fraction of municipal solid waste.* Bioresource Technology, 1010(14), 5728-5732.

149. Schievano, A., D'Imporzano, G., Orzi, V., Adani, F. (2011). *On-field study of anaerobic digestion full-scale plants (Part II): New approaches in monitoring and evaluating process efficiency.* Bioresource Technology, 102, 8814 – 8819.

150. Schüsseler, P. (2008). Measuring, controlling, regulating the production of biogas. Fachagentur für Nachwachsende Rohstoffe (FNR). e.V. 27,8-16.

151. Shi, X-S., Dong, J-J., Yu, J-H., Yin, H., Hu, S-M., Huang, S-X., Yuan, X-Z. (2017). *Effect of hydraulic retention time on AD of wheat straw in the semicontinuous continuous stirred-tank reactors.* BioMed Research International, 1-6.

152. Singh, B., Szamosi, Z., Simenfalvi, Z. (2020). *Impact of mixing intensity and duration on biogas production in an anaerobic digester: A review.* Critical Reviews in Biotechnology, 40(4), 508-521.

153. Singh, B., Kovács, K.L., Bagi, Z., Nyari, J., Szepesi, G.L., Petrik, M., Simenfalvi, Z., Szamosi, Z. (2021). *Enhancing efficiency of AD by optimization of mixing regimes using helical ribbon impeller.* Fermentation, 7, 251-268.

154. Sell, S.T. (2011). *A scale-up procedure for substrate co-digestion in anaerobic digesters through the use of substrate characterization, BMPs, ATAs, and sub pilot-scale digester.* Graduate These and Dissertations. 12044.

155. Souza, T.S.O., Carvajal, A., Donoso-Bravo, A., Pena, M., Fdz-Polanco, F. (2012). *ADM1 calibration using BMP tests for modelling the effect of autohydrolysis pretreatment on the performance of continuous sludge digesters.* Water Research, 47, 3244-3254.

156. Speece, R. E. (1996). *Anaerobic Biotechnology for Industrial Wastewaters*. Nashville, TN: Archae Press.

157. Spyridonidis, A., Vasiliadou, I.A., Akratos, C.S., Stamatelatou, K. (2020). *Performance of a full-scale biogas plant operation in Greece and its impact on the circular economy.* Water, 12, 3074-3093.

158. Strömberg, S., Nistor, M., Liu, J. (2014). *Towards eliminating systematic errors caused by the experimental conditions in biochemical methane potential (BMP) tests.* Waste Management, 34(11), 1939-1948.

159. Switzenbaum, M.S., Farrell, J.B., Pincince, A.B. (2003). *Relationship between the Van Kleeck and mass-balance calculation of volatile solids loss.* Water Environment Research, 75(4), 377-380.

160. Surroop, D., and Mohee, R. (2011). *Power generation from landfill gas.* 2nd International Conference on Environmental Engineering and Applications, IPCEE, 17.

161. Szilagyi, A., Bodor, A., Tolvai, N., Kovacs, K.L., Bodai, L., Wirth, R., Bagi, Z., Szepesi, A., Marko, V., Kakuk, B., Bounedjoum, N., Rakhely, G. (2020). *A comparative analysis of biogas production from tomato bio-waste in mesophilic batch and continuous AD systems.* PLoS ONE, 16(3).

162. Tambone, F., Scaglia, B., D'Imporzano, G., Schievano, A., Orzi, V., Salati, S., Adani, F. (2010). *Assessing amendment and fertilizing properties of digestates from anaerobic digestion through a comparative study with digested sludge and compost.* Chemosphere, 81, 577-583.

163. Theuerl, S., Herrmann, C., Heiermann, M., Grundmann, P., Landwehr, N., Kreidenweis, U., Prochnow, A. (2019). *The future agricultural biogas plant in Germany: A vision.* Energies, 12, 396-428.

164. Tomei, M.C., Braguglia, C.M., Cento, G., Mininni, G. (2009). *Modelling of AD of sludge.* Critical Reviews in Environmental Science and Technology, 39(12), 1003-1051.

165. Torkian, A., Amin, M.M., Movahedian, H., Hashemian, S.J., Salehi, M.S. (2002). *Performance evaluation of UASB system for treating slaughterhouse wastewater.* Scientia Iranica, 9(2), 176-180.

166. Triolo, J.M., Sommer, S.G., Møller, H.B., Weisbjerg, M.R., Jiang, X.Y. (2011). *A New Algorithm to Characterize Biodegradability of Biomass During AD: Influence of Lignin Concentration on Methane Production Potential.* Bioresource Technology, 20, 9395-9402.

167. Tufaner, F., and Avsar, Y. (2016). *Effects of co-substrate on biogas production from cattle manure: a review.* Environmental Science and Technology, 13, 2203-2312.

168. Usack, J.G., Spirito, C.M., Angenent, L.T. (2012). *Continuously-stirred anaerobic digester to convert organic wastes into biogas: system setup and basic operation.* Journal of Visualized Experiments.

169. Van't Riet, K., and Van der Lans, R.G.J.M. (2011). *Mixing in bioreactor vessels: second edition*. Elsevier B.V.

170. Vital-Jacome, M., Cazares-Granillo, M., Carrilo-Reyes, J., Buitron, G. (2020). *Characterization and AD of highly concentrated Mexican wine by-products and effluents.* Water Science & Technology, 81.1, 190-198.

171. VDI 4630 (2016). *Fermentation of organic substances – substrate characterisation, sampling, data collection, fermentation tests*. Dusseldorf, Beuth Verlag.

172. Vlissidis, A., and Zouboulis, A.I. (1993). *Thermophilic anaerobic digestion of alcohol distillery wastewaters.* Bioresource Technology, 43(2), 131-140.

173. Walid, F., El-Fkihi, S., Benbrahim, H., Tagemouati, H. (2021). *Modelling and optimisation of anaerobic digestion: A review.* E3S Web of Conferences, 229:01022.

174. Wang, Z., Jiang, Y., Wang, S., Zhang, Y., Hu, Y., Hu, Z-H., Wu, G., Zhan, X. (2020). *Impact of total solids content on anaco-digestion of pig manure and food wastes: Insights into shifting of the methanogenic pathway.* Waste Management, 114, 96-106.

175. Ward, A.J., Hobbs, P.J., Holliman, P.J., Jones, D.L. (2008). *Optimisation of the anaerobic digestion of agricultural resources.* Bioresource Technology, 99(17), 7928-7940.

176. Water Technology. (2015). *Ultrasonic flowmeters address issues in facility biogas measurement.* Available online: https://www.watertechonline.com/wastewater/article/15549354/ultrasonic-flowmeters-address-issues-in-facility-biogas-measurement [Accessed 21 October 2021].

177. Weinrich, S., Schäfer, F., Bochmann, G., Liebetrau, J., (2018). *Value of batch tests for biogas potential analysis; method comparison and challenges of substrate and efficiency evaluation of biogas plants*. Murphy, J.D. (Ed.) IEA Bioenergy Task 37, 2018: 10

178. Wolmarans, B., and De Villiers, G.H. (2004). *Start-up of a UASB effluent treatment plant on distillery wastewater.* Water South Africa, 28(1), 63 – 68.

179. Wu, M.-C., Sun, K.-W., Zhang, Y. (2006). *Influence of temperature fluctuation on thermophilic AD of municipal organic solid waste.* Journal of Zhejiang University Science, 7(3), 180-185.

180. Yang, L., Xu, F., Ge, X., Li, Y. (2015). *Challenges and strategies for solid-state anaerobic digestion of lignocellulosic biomass.* Renewable and Sustainable Energy Reviews, 44, 824-834.

181. Yi, J., Dong, B., Jin, J., & Dai, X. (2014). *Effect of Increasing Total Solids Contents on anaerobic digestion of Food Waste under Mesophilic Conditions: Performance and Microbial Characteristics Analysis.* PLoS ONE, 9(7), e102548.

182. Yu, L., Ma, J., Chen, S. (2011). *Numerical simulation of mechanical mixing in high solid anaerobic digester.* Bioresource Technology, 102(2), 1012-1018.

183. Zhu, D., Wan, C., Li, Y. (2011). *Anaerobic co-digestion of food wastes and dairy manure for enhanced methane production*. Biological Engineering Transactions, 4(4), 195-206.

## APPENDIX A – ADDITIONAL DATABASES

Table 34: Total and individual feedstock feed rates for Plant 1 (mixed organic wastes) spanning a period of 28 weeks, given as mean values per week.

| Weeks | Total feeding [a] | | Individual feedstocks (kg/week) [b] | | | | | | | | | |
|---|---|---|---|---|---|---|---|---|---|---|---|---|
| | Feed rates (kg/d) | Stdev (kg/d) | Beer | Fruit juice | Chocolate | Sugar | Dairy waste | Apples | Food waste | Expired spices | Cow blood | Cow manure |
| 1 | 8438 | 12292 | 10000 | 14000 | 6000 | 0 | 0 | 15000 | 14000 | 2500 | 6000 | 0 |
| 2 | 14071 | 7960 | 38000 | 17000 | 5500 | 0 | 0 | 18000 | 9500 | 3500 | 7000 | 0 |
| 3 | 10786 | 11782 | 24000 | 8000 | 4000 | 0 | 0 | 16500 | 18000 | 0 | 5000 | 0 |
| 4 | 22571 | 6979 | 46000 | 30000 | 0 | 0 | 0 | 55500 | 21500 | 0 | 5000 | 0 |
| 5 | 22786 | 8741 | 33000 | 28000 | 12500 | 0 | 0 | 54500 | 21500 | 0 | 10000 | 0 |
| 6 | 15786 | 11258 | 41000 | 26000 | 3000 | 0 | 0 | 15000 | 20500 | 0 | 5000 | 0 |
| 7 | 18143 | 8859 | 53000 | 0 | 5000 | 0 | 0 | 25500 | 10000 | 0 | 9000 | 0 |
| 8 | 14714 | 8864 | 70000 | 0 | 0 | 0 | 0 | 18000 | 10000 | 0 | 5000 | 0 |
| 9 | 11857 | 11978 | 43000 | 0 | 0 | 0 | 0 | 21000 | 10000 | 2000 | 7000 | 0 |
| 10 | 21214 | 9327 | 74000 | 4000 | 0 | 0 | 1000 | 47000 | 17500 | 0 | 5000 | 0 |
| 11 | 11357 | 9205 | 31000 | 6000 | 0 | 0 | 3000 | 32500 | 6000 | 0 | 1000 | 0 |
| 12 | 16214 | 6389 | 0 | 10000 | 0 | 0 | 4000 | 56000 | 35500 | 0 | 8000 | 0 |
| 13 | 10071 | 8507 | 0 | 16000 | 2000 | 0 | 1000 | 24000 | 23500 | 0 | 4000 | 0 |
| 14 | 7786 | 10074 | 0 | 6000 | 0 | 0 | 2000 | 28000 | 18500 | 0 | 0 | 0 |
| 15 | 9929 | 11813 | 0 | 12000 | 500 | 0 | 1000 | 27500 | 22500 | 0 | 6000 | 0 |
| 16 | 11000 | 13889 | 0 | 7000 | 5500 | 0 | 2000 | 46500 | 16000 | 0 | 0 | 0 |
| 17 | 3071 | 4401 | 0 | 0 | 0 | 0 | 0 | 4000 | 16000 | 500 | 1000 | 0 |
| 18 | 12857 | 4661 | 0 | 19000 | 2000 | 0 | 1000 | 40000 | 22500 | 0 | 5000 | 0 |
| 19 | 11357 | 3772 | 0 | 6000 | 2000 | 0 | 2000 | 44000 | 20500 | 0 | 5000 | 0 |
| 20 | 12500 | 10190 | 0 | 18000 | 500 | 0 | 1000 | 46000 | 15000 | 1000 | 6000 | 0 |
| 21 | 17143 | 8606 | 0 | 24000 | 3000 | 0 | 500 | 60000 | 26000 | 2500 | 4000 | 0 |
| 22 | 14357 | 9953 | 0 | 14000 | 2000 | 0 | 1500 | 53500 | 23000 | 1500 | 5000 | 0 |
| 23 | 17071 | 8914 | 0 | 5000 | 1000 | 0 | 3000 | 84500 | 21000 | 0 | 5000 | 0 |
| 24 | 17500 | 7863 | 0 | 2000 | 2500 | 0 | 6000 | 90000 | 19000 | 0 | 3000 | 0 |
| 25 | 18214 | 12483 | 0 | 0 | 0 | 0 | 2500 | 100000 | 20000 | 1000 | 4000 | 0 |
| 26 | 35000 | 18797 | 0 | 15000 | 8000 | 0 | 0 | 167000 | 49000 | 0 | 6000 | 0 |
| 27 | 33286 | 19457 | 0 | 23000 | 8000 | 0 | 5000 | 195000 | 40000 | 0 | 7000 | 0 |
| 28 | 0 | 0 | 0 | 0 | 0 | 0 | 0 | 0 | 0 | 0 | 0 | 0 |

[a] : total feed rates are reported as daily mean values; [b] : total masses of individual feedstocks fed to the digester per week.

Table 35: Full-scale operational data for Plant 1 (mixed organic wastes) spanning a period of 28 weeks, given as mean values per week.

| Weeks | Biogas production ($Nm^3/d$) | Stdev ($Nm^3/d$) | Power count (kWh/d) | Stdev (kWh/d) | Methane production [a] ($Nm^3$ $CH_4/d$) | Stdev ($Nm^3$ $CH_4/d$) | $CH_4$ content [b] (%vol) | Stdev | Digester temperature (°C) | Stdev (°C) | Digester pH level | Stdev |
|---|---|---|---|---|---|---|---|---|---|---|---|---|
| 1 | 1494 | 245 | 535 | 56.9 | 354 | 37.6 | 23.9 | 3.53 | 36.8 | 0.6 | 7.12 | 0.02 |
| 2 | 1073 | 319 | 603 | 264.7 | 399 | 175.1 | 37.4 | 10.10 | 37.4 | 0.2 | 7.19 | 0.06 |
| 3 | 921.2 | 263 | 522 | 48.9 | 345 | 32.3 | 41.1 | 13.47 | 37.0 | 0.3 | 7.26 | 0.04 |
| 4 | 1514 | 1150 | 509 | 51.1 | 337 | 33.8 | 19.2 | 11.66 | 37.1 | 0.2 | 7.18 | 0.05 |
| 5 | 1194 | 763 | 517 | 289 | 342 | 190.9 | 39.2 | 14.00 | 37.0 | 0.3 | 7.20 | 0.02 |
| 6 | 958.5 | 685 | 543 | 30.2 | 359 | 20.0 | 37.1 | 24.35 | 36.4 | 0.8 | 7.19 | 0.07 |
| 7 | 895.4 | 532 | 540 | 57.7 | 357 | 38.1 | 49.5 | 21.52 | 37.1 | 0.5 | 7.16 | 0.07 |
| 8 | 732.7 | 432 | 524 | 60.9 | 347 | 40.3 | 46.4 | 16.02 | 36.6 | 0.7 | 7.23 | 0.04 |
| 9 | 909.0 | 699 | 995 | 1099 | 658 | 727.2 | 34.1 | 12.70 | 36.6 | 0.3 | 7.15 | 0.03 |
| 10 | 679.3 | 126 | 512 | 341 | 338 | 225.8 | 40.8 | 24.51 | 35.8 | 0.3 | 7.15 | 0.04 |
| 11 | 1043 | 527 | 562 | 180 | 371 | 119.0 | 45.8 | 27.48 | 18.1 | 2.3 | 7.11 | 0.07 |
| 12 | 1320 | 561 | 617 | 168 | 408 | 111.0 | 35.1 | 18.69 | 0.0 | 0.0 | 7.17 | 0.04 |
| 13 | 1428 | 669 | 586 | 38.1 | 387 | 25.2 | 31.3 | 12.35 | 47.4 | 0.3 | 7.02 | 0.09 |
| 14 | 301.2 | 0 | 335 | - | 222 | - | 73.6 | - | 22.0 | - | 7.05 | 0.04 |
| 15 | 1588 | 707 | 438 | 295 | 290 | 195.3 | 28.1 | 33.22 | 37.1 | 13.1 | 7.04 | 0.05 |
| 16 | 724.9 | 210 | 503 | 158 | 333 | 104.8 | 45.7 | 1.22 | 41.0 | 3.6 | 6.83 | 0.23 |
| 17 | 29.50 | 37 | 470 | 21.2 | 311 | 14.0 | 0.0 | 0.00 | 24.0 | 1.1 | 7.09 | 0.09 |
| 18 | 1055 | 391 | 586 | 16.8 | 387 | 11.1 | 40.8 | 13.42 | 29.3 | 4.2 | 6.99 | 0.06 |
| 19 | 927.2 | 686 | 565 | 322 | 436 | 147.8 | 43.7 | 26.89 | 28.2 | 6.3 | 6.95 | 0.03 |
| 20 | 756.3 | 266 | 539 | 46.5 | 356 | 30.7 | 40.6 | 4.11 | 33.5 | 4.5 | 7.04 | 0.02 |
| 21 | 948.6 | 529 | 555 | 28.4 | 367 | 18.8 | 30.9 | 6.58 | 32.8 | 4.2 | 7.05 | 0.04 |
| 22 | 2289 | 1908 | 598 | - | 396 | - | 10.9 | - | 31.5 | 7.1 | 6.99 | 0.05 |
| 23 | 1156 | 403 | 627 | 16.1 | 414 | 10.6 | 39.5 | 13.49 | 31.9 | 6.1 | 7.02 | 0.04 |
| 24 | 3212 | 2091 | 603 | 17.3 | 399 | 11.4 | 17.6 | 10.77 | 30.2 | 6.9 | 7.00 | 0.09 |
| 25 | 1738 | 1148 | 624 | 12.7 | 413 | 8.4 | 35.6 | 18.95 | 37.4 | 0.5 | 7.01 | 0.08 |
| 26 | 1510 | 516 | 602 | 36.6 | 398 | 24.2 | 30.3 | 14.71 | 35.3 | 7.3 | 7.03 | 0.13 |
| 27 | 1501 | 419 | 1325 | 1753 | 876 | 1159.3 | 31.4 | 0.00 | 38.8 | 0.5 | 7.07 | 0.08 |
| 28 | 478.9 | 323 | 533 | 19.1 | 352 | 12.6 | 48.0 | 0.00 | 30.5 | 7.4 | 7.10 | 0.15 |

[a] : Mean daily methane production rates calculated from mean daily power counts (see sample calculations Appendix B3); [b] : methane content calculated from ratio of daily methane production to daily biogas production;

Table 36: Full-scale feed conditions and operating parameters for Plant 3 (distillery waste) spanning a 34-month period, given as mean values per month.

| Month | Feed conditions | | | | | Operating parameters | | | | |
|---|---|---|---|---|---|---|---|---|---|---|
| | $T_{AMB}$ [a] (°C) | TCOD [b] (mg/L) | Stdev (mg/L) | Feed pH | Stdev | Feed rate ($m^3$/d) | Stdev (m3/d) | HRT [c] (days) | $OLR_T$ [d] (kgCOD/$m^3$/d) | Stdev (kgCOD/$m^3$/d) |
| Jan-18 | 22 | 14156 | 4646 | 6.23 | 0.80 | 400 | 87.1 | 5.5 | 2.6 | 1.0 |
| Feb-18 | 21 | 19950 | 3701 | 5.25 | 0.55 | 410 | 67.4 | 5.4 | 3.8 | 1.0 |
| Mar-18 | 19 | 25969 | 8683 | 5.59 | 1.30 | 444 | 98.0 | 5.0 | 5.2 | 1.3 |
| Apr-18 | 17 | 15537 | 4458 | 6.29 | 0.77 | 480 | 133 | 4.6 | 3.4 | 0.8 |
| May-18 | 16 | 17917 | 6658 | 6.82 | 0.50 | 470 | 157 | 4.7 | 3.7 | 1.0 |
| Jun-18 | 14 | 13619 | 5364 | 6.65 | 0.92 | 439 | 135 | 5.0 | 2.8 | 0.9 |
| Jul-18 | 14 | 9699 | 1596 | 6.89 | 0.35 | 587 | 112 | 3.7 | 2.6 | 0.5 |
| Aug-18 | 12 | 11828 | 2626 | 6.42 | 0.76 | 576 | 82.0 | 3.8 | 3.1 | 1.6 |
| Sep-18 | 14 | 11077 | 1980 | 6.39 | 0.49 | 548 | 58.2 | 4.0 | 2.7 | 0.4 |
| Oct-18 | 19 | 13744 | 4014 | 6.10 | 0.76 | 550 | 58.6 | 4.0 | 3.4 | 1.0 |
| Nov-18 | 18 | 15034 | 3888 | 6.12 | 0.74 | 496 | 92.6 | 4.4 | 3.3 | 0.8 |
| Dec-18 | 21 | 14274 | 4084 | 5.73 | 0.92 | 480 | 87.0 | 4.6 | 3.2 | 1.2 |
| Jan-19 | 21 | 15395 | 6977 | 5.77 | 0.83 | 480 | 115 | 4.6 | 3.4 | 2.1 |
| Feb-19 | 22 | 12639 | 3148 | 5.66 | 1.06 | 542 | 93.2 | 4.1 | 3.2 | 1.1 |
| Mar-19 | 20 | 12856 | 4202 | 6.49 | 0.96 | 466 | 124 | 4.7 | 2.7 | 1.3 |
| Apr-19 | 17 | 12622 | 3526 | 6.79 | 0.65 | 469 | 101 | 4.7 | 2.7 | 0.8 |
| May-19 | 16 | 14082 | 3318 | 6.53 | 0.45 | 553 | 70.4 | 4.0 | 3.6 | 1.0 |
| Jun-19 | 13 | 11905 | 3095 | 6.43 | 0.58 | 549 | 53.8 | 4.0 | 3.0 | 0.9 |
| Jul-19 | 13 | 8835 | 1999 | 6.28 | 0.77 | 540 | 64.9 | 4.1 | 2.2 | 0.5 |
| Aug-19 | 13 | 9578 | 5702 | 6.03 | 0.54 | 557 | 72.3 | 3.9 | 2.5 | 1.6 |
| Sep-19 | 17 | 8983 | 2865 | 6.07 | 0.88 | 569 | 56.5 | 3.9 | 2.3 | 0.7 |
| Oct-19 | 17 | 8301 | 1622 | 5.30 | 1.00 | 620 | 55.7 | 3.5 | 2.4 | 0.5 |
| Nov-19 | 19 | 9375 | 6748 | 4.79 | 1.01 | 639 | 72.0 | 3.4 | 2.7 | 1.9 |
| Dec-19 | 20 | 9099 | 2229 | 5.57 | 0.97 | 643 | 87.0 | 3.4 | 2.7 | 0.9 |
| Jan-20 | 21 | 9435 | 2409 | 4.90 | 0.88 | 600 | 144 | 3.7 | 2.6 | 1.1 |
| Feb-20 | 21 | 11377 | 2656 | 5.18 | 1.94 | 652 | 69.2 | 3.4 | 3.4 | 1.0 |
| Mar-20 | 20 | 10300 | 2691 | 5.64 | 0.77 | 702 | 55.0 | 3.1 | 3.3 | 1.0 |
| Apr-20 | 17 | 10311 | 3359 | 6.67 | 1.05 | 448 | 56.5 | 4.9 | 2.1 | 0.7 |
| May-20 | 15 | 9544 | 2166 | 6.46 | 0.28 | 507 | 60.3 | 4.3 | 2.2 | 0.6 |
| Jun-20 | 14 | 11446 | 8384 | 6.68 | 0.97 | 520 | 132 | 4.2 | 2.8 | 2.5 |
| Jul-20 | 13 | 10046 | 3852 | 6.37 | 0.78 | 591 | 40.2 | 3.7 | 2.7 | 1.0 |
| Aug-20 | 12 | 9224 | 4547 | 6.13 | 0.86 | 597 | 25.2 | 3.7 | 2.5 | 1.2 |
| Sep-20 | 14 | 8959 | 3361 | 7.01 | 1.28 | 597 | 28.7 | 3.7 | 2.4 | 0.9 |
| Oct-20 | 16 | 7440 | 3137 | 6.39 | 1.22 | 556 | 62.1 | 4.0 | 1.9 | 0.9 |
| Nov-20 | 18 | 7603 | 2661 | 6.24 | 0.78 | 611 | 49.9 | 3.6 | 2.1 | 0.9 |

[a] : Ambient temperature; [b] : feed total COD; [c] : hydraulic retention time; [d] : organic loading rate, total COD basis.

Table 37: Full-scale biogas production rates and performance parameters Plant 3 (distillery waste) spanning a 34-month period, given as mean values per month.

| Month | Biogas production ($Nm^3/d$) | Stdev ($Nm^3/d$) | SGY [a] (NL/kgCOD) | Stdev (NL/kgCOD) | Digestate COD (mg/L) | Stdev (mg/L) | CODR [b] (%) | Digestate pH | Stdev |
|---|---|---|---|---|---|---|---|---|---|
| Jan-18 | 1252 | 486.6 | 221 | 80.8 | 488.0 | 246.7 | 96.6 | 7.30 | 0.36 |
| Feb-18 | 1480 | 435.8 | 181 | 51.6 | 387.3 | 94.3 | 98.1 | 7.03 | 0.26 |
| Mar-18 | 1549 | 578.4 | 135 | 197 | 1743.4 | 1093 | 93.3 | 7.19 | 0.30 |
| Apr-18 | 1199 | 404.8 | 161 | 82.6 | 1369.8 | 729.7 | 91.2 | 7.26 | 0.30 |
| May-18 | 1459 | 376.8 | 173 | 73.3 | 2012.3 | 955.0 | 88.8 | 7.08 | 0.28 |
| Jun-18 | 1238 | 292.3 | 207 | 81.7 | 2496.8 | 1891 | 81.7 | 6.86 | 0.30 |
| Jul-18 | 813.7 | 223.0 | 143 | 60.8 | 1133.5 | 938.7 | 88.3 | 7.04 | 0.17 |
| Aug-18 | 1040 | 304.5 | 153 | 68.8 | 407.0 | 314.1 | 96.6 | 7.04 | 0.26 |
| Sep-18 | 1209 | 379.2 | 199 | 55.2 | 233.5 | 72.6 | 97.9 | 7.12 | 0.21 |
| Oct-18 | 1334 | 451.9 | 176 | 77.7 | 198.3 | 33.8 | 98.6 | 7.11 | 0.22 |
| Nov-18 | 830.5 | 196.2 | 111 | 33.5 | 188.4 | 51.2 | 98.7 | 6.98 | 0.26 |
| Dec-18 | 711.5 | 506.2 | 104 | 123.7 | 228.8 | 55.2 | 98.4 | 6.85 | 0.27 |
| Jan-19 | 1649 | 709.5 | 223 | 133.1 | 274.6 | 198.3 | 98.2 | 6.89 | 0.26 |
| Feb-19 | 1893 | 689.2 | 277 | 100 | 571.9 | 407.0 | 95.5 | 6.92 | 0.17 |
| Mar-19 | 1542 | 575.7 | 258 | 197 | 540.9 | 282.9 | 95.8 | 6.97 | 0.26 |
| Apr-19 | 1199 | 404.8 | 203 | 82.6 | 681.8 | 979.3 | 94.6 | 6.89 | 0.35 |
| May-19 | 1459 | 376.8 | 187 | 73.3 | 862.6 | 1928 | 93.9 | 6.94 | 0.26 |
| Jun-19 | 1244 | 293.6 | 190 | 81.7 | 2272.2 | 2445 | 80.9 | 6.86 | 0.60 |
| Jul-19 | 817.4 | 224.0 | 171 | 60.8 | 1584.1 | 1393.5 | 82.1 | 6.91 | 0.52 |
| Aug-19 | 1035 | 303.2 | 194 | 68.8 | 836.9 | 1299 | 91.3 | 7.00 | 0.31 |
| Sep-19 | 961.9 | 112.4 | 188 | 65.4 | 561.1 | 816.6 | 93.8 | 7.03 | 0.28 |
| Oct-19 | 1099 | 198.2 | 214 | 55.2 | 443.6 | 726.6 | 94.7 | 6.92 | 0.26 |
| Nov-19 | 1190 | 150.7 | 199 | 71.4 | 1064.7 | 1201 | 88.6 | 6.94 | 0.21 |
| Dec-19 | 1205 | 236.5 | 206 | 54.3 | 582.1 | 684.9 | 93.6 | 7.04 | 0.26 |
| Jan-20 | 1269 | 523.3 | 224 | 70.2 | 405.1 | 908.8 | 95.7 | 7.20 | 0.29 |
| Feb-20 | 2260 | 555.3 | 305 | 71.2 | 366.7 | 187.0 | 96.8 | 7.12 | 0.31 |
| Mar-20 | 2315 | 577.6 | 320 | 96.6 | 521.9 | 209.9 | 94.9 | 7.14 | 0.36 |
| Apr-20 | 830.3 | 337.0 | 180 | 94.5 | 369.4 | 369.4 | 96.4 | 7.18 | 0.11 |
| May-20 | 821.6 | 149.4 | 170 | 40.3 | 329.9 | 329.9 | 96.5 | 7.16 | 0.12 |
| Jun-20 | 1136 | 501.4 | 191 | 238.4 | 294.2 | 294.2 | 97.4 | 7.09 | 0.18 |
| Jul-20 | 1213 | 320.1 | 204 | 86.5 | 403.6 | 403.6 | 96.0 | 7.00 | 0.12 |
| Aug-20 | 1178 | 224.9 | 214 | 86.8 | 1591.0 | 1591 | 82.8 | 6.94 | 0.11 |
| Sep-20 | 1141 | 143.6 | 213 | 93.9 | 1969.5 | 1970 | 78.0 | 6.93 | 0.09 |
| Oct-20 | 903.7 | 345.9 | 219 | 206 | 2922.0 | 2922 | 60.7 | 6.89 | 0.08 |
| Nov-20 | 1146 | 524.2 | 247 | 164 | 1997.2 | 1997 | 73.7 | 7.00 | 0.13 |

[a] : Specific gas yield; [b] : COD reduction.

Table 38: Estimation of full-scale performance for Plant 3 (distillery waste) using the extrapolation method (Holliger *et al.,* 2017).

| Month | Feed rate ($m^3$/d) | Full-scale TCOD (mg/L) | Extrap. SGY (NL/kgCOD) [a] | Nm3 biogas per day | | SGY (NL/kgCOD) | | Scale factors [b] |
|---|---|---|---|---|---|---|---|---|
| | | | | Full-scale | Estimated | Full-scale | Estimated | Biogas production and SGY |
| Jan-18 | 400 | 14156 | 281,0 | 1252 | 1590 | 221,2 | 281,0 | 0.79 |
| Feb-18 | 410 | 19950 | 258,5 | 1480 | 2112 | 181,2 | 258,5 | 0.70 |
| Mar-18 | 444 | 25969 | 235,1 | 1549 | 2708 | 134,5 | 235,1 | 0.57 |
| Apr-18 | 480 | 15537 | 275,6 | 1199 | 2057 | 160,7 | 275,6 | 0.58 |
| May-18 | 470 | 17917 | 266,4 | 1459 | 2242 | 173,4 | 266,4 | 0.65 |
| Jun-18 | 439 | 13619 | 283,1 | 1238 | 1694 | 206,9 | 283,1 | 0.73 |
| Jul-18 | 587 | 9699 | 298,3 | 814 | 1700 | 142,8 | 298,3 | 0.48 |
| Aug-18 | 576 | 11828 | 290,1 | 1040 | 1976 | 152,6 | 290,1 | 0.53 |
| Sep-18 | 548 | 11077 | 293,0 | 1209 | 1780 | 199,0 | 293,0 | 0.68 |
| Oct-18 | 550 | 13744 | 282,6 | 1334 | 2138 | 176,3 | 282,6 | 0.62 |
| Nov-18 | 496 | 15034 | 277,6 | 831 | 2071 | 111,3 | 277,6 | 0.40 |
| Dec-18 | 480 | 14274 | 280,5 | 712 | 1922 | 103,9 | 280,5 | 0.37 |
| Jan-19 | 480 | 15395 | 276,2 | 1649 | 2039 | 223,4 | 276,2 | 0.81 |
| Feb-19 | 542 | 12639 | 286,9 | 1893 | 1964 | 276,6 | 286,9 | 0.96 |
| Mar-19 | 466 | 12856 | 286,1 | 1542 | 1712 | 257,6 | 286,1 | 0.90 |
| Apr-19 | 469 | 12622 | 287,0 | 1199 | 1699 | 202,5 | 287,0 | 0.71 |
| May-19 | 553 | 14082 | 281,3 | 1459 | 2191 | 187,3 | 281,3 | 0.67 |
| Jun-19 | 549 | 11905 | 289,8 | 1244 | 1895 | 190,1 | 289,8 | 0.66 |
| Jul-19 | 540 | 8835 | 301,7 | 817 | 1438 | 171,5 | 301,7 | 0.57 |
| Aug-19 | 557 | 9578 | 298,8 | 1035 | 1594 | 194,0 | 298,8 | 0.65 |
| Sep-19 | 569 | 8983 | 301,1 | 962 | 1538 | 188,4 | 301,1 | 0.63 |
| Oct-19 | 620 | 8301 | 303,8 | 1099 | 1563 | 213,5 | 303,8 | 0.70 |
| Nov-19 | 639 | 9375 | 299,6 | 1190 | 1795 | 198,5 | 299,6 | 0.66 |
| Dec-19 | 643 | 9099 | 300,7 | 1205 | 1759 | 205,9 | 300,7 | 0.68 |
| Jan-20 | 600 | 9435 | 299,3 | 1269 | 1693 | 224,4 | 299,3 | 0.75 |
| Feb-20 | 652 | 11377 | 291,8 | 2260 | 2164 | 304,7 | 291,8 | 1.04 |
| Mar-20 | 702 | 10300 | 296,0 | 2315 | 2140 | 320,1 | 296,0 | 1.08 |
| Apr-20 | 448 | 10311 | 295,9 | 830 | 1365 | 180,0 | 295,9 | 0.61 |
| May-20 | 507 | 9544 | 298,9 | 822 | 1446 | 169,8 | 298,9 | 0.57 |
| Jun-20 | 520 | 11446 | 291,5 | 1136 | 1736 | 190,7 | 291,5 | 0.65 |
| Jul-20 | 591 | 10046 | 297,0 | 1213 | 1763 | 204,4 | 297,0 | 0.69 |
| Aug-20 | 597 | 9224 | 300,2 | 1178 | 1652 | 214,1 | 300,2 | 0.71 |
| Sep-20 | 597 | 8959 | 301,2 | 1141 | 1612 | 213,2 | 301,2 | 0.71 |
| Oct-20 | 556 | 7440 | 307,1 | 904 | 1269 | 218,7 | 307,1 | 0.71 |
| Nov-20 | 611 | 7603 | 306,5 | 1146 | 1424 | 246,7 | 306,5 | 0.81 |

[a] : Extrapolated specific gas yield using Equation (11); [b] : scale factors calculated from the ratio of full-scale performance to estimated performance.

Table 39: Estimation of full-scale performance for Plant 3 (distillery waste) using the dynamic model (Fiore *et al.,* 2016).

| Month | Feed rate ($m^3$/d) | Full-scale TCOD (mg/L) | Extrap. SGY [a] | Extrap. k-value [b] | Nm3 biogas per day | | SGY (NL/kgCOD) | | Scale factors [c] |
|---|---|---|---|---|---|---|---|---|---|
| | | | | | Full-scale | Modelled | Full-scale | Modelled | Biogas production and SGY |
| Jan-18 | 400 | 14156 | 281,0 | 1,60 | 1252 | 1184 | 221,2 | 209,2 | 1.06 |
| Feb-18 | 410 | 19950 | 258,5 | 1,19 | 1480 | 1358 | 181,2 | 166,2 | 1.09 |
| Mar-18 | 444 | 25969 | 235,1 | 0,76 | 1549 | 1311 | 134,5 | 113,8 | 1.18 |
| Apr-18 | 480 | 15537 | 275,6 | 1,50 | 1199 | 1467 | 160,7 | 196,6 | 0.82 |
| May-18 | 470 | 17917 | 266,4 | 1,33 | 1459 | 1512 | 173,4 | 179,6 | 0.97 |
| Jun-18 | 439 | 13619 | 283,1 | 1,64 | 1238 | 1266 | 206,9 | 211,6 | 0.98 |
| Jul-18 | 587 | 9699 | 298,3 | 1,92 | 814 | 1322 | 142,8 | 232,0 | 0.62 |
| Aug-18 | 576 | 11828 | 290,1 | 1,77 | 1040 | 1492 | 152,6 | 219,0 | 0.70 |
| Sep-18 | 548 | 11077 | 293,0 | 1,82 | 1209 | 1364 | 199,0 | 224,5 | 0.89 |
| Oct-18 | 550 | 13744 | 282,6 | 1,63 | 1334 | 1565 | 176,3 | 206,9 | 0.85 |
| Nov-18 | 496 | 15034 | 277,6 | 1,54 | 831 | 1491 | 111,3 | 199,9 | 0.56 |
| Dec-18 | 480 | 14274 | 280,5 | 1,59 | 712 | 1408 | 103,9 | 205,5 | 0.51 |
| Jan-19 | 480 | 15395 | 276,2 | 1,51 | 1649 | 1459 | 223,4 | 197,6 | 1.13 |
| Feb-19 | 542 | 12639 | 286,9 | 1,71 | 1893 | 1469 | 276,6 | 214,6 | 1.29 |
| Mar-19 | 466 | 12856 | 286,1 | 1,69 | 1542 | 1291 | 257,6 | 215,7 | 1.19 |
| Apr-19 | 469 | 12622 | 287,0 | 1,71 | 1199 | 1286 | 202,5 | 217,2 | 0.93 |
| May-19 | 553 | 14082 | 281,3 | 1,61 | 1459 | 1594 | 187,3 | 204,6 | 0.92 |
| Jun-19 | 549 | 11905 | 289,8 | 1,76 | 1244 | 1433 | 190,1 | 219,1 | 0.87 |
| Jul-19 | 540 | 8835 | 301,7 | 1,98 | 817 | 1140 | 171,5 | 239,1 | 0.72 |
| Aug-19 | 557 | 9578 | 298,8 | 1,93 | 1035 | 1248 | 194,0 | 233,9 | 0.83 |
| Sep-19 | 569 | 8983 | 301,1 | 1,97 | 962 | 1211 | 188,4 | 237,1 | 0.79 |
| Oct-19 | 620 | 8301 | 303,8 | 2,02 | 1099 | 1232 | 213,5 | 239,5 | 0.89 |
| Nov-19 | 639 | 9375 | 299,6 | 1,94 | 1190 | 1391 | 198,5 | 232,1 | 0.86 |
| Dec-19 | 643 | 9099 | 300,7 | 1,96 | 1205 | 1367 | 205,9 | 233,7 | 0.88 |
| Jan-20 | 600 | 9435 | 299,3 | 1,94 | 1269 | 1319 | 224,4 | 233,2 | 0.96 |
| Feb-20 | 652 | 11377 | 291,8 | 1,80 | 2260 | 1625 | 304,7 | 219,1 | 1.39 |
| Mar-20 | 702 | 10300 | 296,0 | 1,88 | 2315 | 1622 | 320,1 | 224,3 | 1.43 |
| Apr-20 | 448 | 10311 | 295,9 | 1,88 | 830 | 1077 | 180,0 | 233,4 | 0.77 |
| May-20 | 507 | 9544 | 298,9 | 1,93 | 822 | 1140 | 169,8 | 235,7 | 0.72 |
| Jun-20 | 520 | 11446 | 291,5 | 1,79 | 1136 | 1328 | 190,7 | 223,0 | 0.86 |
| Jul-20 | 591 | 10046 | 297,0 | 1,89 | 1213 | 1362 | 204,4 | 229,5 | 0.89 |
| Aug-20 | 597 | 9224 | 300,2 | 1,95 | 1178 | 1291 | 214,1 | 234,5 | 0.91 |
| Sep-20 | 597 | 8959 | 301,2 | 1,97 | 1141 | 1263 | 213,2 | 236,0 | 0.90 |
| Oct-20 | 556 | 7440 | 307,1 | 2,08 | 904 | 1021 | 218,7 | 247,0 | 0.89 |
| Nov-20 | 611 | 7603 | 306,5 | 2,07 | 1146 | 1134 | 246,7 | 244,0 | 1.01 |

[a] : Extrapolated specific gas yield using Equation (11); [b] : extrapolated disintegration constants (*k-values*) using Equation (12); scale factors calculated from the ratio of full-scale performance to estimated performance

Table 40: Full-scale feed conditions and operating parameters for Plant 3 (distillery waste) spanning a 34-month period, given as mean values per month.

| Month | Feed conditions | | | | | Operating parameters | | | | |
|---|---|---|---|---|---|---|---|---|---|---|
| | $T_{AMB}$ [a] (°C) | TCOD [b] (mg/L) | Stdev (mg/L) | Feed pH | Stdev | Feed rate ($m^3$/d) | Stdev (m3/d) | HRT [c] (days) | $OLR_T$ [d] (kgCOD/$m^3$/d) | Stdev (kgCOD/$m^3$/d) |
| Jan-18 | 22 | 14156 | 4646 | 6.23 | 0.80 | 400 | 87.1 | 5.5 | 2.6 | 1.0 |
| Feb-18 | 21 | 19950 | 3701 | 5.25 | 0.55 | 410 | 67.4 | 5.4 | 3.8 | 1.0 |
| Mar-18 | 19 | 25969 | 8683 | 5.59 | 1.30 | 444 | 98.0 | 5.0 | 5.2 | 1.3 |
| Apr-18 | 17 | 15537 | 4458 | 6.29 | 0.77 | 480 | 133 | 4.6 | 3.4 | 0.8 |
| May-18 | 16 | 17917 | 6658 | 6.82 | 0.50 | 470 | 157 | 4.7 | 3.7 | 1.0 |
| Jun-18 | 14 | 13619 | 5364 | 6.65 | 0.92 | 439 | 135 | 5.0 | 2.8 | 0.9 |
| Jul-18 | 14 | 9699 | 1596 | 6.89 | 0.35 | 587 | 112 | 3.7 | 2.6 | 0.5 |
| Aug-18 | 12 | 11828 | 2626 | 6.42 | 0.76 | 576 | 82.0 | 3.8 | 3.1 | 1.6 |
| Sep-18 | 14 | 11077 | 1980 | 6.39 | 0.49 | 548 | 58.2 | 4.0 | 2.7 | 0.4 |
| Oct-18 | 19 | 13744 | 4014 | 6.10 | 0.76 | 550 | 58.6 | 4.0 | 3.4 | 1.0 |
| Nov-18 | 18 | 15034 | 3888 | 6.12 | 0.74 | 496 | 92.6 | 4.4 | 3.3 | 0.8 |
| Dec-18 | 21 | 14274 | 4084 | 5.73 | 0.92 | 480 | 87.0 | 4.6 | 3.2 | 1.2 |
| Jan-19 | 21 | 15395 | 6977 | 5.77 | 0.83 | 480 | 115 | 4.6 | 3.4 | 2.1 |
| Feb-19 | 22 | 12639 | 3148 | 5.66 | 1.06 | 542 | 93.2 | 4.1 | 3.2 | 1.1 |
| Mar-19 | 20 | 12856 | 4202 | 6.49 | 0.96 | 466 | 124 | 4.7 | 2.7 | 1.3 |
| Apr-19 | 17 | 12622 | 3526 | 6.79 | 0.65 | 469 | 101 | 4.7 | 2.7 | 0.8 |
| May-19 | 16 | 14082 | 3318 | 6.53 | 0.45 | 553 | 70.4 | 4.0 | 3.6 | 1.0 |
| Jun-19 | 13 | 11905 | 3095 | 6.43 | 0.58 | 549 | 53.8 | 4.0 | 3.0 | 0.9 |
| Jul-19 | 13 | 8835 | 1999 | 6.28 | 0.77 | 540 | 64.9 | 4.1 | 2.2 | 0.5 |
| Aug-19 | 13 | 9578 | 5702 | 6.03 | 0.54 | 557 | 72.3 | 3.9 | 2.5 | 1.6 |
| Sep-19 | 17 | 8983 | 2865 | 6.07 | 0.88 | 569 | 56.5 | 3.9 | 2.3 | 0.7 |
| Oct-19 | 17 | 8301 | 1622 | 5.30 | 1.00 | 620 | 55.7 | 3.5 | 2.4 | 0.5 |
| Nov-19 | 19 | 9375 | 6748 | 4.79 | 1.01 | 639 | 72.0 | 3.4 | 2.7 | 1.9 |
| Dec-19 | 20 | 9099 | 2229 | 5.57 | 0.97 | 643 | 87.0 | 3.4 | 2.7 | 0.9 |
| Jan-20 | 21 | 9435 | 2409 | 4.90 | 0.88 | 600 | 144 | 3.7 | 2.6 | 1.1 |
| Feb-20 | 21 | 11377 | 2656 | 5.18 | 1.94 | 652 | 69.2 | 3.4 | 3.4 | 1.0 |
| Mar-20 | 20 | 10300 | 2691 | 5.64 | 0.77 | 702 | 55.0 | 3.1 | 3.3 | 1.0 |
| Apr-20 | 17 | 10311 | 3359 | 6.67 | 1.05 | 448 | 56.5 | 4.9 | 2.1 | 0.7 |
| May-20 | 15 | 9544 | 2166 | 6.46 | 0.28 | 507 | 60.3 | 4.3 | 2.2 | 0.6 |
| Jun-20 | 14 | 11446 | 8384 | 6.68 | 0.97 | 520 | 132 | 4.2 | 2.8 | 2.5 |
| Jul-20 | 13 | 10046 | 3852 | 6.37 | 0.78 | 591 | 40.2 | 3.7 | 2.7 | 1.0 |
| Aug-20 | 12 | 9224 | 4547 | 6.13 | 0.86 | 597 | 25.2 | 3.7 | 2.5 | 1.2 |
| Sep-20 | 14 | 8959 | 3361 | 7.01 | 1.28 | 597 | 28.7 | 3.7 | 2.4 | 0.9 |
| Oct-20 | 16 | 7440 | 3137 | 6.39 | 1.22 | 556 | 62.1 | 4.0 | 1.9 | 0.9 |
| Nov-20 | 18 | 7603 | 2661 | 6.24 | 0.78 | 611 | 49.9 | 3.6 | 2.1 | 0.9 |

[a]:Ambient temperature; [b] : feed total COD; [c] : hydraulic retention time; [d] : organic loading rate, total COD basis.

Table 41: Full-scale biogas production rates and performance parameters Plant 3 (distillery waste) spanning a 34-month period, given as mean values per month.

| Month | Biogas production ($Nm^3/d$) | Stdev ($Nm^3/d$) | SGY [a] (NL/kgCOD) | Stdev (NL/kgCOD) | Digestate COD (mg/L) | Stdev (mg/L) | CODR [b] (%) | Digestate pH | Stdev |
|---|---|---|---|---|---|---|---|---|---|
| Jan-18 | 1252 | 486.6 | 221 | 80.8 | 488.0 | 246.7 | 96.6 | 7.30 | 0.36 |
| Feb-18 | 1480 | 435.8 | 181 | 51.6 | 387.3 | 94.3 | 98.1 | 7.03 | 0.26 |
| Mar-18 | 1549 | 578.4 | 135 | 197 | 1743.4 | 1093 | 93.3 | 7.19 | 0.30 |
| Apr-18 | 1199 | 404.8 | 161 | 82.6 | 1369.8 | 729.7 | 91.2 | 7.26 | 0.30 |
| May-18 | 1459 | 376.8 | 173 | 73.3 | 2012.3 | 955.0 | 88.8 | 7.08 | 0.28 |
| Jun-18 | 1238 | 292.3 | 207 | 81.7 | 2496.8 | 1891 | 81.7 | 6.86 | 0.30 |
| Jul-18 | 813.7 | 223.0 | 143 | 60.8 | 1133.5 | 938.7 | 88.3 | 7.04 | 0.17 |
| Aug-18 | 1040 | 304.5 | 153 | 68.8 | 407.0 | 314.1 | 96.6 | 7.04 | 0.26 |
| Sep-18 | 1209 | 379.2 | 199 | 55.2 | 233.5 | 72.6 | 97.9 | 7.12 | 0.21 |
| Oct-18 | 1334 | 451.9 | 176 | 77.7 | 198.3 | 33.8 | 98.6 | 7.11 | 0.22 |
| Nov-18 | 830.5 | 196.2 | 111 | 33.5 | 188.4 | 51.2 | 98.7 | 6.98 | 0.26 |
| Dec-18 | 711.5 | 506.2 | 104 | 123.7 | 228.8 | 55.2 | 98.4 | 6.85 | 0.27 |
| Jan-19 | 1649 | 709.5 | 223 | 133.1 | 274.6 | 198.3 | 98.2 | 6.89 | 0.26 |
| Feb-19 | 1893 | 689.2 | 277 | 100 | 571.9 | 407.0 | 95.5 | 6.92 | 0.17 |
| Mar-19 | 1542 | 575.7 | 258 | 197 | 540.9 | 282.9 | 95.8 | 6.97 | 0.26 |
| Apr-19 | 1199 | 404.8 | 203 | 82.6 | 681.8 | 979.3 | 94.6 | 6.89 | 0.35 |
| May-19 | 1459 | 376.8 | 187 | 73.3 | 862.6 | 1928 | 93.9 | 6.94 | 0.26 |
| Jun-19 | 1244 | 293.6 | 190 | 81.7 | 2272.2 | 2445 | 80.9 | 6.86 | 0.60 |
| Jul-19 | 817.4 | 224.0 | 171 | 60.8 | 1584.1 | 1393.5 | 82.1 | 6.91 | 0.52 |
| Aug-19 | 1035 | 303.2 | 194 | 68.8 | 836.9 | 1299 | 91.3 | 7.00 | 0.31 |
| Sep-19 | 961.9 | 112.4 | 188 | 65.4 | 561.1 | 816.6 | 93.8 | 7.03 | 0.28 |
| Oct-19 | 1099 | 198.2 | 214 | 55.2 | 443.6 | 726.6 | 94.7 | 6.92 | 0.26 |
| Nov-19 | 1190 | 150.7 | 199 | 71.4 | 1064.7 | 1201 | 88.6 | 6.94 | 0.21 |
| Dec-19 | 1205 | 236.5 | 206 | 54.3 | 582.1 | 684.9 | 93.6 | 7.04 | 0.26 |
| Jan-20 | 1269 | 523.3 | 224 | 70.2 | 405.1 | 908.8 | 95.7 | 7.20 | 0.29 |
| Feb-20 | 2260 | 555.3 | 305 | 71.2 | 366.7 | 187.0 | 96.8 | 7.12 | 0.31 |
| Mar-20 | 2315 | 577.6 | 320 | 96.6 | 521.9 | 209.9 | 94.9 | 7.14 | 0.36 |
| Apr-20 | 830.3 | 337.0 | 180 | 94.5 | 369.4 | 369.4 | 96.4 | 7.18 | 0.11 |
| May-20 | 821.6 | 149.4 | 170 | 40.3 | 329.9 | 329.9 | 96.5 | 7.16 | 0.12 |
| Jun-20 | 1136 | 501.4 | 191 | 238.4 | 294.2 | 294.2 | 97.4 | 7.09 | 0.18 |
| Jul-20 | 1213 | 320.1 | 204 | 86.5 | 403.6 | 403.6 | 96.0 | 7.00 | 0.12 |
| Aug-20 | 1178 | 224.9 | 214 | 86.8 | 1591.0 | 1591 | 82.8 | 6.94 | 0.11 |
| Sep-20 | 1141 | 143.6 | 213 | 93.9 | 1969.5 | 1970 | 78.0 | 6.93 | 0.09 |
| Oct-20 | 903.7 | 345.9 | 219 | 206 | 2922.0 | 2922 | 60.7 | 6.89 | 0.08 |
| Nov-20 | 1146 | 524.2 | 247 | 164 | 1997.2 | 1997 | 73.7 | 7.00 | 0.13 |

[a] : Specific gas yield; [b] : COD reduction.

Table 42: Estimation of full-scale performance for Plant 3 (distillery waste) using the extrapolation method (Holliger *et al.,* 2017).

| Month | Feed rate ($m^3$/d) | Full-scale TCOD (mg/L) | Extrap. SGY (NL/kgCOD) [a] | Nm3 biogas per day | | SGY (NL/kgCOD) | | Scale factors [b] |
|---|---|---|---|---|---|---|---|---|
| | | | | Full-scale | Estimated | Full-scale | Estimated | Biogas production and SGY |
| Jan-18 | 400 | 14156 | 281,0 | 1252 | 1590 | 221,2 | 281,0 | 0.79 |
| Feb-18 | 410 | 19950 | 258,5 | 1480 | 2112 | 181,2 | 258,5 | 0.70 |
| Mar-18 | 444 | 25969 | 235,1 | 1549 | 2708 | 134,5 | 235,1 | 0.57 |
| Apr-18 | 480 | 15537 | 275,6 | 1199 | 2057 | 160,7 | 275,6 | 0.58 |
| May-18 | 470 | 17917 | 266,4 | 1459 | 2242 | 173,4 | 266,4 | 0.65 |
| Jun-18 | 439 | 13619 | 283,1 | 1238 | 1694 | 206,9 | 283,1 | 0.73 |
| Jul-18 | 587 | 9699 | 298,3 | 814 | 1700 | 142,8 | 298,3 | 0.48 |
| Aug-18 | 576 | 11828 | 290,1 | 1040 | 1976 | 152,6 | 290,1 | 0.53 |
| Sep-18 | 548 | 11077 | 293,0 | 1209 | 1780 | 199,0 | 293,0 | 0.68 |
| Oct-18 | 550 | 13744 | 282,6 | 1334 | 2138 | 176,3 | 282,6 | 0.62 |
| Nov-18 | 496 | 15034 | 277,6 | 831 | 2071 | 111,3 | 277,6 | 0.40 |
| Dec-18 | 480 | 14274 | 280,5 | 712 | 1922 | 103,9 | 280,5 | 0.37 |
| Jan-19 | 480 | 15395 | 276,2 | 1649 | 2039 | 223,4 | 276,2 | 0.81 |
| Feb-19 | 542 | 12639 | 286,9 | 1893 | 1964 | 276,6 | 286,9 | 0.96 |
| Mar-19 | 466 | 12856 | 286,1 | 1542 | 1712 | 257,6 | 286,1 | 0.90 |
| Apr-19 | 469 | 12622 | 287,0 | 1199 | 1699 | 202,5 | 287,0 | 0.71 |
| May-19 | 553 | 14082 | 281,3 | 1459 | 2191 | 187,3 | 281,3 | 0.67 |
| Jun-19 | 549 | 11905 | 289,8 | 1244 | 1895 | 190,1 | 289,8 | 0.66 |
| Jul-19 | 540 | 8835 | 301,7 | 817 | 1438 | 171,5 | 301,7 | 0.57 |
| Aug-19 | 557 | 9578 | 298,8 | 1035 | 1594 | 194,0 | 298,8 | 0.65 |
| Sep-19 | 569 | 8983 | 301,1 | 962 | 1538 | 188,4 | 301,1 | 0.63 |
| Oct-19 | 620 | 8301 | 303,8 | 1099 | 1563 | 213,5 | 303,8 | 0.70 |
| Nov-19 | 639 | 9375 | 299,6 | 1190 | 1795 | 198,5 | 299,6 | 0.66 |
| Dec-19 | 643 | 9099 | 300,7 | 1205 | 1759 | 205,9 | 300,7 | 0.68 |
| Jan-20 | 600 | 9435 | 299,3 | 1269 | 1693 | 224,4 | 299,3 | 0.75 |
| Feb-20 | 652 | 11377 | 291,8 | 2260 | 2164 | 304,7 | 291,8 | 1.04 |
| Mar-20 | 702 | 10300 | 296,0 | 2315 | 2140 | 320,1 | 296,0 | 1.08 |
| Apr-20 | 448 | 10311 | 295,9 | 830 | 1365 | 180,0 | 295,9 | 0.61 |
| May-20 | 507 | 9544 | 298,9 | 822 | 1446 | 169,8 | 298,9 | 0.57 |
| Jun-20 | 520 | 11446 | 291,5 | 1136 | 1736 | 190,7 | 291,5 | 0.65 |
| Jul-20 | 591 | 10046 | 297,0 | 1213 | 1763 | 204,4 | 297,0 | 0.69 |
| Aug-20 | 597 | 9224 | 300,2 | 1178 | 1652 | 214,1 | 300,2 | 0.71 |
| Sep-20 | 597 | 8959 | 301,2 | 1141 | 1612 | 213,2 | 301,2 | 0.71 |
| Oct-20 | 556 | 7440 | 307,1 | 904 | 1269 | 218,7 | 307,1 | 0.71 |
| Nov-20 | 611 | 7603 | 306,5 | 1146 | 1424 | 246,7 | 306,5 | 0.81 |

[a] : Extrapolated specific gas yield using Equation [11]; [b] : scale factors calculated from the ratio of full-scale performance to estimated performance.

Table 43:Estimation of full-scale performance for Plant 3 (distillery waste) using the dynamic model (Fiore *et al.,* 2016).

| Month | Feed rate ($m^3$/d) | Full-scale TCOD (mg/L) | Extrap. SGY [a] | Extrap. k-value [b] | Nm3 biogas per day | | SGY (NL/kgCOD) | | Scale factors [c] |
|---|---|---|---|---|---|---|---|---|---|
| | | | | | Full-scale | Modelled | Full-scale | Modelled | Biogas production and SGY |
| Jan-18 | 400 | 14156 | 281,0 | 1,60 | 1252 | 1184 | 221,2 | 209,2 | 1.06 |
| Feb-18 | 410 | 19950 | 258,5 | 1,19 | 1480 | 1358 | 181,2 | 166,2 | 1.09 |
| Mar-18 | 444 | 25969 | 235,1 | 0,76 | 1549 | 1311 | 134,5 | 113,8 | 1.18 |
| Apr-18 | 480 | 15537 | 275,6 | 1,50 | 1199 | 1467 | 160,7 | 196,6 | 0.82 |
| May-18 | 470 | 17917 | 266,4 | 1,33 | 1459 | 1512 | 173,4 | 179,6 | 0.97 |
| Jun-18 | 439 | 13619 | 283,1 | 1,64 | 1238 | 1266 | 206,9 | 211,6 | 0.98 |
| Jul-18 | 587 | 9699 | 298,3 | 1,92 | 814 | 1322 | 142,8 | 232,0 | 0.62 |
| Aug-18 | 576 | 11828 | 290,1 | 1,77 | 1040 | 1492 | 152,6 | 219,0 | 0.70 |
| Sep-18 | 548 | 11077 | 293,0 | 1,82 | 1209 | 1364 | 199,0 | 224,5 | 0.89 |
| Oct-18 | 550 | 13744 | 282,6 | 1,63 | 1334 | 1565 | 176,3 | 206,9 | 0.85 |
| Nov-18 | 496 | 15034 | 277,6 | 1,54 | 831 | 1491 | 111,3 | 199,9 | 0.56 |
| Dec-18 | 480 | 14274 | 280,5 | 1,59 | 712 | 1408 | 103,9 | 205,5 | 0.51 |
| Jan-19 | 480 | 15395 | 276,2 | 1,51 | 1649 | 1459 | 223,4 | 197,6 | 1.13 |
| Feb-19 | 542 | 12639 | 286,9 | 1,71 | 1893 | 1469 | 276,6 | 214,6 | 1.29 |
| Mar-19 | 466 | 12856 | 286,1 | 1,69 | 1542 | 1291 | 257,6 | 215,7 | 1.19 |
| Apr-19 | 469 | 12622 | 287,0 | 1,71 | 1199 | 1286 | 202,5 | 217,2 | 0.93 |
| May-19 | 553 | 14082 | 281,3 | 1,61 | 1459 | 1594 | 187,3 | 204,6 | 0.92 |
| Jun-19 | 549 | 11905 | 289,8 | 1,76 | 1244 | 1433 | 190,1 | 219,1 | 0.87 |
| Jul-19 | 540 | 8835 | 301,7 | 1,98 | 817 | 1140 | 171,5 | 239,1 | 0.72 |
| Aug-19 | 557 | 9578 | 298,8 | 1,93 | 1035 | 1248 | 194,0 | 233,9 | 0.83 |
| Sep-19 | 569 | 8983 | 301,1 | 1,97 | 962 | 1211 | 188,4 | 237,1 | 0.79 |
| Oct-19 | 620 | 8301 | 303,8 | 2,02 | 1099 | 1232 | 213,5 | 239,5 | 0.89 |
| Nov-19 | 639 | 9375 | 299,6 | 1,94 | 1190 | 1391 | 198,5 | 232,1 | 0.86 |
| Dec-19 | 643 | 9099 | 300,7 | 1,96 | 1205 | 1367 | 205,9 | 233,7 | 0.88 |
| Jan-20 | 600 | 9435 | 299,3 | 1,94 | 1269 | 1319 | 224,4 | 233,2 | 0.96 |
| Feb-20 | 652 | 11377 | 291,8 | 1,80 | 2260 | 1625 | 304,7 | 219,1 | 1.39 |
| Mar-20 | 702 | 10300 | 296,0 | 1,88 | 2315 | 1622 | 320,1 | 224,3 | 1.43 |
| Apr-20 | 448 | 10311 | 295,9 | 1,88 | 830 | 1077 | 180,0 | 233,4 | 0.77 |
| May-20 | 507 | 9544 | 298,9 | 1,93 | 822 | 1140 | 169,8 | 235,7 | 0.72 |
| Jun-20 | 520 | 11446 | 291,5 | 1,79 | 1136 | 1328 | 190,7 | 223,0 | 0.86 |
| Jul-20 | 591 | 10046 | 297,0 | 1,89 | 1213 | 1362 | 204,4 | 229,5 | 0.89 |
| Aug-20 | 597 | 9224 | 300,2 | 1,95 | 1178 | 1291 | 214,1 | 234,5 | 0.91 |
| Sep-20 | 597 | 8959 | 301,2 | 1,97 | 1141 | 1263 | 213,2 | 236,0 | 0.90 |
| Oct-20 | 556 | 7440 | 307,1 | 2,08 | 904 | 1021 | 218,7 | 247,0 | 0.89 |
| Nov-20 | 611 | 7603 | 306,5 | 2,07 | 1146 | 1134 | 246,7 | 244,0 | 1.01 |

[a]: Extrapolated specific gas yield using Equation (11); [b]: extrapolated disintegration constants (*k-values*) using Equation (12); [c]: scale factors calculated from the ratio of full-scale performance to estimated performance

Table 44: ANOVA for actual and estimated full-scale performance parameters for Plant 1 (mixed organic wastes) using the extrapolation method (Holliger *et al.,* 2017).

| **A: Biogas productions** | | | | | | |
|---|---|---|---|---|---|---|
| ***Groups*** | ***Count*** | ***Sum*** | ***Average*** | ***Variance*** | | |
| Full-scale biogas production ($Nm^3/d$) | 5 | 3916.9 | 783.38 | 29847.37 | | |
| Estimated biogas production ($Nm^3/d$) | 5 | 13030.71 | 2606.142 | 2529901 | | |
| **ANOVA** | | | | | | |
| ***Source of Variation*** | ***SS*** [a] | ***df*** [b] | ***MS*** [c] | ***F*** [d] | ***P-value*** [e] | ***F crit*** [f] |
| Between Groups | 8306154 | 1 | 8306154 | 6.489822 | 0.034307 | 5.317655 |
| Within Groups | 10238992 | 8 | 1279874 | | | |
| **Total** | 18545146 | 9 | | | | |
| **B: Specific gas yields (SGY)** | | | | | | |
| ***Groups*** | ***Count*** | ***Sum*** | ***Average*** | ***Variance*** | | |
| Full-scale SGY (NL/kgVS) | 5 | 1601.964 | 320.3929 | 41836.08 | | |
| Estimated SGY (NL/kgVS) | 5 | 3731.627 | 746.3253 | 8238.241 | | |
| **ANOVA** | | | | | | |
| ***Source of Variation*** | ***SS*** | ***df*** | ***MS*** | ***F*** | ***P-value*** | ***F crit*** |
| Between Groups | 453546.1 | 1 | 453546.1 | 18.11492 | 0.002776 | 5.317655 |
| Within Groups | 200297.3 | 8 | 25037.16 | | | |
| **Total** | 653843.4 | 9 | | | | |
| **C: Methane productions** | | | | | | |
| ***Groups*** | *Count* | *Sum* | *Average* | *Variance* | | |
| Full-scale methane production ($Nm^3/d$) | 5 | 1641.534 | 328.3069 | 78.64771 | | |
| Estimated methane production ($Nm^3$ $CH_4/d$) | 5 | 6996.774 | 1399.355 | 829098.4 | | |
| **ANOVA** | | | | | | |
| ***Source of Variation*** | ***SS*** | ***df*** | ***MS*** | ***F*** | ***P-value*** | ***F crit*** |
| Between Groups | 2867860 | 1 | 2867860 | 6.917364 | 0.030174 | 5.317655 |
| Within Groups | 3316708 | 8 | 414588.5 | | | |
| **Total** | 6184568 | 9 | | | | |
| **D: Specific methane yields (SMY)** | | | | | | |
| ***Groups*** | *Count* | *Sum* | *Average* | *Variance* | | |
| Full-scale SMY (NL/kgVS) | 5 | 662.8471 | 132.5694 | 6692.437 | | |
| Modelled SMY (NL $CH_4$/kgVS) | 5 | 1941.265 | 388.2529 | 4718.625 | | |
| **ANOVA** | | | | | | |
| ***Source of Variation*** | ***SS*** | ***df*** | ***MS*** | ***F*** | ***P-value*** | ***F crit*** |
| Between Groups | 163435.2 | 1 | 163435.2 | 28.64504 | 0.000684 | 5.317655 |
| Within Groups | 45644.25 | 8 | 5705.531 | | | |
| **Total** | 209079.4 | 9 | | | | |

[a] : sum of squares; [b] : degrees of freedom; [c] : mean squares; [d] : F-statistic; [e] : significant effect of treatment; [f] : critical value

Table 45: ANOVA for actual and estimated full-scale performance parameters for Plant 1 (mixed organic wastes) using the dynamic model (Fiore *et al.*, 2016).

| **A: Biogas productions** | | | | | | |
|---|---|---|---|---|---|---|
| ***Groups*** | ***Count*** | ***Sum*** | ***Average*** | ***Variance*** | | |
| Full-scale biogas production ($Nm^3/d$) | 5 | 3916.9 | 783.38 | 29847.37 | | |
| Modelled biogas production ($Nm^3/d$) | 5 | 5234.3 | 1046.86 | 148457.1 | | |
| **ANOVA** | | | | | | |
| ***Source of Variation*** | ***SS*** [a] | ***df*** [b] | ***MS*** [c] | ***F*** [d] | ***P-value*** [e] | ***F crit*** [f] |
| Between Groups | 173554.3 | 1 | 173554.3 | 1.946718 | 0.200454 | 5.317655 |
| Within Groups | 713218.1 | 8 | 89152.26 | | | |
| **Total** | 886772.3 | 9 | | | | |
| **B: Specific gas yields (SGY)** | | | | | | |
| ***Groups*** | ***Count*** | ***Sum*** | ***Average*** | ***Variance*** | | |
| Full-scale SGY (NL/kgVS) | 5 | 1601.964 | 320.3929 | 41836.08 | | |
| Modelled SGY (NL/kgVS) | 5 | 3731.627 | 746.3253 | 8238.241 | | |
| ANOVA | | | | | | |
| ***Source of Variation*** | ***SS*** | ***df*** | ***MS*** | ***F*** | ***P-value*** | ***F crit*** |
| Between Groups | 453546.1 | 1 | 453546.1 | 18.11492 | 0.002776 | 5.317655 |
| Within Groups | 200297.3 | 8 | 25037.16 | | | |
| **Total** | 653843.4 | 9 | | | | |
| **C: Methane productions** | | | | | | |
| ***Groups*** | ***Count*** | ***Sum*** | ***Average*** | ***Variance*** | | |
| Full-scale methane production (Nm3/d) | 5 | 1641.534 | 328.3069 | 78.64771 | | |
| Modelled methane production (Nm3 CH4/d) | 5 | 2783.8 | 556.76 | 54779.03 | | |
| **ANOVA** | | | | | | |
| ***Source of Variation*** | ***SS*** | ***df*** | ***MS*** | ***F*** | ***P-value*** | ***F crit*** |
| Between Groups | 130477.1 | 1 | 130477.1 | 4.75693 | 0.060764 | 5.317655 |
| Within Groups | 219430.7 | 8 | 27428.84 | | | |
| **Total** | 349907.8 | 9 | | | | |
| **D: Specific methane yields (SMY)** | | | | | | |
| ***Groups*** | ***Count*** | ***Sum*** | ***Average*** | ***Variance*** | | |
| Full-scale SMY (NL/kgVS) | 5 | 811.3863 | 162.2773 | 8361.196 | | |
| Modelled SMY (NL/kgVS) | 5 | 1941.265 | 388.2529 | 4718.625 | | |
| **ANOVA** | | | | | | |
| ***Source of Variation*** | ***SS*** | ***df*** | ***MS*** | ***F*** | ***P-value*** | ***F crit*** |
| Between Groups | 127662.5 | 1 | 127662.5 | 19.52053 | **0.002232** | 5.317655 |
| Within Groups | 52319.28 | 8 | 6539.91 | | | |
| **Total** | 179981.8 | 9 | | | | |

[a] : sum of squares; [b] : degrees of freedom; [c] : mean squares; [d] : F-statistic; [e] : significant effect of treatment; [f] : critical value

Table 46: ANOVA for actual and estimated full-scale performance parameters for Plant 3 (distillery waste) using the extrapolation method (Holliger *et al.,* 2017).

| **A: Biogas productions** | | | | | | |
|---|---|---|---|---|---|---|
| ***Groups*** | ***Count*** | ***Sum*** | ***Average*** | ***Variance*** | | |
| Full-scale biogas production ($Nm^3/d$) | 35 | 43621.2 | 1246.32 | 135947 | | |
| Estimated biogas production ($Nm^3/d$) | 35 | 63440.7 | 1812.59 | 91179.5 | | |
| **ANOVA** | | | | | | |
| ***Source of Variation*** | ***SS*** [a] | ***df*** [b] | ***MS*** [c] | ***F*** [d] | ***P-value*** [e] | ***F crit*** [f] |
| Between Groups | 5611621 | 1 | 5611621 | 49.414 | 1.3E-09 | 3.9819 |
| Within Groups | 7722315 | 68 | 113563 | | | |
| **Total** | 1.3E+07 | 69 | | | | |
| **B: Specific gas yields (SGY)** | | | | | | |
| ***Groups*** | ***Count*** | ***Sum*** | ***Average*** | ***Variance*** | | |
| Full-scale SGY (NL/kgVS) | 35 | 6959.74 | 198.85 | 2119.07 | | |
| Estimated SGY (NL/kgVS) | 35 | 10120 | 289.142 | 216.575 | | |
| **ANOVA** | | | | | | |
| ***Source of Variation*** | ***SS*** | ***df*** | ***MS*** | ***F*** | ***P-value*** | ***F crit*** |
| Between Groups | 142671 | 1 | 142671 | 122.168 | 7.8E-17 | 3.9819 |
| Within Groups | 79411.9 | 68 | 1167.82 | | | |
| **Total** | 222083 | 69 | | | | |

[a] : sum of squares; [b] : degrees of freedom; [c] : mean squares; [d] : F-statistic; [e] : significant effect of treatment; [f] : critical value

Table 47: ANOVA for actual and estimated full-scale performance parameters for Plant 3 (distillery waste) using the dynamic model (Fiore *et al.,* 2016)

| **A: Biogas productions** | | | | | | |
|---|---|---|---|---|---|---|
| ***Groups*** | ***Count*** | ***Sum*** | ***Average*** | ***Variance*** | | |
| Full-scale biogas production ($Nm^3/d$) | 35 | 43621.17 | 1246.319 | 135947.4 | | |
| Estimated biogas production ($Nm^3/d$) | 35 | **47043** | **1344.086** | **23266.37** | | |
| **ANOVA** | | | | | | |
| ***Source of Variation*** | ***SS*** [a] | ***df*** [b] | ***MS*** [c] | ***F*** [d] | ***P-value*** [e] | ***F crit*** [f] |
| Between Groups | 167270.5 | 1 | 167270.5 | 2.101207 | 0.151779 | 3.981896 |
| Within Groups | 5413268 | 68 | 79606.88 | | | |
| **Total** | **5580538** | **69** | | | | |
| **B: Specific gas yields (SGY)** | | | | | | |
| ***Groups*** | ***Count*** | ***Sum*** | ***Average*** | ***Variance*** | | |
| Full-scale SGY (NL/kgVS) | 35 | 6959.74 | 198.8497 | 2119.071 | | |
| Estimated SGY (NL/kgVS) | 35 | 7609.079 | 217.4023 | 649.8446 | | |
| **ANOVA** | | | | | | |
| ***Source of Variation*** | ***SS*** | ***df*** | ***MS*** | ***F*** | ***P-value*** | ***F crit*** |
| Between Groups | 6023.444 | 1 | 6023.444 | 4.35076 | 0.040747 | 3.981896 |
| Within Groups | 94143.13 | 68 | 1384.458 | | | |
| **Total** | 100166.6 | 69 | | | | |

[a] : sum of squares; [b] : degrees of freedom; [c] : mean squares; [d] : F-statistic; [e] : significant effect of treatment; [f] : critical value

Table 48: ANOVA for actual and estimated full-scale digestate COD content for Plant 3 (distillery waste) using the dynamic model (Fiore *et al.,* 2016).

| ***Groups*** | ***Count*** | ***Sum*** | ***Average*** | ***Variance*** | | |
|---|---|---|---|---|---|---|
| Apparent COD ($kg/m^3$) | 35 | 44.9586 | 1.284531429 | 0.225363 | | |
| Full-scale digestate COD ($kg/m^3$) | 35 | 32.26796159 | 0.92194176 | 0.553184 | | |
| **ANOVA** | | | | | | |
| ***Source of Variation*** | ***SS*** [a] | ***df*** [b] | ***MS*** [c] | ***F*** [d] | ***P-value*** [e] | ***F crit*** [f] |
| Between Groups | 2.300747189 | 1 | 2.300747189 | 5.910363 | 0.0176934 | 3.981896256 |
| Within Groups | 26.47059439 | 68 | 0.389273447 | | | |
| **Total** | 28.77134158 | 69 | | | | |

[a] : sum of squares; [b] : degrees of freedom; [c] : mean squares; [d] : F-statistic; [e] : significant effect of treatment; [f] : critical value

Table 49: ANOVA for actual and estimated full-scale performance parameters for Plant 3 (distillery waste) using the extrapolation method for batch-mode pilot-scale AD tests (Holliger *et al.,* 2017).

| **A: Biogas productions** | | | | | | |
|---|---|---|---|---|---|---|
| ***Groups*** | ***Count*** | ***Sum*** | ***Average*** | ***Variance*** | | |
| Actual BP | 5 | 47.95061768 | 9.590123536 | 47.78456391 | | |
| Modelled BP | 5 | 168.9581035 | 33.7916207 | 0.782753278 | | |
| **ANOVA** | | | | | | |
| ***Source of Variation*** | ***SS*** [a] | ***df*** [b] | ***MS*** [c] | ***F*** [d] | ***P-value*** [e] | ***F crit*** [f] |
| Between Groups | 1464.281 | 1 | 1464.281162 | 60.29903428 | 5.4075E-05 | 5.3176551 |
| Within Groups | 194.2693 | 8 | 24.2836586 | | | |
| Total | 1658.55 | 9 | | | | |
| **B: Specific gas yields (SGY)** | | | | | | |
| ***Groups*** | ***Count*** | ***Sum*** | ***Average*** | ***Variance*** | | |
| Actual SGY | 5 | 445.052031 | 89.01040619 | 4158.20246 | | |
| Modelled SGY | 5 | 1549.105725 | 309.8211449 | 57.47921603 | | |
| **ANOVA** | | | | | | |
| ***Source of Variation*** | ***SS*** | ***df*** | ***MS*** | ***F*** | ***P-value*** | ***F crit*** |
| Between Groups | 121893.5 | 1 | 121893.4559 | 57.82858633 | 6.2784E-05 | 5.3176551 |
| Within Groups | 16862.73 | 8 | 2107.840838 | | | |
| Total | 138756.2 | 9 | | | | |

[a] : sum of squares; [b] : degrees of freedom; [c] : mean squares; [d] : F-statistic; [e] : significant effect of treatment; [f] : critical value

## APPENDIX B – SAMPLE CALCULATIONS

### B1: BMP assay tests calculations

#### (i) Total & volatile solids content determination

Recall Equation (38) for TS% determination:

$$\mathrm{TS}(\%) = \left(\frac{m_3 - m_1}{m_2 - m_1}\right) \times 100$$

Example for Plant 1 (co-digestion of mixed organic wastes), Mixture 1 (apples & food waste).

$$\mathrm{TS}(\%) = \left(\frac{23.18 - 22.34}{28.13 - 22.34}\right) \times 100$$

$$\therefore \mathrm{TS}(\%) = 14.45\% \ (\mathrm{w/w})$$

The VS content was calculated using Equation (39), for the same crucible-sample mass measurements, where $m_4$ represents the burnt crucible-sample mass after 550°C heating:

$$\mathrm{VS}(\%) = \left(\frac{m_3 - m_4}{m_2 - m_1}\right) \times 100 \qquad (37)$$

$$\mathrm{VS}(\%) = \left(\frac{23.18 - 22.38}{28.13 - 22.34}\right) \times 100$$

$$\therefore \mathrm{VS}(\%) = 13.82\% \ (\mathrm{w/w})$$

The proportion of total solids that constitutes volatile solids (VS as TS) is then calculated from the pre-determined TS and VS contents:

$$\therefore \mathrm{VS}(\%\mathrm{TS}) = \frac{13.8}{14.5} \times 100 = 95.6 \ \%\mathrm{TS}$$

#### (ii) BMP tests – reactor bottle (500mL) loadings

BMP reactor bottles were loaded according to (1) an inoculum-to-substrate ratio (ISR) of 2.0 and (2) for a reactor working volume of 400mL, or 400g assuming the densities of substrate and inoculum are the same as water (1.0g/L).

*(a) Volatile solids (% w/w) basis (Plant 1 and Plant 2)*

$$ISR = \frac{m_I VS_I}{m_s VS_s} = 2.0 \qquad [1]$$

$$m_I + m_s = m_{total} = 400 \qquad [2]$$

Where $m_I$ and $m_s$ are the masses of inoculum and substrate added to each reactor bottle, respectively, and $VS_I$ and $VS_s$ are the volatile solids contents of the inoculum and substrate, respectively.

Example for Plant 1:

Mean VS content (Mixture 1, apples & food waste) = $14.45\%$ (w/w)

Mean VS content (inoculum) = $1.01$ % (w/w)

$$\frac{m_I(0.1445)}{m_s(0.0101)} = 2.0 \quad [1]$$

$$m_I = 400 - m_s \quad [2]$$

$$\therefore \frac{(400-m_s)(0.1445)}{m_s(0.0101)} = 2.0$$

$$\therefore m_s = 13.24g$$

$$\therefore m_I = 386.8g$$

*(a) COD (g/L) basis (Plant 3)*

$$ISR = \frac{m_I COD_I}{m_s COD_s} = 2.0 \quad [1]$$

$$m_I + m_s = m_{total} = 0.4L \quad [2]$$

Example for Plant 3:

Mean COD content (distillery waste sample, 29-June-21) $= 9.35$ g/L

Mean COD content (inoculum) $= 9.51$ g/L

$$\frac{m_I(9.51)}{m_s(9.35)} = 2.0 \quad [1]$$

$$m_I = 0.4 - m_s \quad [2]$$

$$\therefore \frac{(0.4-m_s)(9.51)}{m_s(9.35)} = 2.0$$

$$\therefore m_s = 0.135L = 135mL$$

$$\therefore m_I = 0.265L = 265mL$$

**(iii) Calculation of bench-scale specific gas yield (SGY) and biomethane potential (BMP):**

Formulae obtained from the AMPTS II operating manual (Bioprocess Control, 2020):

$$SGY = \frac{(VB_s - VB_I)}{m_{VS,sS}} = \frac{\left(VB_s - VB_B \times \frac{m_{VS,IS}}{m_{VS,IB}}\right)}{m_{VS,sS}} = \frac{\left(VB_s - VB_B \times \frac{m_{IS}}{m_{IB}}\right)}{m_{VS,sS}}$$

$$BMP = \frac{(VM_s - VM_I)}{m_{VS,sS}} = \frac{\left(VM_s - VM_B \times \frac{m_{VS,IS}}{m_{VS,IB}}\right)}{m_{VS,sS}} = \frac{\left(VM_s - VM_B \times \frac{m_{IS}}{m_{IB}}\right)}{m_{VS,sS}}$$

The parameters in each expression above are denoted as the following:

$VB_s$ = Accumulated volume of biogas from reactor containing substrate.

$VB_I$ = Accumulated volume of biogas from reactor containing inoculum.

$VB_B$ = Accumulated volume of biogas from blank tests.

$VM_s$ = Accumulated volume of methane gas from reactor containing substrate.

$VM_I$ = Accumulated volume of methane gas from reactor containing inoculum.

$VM_B$ = Accumulated volume of methane gas from blank tests.

$m_{VS,sS}$ = Organic mass contained in the substrate in a loaded reactor.

$m_{VS,IS}$ = Dry organic mass contained in the inoculum in a loaded reactor.

$m_{VS,IB}$ = Dry organic mass contained in the inoculum in a blank test.

$m_{IS}$ = Total amount of inoculum contained in the sample.

$m_{IB}$ = Total amount of inoculum contained in a blank test.

Example for Plant 1:

Mixture 1 (apples & food waste) BMP tests:

$$SGY(\text{Day } 19) = \frac{\left(1494 - 138.9 \times \frac{3.91}{4.04}\right)}{1.95} = 697\ NL/kgVS$$

$$BMP(\text{Day } 10) = \frac{\left(643 - 75.4 \times \frac{3.91}{4.04}\right)}{1.95} = 292\ NL\ CH_4/kgVS$$

The same calculations were performed for distillery waste (Plant 3) feedstocks investigated in BMP tests, except the organic content was on a COD basis (g/L).

## B2: Pilot-scale loading calculations

Pilot-scale AD reactors were loaded according to working volume of 35L. The quantities of fed material differed between the two investigated feeding modes.

### (i) Semi-continuous feeding mode (Plants 2 & 3):

Semi-continuous pilot-scale tests were fed according to the hydraulic retention time (HRT) established for the full-scale AD plants. The HRT is calculated via Equation (1) in Section 2.2.1.3 (Meegoda *et al.*, 2018).

$$HRT = \frac{V_o}{Q_i}$$

$$\therefore Q_i = \frac{V_o}{HRT}\left[\frac{L}{d}\right]$$

Pilot-scale for Plant 2 (tomato waste):

Plant 2 feeding rate = 1500L/d for 30-minutes (*750 L/d), corresponding to an HRT of 80 days.*

$$\therefore Q_i = \frac{35\ [L]}{80\ [d]}$$

$$\therefore Q_i = 0.438\ L/d$$

$$\therefore Q_i = 438\ mL/d$$

Plant 2 organic loading rate (OLR, Equation (2)) (Sarker *et al.*, 2019) for Day 1:

$$OLR\left[\frac{kg\ VS\ or\ COD}{m^3 \cdot d}\right] = \frac{C}{HRT}$$

$$\therefore OLR = \frac{(0.438[kg/d] \times 2.57\%ww)}{0.035[m^3]} = 0.32\ kgVS/m^3/d$$

Pilot-scale for Plant 3 (distillery waste):

Plant 3 HRT = 4.0 days (feed rate of 550 $m^3$/d):

$$\therefore Q_i = \frac{35\ [L]}{4.0\ [d]}$$

$$\therefore Q_i = 8.75\ L/d$$

Calculation of OLR for Day 28 (COD = 9.98g/L; HRT of 4.4 days; feed rate of 8.0L/d):

$$\therefore OLR = \frac{\left(8.0\left[\frac{L}{d}\right] \times \frac{9.98}{1000}\left[\frac{kg}{L}\right]\right)}{0.035[m^3]} = 2.28\ kgCOD/m^3/d$$

**(ii) Batch feeding mode (Plants 3):**

Batch-mode pilot-scale AD tests were performed under conditions similar to bench-scale BMP tests. Loading of substrate and inoculum was based on an ISR of 2.0 (COD basis):

$$ISR = \frac{m_I COD_I}{m_s COD_s} = 2.0 \quad [1]$$

$$m_I + m_s = m_{total} = 35 \quad [2]$$

For pilot-scale 11 and 12 (duplicates):

$COD_I = 9.51 g/L$

$COD_s = 9.35 g/L$

$$\therefore \frac{m_I}{m_s} \times \left(\frac{9.51}{9.38}\right) = 2.0 \quad [1]$$

$$\therefore m_I = 35 - m_s \quad [2]$$

$$\therefore m_s = \frac{35}{\left(2.0 \times \left(\frac{9.35}{9.51}\right) + 1\right)} = 11.8L$$

$$\therefore m_I = 23.2L$$

**(iii) Calculating pilot-scale gas yields:**

$$SGY = \frac{VB}{m_{COD\ or\ VS}} \left[\frac{NL}{kg\ VS\ or\ COD}\right]$$

For Day 37 (semi-continuous pilot-scale for Plant 3):

$$VB = 12.0\ NL/d$$

$$m_{COD} = 9.98\ g/L$$

$$Q_i = 4.0 L/d$$

$$\therefore SGY = \frac{12.0\ [NL/d]}{\left(\frac{9.98}{1000}\left[\frac{kgCOD}{L}\right] \times 4.0\left[\frac{L}{d}\right]\right)} = 301\ NL/kgCOD$$

## B3: Full-scale datasets

### (i) Normalisation of biogas production data to standard temperature and pressure (STP):

STP conditions: 273.15K, 101.32kPa

STP normalization formulae were derived Bioprocess Control (2020):

$$V_o = f_{T,P} \times f_w \times V_{gas}$$

Where $V_o$ is the normalized biogas/methane volume, $f_{T,P}$ being the temperature and pressure correction factor and $f_w$ being the water content (vapor pressure) correction factor.

The temperature and pressure correction factor is defined below:

$$f_{T,P} = \left(\frac{T_o}{T_{gas}}\right)\left(\frac{p_{gas}}{p_o}\right) = \left(\frac{273.15}{t_{gas} + 273.15}\right)\left(\frac{(p_{gas} + 0.6)}{101.32}\right)$$

Where $T_o$ and $p_o$ are the standard temperature (273.15K or 0°C) and the standard pressure (101.32kPa or 1.0atm), respectively, and $T_{gas}$, $t_{gas}$ and $p_{gas}$ represent the temperature (in Kelvin or °C) and pressure of the gas produced in the reactor at ambient conditions.

The water vapor correction factor $(f_w)$ is calculated using the Antoine equation, which provides an estimation of vapor pressure around atmospheric pressure and in a temperature range of 0 to 100°C (Felder & Rousseau, 2005)

$$f_w = 1 - \frac{p_{vap}}{p_{gas}} = 1 - \frac{10^{8.1962 - \frac{1730.63}{(233.426 + t_{gas})}}}{10 \times (p_{gas} + 0.6)}$$

In accordance with the ideal gas law, the vapor pressure $(p_{vap})$ is assumed to be proportional to the volume of gas produced in an anaerobic digester.

<u>For the example of Plant 3:</u>

Mean daily biogas production on January 2018 $(V_{gas}) = 1381\ m^3/d$

Mean ambient temperature for Stellenbosch (Western Cape, South Africa) in January 2018 $(t_{gas}) = 22\ ^oC$ (Climate-Data.org, 2021):

Ambient pressure $(p_{gas}) = 101.32\ kPa = 1.0atm$

$$\therefore f_{T,P} = \left(\frac{273.15}{22 + 273.15}\right)\left(\frac{(101.32 + 0.6)}{101.32}\right) = 0.931$$

$$\therefore f_w = 1 - \frac{\left(10^{8.1962 - \frac{1731}{(233+22)}}\right)}{10 \times (101.32 + 0.6)} = 0.974$$

$$\therefore V_o = 0.931 \times 0.974 \times 1381\ m^3/d$$

$$\therefore V_o = 1252\ Nm^3/d$$

**(ii) Power calculations for full-scale biogas plants**

(a) Plant 1 (co-digestion of mixed organic wastes) – estimated daily methane productions (MP):

Estimated daily methane production (MP) is calculated using a power equivalent expression (Surroop & Mohee, 2011).

$$MP\ \left[\frac{m^3\mathrm{CH_4}}{d}\right] = \frac{\left(P[kWh] \times 3.6\ \left[\frac{MJ}{kWh}\right]\right)}{\left(LHV\ \left[\frac{MJ}{m^3}\right] \times\ \eta\right)}$$

Where $P$, $LHV$ and $\eta$ represent the actual power detected by the generator, the lower heating value of methane gas (33.9 MJ/m$^3$) (NIST, 2021) and the efficiency of the generator unit (15%). The conversion factor (3.6 MJ/kWh) is included to convert kilowatt-hours to mega-joules:

For an average generator power output of 522 kWh/d (Week 3, Plant 1, FigX):

$$MP\ = \frac{\left(522[kWh] \times 3.6\ \left[\frac{MJ}{kWh}\right]\right)}{\left(33.9\ \left[\frac{MJ}{m^3}\right] \times\ 15\%\right)}$$

$$\therefore MP = \ 345\ m^3\mathrm{CH_4}/d$$

Mean methane concentration (Week 3), for an average daily biogas production of 921 m$^3$/d:

$$[CH_4] = \frac{345\ [m^3\mathrm{CH_4}/d]}{921[m^3/d]} = 37\ \%vol$$

(b) Plant 2 (tomato waste) – estimated daily consumption:

Generator power output (April-2021) $= 7.0\ kVA = 7.0\ kW$

Considering a thermoelectric efficiency of 32%: Actual power $= 7.0kW \times 32\% = 2.24kW$

Run time of farm's borehole pumps $= 8\ hours$

Useful mechanical power: $\therefore = 8\ hours \times 2.24kW = 17.9\ kWh$

$$\therefore MP\ \left[\frac{m^3\mathrm{CH_4}}{d}\right] = \frac{\left(17.9[kWh] \times 3.6\left[\frac{MJ}{kWh}\right]\right)}{\left(33.9\left[\frac{MJ}{m^3}\right] \times\ 20\%\right)} = 9.51\ m^3\ \mathrm{CH_4}/d$$

For a methane concentration of 63.7% vol (measured on site of Plant 2), the daily biogas production (BP) is estimated as:

$$BP\left[\frac{m^3}{d}\right] = \frac{9.51}{0.637} = 14.9\ m^3/d$$

**(iii) Methods for estimating full-scale performance:**

(a) BMP degradation rate (BDR):

Equation (7) proposed by Schievano *et al.* (2011) was used to calculate the BMP degradation rates for each full-scale AD plant, as given below:

$$\mathrm{BMY}_1(\%) = \frac{(BMP_{in} \times TS_{in} - BMP_{out} \times TS_{out})}{(BMP_{in} \times TS_{in})} \times 100$$

The equation above was modified to a COD basis (Plant 3), as given below:

$$\mathrm{BDR}(\%) = \frac{(BMP_{in} \times m_{COD,in} - BMP_{out} \times m_{COD,out})}{BMP_{in} \times m_{COD,in}} \times 100$$

Where $BMP_{in}$ and $BMP_{out}$ represent the BMP values of the feedstock and digestate (blank tests), respectively, and $m_{COD,in}$ and $m_{COD,out}$ represent the quantities of COD (kg) contained in the feedstock and digestate, respectively.

From BMP tests performed on distillery wastes (Plant 3) on 01 June 2021:

$$BMP_{in} = 228\ NL\ CH_4/kgCOD$$

$$m_{COD,in} = 0.0024\ kg$$

$$BMP_{out} = 9.07\ NL\ CH_4/kgCOD$$

$$m_{COD,out} = 0.0038\ kg$$

$$\mathrm{BDR}(\%) = \frac{\left(228\left[\frac{NL\ \mathrm{CH_4}}{kgCOD}\right] \times 0.0024\ [kg] - 9.07\left[\frac{NL\ \mathrm{CH_4}}{kgCOD}\right] \times 0.0038\ [kg]\right)}{\left(228\left[\frac{NL\ \mathrm{CH_4}}{kgCOD}\right] \times 0.0024\ [kg]\right)} \times 100$$

$$\therefore \mathrm{BDR}(\%) = 93.7\%$$

(b) Volatile solids reduction (VSR) and COD reduction (CODR):

The Van Kleeck expression given as Equation (5) was used to calculate the VSR of solid-based feedstocks (Plant 1 and Plant 2) investigated in BMP tests.

$$\mathrm{VSR}(\%) = \frac{\left(\mathrm{VS_{feed}} - \mathrm{VS_{dig}}\right)}{\left(\mathrm{VS_{feed}} - \left(\mathrm{VS_{feed}} \times \mathrm{VS_{dig}}\right)\right)} \times 100$$

Where $\mathrm{VS_{feed}}$ and $\mathrm{VS_{dig}}$ are the VS mass fractions in the feedstock and digestate residue, respectively.

For Plant 1 (Mixture 1; apples and food waste):

Initial and final VS contents determined from BMP tests:

$$\mathrm{VS_{feed}} = 14.7\% ww$$

$$\mathrm{VS_{dig}} = 0.698\% ww$$

$$\mathrm{VSR}(\%) = \frac{(0.147 - 0.00698)}{\left(0.147 - (0.147 \times 0.00698)\right)} \times 100$$

$$\therefore \mathrm{VSR}(\%) = 95.9\%$$

The COD reduction was calculated using a similar method using a COD mass balance:

For Plant 3 (distillery waste, on 01 June 2021):

$$\mathrm{CODR}(\%) = \frac{(COD_{in} - COD_{dig})}{COD_{in}} \times 100$$

$$\mathrm{CODR}(\%) = \frac{\left(7810\ \left[\frac{mg}{L}\right] - 217\ \left[\frac{mg}{L}\right]\right)}{7810\ \left[\frac{mg}{L}\right]} \times 100$$

$$\therefore \mathrm{CODR}(\%) = 97.2\%$$

(c) Extrapolation of BMP test data to full-scale AD processes:

The expression given as Equation (11) was used to compute the daily biogas and methane production rates ($P_{full}$) for each full-scale biogas plant, as given below (Holliger *et al.*, 2017):

$$P_{full}\left[\frac{Nm^3\mathrm{CH_4}}{wk}\right] = Q_i\left[\frac{tonne}{wk}\right] \times \mathrm{TS\%}_i \times \mathrm{VS\%}_i \times \mathrm{BMP}_i\left[\frac{Nm^3\mathrm{CH_4}}{tonne\ \mathrm{VS}}\right]$$

Where $Q_i$ , $TS\%_i$ , $VS\%_i$ , and $\mathrm{BMP_i}$ represent the mass feed rate of material to the full-scale digester, the total and volatile solids content of fed material and the BMP value obtained from BMP tests, respectively.

<u>For Plant 1 (co-digestion of mixed organic wastes):</u>

For daily biogas production:

$Q_i = 9500\ kg/d$

$TS_i = 15.5\%ww$

$VS_i = 95.2\ \%TS$

$\mathrm{BMP_i} = 699\ NL/kgVS$

$$P_{full} = 9500\left[\frac{kg}{d}\right] \times (0.1548 \times 0.9523)[\%\ \mathrm{w/w}] \times \frac{699}{1000}\left[\frac{Nm^3}{kgVS}\right]$$

$$\therefore P_{full} = 979\ Nm^3/d$$

Actual daily biogas production (Mixture 1) = 820 $Nm^3/d$:

$$\therefore Scale\ factor = \frac{820}{979} = 0.838$$

For daily methane production:

$\mathrm{BMP_i} = 292\ NL/kgVS$

$$P_{full} = 9500\left[\frac{kg}{d}\right] \times (0.1548 \times 0.9523)[\%\ \mathrm{w/w}] \times \frac{292}{1000}\left[\frac{Nm^3}{kgVS}\right]$$

$$\therefore P_{full} = 410\ Nm^3\ \mathrm{CH_4}/d$$

Actual daily methane production (Mixture 1) = 318 $Nm^3\ CH_4/d$:

$$\therefore Scale\ factor = \frac{318}{410} = 0.838$$

<u>For Plant 3 (distillery waste), along a COD basis:</u>

Equation (11) was modified to a COD basis, which was referred to in Section 4.2.2:

$$P_{full}\left[\frac{NL}{d}\right] = Q_i\left[\frac{m^3}{d}\right] \times COD\left[\frac{kg}{m^3}\right] \times BMP_i\left[\frac{NL}{kgCOD}\right]$$

The expression above was used to estimate full-scale daily biogas productions, where the BMP value ($BMP_i$) was determined for different feed COD concentrations, as per the linear regression model given in Figure 40 (Equation (30)):

$$\therefore P_{full} = Q_i\left[\frac{m^3}{d}\right] \times COD\left[\frac{kg}{m^3}\right] \times (-3.885 \times [\text{COD}] + 336)\left[\frac{NL}{kgCOD}\right]$$

For the operational month January 2018 (Table 36):

$Q_i = 399.8 m^3/d$

$COD = \frac{14.16g}{L}$

$BMP_i = -3.89 \times 14.16\left[\frac{g}{L}\right] + 336 = 281\ NL/kgCOD$

$$\therefore P_{full} = 399.8\left[\frac{m^3}{d}\right] \times 14.16\left[\frac{kg}{m^3}\right] \times (281)\left[\frac{NL}{kgCOD}\right]$$

$$\therefore P_{full} = 1590\ Nm^3/d$$

Actual mean daily biogas production = 1252 $Nm^3/d$

$$\therefore Scale\ factor = \frac{1252}{1590} = 0.787$$

(d) Computation of CSTR/dynamic model (Fiore *et al.*, 2016):

Equation (12) was used to estimate the daily biogas production rate $[B(t)]$ for all three full-scale AD plants:

$$B(t)\left[\frac{Nm^3}{d}\right] = k_{dis}\left[\frac{1}{day}\right] \times Se(t)\left[\frac{kgVS}{m^3}\right] \times \text{BMP}_o\left[\frac{Nm^3}{kgVS}\right] \times V_w[m^3]$$

Where $k_{dis}$, $Se(t)$, $\text{BMP}_\text{o}$ and $V_w$ represent the degradation rate constant, the apparent VS concentration inside the digester, the BMP value derived from bench-scale AD tests and the full-scale reactor volume, respectively. The apparent VS concentration was solved numerically in MATLAB®, as given by the ordinary differential equation below:

$$V_u\left[\frac{dSe(t)}{dt}\right] = q(t)S_o(t) - q(t)S_e(t) - k_{dis} \times Se(t) \times V_u$$

Where $q(t)$ represents the input/output flowrate of the anaerobic digester ($m^3/d$) of working volume $V_u$ and $S_o(t)$ being the feed VS concentration of the feedstock.

For Plant 1 (co-digestion of mixed organic wastes):

Mixture 1 (apples & food wastes):

$$q(t) = 9500\ kg/d$$

$$k_{dis} = 0.70\ 1/day$$

$$V_u = V_w = 3200 m^3$$

$$\mathrm{BMP_o} = 699\ NL/kgVS$$

$$S_o(t) = 14.75\%ww \qquad \rightarrow \qquad \therefore S_o(t) = \frac{\left(0.1475 \times 9500\left[\frac{kg}{d}\right]\right)}{3200\ [m^3]} = 0.44\frac{kg}{m^3}$$

$$\therefore \frac{dSe(t)}{dt} = \frac{9500\left[\frac{kg}{d}\right]\left(0.44\left[\frac{kg}{m^3}\right] - Se(t)\left[\frac{kg}{m^3}\right]\right) - 0.70\left[\frac{1}{day}\right] \times Se(t)\left[\frac{kg}{m^3}\right] \times 3200[m^3]}{3200\ [m^3]}$$

Solved numerically in MATLAB® (Figure 63)

$$\therefore Se(t) = 0.346\ kg/m^3$$

$$B(t) = 0.70\left[\frac{1}{day}\right] \times 0.346\ \left[\frac{kg}{m^3}\right] \times \frac{699}{1000}\left[\frac{Nm^3}{kgVS}\right] \times 3200[m^3]$$

$$\therefore B(t) = 541\ Nm^3/d$$

Actual daily biogas production (Mixture 1) = 820 $Nm^3/d$:

$$\therefore Scale\ factor = \frac{820}{541} = 1.52$$

For Plant 3 (distillery waste):

Equation (12) was modified for a COD basis (Section 4.2.2), as given below:

$$B(t)\left[\frac{Nm^3}{d}\right] = k_{dis}\left[\frac{1}{d}\right] \times COD_e(t)\left[\frac{kg}{m^3}\right] \times \mathrm{BMP}_o\left[\frac{Nm^3}{kgCOD}\right] \times V_w\ [m^3]$$

$$\frac{dCOD_e(t)}{dt} = \left(\frac{q(t)}{V_u}\right)\left[\frac{m^3}{m^3 \cdot d}\right] \times [COD_o(t) - COD_e(t)]\left[\frac{kg}{m^3}\right] \times COD_e(t)\left[\frac{kg}{m^3}\right]$$

Note that daily biogas productions were estimated from linear regression models approximating disintegration constants (Figure 45, Equation (32)) and BMP values (Figure 40, Equation (30)):

For Plant 3 operating in January 2018:

$$q(t) = 399.8\ m^3/d$$

$$COD_o(t) = 14.16\ g/L$$

$$k_{dis} = -0.0713 \times [COD] + 2.6102 = -0.0713 \times 14.16\left[\frac{g}{L}\right] + 2.6102 = 1.60\ 1/day$$

$$V_u = V_w = 3200 m^3$$

$$\mathrm{BMP_o} = -3.89 \times [COD] + 336 = -3.89 \times 14.16\left[\frac{g}{L}\right] + 336 = 281\ NL/kgCOD$$

$$\therefore \frac{dCOD_e(t)}{dt}$$

$$= \frac{399.8\left[\frac{m^3}{d}\right]\left(14.16\left[\frac{kgCOD}{m^3}\right] - CODe(t)\left[\frac{kg}{m^3}\right]\right) - 1.60\left[\frac{1}{day}\right] \times COD_e(t)\left[\frac{kg}{m^3}\right] \times 2200[m^3]}{2200\ [m^3]}$$

Solved numerically in MATLAB® (Figure 64):

$$\therefore COD_e(t) = 1.20\ kgCOD/m^3$$

$$B(t) = 1.60\left[\frac{1}{day}\right] \times 1.20\ \left[\frac{kgCOD}{m^3}\right] \times \frac{281}{1000}\left[\frac{Nm^3}{kgVS}\right] \times 2200[m^3]$$

$$\therefore B(t) = 1184\ Nm^3/d$$

Actual daily biogas production (Mixture 1) = 820 $Nm^3/d$:

$$\therefore Scale\ factor = \frac{1252}{1184} = 1.06$$

### B4: Statistics calculations

Relative standard deviation (RSD) for BMP test results validation (Holliger *et al.*,2016):

Equation (28) was used to compute the RSD for datasets obtained from bench-scale BMP tests.

$$RSD = \frac{STDEV\ (A_1, A_2, \ldots A_n)}{AVG\ (A_1, A_2, \ldots A_n)} \times 100\%$$

## APPENDIX C – DETAILED METHODOLOGY

### C1: List of materials & consumables required for experimentation

Table 50: Required materials and consumables.

| Required | Purpose | Assay/Est. quantity |
|---|---|---|
| **Chemicals** | | |
| Sodium hydroxide (NaOH) | Raising pH for feedstock & inoculum | 20% |
| Hydrochloric acid (HCl) | Lowering pH for feedstock & inoculum | 32% |
| Micro-crystalline cellulose | Positive control tests for AMPTS | 11 wt.% (20 µm) |
| Sodium hydroxide and Thymolphthalein solution | Required for $CO_2$ absorption units | 1.0L NaOH (3.0M) with 5mL 0.4% Thymolphthalein |
| pH 4.01 buffer solution | Calibration of pH meter | As required |
| pH 7.01 buffer solution | | As required |
| pH 10.01 buffer solution | | As required |
| COD cell test kit (25 vials containing potassium dichromate & sulphuric acid) | COD measurement (photometric) for a range of 5000 to 90 000 mg/L | As required |
| Nitrogen-$CO_2$ gas mixture | Flush gas for bench-scale AD reactors | 60% $N_2$, 40% $CO_2$ |
| Nitrogen | Flush gas for pilot-scale AD reactors | 100% |
| **Laboratory consumables** | | |
| Syringes (20mL and 50mL) | Filtering of feedstock & digestate samples | As required |
| Syringe filters (0.45um) | Filtering of feedstock & digestate samples | As required |
| Pipette tips (100 to 1000uL) | Transferring of samples & chemicals | As required |

## C2: Detailed experimental setup

### Bench-scale (AMPTS II)

Each BMP test bottle was fitted with a multifunction brushless DC stepper motor (24 volts), featuring clockwise and anti-clockwise stirrer agitation, timer control and remote speed control ranging 5% to 100% speed, at a maximum rotation of 145rpm. Each motor is fitted with plastic caps, helical couplings, motor cables (0.2m and 1.5m), signal cables and a hex tool. All motor-fitted reactor vessels are connected via the 0.2m motor cables, as shown in Figure 14, which are all connected to the motor controller (labelled as 3) (Bioprocess Control, 2020). All reactors were identical, having an inside diameter of 80 mm and height of 175 mm. Figure 62 shows a more detailed schematic of each reactor vessel.

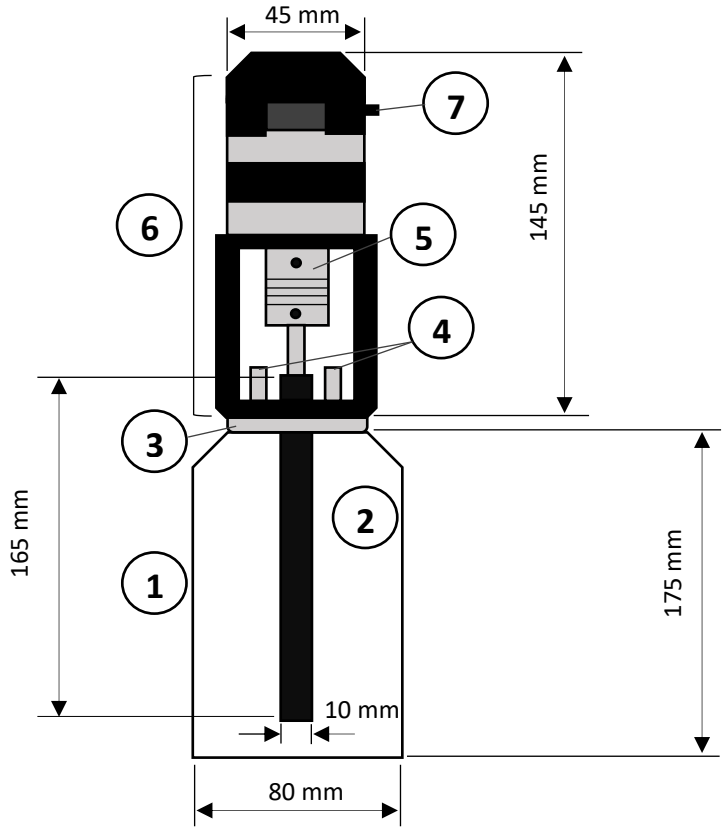


Figure 62: Detailed schematic of a single AMPTS II reactor vessel; (1) 500mL glass bottle, (2) bent stir rod, (3) plastic stopper, (4) gas outlet ports, (5) agitator head, (6) multifunction brushless DC stepper, (7) motor on/off switch.

A maximum of 15 BMP tests (five triplicates) were performed for each AMPTS run using 500mL reactors. The operating temperature for all reactors was controlled using the thermostatic water bath at mesophilic conditions (37 ± 0.1°C). The contents of each reactor were gradually agitated by a rubber-encased bent stir rod. Due to the batch-fed mode of the system only the final pH, total and volatile solids and COD content were measured after the completion of the BMP test runs. The volatile fatty acid (VFA) content was only measured if drastic differences in final and initial pH were recorded.

Two plastic outlet ports extend out from each reactor's stopper cap, where one port served as the gas purge line while the other served as the gas outlet. Clear plastic (PVC) tubing was attached to these outlet ports; the primary outlet gas lines from the reactors (labelled 4 in Figure 14) were connected to the Gas Endeavour's (GE) flotation cells, numbered from 1 to 15. The GE unit (labelled 5 in Figure 14) detects produced bubbles of biogas. When a defined volume of produced biogas flows through each cell, the GE translates these volumes to a digital pulse, which is subsequently sent to the main control system.

From the GE unit produced biogas (measured as normalised millilitres, NmL) flows to the $CO_2$ adsorption vessels (labelled 7 in Figure 14), which contain an alkaline solution (3.0M NaOH). The solution also contains a blue pH indicator (0.4% Thymolphthalein) to indicate the solution's acid binding capacity; as more $CO_2$ and hydrogen sulphide ($H_2S$) binds to NaOH molecules the solution's blue colour fades, and thus daily inspection of each adsorption unit was done to ensure maximum adsorption capacity (Bioprocess Control, 2020).

Following the adsorption of $CO_2$ and $H_2S$ from the biogas, methane gas ($CH_4$) flows via PVC tubing to the AMPTS gas volume measuring device. Similar to the GE, volumes of produced $CH_4$ are monitored via flotation pegs that implement buoyancy and liquid displacement principles. The AMPTS flotation cells are sensitive enough to detect low volumes of produced methane, which subsequently translate registered volumes to a digital pulse. The main control system records and displays all methane production data, and has an integrated embedded data acquisition system (Bioprocess Control, 2020).

According to standardised BMP protocol, AD tests via AMPTS II were terminated when the daily methane production over three consecutive days was <1.0% of the cumulative methane volume (Holliger *et al*., 2016). Upon termination of such tests the final pH, total solids (TS) and/or volatile solids (VS) content of each reactor's media were measured.

TS content is determined as follows:

1. A crucible dish of known mass is used for holding the feedstock (approx. 5g of sample).
2. The combined crucible-sample mass is recorded and then placed in a drying oven at 105°C.
3. The sample is dried until all moisture evaporates from it, i.e. until a constant mass is measured.
4. Equation (38) is then used to calculate the TS content of the feedstock:

$$\mathrm{TS}(\%) = \left(\frac{m_3 - m_1}{m_2 - m_1}\right) \times 100 \tag{38}$$

$m_1$ = mass of empty crucible

$m_2$ = mass of crucible containing sample

$m_3$ = mass of crucible (and sample) after drying

Determining a substrate's VS content is a subsequent step from the TS analysis procedure (VDI 4630, 2016):

1. Following the initial TS analysis method, the crucible (with dried sample) is placed in a muffle furnace to undergo a two-step calcination (high temperature) process:
    1.1. Samples are heated at 220°C for 30 minutes.
    1.2. Samples are further heated at 550°C for 2 hours.
2. Following calcination, the samples are removed from the furnace and left to cool at 25°C.
3. The final crucible-sample masses are then recorded, which are used in Equation (39) below to compute the VS content:

$$\mathrm{VS}(\%) = \left(\frac{m_3 - m_4}{m_2 - m_1}\right) \times 100 \tag{39}$$

$m_1$ = mass of empty crucible

$m_2$ = mass of crucible containing sample

$m_3$ = mass of crucible (and sample) after drying

$m_4$ = mass of crucible (and sample) after calcination

## C3: MATLAB® and Simulink input screens

**A**

```
%% Mixture 1 specs: SGY

BMP = 699.0;                    % SGY: NL/kgVS  mean value
%BMP = 675.5;
%BMP = 661.6;
%BMP = 759.9;

Vu = 3200;                      % m3
k_dis = 0.7;                    % per day
So = 0.43775309454608;          % Input VS concentration kg_VS/m3
q = 9500;                       % Feed flow kg/d
```

**B**

```
%% TW (15-04-21)

%BMP = 651.6;                   % SGY: NL/kgVS  mean value
BMP = 455.8;                    % SMY: NL CH4/kgVS mean value

Vu = 60;                        % m3
k_dis = 0.35;                   % per day
So = 0.4283;                    % Input VS concentration kg_VS/m3
q = 1000;                       % Feed flow kg/d (expressed as m3/d)
```

**C**

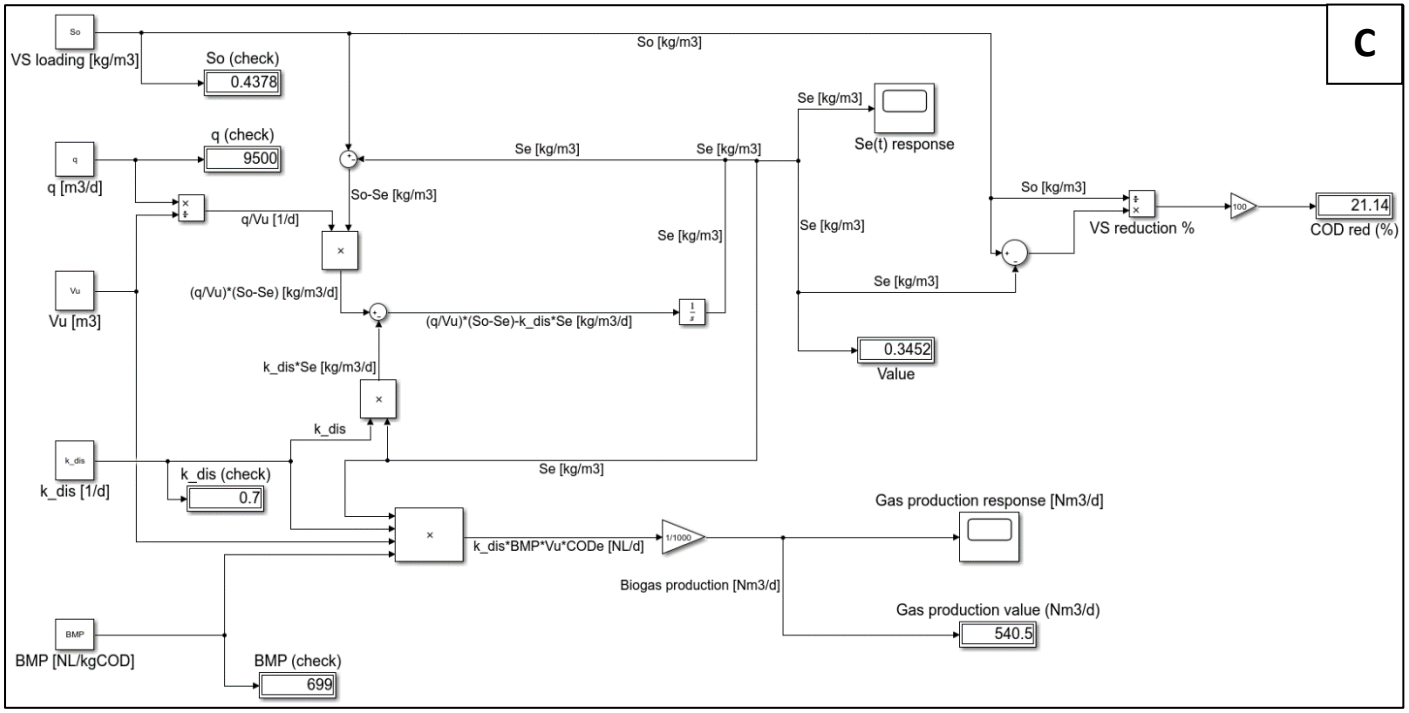


Figure 63: Use of MATLAB® software for dynamic modelling of full-scale performance parameters for solid-based AD installations Plant 1 and Plant 2: (a) input screen for Plant 1, (b) input screen for Plant 2, (c) Simulink diagram for both AD plants.

A

```
%% Input variables - 26-Oct-2020

BMP = 292.619220527717;          % SGY: NL/kgCOD
Vu = 2200;                       % m3
k_dis = 2.0;                     % per day
COD_o = 15.29;                   % kg/m3
q = 479.545454545455;            % m3/d (Plant 3: Oct. 2020 avg flow rate)
```

B

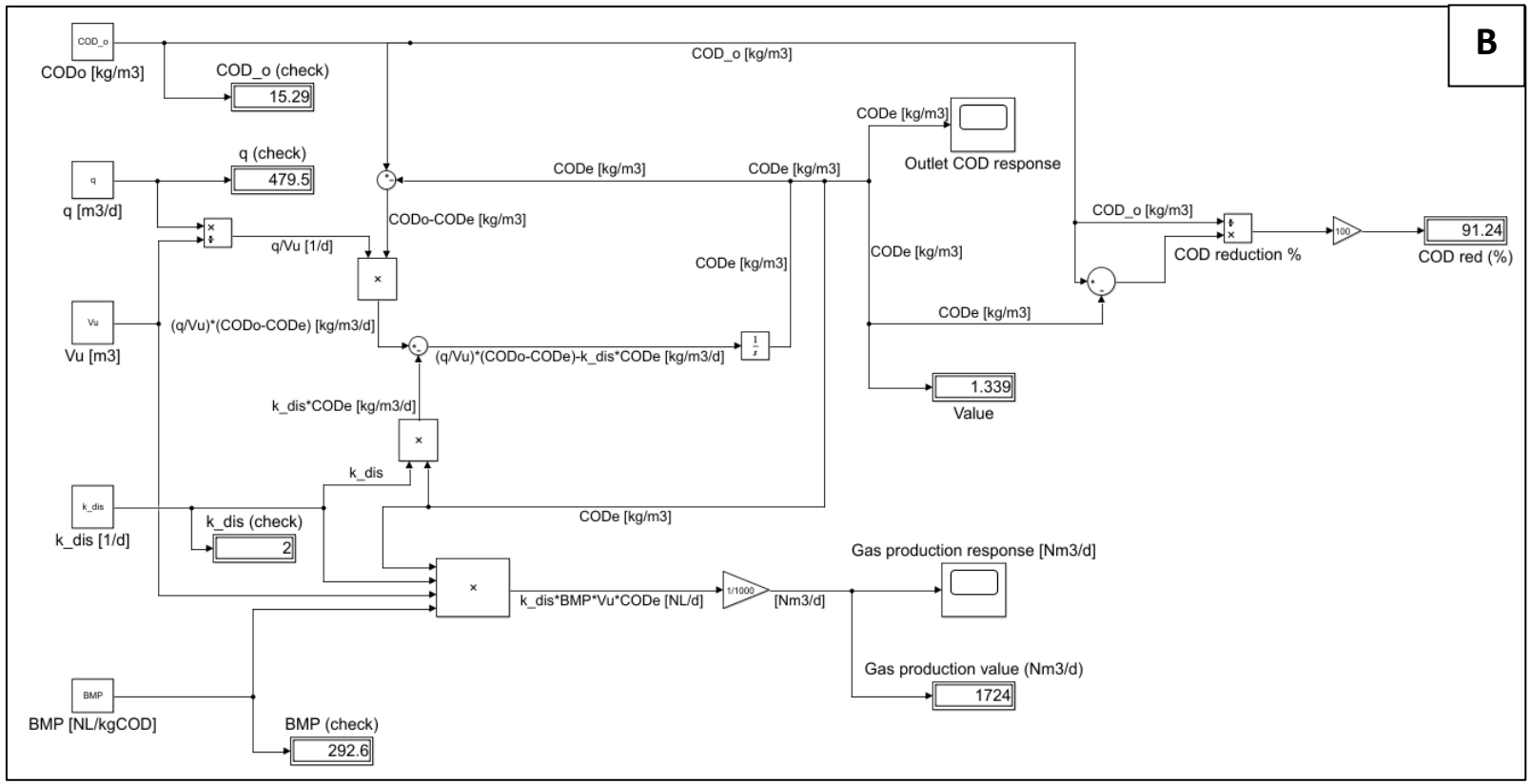


Figure 64: Use of MATLAB® software for dynamic modelling of full-scale performance parameters for liquid-based AD Plant 3 (a) input screen and work space, (b) Simulink diagram.